

ACCURATE, EMPIRICAL RADII AND MASSES OF PLANETS AND THEIR HOST STARS WITH *GAIA* PARALLAXES

KEIVAN G. STASSUN,^{1,2} KAREN A. COLLINS,^{1,2} AND B. SCOTT GAUDI^{3,4}

¹ Vanderbilt University, Department of Physics & Astronomy, 6301 Stevenson Center Ln., Nashville, TN 37235, USA

² Fisk University, Department of Physics, 1000 17th Ave. N., Nashville, TN 37208, USA

³ The Ohio State University, Department of Astronomy, 140 W. 18th Ave., Columbus, OH 43210, USA

⁴ Jet Propulsion Laboratory, California Institute of Technology, 4800 Oak Grove Dr., Pasadena, CA 91109, USA

ABSTRACT

We present empirical measurements of the radii of 116 stars that host transiting planets. These radii are determined using only direct observables—the bolometric flux at Earth, the effective temperature, and the parallax provided by the *Gaia* first data release—and thus are virtually model independent, extinction being the only free parameter. We also determine each star’s mass using our newly determined radius and the stellar density, itself a virtually model independent quantity from previously published transit analyses. These stellar radii and masses are in turn used to redetermine the transiting planet radii and masses, again using only direct observables. The median uncertainties on the stellar radii and masses are 8% and 30%, respectively, and the resulting uncertainties on the planet radii and masses are 9% and 22%, respectively. These accuracies are generally larger than previously published model-dependent precisions of 5% and 6% on the planet radii and masses, respectively, but the newly determined values are purely empirical. We additionally report radii for 242 stars hosting radial-velocity (non-transiting) planets, with median achieved accuracy of $\approx 2\%$. Using our empirical stellar masses we verify that the majority of putative “retired A stars” in the sample are indeed more massive than $\sim 1.2 M_{\odot}$. Most importantly, the bolometric fluxes and angular radii reported here for a total of 498 planet host stars—with median accuracies of 1.7% and 1.8%, respectively—serve as a fundamental dataset to permit the re-determination of transiting planet radii and masses with the *Gaia* second data release to $\approx 3\%$ and $\approx 5\%$ accuracy, better than currently published precisions, and determined in an entirely empirical fashion.

1. INTRODUCTION

Precise and accurate estimates of the radii and masses of extrasolar planets are essential for a wide variety of reasons. In the most basic sense, these parameters allow one to estimate the bulk density of an exoplanet, and thus broadly categorize its nature, in other words, determine if it is, e.g., a gas giant, ice giant, mini-Neptune, or rocky planet. Indeed, it was the discovery of the first transiting planet HD 209458 b (Charbonneau, Brown, Latham, & Mayor 2000; Henry, Marcy, Butler, & Vogt 2000) that ultimately cemented the interpretation of the Doppler signals of “Hot Jupiters” (first discovered with the detection of 51 Peg b; Mayor & Queloz 1995) as due to roughly Jupiter-mass objects with roughly Jupiter-like densities, and thus that these objects must be primarily composed of hydrogen and helium. Given that the “Hot Jupiters” have periods of only a few days, this discovery, along with the fairly robust theoretical conclusion that the majority of gas giants must form beyond the “snow line” at several AU (Pollack et al. 1996; Kennedy & Kenyon 2008), also cemented the paradigm-shifting idea that a significant subset of giant planets undergo large-scale migration, thus revolutionizing our ideas about the evolution of planetary systems.

Similarly, estimates of the masses and radii of planets, when coupled with information about their demographics (e.g., their periods and host star properties), can provide important insight into both the physics of planetary atmospheres and interiors, and the physics of planet formation and evolution. For example, a significant fraction of planets in the range of $\sim 0.1\text{--}2 M_J$ have much larger radii than are predicted from standard models of the evolution of hot Jupiters, given their probable irradiation history (e.g., Burrows et al. 2000). Despite many suggested solutions to this ‘inflated Hot Jupiter’ problem (Burrows et al. 2007; Guillot & Showman 2002; Jackson et al. 2009; Batygin et al. 2011; Chabrier & Baraffe 2007; Arras & Socrates 2010), no one explanation has emerged as the leading contender, although empirical trends with stellar insolation (Demory & Seager 2011) and perhaps age (Hartman et al. 2016) may provide clues to the correct physical model. Regardless, whichever physical mechanism turns out to be dominant, measurements of their radii as a function of the other properties of the system will provide important constraints on the physics of, e.g., tides, magnetic fields, and/or winds in these planets.

As another example, estimates of the density of ‘warm Jupiters’, i.e., those which do not appear to be affected by the inflation effect discussed above, can provide constraints on their heavy element content, and therefore potentially on the existence of a solid core (Sato et

al. 2005). Such cores are a ‘smoking gun’ of the core-accretion, bottom-up formation scenario for giant planets (Pollack et al. 1996), but are generally not expected in the gravitational instability scenario (Boss 1997). Indeed, evidence for a correlation between the inferred core mass of warm Jupiters and the heavy element composition of the host star lends credence to the idea that most, if not all, close-in giant planets form via core accretion (Miller & Fortney 2011).

More recently, estimates of the masses and radii of less massive planets ($M_p \lesssim 10M_\oplus$) detected via Kepler (Borucki et al. 2010) have uncovered an apparent dichotomy in the properties of planets with radii $\lesssim 1.5 R_\oplus$ compared to those larger than this (Rogers 2015). In particular, the larger planets appear to have significant hydrogen and helium envelopes, whereas the smaller planets appear to be much more similar to the terrestrial planets in our solar system, with little to no atmospheres. Indeed, the most precise estimates of the masses and radii of the smallest planets reveal densities that are consistent with a Mg-Si-O composition that is identical to that of the Earth (Dressing et al. 2015).

Thus, accurate and precise estimates of the masses and radii of exoplanets have played, and will continue to play, an essential role in understanding the physical processes at work in these planets, and their formation and evolutionary histories.

1.1. *The challenge of direct and accurate measurements of host-star radii and masses*

Essentially all exoplanets with measured masses and radii are those found in transiting systems. Unfortunately, as is well known, the masses and radii of transiting planets are generally not measured directly; the planets’ masses and radii depend, through direct transit observables, on the assumed masses and radii of their host stars. The observables are the depth of the transit, which (in the absence of limb darkening) is simply $\delta_{\text{tr}} = k^2$, where $k \equiv R_p/R_\star$ and R_p and R_\star are the radius of the planet and star, respectively, and the velocity semi-amplitude K_{RV} , which is given by

$$K_{\text{RV}} \equiv \left(\frac{2\pi G}{P} \right)^{1/3} \frac{M_p \sin i}{(M_\star + M_p)^{2/3}} (1 - e^2)^{-1/2}, \quad (1)$$

where P , e , and i are period, eccentricity, and inclination of the planet’s orbit, respectively, M_p is the mass of the planet and M_\star is the mass of the star. The eccentricity of the orbit can be determined from the precise shape of the Doppler reflex (radial velocity, or RV) motion of the star, and the inclination can be measured from the relative duration of the ingress/egress τ and full-width half-maximum T of the transit (Carter et al.

2008). Thus, in order to estimate R_p and M_p , one must be able to measure R_* and M_* .

Unfortunately, it is not possible to estimate the mass or radius of the host purely from photometric follow-up of the primary transit and RV measurements of the host star, *regardless of how precise these measurements are*. This is due to a well-known degeneracy, first pointed out in the case of transiting planets by Seager & Mallén-Ornelas (2003). As they note, the only parameter about the star that can be directly measured from observables is the ratio of the semimajor axis of the orbit a to the radius of the star a/R_* (Winn 2010),

$$\frac{a}{R_*} = \frac{\delta_{\text{tr}}^{1/4}}{\pi} \frac{P}{\sqrt{T\tau}} \left(\frac{\sqrt{1-e^2}}{1+e \sin \omega} \right), \quad (2)$$

where ω is the argument of periastron, which is also an observable from the RV curve. However, this quantity is closely related to the density of the star (Seager & Mallén-Ornelas 2003; Winn 2010),

$$\rho_* = \frac{3\pi}{GP^2} \left(\frac{a}{R_*} \right)^3 - k^3 \rho_p \simeq \frac{3\pi}{GP^2} \left(\frac{a}{R_*} \right)^3, \quad (3)$$

where ρ_p is the density of the planet (and is typically $\sim \rho_*$) and the last equality follows from the fact that typically $k^3 \ll 1$.

Thus ρ_* can essentially be inferred from direct observables. Nevertheless, there remains a one-parameter degeneracy that makes it impossible to estimate the mass and radius of the star independently. All transiting planet systems (with only photometry of the primary transit and RV observations) are subject to this degeneracy. To break the degeneracy, one must bring in additional external constraints, such as a measurement of the surface gravity of the star, $\log g$ (which is a direct observable from high-resolution spectra), astroseismological inferences of the stellar mass and radius (e.g., Huber et al. 2013), or a measurement of the radius of the star (which, as we will show is a direct observable from the bolometric flux and effective temperature of the star, and the distance to the system).

Up until now, these observables of the host stars, while preferred because they are direct, have been either poorly measured, subject to systematic errors, or not constrained at all.

1.2. The value of reducing reliance on, and testing, stellar models and empirical relations

Instead, most authors typically use theoretical and/or empirically-calibrated relations between observable properties of the star. Stellar evolution is reasonably well understood, and it is known that a star of a given

effective temperature, metallicity, and density cannot have an arbitrary mass and radius. Indeed, to first order, these three parameters essentially fix the luminosity and age of the star, and thus its radius and mass. Therefore, adopting these constraints, while not direct, typically lead to much more precise estimates of the parameters of the system.

Nevertheless, they are subject to uncertainties in stellar evolution models and second-order parameters (i.e., stellar rotation), and/or inaccurate calibrations of the empirical relations. One might therefore be concerned that these estimates, while precise, are not *accurate*. One clear demonstration of this is the case of KELT-6b (Collins et al. 2014), where the parameters inferred using the Yonsei-Yale isochrones (Demarque et al. 2004) to break the degeneracy disagreed significantly (by as much as 4σ) from those inferred using the Torres et al. (2010) empirical relations. Likely this was due to the low metallicity $[\text{Fe}/\text{H}] \approx -0.3$ of the KELT-6 host star, and the fact that neither the isochrones nor the empirical relations are well-calibrated at such low metallicities.

While slightly erroneous inferences about the properties of individual systems (as in the case of Collins et al. 2014) are troubling, the difficulty with estimating accurate parameters of host stars and thus their transiting planets can be, and indeed has proven to be, quite deleterious in some cases, sometimes leading to markedly incorrect or inconsistent inferences about individual systems or even entire populations of planets. An early example of this is the case of the supermassive ($\sim 12 M_J$) planet XO-3 b (Johns-Krull et al. 2008), in which initial estimates of R_p differed by nearly a factor of two, from $\sim 1.2 R_J$ to $\sim 2.1 R_J$. The latter value would have implied that the planet was highly inflated relative to standard models, which would have been particularly interesting given its relatively large inferred mass. With improved photometry and thus an improved estimate of ρ_* , Winn et al. (2008) were able to demonstrate that the true planetary radius was likely at the lower end of this range. Indeed, as we show in this work, our revised determinations with the *Gaia* distance—which places the star at a significantly shorter distance than previously assumed—reveal the planet to be $M_p \approx 7 M_J$ and $R_p \approx 1.4 R_J$. We defer additional case studies of problems arising from current poor constraints on models and empirical relations to the Discussion (Sec. 4).

However, the difficulties with interpreting the properties of planetary populations due to uncertainties about the properties of the host stars became quite prominent and acute with the discoveries of thousands of planets via *Kepler* (Borucki et al. 2010). Here the difficulties were threefold. First, the *Kepler* transiting planet hosts

tended to be fairly faint compared to those found via ground based transit surveys, making characterization of the host stars more difficult. Second, the sheer number of hosts made systematic assays of their properties via high-resolution spectroscopy extremely resource-intensive; this was obviously exacerbated by the faintness of the hosts. Finally, the wide *Kepler* bandpass, poor cadence, and/or low signal-to-noise ratio of the majority of the transit signals made estimates of the ingress/egress time, and thus stellar densities, generally imprecise. This has led to herculean efforts to characterize the properties of the host stars, often resulting in quite different conclusions as to the radius distribution of the *Kepler* target stars and thus their transiting planetary companions (see, e.g., Pinsonneault et al. 2012; Mann et al. 2012; Dressing & Charbonneau 2013; Huber et al. 2014; Gaidos et al. 2016).

1.3. Aim of this paper: A path to precision exoplanetology in the era of *Gaia*

Three recent advances now permit the determination of accurate *and* empirical radii and masses for a large sample of transiting planets. First, there now exist all-sky, broadband photometric measurements for stars spanning a very broad range of wavelengths, from the *GALEX* far-UV at $\sim 0.15 \mu\text{m}$ to the *WISE* mid-IR at $\sim 22 \mu\text{m}$. These measurements permit construction of spectral energy distributions (SEDs) that effectively sample the majority of the flux for all but the hottest stars. Consequently the bolometric fluxes (F_{bol}), and in turn the stars' angular radii (Θ , via the stellar effective temperature, T_{eff}), can in principle be determined in a largely empirical manner. Using a set of eclipsing binary stars as benchmarks, Stassun & Torres (2016) have shown that with such data F_{bol} can be measured with a precision that is typically $\lesssim 3\%$. Second, the *Gaia* mission's first data release (Gaia Collaboration 2016) has delivered trigonometric parallaxes for $\sim 2 \times 10^6$ stars in common with *Tycho-2* (Høg et al. 2000), with a precision for the best $\sim 10\%$ of stars of $240 \mu\text{as}$. These parallaxes permit Θ to be converted to R_* . Third, a large sample of transiting planets orbiting stars that are sufficiently bright to have been included in *Tycho-2*, and consequently in the *Gaia* first data release, have been published with quantities that follow from direct observables such as the stellar density, ρ_* , the ratio of planet-to-star radii, and the orbital radial-velocity semi-amplitude. With R_* , these quantities yield R_p as well as the stellar mass, which in turn yields the planet mass.

In this paper, we perform this procedure to measure F_{bol} and Θ for 498 planet host stars, which will serve as fundamental stellar parameters for use with upcoming

data releases from *Gaia*. We also report empirical stellar and planet radii and masses as described above for 116 stars that host transiting planets, have the necessary direct observables published in the literature, and have parallaxes newly reported in the *Gaia* first data release (Gaia Collaboration 2016). We additionally perform this procedure for 242 stars that host non-transiting (radial-velocity only) planets, for which the newly derived planet properties remain modulo factors of $\sin i$.

Importantly, the stellar and planet properties that we determine are independent of stellar models and of empirically calibrated stellar relations; thus the properties that we determine for the stars and their planets do not require the assumption that individual systems behave according to theoretical expectation or within the limits of mean relations. We argue, moreover, that the stellar and planet properties that we determine are *empirical and accurate*, even if the *Gaia* parallaxes do not yet yield *precisions* that rival those typically achieved via model-dependent analyses reported in the literature. However, the Θ measurements that we determine are sufficiently accurate and precise that upcoming, improved parallax measurements from *Gaia* should enable the stellar and planet properties to be re-determined with accuracies and precisions superior to those currently available in many cases—in an entirely empirical, model-free fashion. As we enter the *TESS* era of superb precision in the transit parameters of very bright stars, such empirical and accurate stellar properties will become even more important than they have been for *Kepler* targets for which precision followup often proved challenging.

In Section 2 we describe our study sample, the data used, and our methodological approach. The primary results of this study are presented in Section 3, including F_{bol} , Θ , R_* , and M_* , followed by the planet properties, R_p and M_p . In Section 4 we present additional motivation for the importance of reducing reliance on stellar models, explore the degree to which the approach laid out in this paper is truly empirical, discuss our results in the context of previously published results, and briefly discuss the prospects for improving on the stellar and planet properties reported here with the anticipated advent of improved parallaxes from the *Gaia* second data release. Finally, Section 5 provides a summary of our results and conclusions.

2. DATA AND METHODS

2.1. Study Sample, Data from the Literature, and *Gaia* Parallaxes

We began by selecting all planet hosting stars found in the [exoplanets.org](#) database (Han et al. 2014, accessed on 31 August 2016) and added 12 well character-

ized transiting planets that were present in the NASA Exoplanet Archive¹ but missing from [exoplanets.org](#). We then selected systems with host stars that are also present in the *Tycho-2* catalog, resulting in 560 unique stars. Of these, 62 stars were removed because they lacked one or more of the minimal set of parameters required for our analysis (see Sec. 2.2); nearly all of these were *Kepler* planets for which radial-velocity semi-amplitudes were not reported. The remaining 498 stars form our master study sample, for which we perform our SED fitting procedures, resulting in fundamental F_{bol} and Θ measurements, as discussed below. The *Gaia* DR1 provides parallaxes for 358 of these stars, of which 116 were listed as hosting transiting planets and 242 were listed as hosting radial-velocity planets. We updated the XO-3 stellar radius and distance from the [exoplanets.org](#) database to the more recent values reported in Winn et al. (2008) (see §4).

For each of the transiting planet hosts, we adopted the literature values from the [exoplanets.org](#) database for each of the following quantities: the orbital period, P , and its uncertainty; the transit depth, δ_{tr} , and its uncertainty; the ratio of the orbital semi-major axis to the stellar radius, a/R_{\star} , and its uncertainty; the orbital inclination angle to the line of sight, i , and its uncertainty; and the orbital radial-velocity semi-amplitude, K_{RV} , and its uncertainty. In this paper we analyze only the ‘b’ planet in each system; however, the stellar properties that we newly determine here (e.g., F_{bol} , Θ , R_{\star} , M_{\star}) can be readily applied to other planets in the case of currently known or future discovered additional planets.

We also adopted the parallax measurements newly available from *Gaia* (Gaia Collaboration 2016). We adopt the *Gaia* parallax, π , and its uncertainty as provided by the *Gaia* first data release² (see Table 4). We note that, at the time of this writing, the *Gaia* π values potentially have systematic uncertainties that are not yet fully characterized but that could reach $\sim 300 \mu\text{as}$ ³. Preliminary assessments suggest a global offset of -0.25 mas (where the negative sign indicates that the *Gaia* parallaxes are underestimated) for $\pi \gtrsim 1 \text{ mas}$ (Stassun & Torres 2016), corroborating the *Gaia* claim, based on comparison to directly-measured distances to well-studied eclipsing binaries by Stassun & Torres (2016). Gould & Kollmeier (2016) similarly claim a systematic uncertainty of 0.12 mas. Casertano et al. (2016) used a large sample of Cepheids to show that there is likely little to no systematic error in the *Gaia*

parallaxes for $\pi \lesssim 1 \text{ mas}$, but find evidence for an offset at larger π consistent with Stassun & Torres (2016). Thus the available evidence suggests that any systematic error in the *Gaia* parallaxes is likely to be small. Thus, for the purposes of this work, we use and propagate the reported *random* uncertainties on π only, emphasizing that (a) the fundamental F_{bol} and Θ measurements that we report are independent of π , and (b) additional (or different) choices of π uncertainties may be applied to our F_{bol} and Θ measurements following the methodology, equations, and error propagation coefficients supplied below.

The assembled set of literature parameters for the 498 stars in our master sample—including the 116 transiting planet hosts and the 242 non-transiting planet hosts in our study for which *Gaia* DR1 parallaxes are available—are tabulated in Table 5 and Table 6, respectively.

2.2. Basic Methodology

For all planets in the study sample, we first collect high-quality spectroscopic values of host star T_{eff} , $\log g$, and [Fe/H] as described in §2.3 and broadband photometric data as described in §2.4. Then, for each planetary system, we fit a spectroscopic parameter-based stellar atmosphere model to a broadband photometry-based SED as described in §2.5. We directly sum the unreddened SED model over all wavelengths to obtain F_{bol} , and use the Stefan-Boltzmann law to calculate the host star radius, R_{\star} , from F_{bol} , T_{eff} , and the *Gaia* parallax, as described in §2.6.

For the transiting planets, we calculate the planet radius R_p from the transit depth, $\delta_{\text{tr}} \equiv (R_p/R_{\star})^2$, and the empirically calculated stellar radius, R_{\star} . The stellar density, ρ_{\star} , is calculated from the transit model parameter a/R_{\star} and the orbital period, P , (see §2.6) and then the stellar mass, M_{\star} , is calculated from ρ_{\star} and R_{\star} . Planet mass, M_p , is then empirically calculated from M_{\star} , the radial velocity semi-amplitude, K_{RV} , and the orbital period, P , and eccentricity, e (see §2.7). Finally, we calculate planet surface gravity, $\log g_p$, from K_{RV} , the transit parameters a/R_{\star} and δ_{tr} , and P , e , and orbital inclination, i , and we calculate the insolation at the planet, $\langle F \rangle$, from F_{bol} , the distance to the star, and the semi-major axis of the orbit, a (see §2.7).

For the non-transiting planets, we calculate M_{\star} from our empirical R_{\star} and the spectroscopic $\log g$. We also calculate the minimum planet mass, $M_p \sin i$, in the same way that we calculate M_p for the transiting planets, but with the spectroscopic $\log g$ -based stellar mass rather than the generally higher accuracy transit-based ρ_{\star} . We calculate the insolation at the planet in the same way as for the transiting planets.

¹ exoplanetarchive.ipac.caltech.edu

² Accessed on 14 September 2016.

³ See <http://www.cosmos.esa.int/web/gaia/dr1>.

We determine uncertainties for all calculated parameters by propagating the measured parameter uncertainties through the relevant equations. We also include the effects of typical parameter correlations for the transit, orbital, and RV parameters, as part of error propagation (see §2.7).

2.3. Stellar Effective Temperatures, Surface Gravities, and Metallicities

For most of the stars in our study sample, values of T_{eff} , $\log g$, and $[\text{Fe}/\text{H}]$ are available in the exoplanet archives as obtained from the original literature. We adopted these values if no other independent, spectroscopic values were available. However, where possible, we opted to instead use T_{eff} , $\log g$, and $[\text{Fe}/\text{H}]$ from the recently updated PASTEL catalog (Soubiran et al. 2016), which compiles stellar properties determined from high-quality⁴ spectroscopic analyses in the literature. We did this in order to ensure that the stellar properties used were as independent as possible from the transit-based parameters, so as to avoid hidden correlations in the derived parameters (see also Sec. 2.7).

Where multiple values were available in the PASTEL catalog, we adopted the mean and uncertainty on the mean. Where no values were available in the PASTEL catalog, we adopted the values reported in the archive. For a small number of stars with values in neither PASTEL nor in the archive, we adopted the values reported by Santos et al. (2013). Finally, for a few stars our initial SED fits clearly indicated a poor choice of T_{eff} , so we adopted an alternate T_{eff} from the literature, as indicated in Tables 5 and 6.

2.4. Broadband photometric data from the literature

In order to systematize and simplify our procedures, we opted to assemble for each host star the available broadband photometry from the following large, all-sky catalogs (listed here in approximate order by wavelength coverage) via the VizieR⁵ query service:

- GALEX All-sky Imaging Survey (AIS): FUV and NUV at $\approx 0.15 \mu\text{m}$ and $\approx 0.22 \mu\text{m}$, respectively.
- Catalog of Homogeneous Means in the *UBV* System for bright stars from Mermilliod (2006): Johnson *UBV* bands (≈ 0.35 – $0.55 \mu\text{m}$).

⁴ The parameters compiled in the PASTEL catalog derive from high-resolution ($R \geq 25000$), high signal-to-noise ($S/N \geq 50$) spectra via a variety of analysis methods (e.g., spectral synthesis, equivalent width measurements, etc.) from a large number of published papers.

⁵ <http://vizier.u-strasbg.fr/>

- Tycho-2: Tycho *B* (B_T) and Tycho *V* (V_T) bands ($\approx 0.42 \mu\text{m}$ and $\approx 0.54 \mu\text{m}$, respectively).
- Strömgren Photometric Catalog by Paunzen (2015): Strömgren *uvby* bands (≈ 0.34 – $0.55 \mu\text{m}$).
- AAVSO Photometric All-Sky Survey (APASS) DR6 (obtained from the UCAC-4 catalog): Johnson *BV* and SDSS *gri* bands (≈ 0.45 – $0.75 \mu\text{m}$).
- Two-Micron All-Sky Survey (2MASS): *JHK_S* bands (≈ 1.2 – $2.2 \mu\text{m}$).
- All-WISE: *WISE1*–*4* bands (≈ 3.5 – $22 \mu\text{m}$).

We found *BV*, *JHK_S*, and *WISE1*–*3* photometry—spanning a wavelength range ≈ 0.4 – $10 \mu\text{m}$ —for nearly all of the stars in our study sample. Most of the stars also have *WISE4* photometry, and many of the stars also have Strömgren and/or *GALEX* photometry, thus extending the wavelength coverage to ≈ 0.15 – $22 \mu\text{m}$. We adopted the reported measurement uncertainties unless they were less than 0.01 mag, in which case we assumed an uncertainty of 0.01 mag. In addition, to account for an artifact in the Kurucz atmospheres at $10 \mu\text{m}$ (see, e.g., Stassun & Torres 2016, and note that the contribution to F_{bol} for $\lambda \geq 10 \mu\text{m}$ is $\lesssim 10^{-4}$), we artificially inflated the *WISE3* uncertainty to 0.1 mag unless the reported uncertainty was already larger than 0.1 mag. Stassun & Torres (2016) found no evidence for systematic effects in any of the other passbands, although individual outlier cases do occur; see Sec. 2.5. The assembled SEDs are presented in Appendix A.

2.5. Spectral energy distribution fitting

To measure the F_{bol} of each of the 498 stars in our master sample, we followed the SED fitting procedures described in Stassun & Torres (2016). Briefly, the observed SEDs were fitted with standard stellar atmosphere models, and F_{bol} measured by summation of the model after correction for extinction. For the stars in our sample with $T_{\text{eff}} > 4000 \text{ K}$, we adopted the atmospheres of Kurucz (2013), whereas for the stars with $T_{\text{eff}} < 4000 \text{ K}$ we adopted the NextGen atmospheres of Hauschildt et al. (1999). As discussed in Stassun & Torres (2016), because the photometric data span such a large portion of the SED, and because there is only one free parameter (A_V) in the SED fit, the determination of F_{bol} via this procedure is virtually model independent, the model atmosphere serving essentially as an “intelligent interpolation” between the photometric measurements.

As summarized in Tables 5 and 6, for each star we have T_{eff} , $\log g$, and $[\text{Fe}/\text{H}]$. We interpolated in the

model grid to obtain the appropriate model atmosphere for each star in units of emergent flux. To redden the SED model, we adopted the interstellar extinction law of Cardelli et al. (1989) with the usual ratio of total-to-selective extinction, $R_V = 3.1^6$. We then fitted the atmosphere model to the flux measurements to minimize χ^2 by varying just two fit parameters: extinction (A_V) and overall normalization (effectively the ratio of the stellar radius to the distance, R_\star^2/d^2). (The uncertainty in the adopted stellar T_{eff} is handled in a later step via the propagation of errors through the stellar angular radius, Θ ; see Section 2.6.) We estimated A_V from the three-dimensional Galactic dust model of Amôres & Lépine (2005, Model A) for each star’s line of sight and distance, but we allowed the fit to vary A_V from this initial guess by as much as 20%, limited by the maximum line-of-sight extinction from the dust maps of Schlegel et al. (1998). The best-fit model SED with extinction is shown for each star in Appendix A, and the best-fit A_V and reduced χ^2 values (χ_ν^2) are given in Table 7.

Inspection of the SEDs shows generally excellent fits (see below for discussion of χ^2), with only a few exhibiting clear outlier behavior. These include HD 208527, α Ari, XO-4, 6 Lyn, HD 190360, HAT-P-15, HD 132563, and 14 And. Such outliers could occur for a number of possible reasons, including close neighbors that are unresolved in the available photometric catalogs and/or excesses arising from circumstellar material; in principle, multi-component SED fits could improve these in the future. Here we simply note these few cases, and remind the reader that these are readily flagged by the χ_ν^2 of the fit provided in Table 7. These are also excluded from our analyses below.

The primary quantity of interest for each star is F_{bol} , which we obtained via direct summation of the fitted SED, *without* extinction, over all wavelengths. The formal uncertainty in F_{bol} was determined according to the standard criterion of $\Delta\chi^2 = 2.30$ for the case of two fitted parameters (e.g., Press et al. 1992), where we first renormalized the χ^2 of the fits such that $\chi_\nu^2 = 1$ for the best fit model. Because χ_ν^2 is in almost all cases greater than 1 (see Table 7), this χ^2 renormalization is equivalent to inflating the photometric measurement errors by a constant factor and results in a more conservative final uncertainty in F_{bol} according to the $\Delta\chi^2$ criterion.

⁶ As noted in Stassun & Torres (2016), experiments with varying the value of R_V showed a negligible effect on F_{bol} , mainly because the available broadband photometry spans such a large wavelength range that the fitted atmosphere model is essentially an interpolator, and the extrapolated flux is a very small fraction of the total F_{bol} in virtually all cases.

Figure 1 (left) shows the dependence of the fractional F_{bol} uncertainty as functions of the goodness of the SED fit and of the uncertainty on T_{eff} . For stars with T_{eff} uncertainties of $\lesssim 1\%$, the F_{bol} uncertainty is dominated by the SED goodness-of-fit. With the exception of a few outliers, we achieve an uncertainty on F_{bol} of at most 6% for $\chi_\nu^2 \leq 5$. Adopting this as a goodness-of-fit threshold thus yields a sample of 114 transiting-planet host stars with *Gaia* DR1 parallaxes for which we can in principle achieve an uncertainty in R_\star of $\approx 3\%$ (see Eq. 4).

Figure 1 (right) shows the distribution of fractional F_{bol} uncertainties for the transiting-planet sample (blue) and for all stars (black). For the transiting-planet hosts with $\chi_\nu^2 \leq 5$, the median uncertainty on F_{bol} is 2% and is at most 5.7%. For the full sample, which includes the radial-velocity sample that is brighter on average than the transit sample, the median uncertainty is 1.7%, with 95% of the sample having an uncertainty of less than 5%.

2.6. Host Star Parameters and Uncertainties

Finally, we derived stellar radii R_\star by combining our F_{bol} values derived from SED fitting with our T_{eff} values derived from photometry and spectra. These quantities are related by

$$\Theta = (F_{\text{bol}}/\sigma_{\text{SB}} T_{\text{eff}}^4)^{1/2}, \quad (4)$$

where Θ is the stellar angular radius ($\Theta \equiv R_\star/d$), d is the distance to the star, and σ_{SB} is the Stefan-Boltzmann constant. Errors propagating into R_\star come from random and systematic errors on T_{eff} , and uncertainties on F_{bol} , A_V , and d . We note that the calculation of d from π can become non-trivial when $\sigma_\pi/\pi \gtrsim 20\%$ (see, e.g., Bailer-Jones 2015). The actual σ_π/π from *Gaia* DR1 for our study sample has a median of 2.3%, and is less than 20% for 98% of the sample. We therefore proceed in this paper to compute d via the straightforward $1/\pi$ conversion.

For transiting planets, we determine the stellar density, ρ_\star , from the transit model parameter a/R_\star and the orbital period, P , through the relation

$$\rho_\star = \frac{3\pi}{GP^2} (a/R_\star)^3, \quad (5)$$

for $\rho_p \sim \rho_\star$ and $k^3 \equiv (R_p/R_\star)^3 \ll 1$.

Combining ρ_\star with our determination of R_\star provides a direct measure of the stellar mass, M_\star . For the non-transiting planets, we calculate M_\star from our R_\star and the spectroscopic $\log g$.

As a check that our procedures result in accurate Θ and F_{bol} , we applied our procedures to the interferometrically observed planet-hosting stars HD 189733 and HD 209458 reported by Boyajian et al. (2015). Our SED

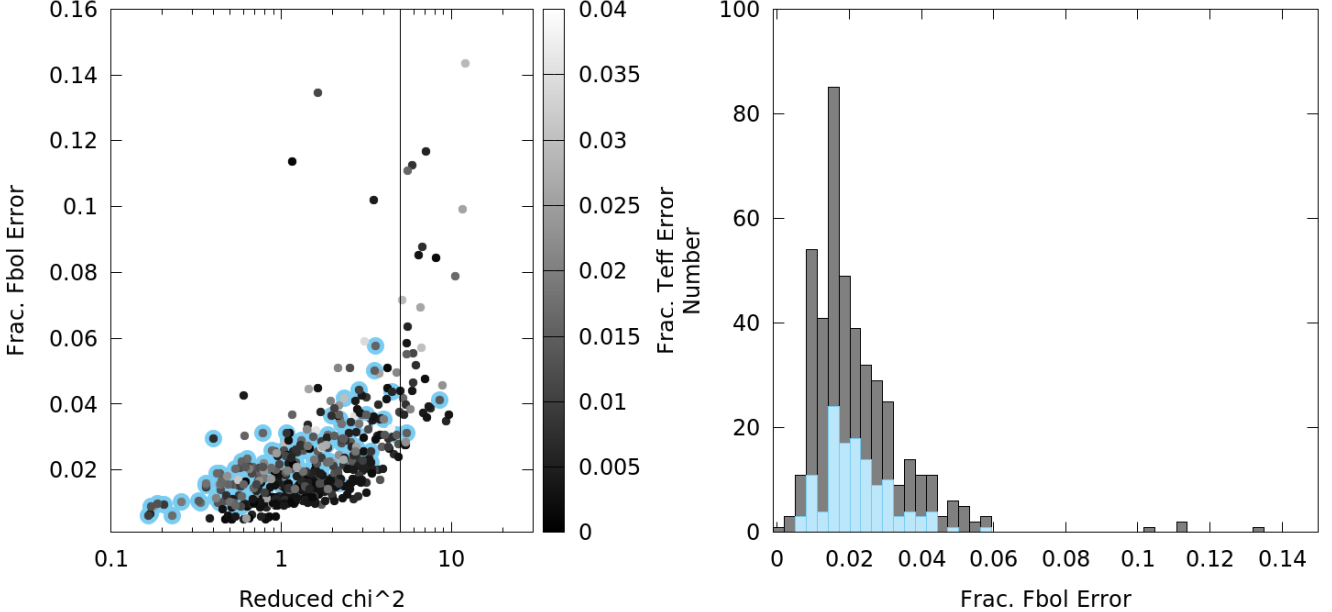


Figure 1. (Left:) Fractional uncertainty on F_{bol} from the SED fitting procedure as a function of χ_{ν}^2 and of T_{eff} uncertainty. The vertical line represents the cutoff of $\chi_{\nu}^2 \leq 5$ for which the uncertainty on F_{bol} is at most 6% for most stars, thus permitting a determination of R_{\star} to $\approx 3\%$. Points with blue haloes represent stars with transiting planets. (Right:) Distribution of fractional F_{bol} uncertainties for stars with $\chi_{\nu}^2 \leq 5$. The median uncertainty on F_{bol} for transiting-planet host stars (blue) is 2%; it is 1.7% for all stars.

Table 1. Comparison of stellar angular diameters ($2 \times \Theta$) and bolometric fluxes (F_{bol}) for stars with interferometrically measured angular diameters from Boyajian et al. (2015).

	Boyajian et al. (2015)	This work
HD 189733 ($T_{\text{eff}}=4875 \pm 43$ K)		
$2 \times \Theta$ (mas)	0.3848 ± 0.0055	0.391 ± 0.008
F_{bol} (10^{-8} erg s $^{-1}$ cm $^{-2}$)	2.785 ± 0.058	2.87 ± 0.06
HD 209458 ($T_{\text{eff}}=6092 \pm 103$ K)		
$2 \times \Theta$ (mas)	0.2254 ± 0.0072	0.225 ± 0.008
F_{bol} (10^{-8} erg s $^{-1}$ cm $^{-2}$)	2.331 ± 0.051	2.33 ± 0.05

fits are shown in Figure 2 and the Θ and F_{bol} values directly measured by those authors versus those derived in this work are compared in Table 1, where the agreement is found to be excellent and within the uncertainties.

2.7. Planet Parameters and Uncertainties

From our empirically calculated R_{\star} , we then directly obtain R_p via $R_p/R_{\star} = \sqrt{\delta_{\text{tr}}}$ for the transiting planets. From our empirically calculated M_{\star} , we can directly calculate M_p ($M_p \sin i$ for the RV planets) for all samples

in the study via

$$M_p = \frac{K_{\text{RV}} \sqrt{1 - e^2}}{\sin i} \left(\frac{P}{2\pi G} \right)^{1/3} M_{\star}^{2/3}, \quad (6)$$

in the limit $M_p \ll M_{\star}$.

For the transiting planets, we also directly calculate the planet surface gravity, $\log g_p$, from the RV, orbital, and transit parameters via

$$\log g_p = \frac{2\pi K_{\text{RV}} \sqrt{1 - e^2} (a/R_{\star})^2}{P \delta_{\text{tr}} \sin i}. \quad (7)$$

Note that this is a direct observable and does *not* depend on the properties of the host star (Winn 2010).

Finally, we directly calculate the insolation at the planet, $\langle F \rangle$, for all samples in the study from the relation

$$\langle F \rangle = F_{\text{bol}} \left(\frac{d}{a} \right)^2, \quad (8)$$

where d is the distance from Earth to the planetary system determined from the *Gaia* parallax, and a is the semi-major axis of the planetary orbit. For the transiting planets, a is determined from a/R_{\star} and our empirically determined R_{\star} . For the non-transiting planets, we use the values of a from the literature.

We determine uncertainties for all calculated parameters by propagating the measured parameter uncertainties through the relevant equations. For the purposes

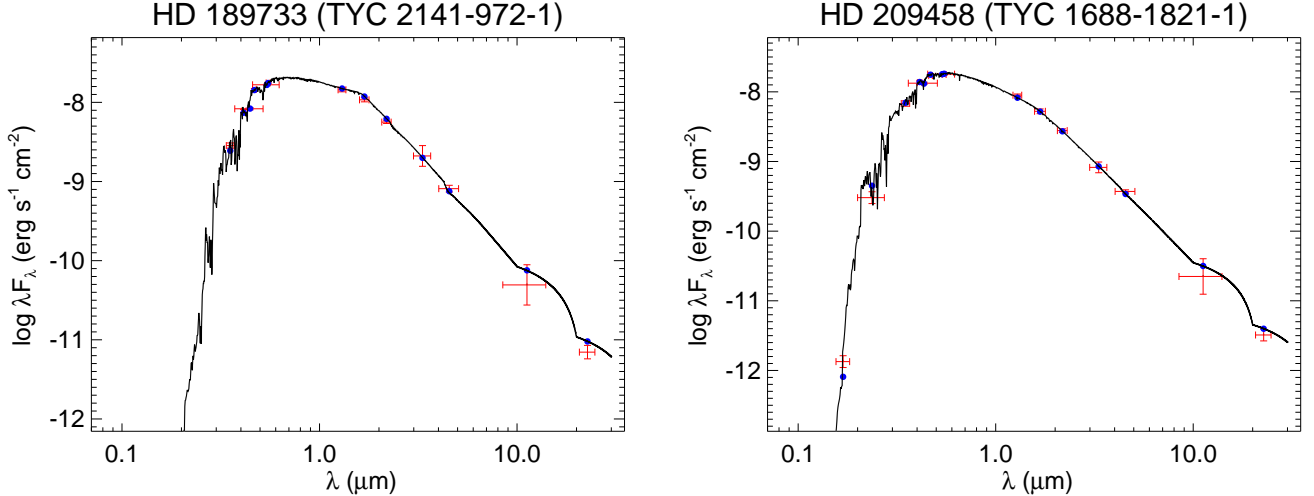


Figure 2. SED fits for the stars HD 189733 (left) and HD 209458 (right), for which interferometric angular radii have been reported (Boyajian et al. 2015) as a check on the Θ and F_{bol} values derived in this work. The two SED fits have χ^2_ν of 1.65 and 1.67, respectively. The Θ and F_{bol} comparisons are presented in Table 1. Symbols and colors are as in Figure 14.

of this paper, we assume first-order linear perturbations for the error propagation, and we also include the effects of typical parameter correlations for the transit, orbital, and RV parameters, as part of error propagation (see below). In principle our use of simple linear error propagation could underestimate the true errors for systems where the observational uncertainties are large and thus higher order terms would be needed. However, because this paper utilizes the *Gaia* DR1 parallaxes which currently are the limiting factor for most of the systems in our study sample (see Section 3.3 and Figure 4), this simplification of approach should be sufficient (see also below). The eventual arrival of the *Gaia* DR2 parallaxes may very well require more sophisticated error analysis procedures, such as through the use of full MCMC chains.

It is beyond the scope of this work to calculate parameter correlations for all planets in our study, so we use KELT-15 (Rodriguez et al. 2016) as an exemplar planetary system to estimate parameter correlations and to verify our full error propagation methodology. To be sure, the KELT-15 correlations do not exactly represent the parameter correlations for all planets in our study. Nonetheless, we expect they are reasonable representations, and since the *Gaia* DR1 parallaxes currently dominate the errors, this approximation should not compromise the accuracy of our results. To verify this expectation, we compared the results of several systems with and without the KELT-15 covariance terms included in the error propagation and found that indeed the results were identical to within ± 1 in the least significant digit of most reported parameter values. Rodriguez et al. (2016) used a custom version of EXOFAST (Eastman,

Gaudi, & Agol 2013), which allows multiple RV and transit datasets to be simultaneously fitted (see Siverd et al. 2012 for more details), to perform a KELT-15 global system fit to spectroscopic parameters, RV data, and photometric follow-up light curves. EXOFAST uses MCMC to robustly determine system parameter uncertainties. We used the resulting MCMC chains to calculate transit parameter correlations for KELT-15b. The resulting parameter correlation values are listed in Table 2, and are adopted for all planets for the purposes of error propagation.

We compare our calculated KELT-15b parameter values and uncertainties to those of Rodriguez et al. (2016) in Table 3. We find host star and planet radii and masses that are $\sim 1\sigma$ higher than the literature values. Since ρ_* and $\log g_p$ are calculated solely from the transit light curve and RV parameters (i.e., they do not involve R_*), those values are nearly identical to the literature values. Our $\langle F \rangle$ is consistent with the literature value. Our propagated stellar and planet radii uncertainties are $\sim 3\times$ the literature values. The stellar mass uncertainty is significantly higher and the planet mass uncertainty is $\sim 2\times$ higher than the literature values. To the extent that KELT-15b is representative of the systems in our study sample, this suggests that in fact our simplified linear error propagation approach discussed above results in conservative error estimates.

3. RESULTS

3.1. Stellar Bolometric Fluxes and Angular Radii

Two fundamental products of this work are the newly determined F_{bol} for each of the 498 planet host stars in

Table 2. Parameter correlation values used for error propagation as determined from the KELT-15b global system fit.

Param. 1	Param. 2	Correlation
a/R_\star	δ_{tr}	-0.152
a/R_\star	K_{RV}	-0.134
a/R_\star	P	-0.217
a/R_\star	i	0.517
a/R_\star	e	-0.645
δ_{tr}	K_{RV}	-0.015
δ_{tr}	P	0.090
δ_{tr}	i	-0.406
δ_{tr}	e	-0.007
K_{RV}	P	-0.049
K_{RV}	i	-0.051
K_{RV}	e	0.086
P	i	-0.043
P	e	0.366
i	e	-0.187

Table 3. KELT-15b empirical parameter values and uncertainties (this work) compared to Rodriguez et al. (2016).

Parameter	Units	This Work	Literature
R_\star	Stellar Radius (R_\odot)	1.783 ± 0.205	1.481 ± 0.066
M_\star	Stellar Mass (M_\odot)	2.065 ± 0.748	1.181 ± 0.051
ρ_\star	Stellar Density (cgs)	0.513 ± 0.056	0.514 ± 0.055
R_p	Planet Radius (R_J)	1.737 ± 0.203	1.443 ± 0.084
M_p	Planet Mass (M_J)	1.311 ± 0.434	0.910 ± 0.220
$\log g_p$	Planet Surface Gravity (cgs)	3.032 ± 0.106	3.020 ± 0.115
$\langle F \rangle$	Incident Flux ($10^9 \text{ erg s}^{-1} \text{ cm}^{-2}$)	1.642 ± 0.544	1.652 ± 0.145

our master sample, and from them the newly determined Θ for each of the stars. These are presented in Table 7.

Because the precision on F_{bol} is typically 2% and the precision on T_{eff} is typically 1–2% (Fig. 1), the achieved median precision on Θ is 3% for the transiting hosts and 1.8% for all stars (Fig. 3, left). In absolute units, the median precision is 0.8 μas for the transiting hosts and 1.6 μas for all stars (Fig. 3, right). The transiting planet hosts are at greater distances, on average, than the radial-velocity planet hosts, and thus have smaller absolute Θ uncertainties despite having larger relative Θ uncertainties.

Importantly, these two newly determined properties— F_{bol} and Θ —do not depend on d . Thus, these results

serve as a fundamental, accurate and purely empirical data set to permit the re-determination of stellar and planet radii and masses as measurements of d improve.

3.2. Host Star Radii and Masses

We can use the newly available parallaxes from the *Gaia* first data release to estimate R_\star and M_\star from our newly measured F_{bol} and Θ . The linear radii and masses newly determined here for the planet hosting stars in our sample are presented in Table 7. In Figure 4 we show the achieved precision on the stellar radii and masses as a function of the *Gaia* distance and the T_{eff} precision. The stellar radii and masses for the transiting-planet host stars are determined with a median precision of 8% and 30%, respectively. Importantly, as shown in the figure, for most of the transiting planet host stars, the limiting factor on the radius precision is the precision on the current *Gaia* distance.

Figure 5 presents the H-R diagram of the planet host stars, where all of the quantities represented are now measured entirely empirically. The separation of metal-poor stars below the metal-rich stars on the main sequence is readily apparent.

3.3. Planet Radii and Masses

The resulting planet radii and masses, R_p and M_p , are presented in Table 7. We also calculate directly the planet surface gravity, $\log g_p$, and the insolation received by the planet, $\langle F \rangle$. These quantities are displayed together in Figure 6 for the transiting planets. The effect of insolation on the planet radii and surface gravities is evident, in the sense that more highly insolated planets of high mass have significantly larger radii and lower surface gravities at fixed mass. This effect is not clearly evident among lower mass planets below $M_p \lesssim 0.1M_J$. This may simply be due to the small sample size, but it has been suggested that the lowest mass planets at high insolation may have had their atmospheres photo-evaporated (Owen & Wu 2013).

The precisions on R_p and M_p are shown in Figure 7. The median uncertainty on R_p (we determine R_p for transiting planets only) is 9%. The median uncertainty on M_p is 22% for the transiting planets. The median uncertainty on $M_p \sin i$ is 10% for the radial-velocity planets. Three planets with low signal-to-noise K_{RV} have fractional M_p uncertainties above 0.5 and are not shown on the plot.

4. DISCUSSION

In this section we compare our results to previous results, and we also consider how the results from the approach laid out in this study should improve when the

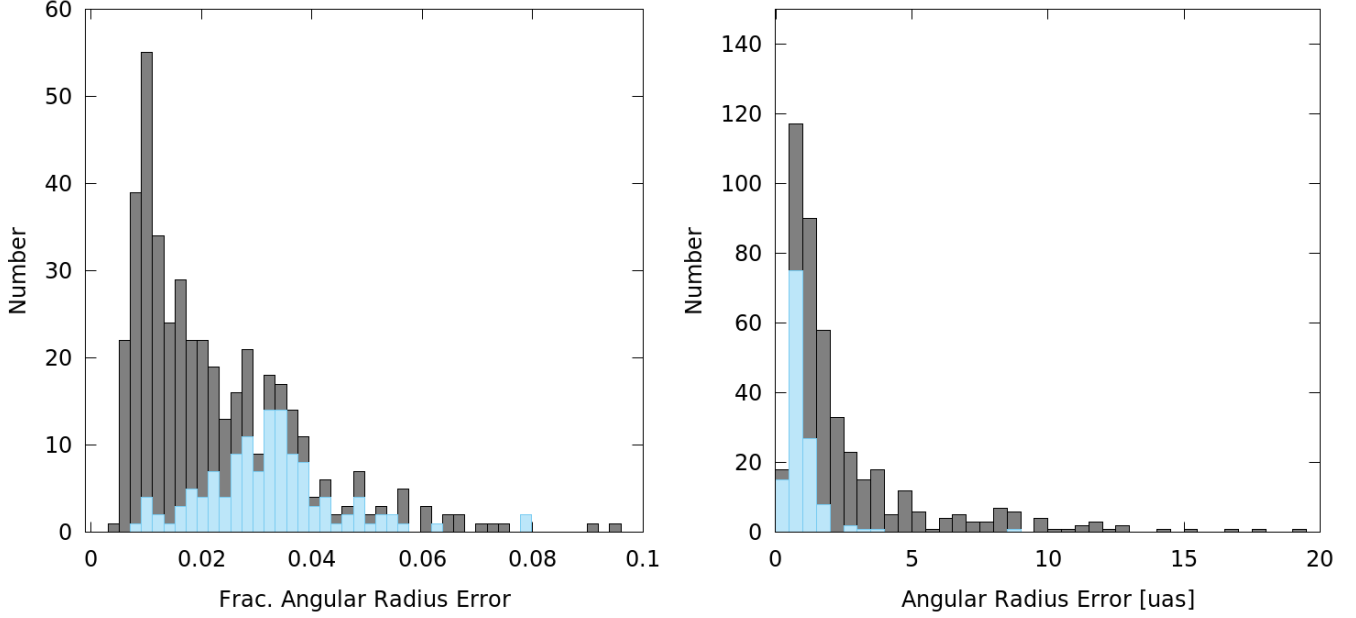


Figure 3. Fractional uncertainty (left) and absolute uncertainty (right) on Θ for transiting planet host stars (blue) and for all stars (black). One star with a fractional uncertainty larger than 0.1 is not shown at left, and 15 stars with uncertainty larger than $20 \mu\text{as}$ are not shown at right.

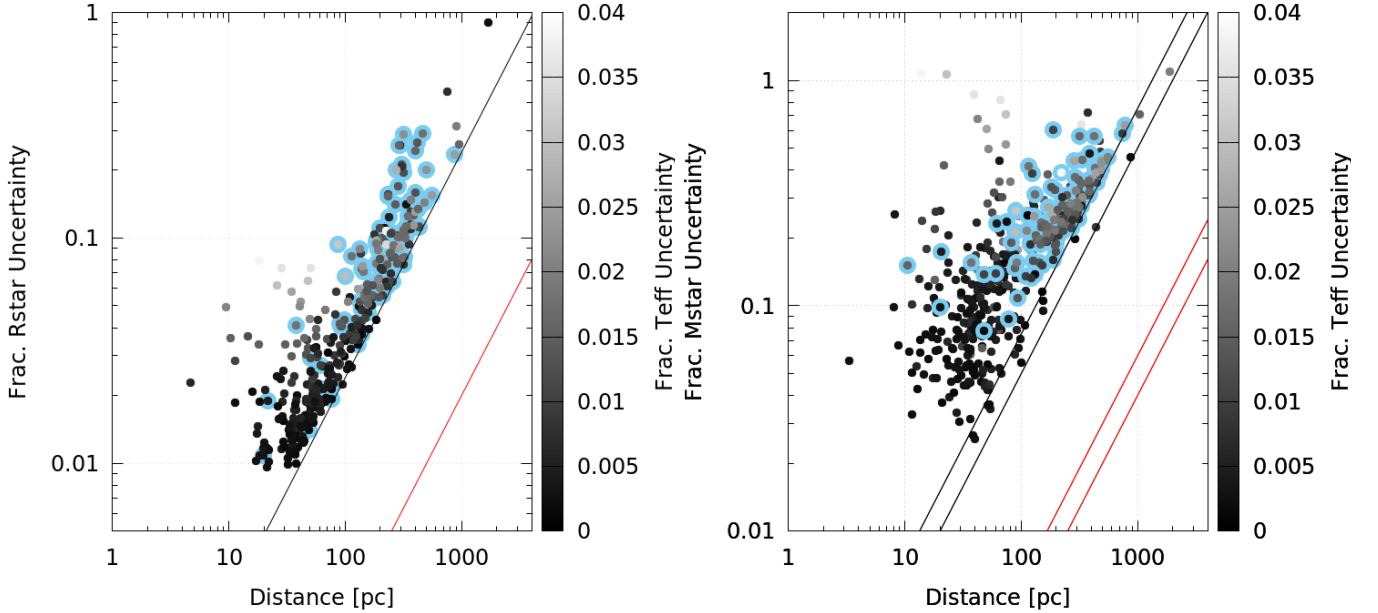


Figure 4. Fractional uncertainties in stellar radii (left) and stellar mass (right) versus distance. Points with blue halos represent transiting planet host stars. The diagonal lines represent the fractional error expected for a current nominal parallax error floor of $240 \mu\text{as}$ (black) and for an expected future parallax error of $20 \mu\text{as}$ (red). In the case of stellar mass (right), there are two diagonal lines representing the dependence of σ_{M_*}/M_* on σ_d for the transiting planets (where M_* is determined directly from ρ_* and R_* ; upper line) and radial-velocity planets (where M_* is determined from $\log g$ and R_* ; lower line).

second data release from *Gaia* becomes available. We begin, however, by expanding the discussion from Section 1 of the need to reduce reliance on, and to test, stellar models and empirical relations, as well as to ex-

plore the extent to which the approach laid out in this paper is truly empirical.

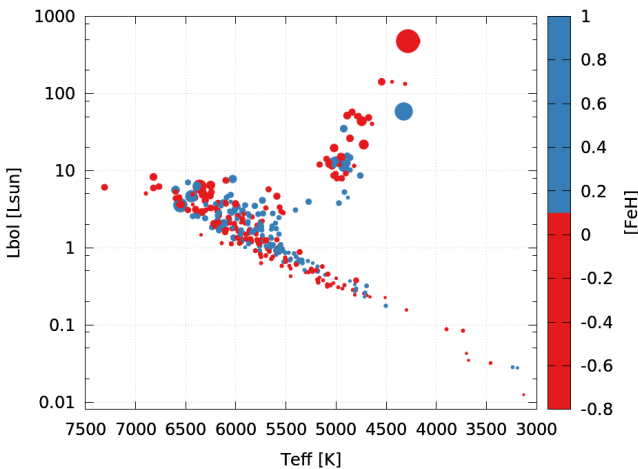


Figure 5. Hertzsprung-Russel Diagram of all planets in our study sample. Symbol size is proportional to M_* , which for transiting planets is derived from the transit-based ρ_* and for RV planets is derived from $\log g$ (see the text). Color represents $[Fe/H]$. The separation of metal-poor stars below the metal-rich stars on the main sequence is readily apparent. All quantities represented are determined empirically.

4.1. In Defense of the Empirical Approach Taken in this Study

4.1.1. The importance of reducing reliance on, and testing, stellar models and empirical relations

In Section 1, we asserted that there remain numerous areas in which theoretical stellar models, as well as empirically calibrated stellar relations, are not yet accurate and require additional testing. Here we present a number of additional examples to justify this assertion.

One particularly relevant example, which we explore in detail in §4.2.3, is the controversy over the masses of subgiants and giants dubbed “retired A stars”⁷. These are stars that were targeted by the radial velocity survey of Johnson et al. (2007) because it was thought that their main-sequence progenitors were massive ($M \gtrsim 1.5 M_\odot$), and thus could be used to explore the dependence of planet occurrence on host star mass. However, because the majority of their masses and radii were not measured directly, and because of intrinsic degeneracies and uncertainties in the models of stars in the part of the H-R diagram where they reside, there has been some controversy over their true mass (e.g., Lloyd 2013). Our empirically-measured radii and thus inferred masses (via $\log g$) speak directly to this controversy, and provide an

⁷ We thank the referee for pointing out this particularly important application of direct stellar mass and radius measurements.

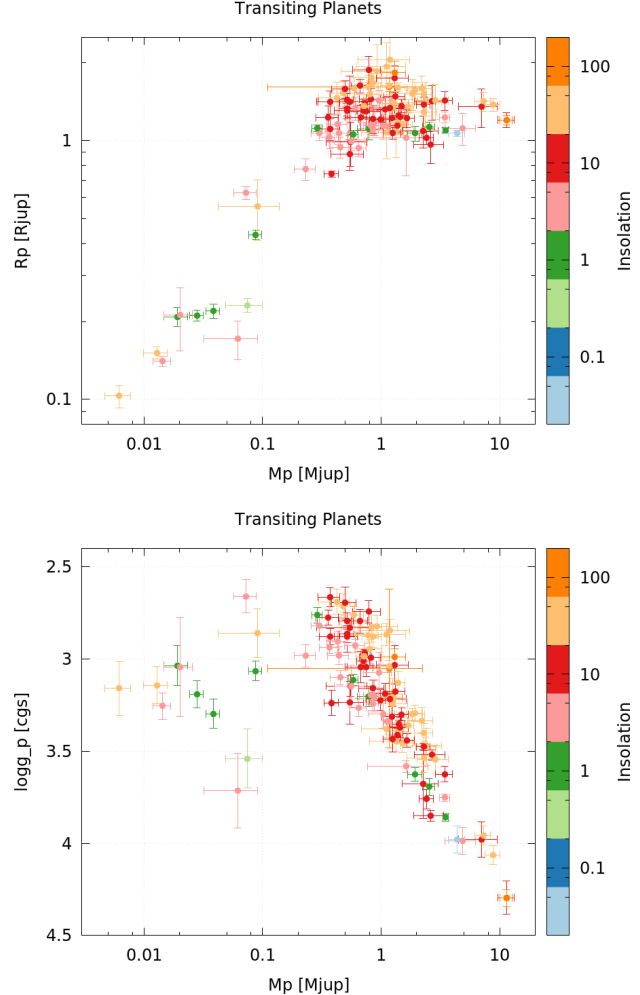


Figure 6. (Top) Radius versus mass, and (bottom) $\log g_p$ versus mass, for transiting planets in our study sample. Color represents the received insolation by the planet, in units of $10^8 \text{ erg s}^{-1} \text{ cm}^{-2}$, where warm colors represent insolation above the empirical threshold of $\sim 2 \times 10^8 \text{ erg s}^{-1} \text{ cm}^{-2}$ for planet inflation (Demory & Seager 2011).

excellent example of how such direct, empirical measurements can be important.

Another well-known discrepancy between models and empirical measurements is the “inflated radius” problem of low-mass stars. Specifically, stars of mass $\lesssim M_\odot$ with empirically-measured stellar radii are often observed to be inflated by $\sim 10\%$, and their empirically-measured stellar effective temperatures to be lower by $\sim 5\%$, relative to the predictions of standard theoretical stellar evolution models. It is thought that this inflation problem is likely due to magnetic activity, which can suppress energy transport by increasing the spot coverage of the photosphere (Stassun et al. 2012). Because mass-radius and mass- T_{eff} relationships are critical to our understanding of stellar evolution, resolving these dis-

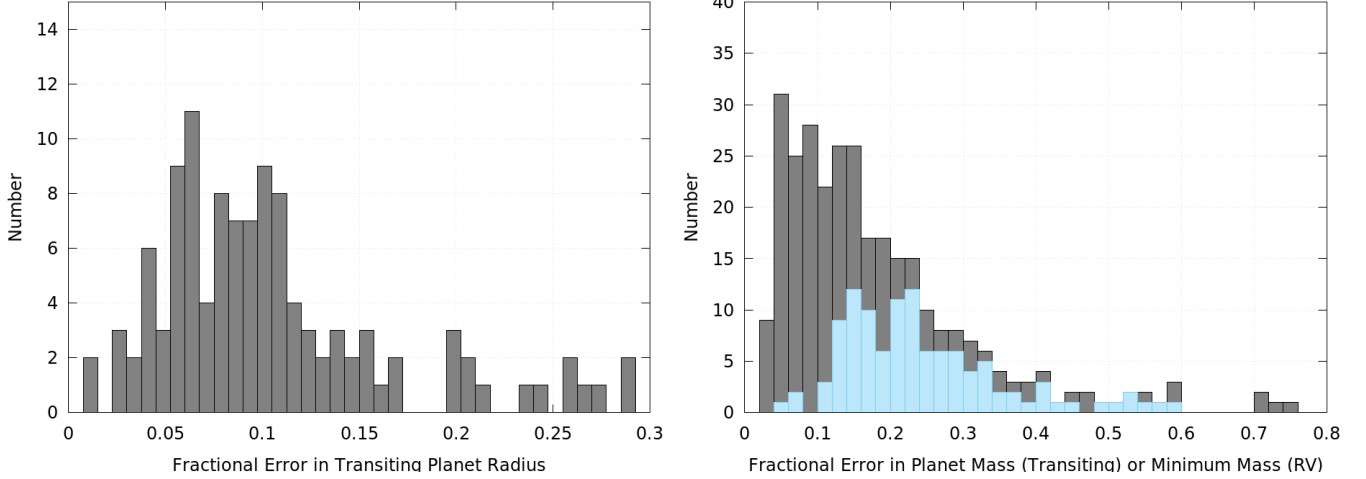


Figure 7. Distributions of fractional uncertainties on R_p (left) and M_p ($M_p \sin i$ for the RV planets) (right) determined in this work. Transiting planets are represented in blue in the right panel.

crepancies is essential for our development of accurate theoretical stellar models of low-mass stars.

We previously mentioned the case of KELT-6b (Collins et al. 2014), where applying the empirical models of Torres et al. (2010) to the observational data resulted in inferences for the parameters of the system that were inconsistent with those inferred by applying the YY isochrones (Demarque et al. 2004) by a much as $\sim 4\sigma$. As we suggested previously, this is likely due to the relatively low metallicity of the star ($[\text{Fe}/\text{H}] \sim -0.3$), but nevertheless clearly indicates that we need to calibrate both the empirical relations and isochrones over a much broader range of stellar parameters, thereby requiring more extensive empirical measurements.

As another example, Tayar et al. (submitted) demonstrate that theoretical models of red giants exhibit a metallicity-dependent offset in the predicted temperatures when compared to observations, which can result in inferred ages that are incorrect by as much as a factor of two, even for modest deviations from solar metallicity.

Another final example that is both more subtle but also much more disturbing is the case of the properties of the Sun. Standard solar models (SSMs) have existed for well over fifty years, and were used to, e.g., uncover the solar neutrino problem (e.g., Bahcall & Pinsonneault 1992), which eventually lead to the discovery that neutrinos have mass and thus that the standard model of particle physics was incomplete (e.g., Fukuda et al. 2001). While a seemingly impenetrable success of SSMs, a later revised estimate of the oxygen abundance of the Sun (Allende Prieto et al. 2001; Asplund et al. 2009), resulted in predictions for helioseismology from SSMs that were grossly inconsistent with observations (Bahcall et al. 2005). While this “Solar Oxygen Crisis” now appears to be largely resolved (e.g., Caffau et al.

2008), this example demonstrates how even our nearest star, for which we have the most information and which we use as an anchor point for essentially all of our stellar evolutionary models, can still have uncertainties and thus can still benefit from improved direct observational constraints.

Indeed, even the often-used Torres et al. (2010) empirical relations between (T_{eff} , $\log g$, and $[\text{Fe}/\text{H}]$) and M_{\star} and R_{\star} do not reproduce the mass and radius of the Sun to better than $\sim 5\%$ and $\sim 2\%$, respectively. While such “small” discrepancies may appear inconsequential given our current ability to measure the masses and radii of other stars, there is no reason that we cannot and should not demand better accuracy and precision in our knowledge of a larger sample of other stars. In this paper, we demonstrate a path forward to achieving this goal.

4.1.2. Are the stellar and planet properties truly empirical?

Few measured quantities in astronomy are truly, unequivocally empirical. Arguably, the only stellar properties that one can measure in a fully empirical manner—that is, without invoking models or even basic laws of physics—are parallax, color, brightness at a given wavelength, and in some cases an interferometric angular diameter at a given wavelength. All other measurable stellar quantities rely on basic physical laws together with the above direct observables. For example, stellar T_{eff} are determined either through fitting observed spectra to synthetic spectra, or through measurement of the equivalent widths of absorption lines and the subsequent use of models or empirical relations to convert them to T_{eff} . Similarly, the determination of the stellar F_{bol} makes use of an adopted extinction law. In fact, even the stellar parallaxes involve analysis pipelines from the *Gaia* team

that, based on the experience of the *Hipparcos* distance to the Pleiades, might be considered in doubt.

The planet properties in turn depend on the stellar properties, as well as on observables that themselves involve some basic assumptions. For example, transit light curve parameters depend on adopted stellar limb darkening coefficients, algorithms for the removal of systematics in the transit light curves and for the extraction of radial velocities from spectra, and indeed the assumption of Keplerian orbits.

For the reasons described in the previous section, we have attempted in this paper to lay out an approach that is empirical to the extent possible, making use only of *observational measures* that are either direct (e.g., apparent brightness) or that follow simply from direct observables (e.g., light curves and radial velocities) via well understood, basic physics (e.g., Kepler's laws). This then leaves only a very small number of observational quantities that depend mildly on standard assumptions (e.g., reddening) but that affect the stellar and planet properties of interest only negligibly, as we now discuss.

First, and most fundamentally for the purposes of this work, is the empirical measurement of F_{bol} , which is the most basic quantity that we measure for all 498 stars in our study sample. It could be argued that our procedure is dependent on the model atmospheres used, which of course it is to some extent. This model dependence is mitigated, however, by the very large wavelength range covered by the actual broadband flux measurements, which for most of the stars includes a very large fraction of the emergent stellar flux. This was examined in detail by [Stassun & Torres \(2016\)](#), who calculated the fraction of the stellar F_{bol} that is from beyond the span of the flux measurements, for stars of various T_{eff} . They found that for $T_{\text{eff}} \lesssim 7000$ K (which is the case for all but one star in our sample here), this flux fraction is in the range 1–4%. Indeed, this is the range of F_{bol} uncertainty that we determine for our sample here (Figure 1), which reflects this “extrapolated” flux in the SED fitting procedure. Other concerns may be that we have had to assume solar metallicity for some of the stars, if a spectroscopic [Fe/H] was not available. [Stassun & Torres \(2016\)](#) performed a check by varying the adopted [Fe/H] from -0.5 to $+0.3$ —representing the range of metallicity for the vast majority of Milky Way stars—for several stars spanning the full range of T_{eff} considered here. They found that the effect on the resulting F_{bol} is negligible for hot stars and as much as $\sim 0.5\%$ for cool stars, in all cases much smaller than our typical F_{bol} uncertainty of 2%. Arguably the most important purpose of the fitting procedure is to determine A_V , for determining what F_{bol} would be in the absence

of extinction. We have adopted a single ratio of total-to-selective extinction, $R_V = 3.1$ in our fits. R_V values in the literature span the range ≈ 2.5 –4 for most Galactic sight lines, and thus in principle fitting for R_V could further improve the SED fits. However, we have opted for simplicity not to introduce another free parameter to the SED fitting procedure. In any event, if any of the SED fits are poorer due to our choice of R_V , the resulting increased χ^2_ν will in turn result in more conservative uncertainties on F_{bol} .

Next, the determination of Θ from F_{bol} requires one additional datum, namely T_{eff} (Equation 4). Stellar T_{eff} determinations are most reliable when measured from high-resolution spectroscopic analysis, as we have done here by drawing T_{eff} from the PASTEL catalog (Sec. 2). It is true that determining the proper physical temperature of a star can be complicated by, e.g., the spectral analysis method used, temperature inhomogeneities on stellar surfaces, etc. However, T_{eff} is a *defined* quantity, namely, defined in the context of the Stefan-Boltzmann Law. Numerous calibrations of T_{eff} for stars in various color/mass/age ranges have been performed (see, e.g., [Casagrande et al. 2008, 2010; Boyajian et al. 2012, 2013; Mann et al. 2015](#)), and thus while there remain systematic uncertainties, in general these uncertainties are well characterized and they are propagated into our Θ uncertainties (see also [Casagrande et al. 2014](#), for extensive discussion of progress toward T_{eff} and Θ at percent-level accuracy).

Furthermore, while spectroscopic determinations of $\log g$ and [Fe/H] can be subject to larger uncertainties and systematics (e.g., [Torres et al. 2012](#)), our results are almost entirely independent of these quantities, at least for the transiting planet systems. Similarly, the effect of stellar limb darkening coefficients on ρ_* determined from the planet transit durations is exceptionally small, and in any case it is always possible to obtain transit duration measurements in the infrared where the effect is nearly nonexistent.

In summary, we have attempted in this work to lay out a set of procedures that utilize the *Gaia* parallaxes to determine stellar and planet properties that are as direct and empirical as possible. For the reasons discussed here, it is our assertion that the fundamental quantities we have measured for the 498 stars in our sample— F_{bol} and Θ —may be regarded as truly empirical, with effectively only one free parameter, A_V . Moreover, to the extent that trigonometric parallax is empirical, then so is R_* , which follows directly from the above. And, because they follow from the above empirical stellar properties together with observables that are virtually free of assumptions, R_p and M_p , in particular for transit planets,

are, we argue, empirically measured, at least according to the precepts and procedures laid out in this work.

4.2. Comparison to Previously Published Results

4.2.1. Previous compilations of planet host star radii

Several authors have previously published compilations of estimated stellar radii for stars with *Hipparcos* parallaxes. These include, e.g., 32 early-type stars in [Jerzykiewicz & Molenda-Zakowicz \(2000\)](#), 1000 FGK stars in [Valenti & Fischer \(2005\)](#), 125 A–M dwarfs in [Boyajian et al. \(2012, 2013\)](#), and 166 stars known (at the time) to host exoplanets in [van Belle & von Braun \(2009\)](#). In general these and other works have used spectroscopic and/or photometric measures of T_{eff} together with individual colors, bolometric corrections, and the *Hipparcos* distance to estimate R_* . The studies of [Boyajian et al. \(2013\)](#), and other papers in the series) used directly measured interferometric Θ , including the planet-hosting stars that we have used to check our procedures (see Section 2.6; [Boyajian et al. 2015](#)).

The previous study most directly comparable to our work is that of [van Belle & von Braun \(2009\)](#), which used full broad-band SED fitting to estimate A_V , spectral type templates to estimate T_{eff} , and thereby to estimate Θ and finally R_* via the *Hipparcos* distance. Our work complements and extends this study by including a considerably expanded set of planet-hosting stars now known possessing suitable measurements (498 here versus 166 in that work) and the newly available *Gaia* parallaxes. In addition, our work includes any and all direct observables of the planets in order to also determine M_* as well as revised planet radii, masses, and surface gravities—all of these involving only direct, empirical measures.

4.2.2. Planet and host-star radii and masses: This study versus previously published values

While we anticipate that the R_* , M_* , R_p , and M_p values derived from our F_{bol} and Θ determinations will be greatly improved with the *Gaia* second data release (see below), we can already assess the impact of *Gaia* parallaxes from the first data release on the inferred stellar and planet properties. We present a direct comparison of our newly determined R_* versus those reported in [exoplanets.org](#) in Fig. 8.

Our revised R_* values range from $\sim 50\%$ smaller to $\sim 100\%$ larger than the previous literature values, and these differences are clearly the result principally of the improved *Gaia* distances, the one exception being XO-3 for which the updated R_* is small despite a change in d of nearly 25%. We have traced the XO-3 anomaly to the complicated history of this system in the litera-

ture; see below. For the transiting-planet host stars, because the fractional changes in d are generally relatively small, there is good overall agreement with previously reported R_* ; the median difference is 3% with no strong systematic dependence on T_{eff} , and for 90% of the sample the change in R_* is at most 15%. On the other hand, for the radial-velocity planet-host stars, there are significant differences, and in particular among the coolest stars there is a clear tendency for large changes in R_* . We have compared our adopted T_{eff} with those previously used in the literature, and confirm that this is not the cause of these large R_* differences (the difference in T_{eff} being $0.0 \pm 0.3\%$). Comparison between the new stellar distances from *Gaia* and those previously reported in the literature suggests that the errors in the previous distances, particularly among the cooler very nearby stars, may be the culprit; here the differences in d can be as large as $\sim 100\%$, most notably for the red giants in the sample (Figure 8, right).

Similarly, we compare our newly determined M_* to those previously reported in Figure 9, where the M_* for the transiting planet host stars are determined directly from transit-based ρ_* and R_* , whereas for the radial-velocity planet hosts it is determined from the spectroscopic $\log g$ and R_* . Once again, for the transit-planet host stars, there is good overall agreement. However, again for the radial-velocity host stars, there are significant differences, and these show systematics with T_{eff} . We suspect that these differences arise from the fact that, for the transiting systems, we have a very direct measure of M_* from ρ_* and R_* , whereas for the radial-velocity planet hosts we are subject to the well known challenges with spectroscopic $\log g$ ([Torres et al. 2012](#)). Recall that we have opted to use spectroscopically determined $\log g$ that are measured independent of the planet discovery papers.

[Mortier et al. \(2014\)](#) proposed empirical corrections for spectroscopic based $\log g$ on the basis of transits and asteroseismology. We can use our transit-derived $\log g$ for the transiting planet host stars to test this (Figure 10). Indeed, we find a tendency for stars with $T_{\text{eff}} \gtrsim 6000$ K to have spectroscopic $\log g$ that are overestimated by ~ 0.1 dex, and for the cooler stars to have spectroscopic $\log g$ that are underestimated by a similar amount. This trend ($\Delta \log g = 1.6 \times 10^{-4} T_{\text{eff}} - 0.95$, spectroscopic minus transit) is somewhat less steep than that proposed by [Mortier et al. \(2014\)](#). Nonetheless, the effect is in the correct sense to at least partially explain the systematics in M_* for the radial-velocity planet hosts (Fig. 9, right).

Based on the updated stellar R_* and M_* , we can compare our newly determined R_p and M_p to those previ-

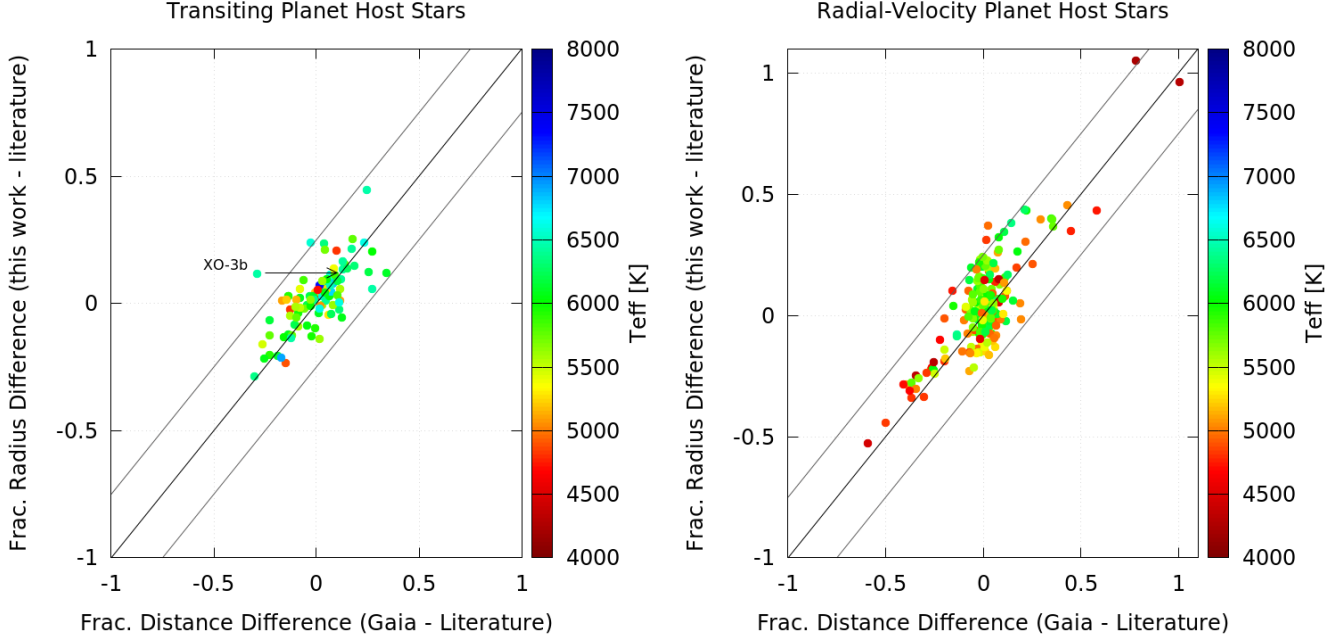


Figure 8. Fractional difference in the newly determined R_* versus those previously reported in the literature, as a function of the fractional change in the distance, for transiting planet hosts (left) and radial-velocity planet hosts (right). Color represents T_{eff} . Lines represent the one-to-one relationship of $\Delta R_* \sim \Delta d$ and the range of variation arising from the R_* errors determined in this work (see also Figure 7). The case of XO-3b is identified and discussed further in the text (see also Figure 11).

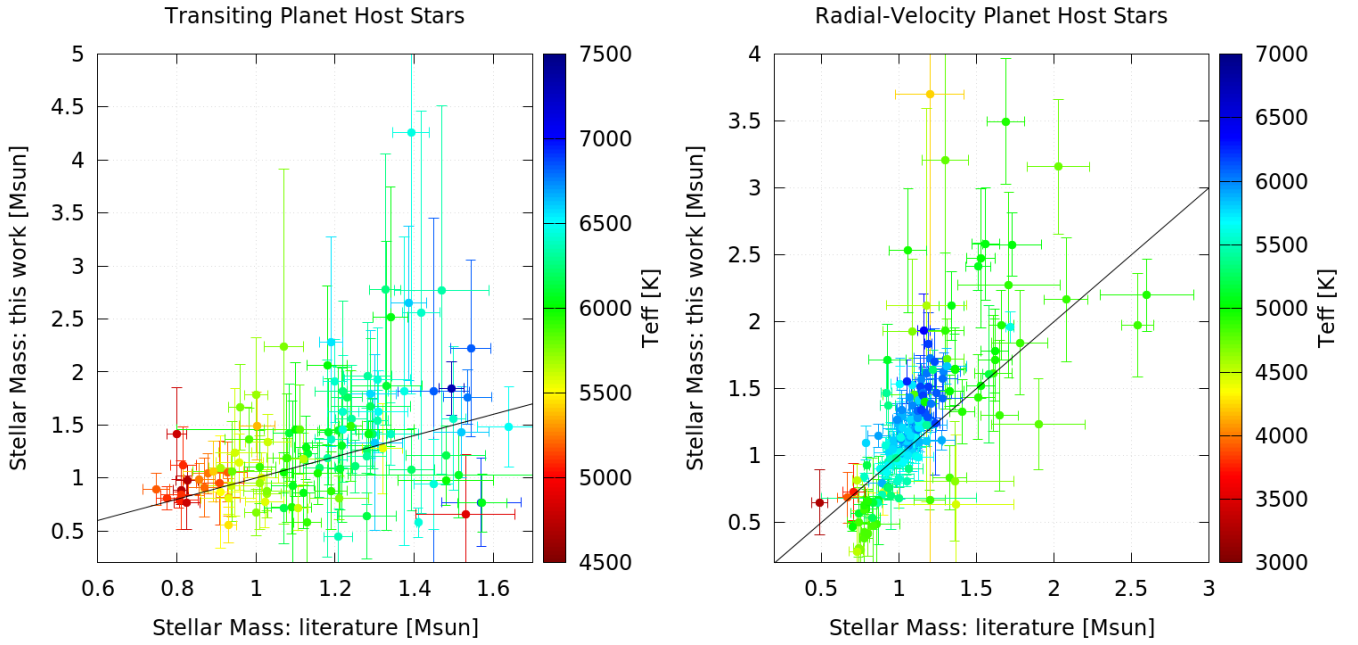


Figure 9. Comparison of newly determined M_* versus those previously reported in the literature for transiting planet hosts (left) and radial-velocity planet hosts (right).

ously published. These comparisons are shown in Figures 11 and 12, respectively. The outlier planet radius labeled in Figure 11 is Kepler-454b. Gettel et al. (2016) reported its radius as $2.37 \pm 0.13 R_{\oplus}$, but the value

in exoplanets.org is $2.37 \pm 0.13 R_J$. The tip of the light grey arrow on the plot shows the proper position of Kepler-454b for the correct value from Gettel et al. (2016). The planet with mass significantly below the

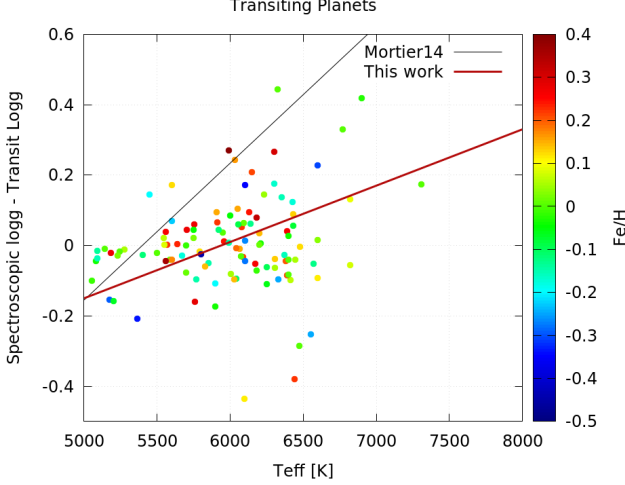


Figure 10. Comparison of spectroscopic $\log g$ versus transit-derived $\log g$ for transiting planet host stars. There is a tendency (red solid line) for the spectroscopic $\log g$ to be overestimated at high T_{eff} and underestimated at low T_{eff} , by ~ 0.1 dex. The sense of this trend is in the same sense as the systematics observed in the masses derived from spectroscopic $\log g$ for the radial-velocity planet hosts (Fig. 9, right). The correction previously suggested by Mortier et al. (2014) (solid black line) is somewhat larger than what we find here.

line in Figure 12 is XO-3 b. The distance to XO-3 b is reported as $d = 282^{+27}_{-23}$ pc in [exoplanets.org](#). In the XO-3 b discovery paper, Johns-Krull et al. (2008) reported a mass of $M_p = 13.25 \pm 0.64 M_J$ and a radius of $R_p = 1.95 \pm 0.16 R_J$ based primarily on a host star stellar radius derived from the spectroscopic $\log g$. In a follow-up paper, Winn et al. (2008) found a slightly lower mass $M_p = 11.79 \pm 0.59 M_J$ and a significantly lower radius $R_p = 1.217 \pm 0.073 R_J$ and distance $d = 174 \pm 18$ pc based the stellar density from the transit light curves⁸. We find a significantly lower empirical value of planet mass $M_p = 7.290 \pm 1.188 M_J$ and a slightly higher planet radius $R_p = 1.414 \pm 0.121 R_J$ and distance $d = 201.7 \pm 14.2$ pc compared to Winn et al. (2008).

4.2.3. Occurrence of “retired A stars”

Finally, one of the outstanding questions in the literature is that of the so-called “retired A stars.” In brief, it has been suggested that planets orbiting evolved subgiants and red giants may serve as probes of planet formation and evolution in massive stars (e.g., Johnson et al. 2007), which is particularly useful given the paucity of known planets orbiting unevolved (i.e., main sequence) stars more massive than the Sun. The utility of the subgiant and red giant planets in this context is of course predicated on the assumption that the stars are indeed the evolved (“retired”) counterparts of stars that were formerly A-type stars on the main sequence. However, this has been called into question (e.g., Lloyd 2011, 2013), considering the challenge of disambiguating stars by mass in the subgiant and red giant regions of the H-R diagram, where T_{eff} and L_{bol} become largely degenerate with M_* , particularly when uncertainties and systematic errors in the determination of $[\text{Fe}/\text{H}]$ and $\log g$ are considered. These degeneracies are compounded by uncertainties in the accuracy of stellar evolution models in these parts of the H-R diagram. As a result, the arguments and counter-arguments presented by, e.g., Lloyd (2011, 2013), Johnson & Wright (2013), and Schlaufman & Winn (2013), have largely relied on indirect lines of evidence, such as the proper application of priors, sample biases, Galactic models and stellar spins. One exception is Johnson et al. (2014), who used asteroseismology to directly measure the mass of one “retired A star” to be $\sim 2 M_\odot$.

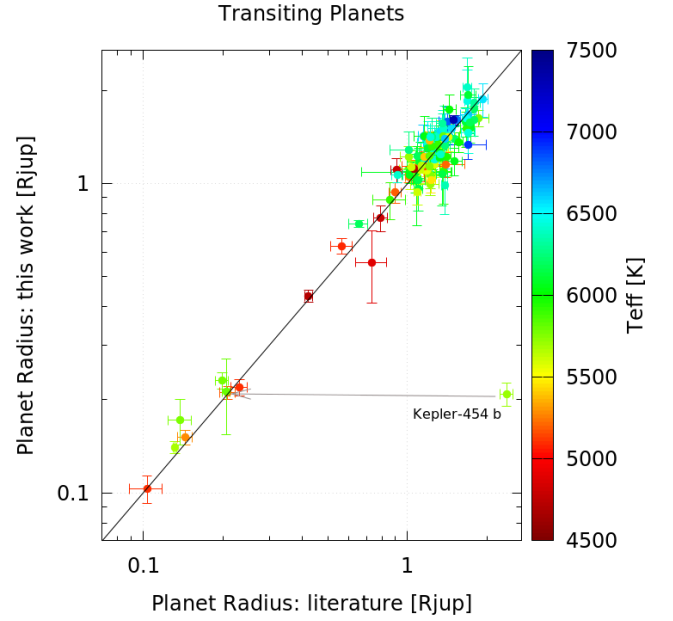


Figure 11. Comparison of newly determined R_p versus those previously reported in the literature. One notably discrepant case is labeled and discussed in the text.

With our new, empirically determined stellar properties—including in particular M_* —we are in a position to assess the occurrence of stars with $M_* \gtrsim 1.2 M_\odot$ in the subgiant and red giant branches of the H-R diagram, at

⁸ At the time of writing, the [exoplanets.org](#) database contains the updated R_p , but not the updated R_* and distance. We have updated our literature R_* and distance to the values from Winn et al. (2008).

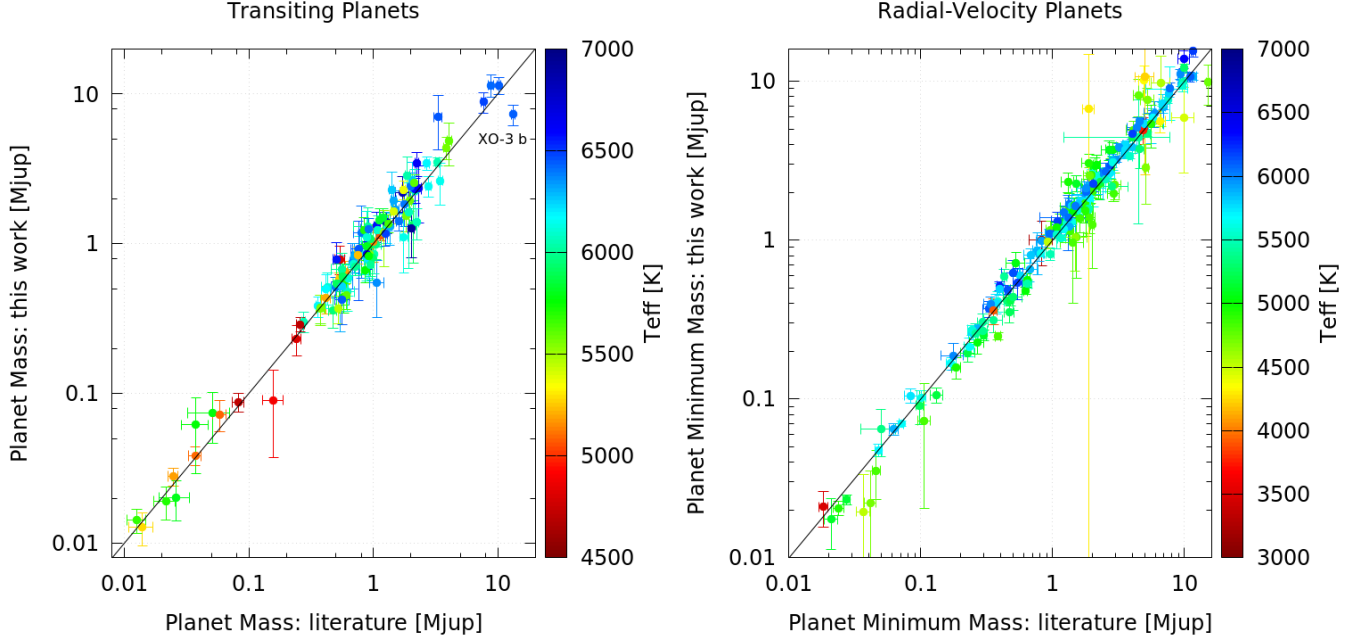


Figure 12. Comparison of newly determined M_p ($M_p \sin i$ for radial-velocity planets) versus those previously reported in the literature for transiting planets (left) and radial-velocity planets (right). One notably discrepant case is labeled and discussed in the text.

least among the systems in our study sample. Figure 13 shows the 134 stars in our study with the currently most accurately determined M_* , for which $\sigma_{M_*} < 15\%$. Thirty of these are in the region of the H-R diagram often dubbed “retired A stars.” The mean and median stellar mass of these 30 stars is $M_* = 1.58 M_\odot$ and $1.45 M_\odot$, respectively, and the inter-quartile range is $1.22\text{--}1.66 M_\odot$. Only $\sim 20\%$ of these stars have $M_* < 1.2 M_\odot$. Thus, we conclude that in our sample there is strong evidence for a preponderance of *bona fide* “retired A stars,” though there do appear to be some stars that are less massive.

4.3. Prospects with Gaia Second Data Release

The anticipated second data release from *Gaia* should enable the fundamental stellar F_{bol} and Θ reported here to achieve their full potential. In particular, whereas the accuracy that we currently achieve on R_p and M_p is limited for the transiting planets by the current *Gaia* parallax error floor of 240 μas (see Figure 4), the parallax precision for the *Gaia* second data release should be 20 μas for the bright stars in our study sample, and consequently the final R_p and M_p will in most cases be limited only by the accuracy of Θ , which in this work we already determine to be 1.8%. Thus, we may expect that the application of our Θ to the *Gaia* second data release parallaxes should yield R_p and M_p for the transiting planets in our sample to $\approx 3\%$ and $\approx 5\%$, respectively, assuming that the uncertainties in the observed

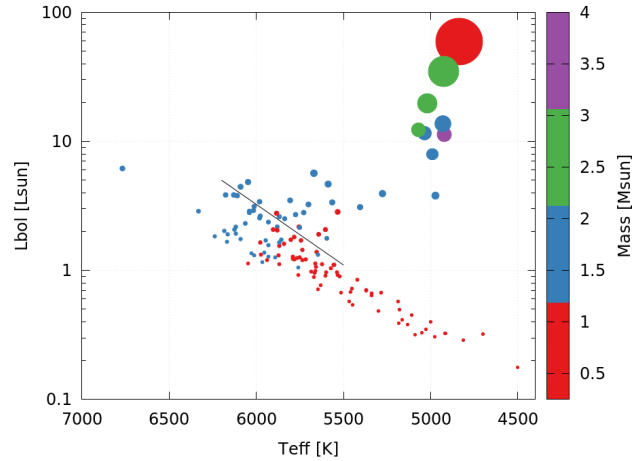


Figure 13. H-R diagram of stars in our sample with the most accurate stellar mass determinations, $\sigma_{M_*} < 15\%$. Color represents M_* , and symbol size is proportional to R_* . The black line denotes our separation of dwarfs from subgiants/giants. The majority of the evolved stars have $M_* > 1.2 M_\odot$ (blue, green, or purple colors).

δ_{tr} and ρ_* are negligible. At present, the median uncertainties on δ_{tr} and ρ_* for the transit planet host stars are $\approx 2\%$ and $\approx 14\%$; thus the accuracy in R_p should indeed be close to $\approx 3\%$, whereas for M_p it would be closer to $\approx 10\%$. Still, improvements in the ρ_* from high-precision transit observations, such as expected from the bright

TESS targets, will allow the methodology laid out here to achieve $\approx 5\%$ accuracy in M_p with the *Gaia* DR2 parallaxes.

Finally, we note that once we have many more precise and accurate empirical measurements of these stars from *Gaia* DR2, it will then be possible to refine and extend both stellar evolutionary models and empirical relations. These can then be more confidently applied to systems where direct empirical measurements are not possible, in order to derive precise and presumably more accurate parameters for vastly larger numbers of star/planet systems.

5. SUMMARY AND CONCLUSIONS

We have demonstrated that several new observational advances have enabled direct measurements of the fundamental properties for a much larger sample of bright ($V \lesssim 12$) stars than has heretofore been available. These advances include the availability of broadband photometric measurements spanning a very broad range of wavelengths, thanks to several all-sky panchromatic surveys (e.g., GALEX, APASS, 2MASS, WISE). These photometric measurements permit construction of empirical SEDs that encompass a very large fraction of the stellar SED, which in turn enable nearly direct measurements of the bolometric fluxes of all but the hottest of these bright stars, to a precision of typically $\lesssim 3\%$ (Stassun & Torres 2016). When combined with estimates of the stellar effective temperatures, ideally measured from high-resolution spectra, the angular diameter of the star (as well as the extinction) can in principle be determined in a largely empirical manner. Finally, the newly available *Gaia* parallaxes can then be used to estimate the radii of the stars, essentially directly.

With the current data available, we find that stellar radii can be determined to a precision of $\sim 8\%$. This precision is limited by the current *Gaia* parallaxes themselves. However, with the final *Gaia* data release, we can expect typical (systematics-limited) parallax uncertainties of $\sim 20\ \mu\text{as}$ for stars with $V \lesssim 12$ (Gaia Collaboration 2016). In this regime, the uncertainty in R_\star will be dominated by the uncertainties in F_{bol} and T_{eff} . Fortunately, there are excellent prospects for improving the uncertainties (and accuracy) in F_{bol} even beyond the few-percent precision already provided in this paper. *Gaia* DR3 will release low-resolution ($R \sim 10 - 20$) spectrophotometry covering wavelengths of $0.33 - 1.05\ \mu\text{m}$, and the proposed Explorer mission Spectro-Photometer for the History of the Universe, Epoch of Reionization, and Ices Explorer (SPHEREx; Doré et al. 2016), should it be selected, will provide low-resolution ($R \sim 40 - 100$) spectrophotometry from $0.75 - 5.0\ \mu\text{m}$. Together these

would directly measure $\sim 98\%$ of the bolometric flux of the majority of the $V \lesssim 12$ stars with $T_{\text{eff}} \lesssim 8500\text{K}$ (as well as the extinction as a function of wavelength to these stars from $\sim 0.3 - 5\ \mu\text{m}$). Ultimately, the precision with which R_\star can be measured for these stars will likely be limited by the uncertainty in T_{eff} , which can optimistically be reduced to $\sim 1\%$ with a combination of high-resolution spectroscopy and SED fitting. The precision with which the stellar mass, and planetary mass and radius, can then be inferred will then ultimately be limited by the precision of the follow-up photometry of the primary transit, and the radial velocity measurements of the stellar reflex motion due to the planet, which together allow one to estimate ρ_\star and the velocity semiamplitude, K_{RV} . These parameters, together with the measurement of R_\star , allow a complete solution of the system, and thus a measurement of M_\star , M_p , and R_p . In principle, with sufficient perseverance and strict control systematic errors, these can be reduced to arbitrarily low precisions. Ultimately, we can expect precisions on R_p and M_p of several percent in the best cases (Stevens et al. 2017).

We are therefore poised to enter the era of precision exoplanetology, whereby we will be able to accurately measure the host star and planetary masses and radii of bright transiting systems to a precision of, at best, a few percent, likely limited by the total amount of available follow-up resources. Most importantly, these measurements will be direct, and will not rely on stellar models (e.g., Demarque et al. 2004) or (externally-calibrated) empirical relations (e.g., Torres et al. 2010). Given that the Transiting Exoplanet Survey Satellite (TESS, Ricker et al. 2014) is expected to find ~ 1700 transiting planets, including ~ 600 with $R_p \lesssim 2R_\oplus$, this will clearly be transformative for our understanding of the physical properties of exoplanets, as well as their formation and evolution. For example, it will be possible to estimate the masses and radii of essentially all known transiting Hot Jupiters in a consistent, uniform, precise, and accurate manner, thereby potentially allowing for the identification of trends within this population that have been heretofore hidden by large uncertainties, systematics, and/or inhomogeneous analysis methodology. Perhaps even more exciting is the prospect of constraining the properties of low-mass terrestrial planets, given the availability of such precise estimates of their masses, radii, and densities. This may allow for the identification of terrestrial planets that have bulk heavy element compositions that differ significantly from that of the Earth (e.g., Rogers & Seager 2010; Unterborn & Panero 2016), and to look for trends of these parameters with the atmospheric composition of the host stars themselves.

Importantly, these precise estimates of the planetary properties will be anchored to the equally precise estimates of their host star properties. For stars more massive than the sun, and older than a few Gyr, it will be possible to estimate a robust (albeit model-dependent) age of the star via its (directly-measured) luminosity. Therefore, it will be possible to better recognize and quantify trends of planet properties with host star mass, radius, luminosity, effective temperature, and age.

Notably, these host stars will themselves provide stringent tests of stellar evolutionary models, increasing the sample of stars with precise (few percent) and directly-measured masses and radii by nearly an order of magnitude above the largest such samples current available (Torres et al. 2010). Furthermore, these stars will sample a much broader range of effective temperatures (particularly at the low T_{eff} range), and many will be effectively single, and therefore will not inherit any potential biases in their parameters arising from the formation and evolution of close binaries.

Already, we have been able to use the empirical stellar masses newly determined here to verify that the majority of putative “retired A stars” in the sample are indeed more massive than $\sim 1.2 M_{\odot}$.

Most importantly, the fundamental stellar bolometric fluxes and angular radii supplied in this work will help to enable these future improvements for the 498 planet-hosting stars studied here. And the much deeper reach

of future *Gaia* data releases should enable application of the methods laid out here to most if not all of the known planet-hosting stars in the Galaxy.

The authors are grateful to R. Oelkers for assistance with accessing and using the *Gaia* DR1 data. We also gratefully acknowledge the meticulous and helpful review by the anonymous referee. K.G.S. acknowledges partial support from NSF PAARE grant AST-1358862. Work by B.S.G. was partially supported by NSF CAREER Grant AST-1056524, and by the Jet Propulsion Laboratory and NASA’s Exoplanet Exploration Program. This work has made extensive use of the Filtergraph data visualization service (Burger et al. 2013) at filtergraph.vanderbilt.edu. This research has made use of the VizieR catalogue access tool, CDS, Strasbourg, France. The Exoplanet Archive is funded through NASA’s Exoplanet Exploration Program, administered by the Jet Propulsion Laboratory, California Institute of Technology. This work has made use of data from the European Space Agency (ESA) mission *Gaia* (<http://www.cosmos.esa.int/gaia>), processed by the *Gaia* Data Processing and Analysis Consortium (DPAC, <http://www.cosmos.esa.int/web/gaia/dpac/consortium>). Funding for the DPAC has been provided by national institutions, in particular the institutions participating in the *Gaia* Multilateral Agreement.

REFERENCES

- Allende Prieto, C., Lambert, D. L., & Asplund, M. 2001, ApJL, 556, L63
- Ammons, S. M., Robinson, S. E., Strader, J., et al. 2006, ApJ, 638, 1004
- Amôres, E. B., & Lépine, J. R. D. 2005, AJ, 130, 659
- Arras, P., & Socrates, A. 2010, ApJ, 714, 1
- Asplund, M., Grevesse, N., Sauval, A. J., & Scott, P. 2009, ARA&A, 47, 481
- Bahcall, J. N., & Pinsonneault, M. H. 1992, Reviews of Modern Physics, 64, 885
- Bahcall, J. N., Basu, S., Pinsonneault, M., & Serenelli, A. M. 2005, ApJ, 618, 1049
- Bailer-Jones, C. A. L. 2015, PASP, 127, 994
- Batygin, K., Stevenson, D. J., & Bodenheimer, P. H. 2011, ApJ, 738, 1
- Borucki, W. J., Koch, D., Basri, G., et al. 2010, Science, 327, 977
- Boss, A. P. 1997, Science, 276, 1836
- Boyajian, T., von Braun, K., Feiden, G. A., et al. 2015, MNRAS, 447, 846
- Boyajian, T. S., von Braun, K., van Belle, G., et al. 2013, ApJ, 771, 40
- Boyajian, T. S., von Braun, K., van Belle, G., et al. 2012, ApJ, 757, 112
- Burger, D., Stassun, K. G., Pepper, J., et al. 2013, Astronomy and Computing, 2, 40
- Burrows, A., Guillot, T., Hubbard, W. B., et al. 2000, ApJL, 534, L97
- Burrows, A., Hubeny, I., Budaj, J., & Hubbard, W. B. 2007, ApJ, 661, 502
- Caffau, E., Ludwig, H.-G., Steffen, M., et al. 2008, A&A, 488, 1031
- Cardelli, J. A., Clayton, G. C., & Mathis, J. S. 1989, ApJ, 345, 245
- Carter, J. A., Yee, J. C., Eastman, J., Gaudi, B. S., & Winn, J. N. 2008, ApJ, 689, 499–512
- Casagrande, L., Portinari, L., Glass, I. S., et al. 2014, MNRAS, 439, 2060
- Casagrande, L., Ramírez, I., Meléndez, J., Bessell, M., & Asplund, M. 2010, A&A, 512, A54

- Casagrande, L., Flynn, C., & Bessell, M. 2008, MNRAS, 389, 585
- Casertano, S., Riess, A. G., Bucciarelli, B., & Lattanzi, M. G. 2016, arXiv:1609.05175
- Chabrier, G., & Baraffe, I. 2007, ApJL, 661, L81
- Charbonneau, D., Brown, T. M., Latham, D. W., & Mayor, M. 2000, ApJL, 529, L45
- Collins, K. A., Eastman, J. D., Beatty, T. G., et al. 2014, AJ, 147, 39
- Demarque, P., Woo, J.-H., Kim, Y.-C., & Yi, S. K. 2004, ApJS, 155, 667
- Demory, B.-O., & Seager, S. 2011, ApJS, 197, 12
- Doré, O., Werner, M. W., Ashby, M., et al. 2016, arXiv:1606.07039
- Dressing, C. D., & Charbonneau, D. 2013, ApJ, 767, 95
- Dressing, C. D., Charbonneau, D., Dumusque, X., et al. 2015, ApJ, 800, 135
- Eastman, J., Gaudi, B. S., & Agol, E. 2013, PASP, 125, 83
- Fukuda, S., Fukuda, Y., Ishitsuka, M., et al. 2001, Physical Review Letters, 86, 5651
- Gaidos, E., Mann, A. W., Kraus, A. L., & Ireland, M. 2016, MNRAS, 457, 2877
- A. G. A. Brown, A. Vallenari, T. Prusti, J. H. J. de Bruijne, F. Mignard and et al. 2016, A&A, special Gaia volume
- Gettel, S., Charbonneau, D., Dressing, C. D., et al. 2016, ApJ, 816, 95
- Gould, A., & Kollmeier, J. A. 2016, arXiv:1609.00728
- Guillot, T., & Showman, A. P. 2002, A&A, 385, 156
- Han, E., Wang, S. X., Wright, J. T., et al. 2014, PASP, 126, 827
- Hartman, J. D., Bakos, G. Á., Bhatti, W., et al. 2016, arXiv:1609.02767
- Hauschildt, P. H., Allard, F., & Baron, E. 1999, ApJ, 512, 377
- Henry, G. W., Marcy, G. W., Butler, R. P., & Vogt, S. S. 2000, ApJL, 529, L41
- Høg, E., Fabricius, C., Makarov, V. V., et al. 2000, A&A, 355, L27
- Huber, D., Chaplin, W. J., Christensen-Dalsgaard, J., et al. 2013, ApJ, 767, 127
- Huber, D., Silva Aguirre, V., Matthews, J. M., et al. 2014, ApJS, 211, 2
- Jackson, B., Barnes, R., & Greenberg, R. 2009, ApJ, 698, 1357
- Jerzykiewicz, M., & Molenda-Zakowicz, J. 2000, AcA, 50, 369
- Johns-Krull, C. M., McCullough, P. R., Burke, C. J., et al. 2008, ApJ, 677, 657-670
- Johnson, J. A., Fischer, D. A., Marcy, G. W., et al. 2007, ApJ, 665, 785
- Johnson, J. A., & Wright, J. T. 2013, arXiv:1307.3441
- Johnson, J. A., Huber, D., Boyajian, T., et al. 2014, ApJ, 794, 15
- Kennedy, G. M., & Kenyon, S. J. 2008, ApJ, 673, 502-512
- Kurucz, R. L. 2013, Astrophysics Source Code Library, ascl:1303.024
- Lloyd, J. P. 2013, ApJL, 774, L2
- Lloyd, J. P. 2011, ApJL, 739, L49
- Mann, A. W., Feiden, G. A., Gaidos, E., Boyajian, T., & von Braun, K. 2015, ApJ, 804, 64
- Mann, A. W., Gaidos, E., Lépine, S., & Hilton, E. J. 2012, ApJ, 753, 90
- Mayor, M., & Queloz, D. 1995, Nature, 378, 355
- McDonald, I., Zijlstra, A. A., & Boyer, M. L. 2012, MNRAS, 427, 343
- Mermilliod, J. C. 2006, VizieR Online Data Catalog, 2168,
- Miller, N., & Fortney, J. J. 2011, ApJL, 736, L29
- Mortier, A., Sousa, S. G., Adibekyan, V. Z., Brandão, I. M., & Santos, N. C. 2014, A&A, 572, A95
- Owen, J. E., & Wu, Y. 2013, ApJ, 775, 105
- Paunzen, E. 2015, A&A, 580, A23
- Pinsonneault, M. H., An, D., Molenda-Żakowicz, J., et al. 2012, ApJS, 199, 30
- Pollack, J. B., Hubickyj, O., Bodenheimer, P., et al. 1996, Icarus, 124, 62
- Press, W. H., Teukolsky, S. A., Vetterling, W. T., & Flannery, B. P. 1992, Cambridge: University Press, —c1992, 2nd ed.,
- Ricker, G. R., Winn, J. N., Vanderspek, R., et al. 2014, Proc. SPIE, 9143, 914320
- Rodriguez, J. E., Colón, K. D., Stassun, K. G., et al. 2016, AJ, 151, 138
- Rogers, L. A., & Seager, S. 2010, ApJ, 712, 974
- Rogers, L. A. 2015, ApJ, 801, 41
- Santos, N. C., Sousa, S. G., Mortier, A., et al. 2013, VizieR Online Data Catalog, 355,
- Seager, S., & Mallén-Ornelas, G. 2003, ApJ, 585, 1038
- Schlaufman, K. C., & Winn, J. N. 2013, ApJ, 772, 143
- Schlegel, D. J., Finkbeiner, D. P., & Davis, M. 1998, ApJ, 500, 525
- Sato, B., Fischer, D. A., Henry, G. W., et al. 2005, ApJ, 633, 465
- Siverd, R. J., Beatty, T. G., Pepper, J., et al. 2012, ApJ, 761, 123
- Soubiran, C., Le Campion, J.-F., Brouillet, N., & Chemin, L. 2016, A&A, 591, A118
- Stassun, K. G., Kratter, K. M., Scholz, A., & Dupuy, T. J. 2012, ApJ, 756, 47
- Stassun, K. G., & Torres, G. 2016, AJ, 152, 180
- Stassun, K. G., & Torres, G. 2016, ApJL, 831, L6

- Stevens, D.J., et al. 2017, in preparation
- Sullivan, P. W., Winn, J. N., Berta-Thompson, Z. K., et al. 2015, *ApJ*, 809, 77
- Torres, G., Fischer, D. A., Sozzetti, A., et al. 2012, *ApJ*, 757, 161
- Torres, G., Andersen, J., & Giménez, A. 2010, *A&A Rv*, 18, 67
- Unterborn, C. T., & Panero, W. R. 2016, arXiv:1604.08309
- Valenti, J. A., & Fischer, D. A. 2005, *ApJS*, 159, 141
- van Belle, G. T., & von Braun, K. 2009, *ApJ*, 694, 1085
- Winn, J. N., Holman, M. J., Torres, G., et al. 2008, *ApJ*, 683, 1076-1084
- Winn, J. N. 2010, *Exoplanets*, 55
- Wright, C. O., Egan, M. P., Kraemer, K. E., & Price, S. D. 2003, *AJ*, 125, 359

Table 4. *Gaia* parallax data used in this study.

Tycho	Name	d (pc)	σ_d (pc) ^a
2-1155-1	WASP-32 b	232.42	34.72
12-104-1	HD 5319 b	119.64	3.83
30-116-1	WASP-71 b	299.15	28.71
32-383-1	HD 10442 b	129.65	4.83
88-57-1	WASP-82 b	277.72	19.74
90-645-1	HD 28678 b	191.09	8.98
96-602-1	GJ 179 b
107-1139-1	HD 33636 b	29.44	0.71
112-182-1	HD 34445 b	45.37	0.60
116-1316-1	HD 38529 b
127-402-1	HD 37605 b	46.34	0.59
154-891-1	HD 46375 b
203-1079-1	HAT-P-35 b	1380.91	1894.99
208-722-1	HAT-P-30 b	204.16	19.49
211-706-1	WASP-84 b
213-177-1	GJ 328 b
219-1438-1	HD 74156 b
255-946-1	HD 95089 b
267-1200-1	HD 99492 b	18.22	0.09
275-157-1	HD 102195 b	29.40	0.22
275-243-1	HD 102329 b	229.31	15.80
320-1027-1	HAT-P-26 b	145.45	6.24
339-329-1	WASP-24 b	337.78	36.16
356-1276-1	omega Ser b
386-86-1	HD 149143 b	74.33	1.38
426-1099-1	HD 159243 b	74.14	1.81
430-2613-1	HD 164509 b	53.86	0.70
457-495-1	HD 175541 b	136.02	5.16
458-1450-1	HD 171028 b	112.87	2.89
488-2442-1	HAT-P-41 b	402.98	97.54
504-2358-1	HD 192699 b	69.56	1.69
534-2537-1	HD 200964 b	71.67	2.65
585-774-1	HIP 116454 b	61.63	0.91
601-636-1	HD 1502 b
604-1102-1	HD 4313 b	132.29	6.50
692-497-1	HD 31253 b	58.04	1.13
736-601-1	HD 45652 b	34.75	0.38
774-1441-1	HAT-P-24 b	402.83	63.14
794-1622-1	bet Cnc b
805-24-1	HD 73534 b	85.79	2.08
813-2344-1	M 67 SAND 364 b	1693.67	1532.24
817-1748-1	HD 75784 b	83.72	4.44
843-568-1	HD 89307 b	32.18	0.26
869-1019-1	HD 106252 b	37.79	0.49
870-114-1	HD 102272 b	355.38	32.49
898-1042-1	70 Vir b	18.28	0.29
910-165-1	HD 128311 b

Table 4 continued

Table 4 (*continued*)

Tycho	Name	d (pc)	σ_d (pc) ^a
950-1156-1	WASP-38 b	137.77	5.83
983-872-1	HD 152581 b	167.89	7.72
1014-973-1	HAT-P-57 b	313.95	64.16
1031-1530-1	HD 170469 b	60.55	0.86
1055-3415-1	HD 183263 b	54.01	0.85
1058-3400-1	xi Aql b
1092-1778-1	HD 196885 b
1107-2709-1	18 Del b
1117-615-1	BD +14 4559 b	49.74	0.60
1162-750-1	HD 220773 b	49.93	0.76
1193-2072-1	HD 3651 b
1194-26-1	HD 4203 b	78.95	2.76
1195-588-1	HD 5891 b	272.48	20.73
1211-1730-1	HD 10697 b
1231-1727-1	HIP 14810 b	50.77	0.80
1242-608-1	BD+20 594 b	173.13	7.37
1250-4-1	HD 285507 b	44.70	0.56
1252-844-1	HD 24040 b	45.84	0.56
1273-1104-1	epsilon Tau b
1275-2034-1	GJ 176 b	9.41	0.05
1310-2544-1	HD 37124 b
1391-121-1	K2-34 b	305.23	63.17
1398-321-1	Pr 201 b	177.46	18.12
1408-143-1	HD 81040 b	34.31	0.29
1422-614-1	TYC 1422-614-1 b
1422-790-1	BD +20 2457 b	2519.91	2610.42
1422-1130-1	HD 88133 b	74.04	1.28
1440-2597-1	HD 100655 b	135.94	11.10
1445-2560-1	11 Com b
1447-2345-1	HD 108863 b	170.93	8.88
1454-315-1	HD 114762 b	38.64	0.68
1460-132-1	tau Boo b
1481-485-1	HD 131496 b	137.84	4.78
1482-882-1	WASP-14 b	171.05	7.77
1496-1841-1	HD 142245 b	99.83	2.61
1601-1129-1	HD 231701 b	110.04	3.55
1622-1261-1	HAT-P-34 b	282.37	47.02
1632-1396-1	HAT-P-23 b	303.83	63.65
1640-113-1	HD 195019 b	37.82	0.48
1681-1751-1	HD 210702 b
1688-1821-1	HD 209458 b	48.86	0.54
1691-1788-1	HD 208527 b
1716-1182-1	HD 219828 b	71.41	1.61
1717-2193-1	51 Peg b
1754-192-1	HD 8574 b	44.35	0.47
1755-1637-1	HD 9446 b
1758-2416-1	alpha Ari b
1761-192-1	HD 12661 b	37.94	0.32
1771-1397-1	30 Ari B b	46.68	1.30
1818-1428-1	K2-29 b

Table 4 continued

Table 4 (*continued*)

Tycho	Name	d (pc)	σ_d (pc) ^a
1853-1187-1	HD 32963 b
1891-1178-1	WASP-12 b	388.04	39.92
1894-1961-1	HD 50554 b
1901-976-1	HAT-P-56 b	319.49	23.82
1949-2012-1	55 Cnc b
1951-1006-1	HD 79498 b
1964-1473-1	mu Leo b
1973-954-1	KELT-4 A b
1981-1168-1	HD 97658 b	21.53	0.11
1984-2613-1	GJ 436 b
1986-1561-1	WASP-56 b	259.04	21.62
1989-2141-1	HD 108874 b	59.26	0.86
1994-2335-1	HD 116029 b	122.38	4.32
2031-1389-1	omicron CrB b
2037-1826-1	epsilon CrB b
2038-1873-1	HD 145457 b	140.73	4.65
2041-1657-1	XO-1 b	155.22	7.88
2063-479-1	GJ 649 b	10.38	0.04
2073-136-1	HD 156668 b
2082-1290-1	HD 158038 b	96.13	2.85
2099-908-1	HAT-P-31 b	325.05	24.29
2099-2717-1	HD 164922 b	22.04	0.14
2109-49-1	KELT-8 b	207.99	9.91
2126-1196-1	HD 177830 b	62.74	1.45
2141-972-1	HD 189733 b	19.84	0.09
2148-1948-1	HD 188015 b
2150-5013-1	HD 185269 b	52.36	1.12
2153-1463-1	HD 190228 b
2153-2883-1	HD 190360 b	16.03	0.15
2163-549-1	HAT-P-49 b	366.44	39.32
2261-371-1	HD 1605 b	89.71	2.10
2265-107-1	WASP-1 b
2285-553-1	HD 5608 b	58.36	1.11
2313-437-1	HD 13189 b	476.86	51.91
2340-1714-1	WASP-11 b	133.48	10.39
2355-246-1	HD 22781 b
2393-852-1	KELT-7 b	138.09	4.98
2420-899-1	KELT-2 A b	133.92	5.99
2461-988-1	HAT-P-33 b	417.21	110.02
2463-281-1	HAT-P-9 b
2469-686-1	HD 67087 b	76.92	1.62
2488-663-1	HD 75898 b	76.86	1.61
2496-1114-1	WASP-13 b	200.38	21.55
2497-418-1	HD 82886 b	127.97	4.19
2506-894-1	HD 87883 b	18.09	0.08
2524-2128-1	HIP 57274 b	26.12	0.17
2532-556-1	KELT-6 b	244.59	16.31
2569-1599-1	HAT-P-4 b
2576-2228-1	rho CrB b
2578-1609-1	kappa CrB b

Table 4 continued

Table 4 (*continued*)

Tycho	Name	d (pc)	σ_d (pc) ^a
2595-1464-1	HD 155358 b	44.02	0.46
2620-648-1	TrES-4 b	433.05	47.13
2634-1087-1	HAT-P-5 b	310.54	23.05
2636-195-1	WASP-3 b	245.81	19.57
2648-2151-1	HD 178911 B b	41.51	0.39
2649-1153-1	HD 173416 b
2652-1324-1	TrES-1 b	159.90	8.16
2653-91-1	HD 180314 b	121.37	4.08
2664-550-1	HD 187123 b
2717-417-1	HAT-P-17 b	92.17	2.34
2757-1152-1	HAT-P-8 b	219.26	20.23
2767-1746-1	WASP-60 b	345.66	41.35
2792-1700-1	HAT-P-16 b
2794-157-1	GJ 15 A b	3.56	0.00
2822-2210-1	upsilon And b
2831-594-1	WASP-33 b	117.53	3.34
2840-1669-1	HD 16175 b	58.35	0.90
2842-200-1	HD 13931 b	46.75	0.53
2845-2243-1	HD 16760 b
2867-1318-1	HD 23596 b	52.16	0.74
2883-1687-1	HAT-P-15 b	195.39	10.82
2927-323-1	HD 45350 b
2930-2105-1	HD 43691 b
2937-1747-1	HD 40979 b	33.95	0.34
2946-426-1	HD 49674 b	42.85	0.42
2996-683-1	KELT-3 b	210.53	14.74
3004-578-1	HD 89744 b
3009-2703-1	47 UMa b
3011-791-1	HD 95127 b	760.61	337.54
3012-667-1	HD 96127 b	534.52	237.93
3013-1229-1	HAT-P-21 b	268.30	36.91
3015-1137-1	HD 99706 b	148.54	4.90
3020-2221-1	HAT-P-36 b	288.32	23.72
3048-172-1	HD 136418 b	106.90	2.73
3050-1243-1	HD 132563 B b
3063-1587-1	HD 149026 b	76.68	1.28
3065-1195-1	HAT-P-2 b	128.84	4.14
3067-576-1	14 Her b	17.88	0.08
3086-152-1	HAT-P-14 b	252.17	19.20
3120-1368-1	Kepler-454 b	224.45	14.12
3131-1199-1	Kepler-37 b	65.40	1.17
3134-218-1	Kepler-93 b	98.70	3.30
3140-349-1	KOI-12 b	460.40	132.82
3147-188-1	Kepler-78 b	124.76	3.83
3161-126-1	HD 197037 b	33.32	0.35
3227-413-1	HD 216536 b	369.02	47.33
3231-323-1	14 And b
3239-992-1	HAT-P-6 b	278.66	27.52
3281-800-1	HAT-P-32 b	264.08	20.34
3293-1539-1	HAT-P-29 b	329.14	33.17

Table 4 continued

Table 4 (*continued*)

Tycho	Name	d (pc)	σ_d (pc) ^a
3304-101-1	HD 17092 b	225.31	12.69
3304-323-1	BD +48 738 b
3413-5-1	XO-2 b
3413-210-1	XO-2S b	149.76	5.08
3416-543-1	HAT-P-13 b
3425-1596-1	HD 81688 b
3431-46-1	HD 80606 b	65.21	1.11
3441-925-1	HAT-P-22 b	84.10	2.62
3466-819-1	HAT-P-3 b	137.77	9.02
3501-1373-1	HD 154345 b	18.26	0.07
3525-76-1	WASP-58 b	297.46	21.86
3546-413-1	Kepler-14 b
3547-1402-1	HAT-P-7 b	334.43	46.57
3549-2811-1	TrES-2 b	231.62	13.22
3551-189-1	Kepler-68 b	148.84	5.38
3561-2092-1	HAT-P-11 b	37.89	0.34
3565-1525-1	16 Cyg B b	21.22	0.10
3607-1028-1	HAT-P-40 b	432.64	46.27
3646-2286-1	HD 222155 b	51.15	0.73
3658-583-1	HD 2952 b	110.38	5.32
3727-1064-1	XO-3 b	201.70	14.23
3777-2071-1	6 Lyn b
3793-1994-1	XO-4 b	257.48	15.28
3839-846-1	HD 102956 b	122.95	3.61
3850-458-1	HD 118203 b	91.07	2.17
3861-267-1	HD 132406 b	70.35	1.50
3869-494-1	HD 139357 b
3875-1620-1	iota Dra b
3903-2143-1	HD 167042 b
3910-257-1	HD 163607 b	66.94	1.01
3925-739-1	WASP-48 b	398.21	47.75
4006-19-1	HD 240237 b	875.60	200.45
4006-980-1	HD 240210 b
4054-322-1	HD 13908 b	79.97	1.89
4126-818-1	HD 68988 b	59.96	0.87
4127-2431-1	omicron UMa b
4130-2355-1	4 UMa b
4166-541-1	HD 113337 b
4202-656-1	HD 156279 b	36.52	0.31
4215-406-1	HIP 91258 b	45.81	0.57
4222-2311-1	42 Dra b
4283-211-1	HD 220074 b	276.64	35.32
4321-1320-1	HD 17156 b	79.82	1.58
4322-1310-1	HD 11755 b	218.34	20.66
4339-2274-1	HD 24064 b	300.33	25.28
4346-320-1	HD 32518 b
4400-99-1	HD 109246 b	68.13	1.01
4414-2315-1	11 UMi b	133.86	11.85
4416-1799-1	bet UMi b
4417-267-1	8 UMi b	162.84	5.68

Table 4 continued

Table 4 (*continued*)

Tycho	Name	d (pc)	σ_d (pc) ^a
4428-1943-1	GJ 687 b	4.54	0.01
4494-1346-1	HD 7924 b	17.01	0.07
4532-2096-1	HD 33564 b
4550-2113-1	HD 104985 b
4561-2319-1	HD 120084 b
4606-3584-1	gamma Cep b
4620-542-1	HD 12648 b	185.89	7.87
4671-94-1	HD 2638 b	56.23	1.13
4683-883-1	HD 7449 b	36.85	0.56
4697-201-1	WASP-77 A b	100.97	2.45
4698-1302-1	75 Cet b
4701-1094-1	81 Cet b
4701-1095-1	HD 16141 b	37.29	0.41
4708-1423-1	HD 19994 b
4748-1630-1	HD 30562 b	26.35	0.44
4757-731-1	HD 290327 b	57.04	0.93
4762-714-1	WASP-35 b	194.26	9.11
4799-1733-1	CoRoT-7 b	158.88	6.62
4822-3681-1	HD 52265 b	29.79	0.26
4846-68-1	HD 66428 b	53.43	0.71
4862-360-1	HD 72659 b	51.83	0.69
4899-942-1	HD 86081 b	102.86	2.44
4905-1374-1	24 Sex b
4913-618-1	HD 92788 b	34.63	0.29
4923-464-1	HD 99109 b	54.95	0.86
4924-460-1	HD 96063 b
4927-1063-1	WASP-106 b	317.52	90.22
4933-678-1	HD 100777 b	49.36	0.65
4943-39-1	HD 107148 b
4958-894-1	HD 114783 b
4967-678-1	WASP-54 b	253.12	25.39
4983-226-1	HD 126614 A b	74.40	1.94
4986-302-1	HD 130322 b
5002-997-1	HD 136118 b	52.02	0.74
5133-750-1	HD 179079 b	70.71	1.32
5146-2250-1	HIP 97233 b	99.48	2.89
5161-868-1	HD 192263 b	19.68	0.09
5162-1142-1	WASP-74 b	143.22	8.43
5200-1560-1	WASP-69 b	50.30	0.93
5221-210-1	HD 206610 b	155.65	8.00
5227-1521-1	GJ 849 b	8.83	0.03
5235-1468-1	HD 217107 b	20.00	0.13
5242-229-1	HD 218566 b	28.73	0.21
5242-591-1	HD 217786 b	56.45	0.84
5258-491-1	HD 222582 b	42.32	0.54
5261-789-1	HD 1461 b
5262-825-1	HD 1690 b	673.70	189.60
5273-16-1	HD 6718 b	50.66	1.05
5278-2314-1	HD 11964 b
5290-462-1	WASP-50 b	183.57	12.17

Table 4 continued

Table 4 (*continued*)

Tycho	Name	d (pc)	σ_d (pc) ^a
5296-1533-1	epsilon Eri b
5317-733-1	HD 28185 b	39.29	0.41
5342-401-1	HD 33844 b	105.74	3.31
5342-891-1	HD 33142 b	115.98	3.99
5347-367-1	HD 38801 b	91.28	2.27
5367-701-1	HD 44219 b	52.83	0.68
5409-2156-1	NGC 2423 3 b	950.55	243.51
5435-2991-1	HD 69830 b
5469-1000-1	HD 82943 b
5480-20-1	BD -08 2823 b	41.18	0.40
5503-946-1	BD -10 3166 b	82.15	3.06
5504-418-1	HD 96167 b	85.38	2.03
5519-1520-1	HD 106270 b
5521-1086-1	HD 103774 b	56.46	1.32
5594-1093-1	GJ 581 b
5639-555-1	HD 148427 b	70.56	2.11
5681-1576-1	HD 168443 b
5685-2670-1	HD 168746 b	42.04	0.54
5782-970-1	WASP-70 A b
5803-1956-1	HD 210277 b	21.30	0.12
5811-835-1	K2-39 b	298.18	76.81
5819-1255-1	GJ 876 b	4.67	0.02
5839-876-1	WASP-26 b	238.58	29.15
5840-482-1	HIP 2247 b	34.67	0.34
5842-736-1	HD 1666 b	118.03	3.25
5853-449-1	HIP 5158 b	50.44	0.64
5858-2028-1	HD 11506 b	50.26	0.72
5870-602-1	HD 18742 b	160.66	5.77
5889-271-1	WASP-78 b	871.07	200.25
5936-2086-1	WASP-49 b	183.72	14.64
5956-2621-1	7 CMa b
5991-217-1	HD 60532 b
6045-1121-1	HD 86264 b
6083-1275-1	HD 95872 b	67.98	1.92
6087-1053-1	WASP-31 b
6100-1491-1	HD 104067 b	20.45	0.11
6107-663-1	WASP-83 b
6116-1517-1	61 Vir b
6125-113-1	WASP-55 b	284.62	26.86
6143-1696-1	HD 125612 b	57.07	0.97
6147-229-1	WASP-16 b	207.84	12.75
6191-172-1	HD 141937 b	32.66	0.37
6209-1322-1	HIP 79431 b	14.65	0.14
6242-339-1	HD 156846 b	47.37	0.90
6244-136-1	HD 155233 b
6307-1388-1	WASP-67 b	192.54	14.87
6336-204-1	WASP-68 b	244.67	25.10
6359-848-1	HD 202206 b	45.58	0.54
6373-214-1	HD 204941 b	28.75	0.21
6373-682-1	HD 204313 b	47.60	0.51

Table 4 continued

Table 4 (*continued*)

Tycho	Name	d (pc)	σ_d (pc) ^a
6385-788-1	HD 212771 b	111.69	2.88
6411-109-1	HD 224693 b
6413-439-1	WASP-20 b
6421-1078-1	HD 4732 b
6423-1832-1	HD 4208 b	34.01	0.29
6434-494-1	HIP 12961 b	23.27	0.17
6445-136-1	HD 20782 b	35.85	0.35
6446-326-1	WASP-22 b	318.63	32.74
6466-1769-1	HD 30856 b	132.10	4.23
6469-1972-1	WASP-61 b	552.13	80.56
6481-1002-1	HD 33283 b	88.35	1.74
6507-2660-1	WASP-101 b	197.88	9.12
6516-711-1	HD 47186 b	37.42	0.34
6517-2108-1	HD 43197 b	61.20	0.82
6589-761-1	HD 77338 b	45.76	0.56
6631-431-1	HD 90156 b
6636-540-1	WASP-34 b	112.75	8.46
6649-807-1	HD 98219 b	114.54	4.35
6706-861-1	WASP-25 b	193.29	17.53
6766-877-1	HD 134987 b	26.12	0.58
6779-268-1	K2-38 b	235.35	36.21
6787-1927-1	WASP-17 b	389.03	47.60
6801-585-1	HD 145377 b	52.78	0.70
6854-175-1	HD 164604 b	38.54	0.41
6866-1721-1	HD 171238 b
6869-1277-1	HD 169830 b
6875-192-1	HD 181342 b	119.98	3.75
6875-222-1	HD 180902 b	98.88	2.75
6875-3273-1	HD 179949 b
6914-1943-1	HD 192310 b
6926-454-1	HATS-3 b	316.74	61.17
6956-378-1	HD 207832 b	59.07	0.80
6972-75-1	WASP-6 b	184.57	15.69
6974-283-1	HD 216770 b	36.65	0.33
6996-583-1	WASP-45 b	225.07	16.32
7011-487-1	WASP-72 b	422.93	55.06
7014-630-1	HD 16417 b
7023-236-1	HD 20868 b	48.19	0.60
7038-834-1	WASP-79 b	243.98	19.37
7073-2172-1	HD 45364 b
7096-565-1	HD 50499 b
7136-2007-1	HD 73256 b	35.88	0.34
7144-1553-1	HD 73267 b
7190-2048-1	HD 93083 b
7193-1804-1	WASP-66 b	499.34	97.17
7220-1321-1	GJ 433 b	9.13	0.03
7247-587-1	WASP-41 b	156.56	6.14
7258-1542-1	HD 114386 b	27.94	0.19
7263-2071-1	HD 114729 b	37.69	0.37
7272-1998-1	HD 117207 b	32.42	0.26

Table 4 continued

Table 4 (*continued*)

Tycho	Name	d (pc)	σ_d (pc) ^a
7283-1162-1	WASP-15 b	290.47	74.10
7287-1874-1	HIP 67851 b
7428-2738-1	HD 181720 b	58.80	2.40
7449-1245-1	HD 190647 b	53.74	0.74
7466-1400-1	WASP-94 A b	198.61	15.16
7487-1980-1	HD 205739 b	93.19	2.73
7522-505-1	WASP-8 b	89.29	2.13
7532-852-1	HD 4113 b	41.69	0.41
7533-1111-1	HD 6434 b	42.40	0.44
7544-986-1	HD 8535 b	55.28	0.93
7567-1183-1	HD 20794 b
7612-556-1	WASP-63 b	296.20	27.55
7665-696-1	HD 70642 b	29.19	0.21
7670-3068-1	HD 73526 b	95.37	1.91
7683-1503-1	HD 75289 b	28.97	0.38
7704-39-1	HD 83443 b	40.42	0.37
7706-1752-1	HD 85512 b	11.32	0.04
7745-1381-1	HD 102365 b
7762-1479-1	HD 109749 b	62.69	1.18
7774-1925-1	HD 114613 b
7809-2461-1	HD 125595 b	28.27	0.22
7853-621-1	HD 147513 b
7863-1386-1	HD 143361 b	68.73	1.28
7881-474-1	HD 153950 b	48.04	0.81
7890-1378-1	HD 162020 b	30.75	0.22
7896-3839-1	HD 159868 b	55.36	1.06
7963-1570-1	WASP-7 b	158.13	6.26
7979-47-1	HIP 105854 b
7982-636-1	HD 208487 b
8015-1020-1	WASP-29 b	87.13	6.04
8017-108-1	WASP-4 b	275.40	53.06
8025-341-1	HD 142 b
8031-1-1	HD 5388 b	53.02	0.91
8040-72-1	WASP-18 b	126.47	4.75
8048-1022-1	GJ 86 b	11.25	0.12
8055-876-1	WASP-117 b	156.37	6.68
8056-948-1	WASP-99 b	154.77	6.92
8056-1164-1	iota Hor b	17.37	0.17
8075-1657-1	HD 28254 b
8108-493-1	HD 48265 b	89.77	1.71
8146-86-1	KELT-15 b	369.95	42.01
8189-1278-1	HD 85390 b	33.30	0.33
8224-925-1	HD 103197 b	56.38	0.77
8265-2722-1	HD 117618 b	38.17	0.35
8312-3251-1	HD 148156 b	57.15	0.99
8317-525-1	HD 330075 b	45.66	0.51
8345-4656-1	HD 156411 b
8346-37-1	GJ 674 b
8354-785-1	GJ 676 A b	15.86	0.15
8355-436-1	mu Ara b

Table 4 continued

Table 4 (*continued*)

Tycho	Name	d (pc)	σ_d (pc) ^a
8378-64-1	KELT-10 b
8411-1384-1	WASP-88 b	482.05	65.81
8431-60-1	GJ 832 b
8442-960-1	WASP-95 b	140.79	8.04
8449-868-1	HD 213240 b	41.39	0.50
8450-1093-1	tau Gru b
8468-177-1	HD 2039 b	86.92	1.73
8475-527-1	HD 10647 b
8478-1241-1	WASP-97 b	145.98	5.92
8500-534-1	HD 23079 b	33.17	0.25
8502-1934-1	GJ 163 b
8508-1724-1	HD 27894 b
8508-2041-1	epsilon Ret b
8515-1843-1	HD 30177 b	54.27	1.66
8553-2637-1	HD 63765 b	32.37	0.22
8638-692-1	HD 101930 b	29.84	0.25
8642-742-1	HD 102117 b	39.50	0.40
8668-674-1	HD 121504 b	41.25	0.43
8735-1682-1	HD 154857 b	64.29	1.62
8735-1768-1	HD 154672 b	62.04	0.96
8805-131-1	WASP-73 b	363.39	51.43
8826-247-1	HD 215497 b	40.59	0.38
8838-463-1	HD 221287 b
8847-598-1	HD 4308 b	22.03	0.12
8855-128-1	HD 7199 b	36.16	0.29
8867-913-1	HD 23127 b	93.39	2.13
8874-376-1	HD 25171 b	56.83	0.80
8884-719-1	WASP-100 b	331.84	30.88
8892-1247-1	HD 40307 b
8900-874-1	WASP-62 b	171.79	9.63
8915-2808-1	HD 65216 b	35.31	0.29
8939-306-1	HD 76700 b	60.46	0.79
8975-2606-1	NGC 4349 127 b	896.06	276.60
8983-384-1	HD 108147 b
9023-815-1	HD 142415 b	35.67	0.33
9037-233-1	HD 147018 b	40.36	0.41
9083-198-1	HD 181433 b	26.91	0.16
9100-354-1	HD 196050 b	51.35	0.68
9143-238-1	HD 11977 b
9175-83-1	HD 38283 b	37.89	0.31
9236-2866-1	HD 108341 b
9241-249-1	HD 111232 b	28.62	0.18
9270-1491-1	HD 131664 b	52.27	0.71
9296-423-1	HD 175167 b	71.73	1.29
9340-1818-1	HD 216437 b
9354-780-1	HD 1237 b
9385-1045-1	HD 63454 b	38.07	0.35
9386-2614-1	HD 39091 b
9437-1921-1	HD 137388 b	40.34	0.36
9479-407-1	HD 212301 b	53.49	0.89

Table 4 continued

Table 4 (*continued*)

Tycho	Name	d (pc)	σ_d (pc) ^a
9522-552-1	HD 142022 b	34.33	0.25

^a Random uncertainty only; does not include systematic uncertainty that is potentially as large as $\sim 300 \mu\text{as}$ (see the text).

Table 5. Sample of transiting planets used in this study.

Tycho	Name	T_{eff}	$\sigma_{T_{\text{eff}}}$	$\log g$	$\sigma_{\log g}$	[Fe/H]	Source ^a	P_{orb}	$\sigma_{P_{\text{orb}}}$	e	σ_e	K_{RV}	$\sigma_{K_{\text{RV}}}$	i	σ_i	δ_{tr}	$\sigma_{\delta_{\text{tr}}}$	a/R_{\star}	$\sigma_{a/R_{\star}}$	AU/R_{\odot}	AU/R_{\odot}
		K	K	[cgs]	[cgs]			d	d			m s ⁻¹	m s ⁻¹	deg.	deg.						
2-1155-1	WASP-32 b	6140	95	4.40	0.02	-0.13	EXO	2.71866	2.0e-06	0.00	...	478.0	11.0	85.10	0.20	1.1e-02	1.0e-04	7.72	0.25		
30-116-1	WASP-71 b	6050	100	3.90	0.05	0.15	EXO	2.90367	6.8e-06	0.00	...	236.4	3.7	84.20	1.80	4.4e-03	1.5e-04	4.30	0.27		
88-57-1	WASP-82 b	6480	90	3.96	0.03	0.12	EXO	2.70579	2.0e-06	0.00	...	130.7	1.9	87.90	1.65	6.3e-03	1.0e-04	4.43	0.15		
203-1079-1	HAT-P-35 b	6096	88	4.21	0.04	0.11	EXO	3.64671	2.1e-05	0.03	0.02	120.7	2.2	87.30	1.00	9.1e-03	5.2e-04	7.48	0.45		
208-722-1	HAT-P-30 b	6304	88	4.36	0.30	0.13	EXO	2.81060	5.0e-06	0.04	0.02	88.1	3.3	83.60	0.04	1.3e-02	4.5e-04	7.43	0.34		
211-706-1	WASP-84 b	5300	100	4.40	0.10	0.00	EXO	8.52349	7.0e-06	0.00	...	77.4	2.0	88.37	0.05	1.7e-02	1.5e-04	22.22	0.58		
320-1027-1	HAT-P-26 b	5079	88	4.56	0.06	-0.04	EXO	4.23452	1.5e-05	0.12	0.06	8.5	1.0	88.60	0.70	5.4e-03	1.3e-05	13.09	1.19		
339-329-1	WASP-24 b	6075	100	4.26	0.17	0.00	EXO	2.34121	2.0e-06	0.00	...	148.2	2.5	83.64	0.29	1.0e-02	1.2e-04	5.91	0.17		
488-2442-1	HAT-P-41 b	6390	100	4.14	0.02	0.21	EXO	2.69405	4.0e-06	0.00	...	92.5	11.6	87.70	1.00	1.1e-02	3.3e-04	5.45	0.18		
585-774-1	HIP 116454 b	5089	50	4.59	0.03	-0.16	EXO	9.12050	5.0e-04	0.20	0.07	4.4	0.5	88.43	0.40	9.7e-04	1.1e-04	23.62	0.88		
774-1441-1	HAT-P-24 b	6373	80	4.27	0.04	-0.16	EXO	3.35524	7.0e-06	0.07	0.02	83.0	3.4	88.60	0.70	9.4e-03	2.3e-04	7.61	0.41		
950-1156-1	WASP-38 b	6180	50	4.25	0.01	-0.02	EXO	6.87188	1.0e-05	0.03	0.00	252.0	4.0	89.50	0.35	6.9e-03	1.0e-04	12.11	0.27		
1014-973-1	HAT-P-57 b	6330	124	4.25	0.02	-0.25	Ammons	2.46530	3.2e-06	0.00	...	215.2	...	88.26	0.85	9.4e-03	2.9e-04	5.82	0.09		
1242-608-1	BD+20 594 b	5766	99	4.50	0.08	-0.15	EXO	41.68550	3.0e-03	0.00	...	3.1	1.1	89.55	0.16	4.9e-04	2.5e-05	55.80	3.30		
1391-121-1	K2-34 b	6132	47	4.17	0.03	0.24	EXO	2.99561	1.7e-05	0.00	...	209.0	12.0	82.06	0.51	8.2e-03	3.1e-04	6.20	0.25		
1482-882-1	WASP-14 b	6475	100	4.07	0.20	0.00	EXO	2.24375	1.0e-05	0.09	0.00	993.0	3.0	84.32	0.62	1.0e-02	2.5e-04	6.05	0.34		
1622-1261-1	HAT-P-34 b	6442	88	4.21	0.06	0.22	EXO	5.45265	1.6e-05	0.44	0.03	343.1	21.3	87.10	1.20	6.4e-03	4.2e-04	12.20	1.14		
1632-1396-1	HAT-P-23 b	5905	80	4.33	0.05	0.15	EXO	1.21288	2.0e-06	0.11	0.04	368.5	17.6	85.10	1.50	1.4e-02	2.8e-04	4.16	0.26		
1688-1821-1	HD 209458 b	6091	10	4.45	0.02	0.01	PASTEL	3.52475	3.8e-07	0.00	...	84.7	0.7	86.71	0.05	1.5e-02	2.4e-05	8.81	0.19		
1818-1428-1	K2-29 b	5358	38	4.54	0.01	0.16	EXO	3.25883	1.9e-06	0.07	0.02	103.5	5.4	86.66	0.09	2.0e-02	1.8e-04	10.51	0.15		
1891-1178-1	WASP-12 b	6300	150	4.38	0.10	0.30	EXO	1.09142	3.3e-07	0.05	0.01	226.0	4.0	82.50	0.75	1.4e-02	1.6e-04	2.98	0.15		
1901-976-1	HAT-P-56 b	6586	50	3.39	0.19	0.00	EXO	2.79083	4.7e-06	...	0.12	262.0	30.0	82.13	0.18	1.1e-02	7.4e-07	6.37	0.11		
1973-954-1	KELT-4 A b	6206	75	4.11	0.01	-0.12	EXO	2.98959	4.9e-06	0.00	...	111.8	6.3	83.16	0.22	1.2e-02	1.2e-04	5.79	0.08		
1981-1168-1	HD 97658 b	5175	25	4.49	0.04	-0.30	PASTEL	9.49090	1.6e-03	0.06	0.05	2.9	0.3	89.45	0.40	8.5e-04	7.9e-05	24.41	1.33		
1984-2613-1	GJ 436 b	3416	53	4.50	...	0.00	PASTEL	2.64385	9.0e-05	0.16	0.02	18.3	0.5	86.36	0.17	7.0e-03	1.2e-04	13.34	0.36		
1986-1561-1	WASP-56 b	5600	100	4.50	...	0.12	EXO	4.61710	3.0e-06	0.00	...	69.0	4.0	88.50	0.15	1.0e-02	4.1e-04	10.88	0.30		
2041-1657-1	XO-1 b	5750	75	4.51	0.02	0.02	EXO	3.94153	2.7e-05	0.00	...	116.0	9.0	88.81	0.50	1.8e-02	1.2e-04	11.37	0.47		
2099-908-1	HAT-P-31 b	6065	100	4.26	0.12	0.15	EXO	5.00542	9.1e-05	0.25	0.00	232.5	1.1	87.10	2.25	6.5e-03	1.5e-03	9.70	1.62		
2109-49-1	KELT-8 b	5754	54	4.08	0.05	0.27	EXO	3.24406	1.6e-04	0.04	0.05	104.0	6.4	82.65	0.90	1.3e-02	6.0e-04	5.90	0.38		
2141-972-1	HD 189733 b	5052	16	4.49	0.05	-0.02	PASTEL	2.21858	1.5e-07	0.00	...	205.0	6.0	85.71	0.00	2.4e-02	5.8e-05	8.84	0.27		
2163-549-1	HAT-P-49 b	6820	52	4.10	0.04	0.07	EXO	2.69155	6.0e-06	0.00	...	188.7	21.9	86.20	1.70	6.3e-03	3.0e-04	5.15	0.31		
2265-107-1	WASP-1 b	6110	45	4.19	0.02	0.26	EXO	2.51994	1.3e-06	0.00	...	109.4	5.6	88.65	0.53	1.1e-02	1.2e-04	5.47	0.20		
2340-1714-1	WASP-11 b	4800	100	4.45	0.20	0.00	EXO	3.72247	7.0e-06	0.00	...	82.1	7.4	89.80	0.50	1.6e-02	2.5e-04	12.71	0.64		
2393-852-1	KELT-7 b	6768	7	4.50	...	0.00	PASTEL	2.73477	3.9e-06	0.00	...	138.0	19.0	83.76	0.38	8.3e-03	1.2e-04	5.50	0.17		

Table 5 continued

Table 5 (*continued*)

Tycho	Name	T_{eff}	$\sigma_{T_{\text{eff}}}$	$\log g$	$\sigma_{\log g}$	[Fe/H]	$\sigma_{\text{[Fe/H]}}$	Source ^a	P_{orb}	$\sigma_{P_{\text{orb}}}$	e	σ_e	K_{RV}	$\sigma_{K_{\text{RV}}}$	i	σ_i	δ_{tr}	$\sigma_{\delta_{\text{tr}}}$	a/R_*	AU/R_{\odot}	σ_a/R_*	AU/R_{\odot}
		K	K	[cgs]	[cgs]			d	d				m s ⁻¹	m s ⁻¹	deg.	deg.						
2420-899-1	KELT-2 A b	6327	80	4.50	...	0.00	PASTEL	4.11379	1.0e-05	0.00	...	161.1	7.8	88.60	1.20	5.2e-03	2.5e-04	6.48	0.21			
2461-988-1	HAT-P-33 b	6446	88	4.15	0.01	0.05	EXO	3.47447	1.0e-06	0.00	0.00	82.7	10.8	87.20	0.05	1.1e-02	2.3e-04	6.57	0.18			
2463-281-1	HAT-P-9 b	6350	150	4.29	0.04	0.12	EXO	3.92289	4.0e-05	0.00	...	84.7	7.9	86.50	0.20	1.2e-02	1.1e-04	8.63	0.54			
2496-1114-1	WASP-13 b	5950	70	4.06	0.10	0.00	EXO	4.35301	2.7e-06	0.00	...	55.5	3.6	85.43	0.29	8.4e-03	1.6e-04	7.35	0.26			
2532-556-1	KELT-6 b	6102	43	4.07	0.06	-0.28	EXO	7.84570	2.0e-04	0.22	0.11	42.8	4.3	88.81	0.85	6.0e-03	1.5e-04	10.83	0.89			
2569-1599-1	HAT-P-4 b	5860	80	4.36	0.11	0.24	EXO	3.05654	5.7e-05	0.00	...	81.1	1.9	89.91	1.14	6.7e-03	7.2e-05	5.99	0.29			
2620-648-1	TrES-4 b	6200	75	4.06	0.02	0.14	EXO	3.55395	7.5e-05	0.00	...	97.4	7.2	82.81	0.33	9.8e-03	1.7e-04	6.04	0.23			
2634-1087-1	HAT-P-5 b	5960	100	4.37	0.03	0.24	EXO	2.78849	2.5e-05	0.00	...	138.0	14.0	86.75	0.44	1.2e-02	1.3e-04	7.53	0.34			
2636-195-1	WASP-3 b	6400	100	4.25	0.05	0.00	EXO	1.84683	2.0e-06	0.00	...	290.5	9.5	85.06	0.16	1.0e-02	1.8e-03	5.18	0.35			
2652-1324-1	TrES-1 b	5230	50	4.57	0.01	0.02	EXO	3.03007	8.0e-06	0.00	...	115.2	6.2	90.00	0.05	1.8e-02	9.1e-05	10.48	0.28			
2717-417-1	HAT-P-17 b	5246	80	4.53	0.02	0.00	EXO	10.33852	9.0e-06	0.35	0.01	58.4	0.9	89.20	0.15	1.5e-02	2.2e-04	22.72	0.68			
2737-1152-1	HAT-P-8 b	6200	80	4.15	0.03	0.01	EXO	3.07634	3.6e-06	0.00	...	153.1	3.9	87.80	0.76	8.3e-03	1.6e-04	6.13	0.29			
2767-1746-1	WASP-60 b	5900	100	4.20	0.10	-0.04	EXO	4.30500	6.2e-06	0.00	...	60.8	3.8	87.90	1.60	6.0e-03	6.0e-04	10.04	1.16			
2792-1700-1	HAT-P-16 b	6158	80	4.34	0.03	0.17	EXO	2.77596	3.0e-06	0.04	0.00	531.1	2.8	86.60	0.70	1.1e-02	3.0e-04	7.20	0.34			
2831-594-1	WASP-33 b	7308	71	4.50	...	0.00	PASTEL	1.21987	4.5e-07	0.00	...	0.0	295.0	87.67	1.81	1.1e-02	1.9e-04	3.81	0.11			
2883-1687-1	HAT-P-15 b	5568	90	4.38	0.03	0.22	EXO	10.86350	2.7e-05	0.19	0.02	180.6	3.5	89.10	0.20	1.0e-02	1.8e-04	19.25	0.77			
2936-683-1	KELT-3 b	6304	49	4.20	0.03	0.05	EXO	2.70339	1.0e-05	0.00	...	179.6	5.8	84.14	0.57	8.9e-03	2.0e-04	6.00	0.27			
3013-1229-1	HAT-P-21 b	5588	80	4.33	0.06	0.01	EXO	4.12448	7.0e-06	0.23	0.02	548.3	14.2	87.20	0.70	9.0e-03	4.2e-04	9.65	0.74			
3020-2221-1	HAT-P-36 b	5560	100	4.37	0.04	0.26	EXO	1.32735	3.0e-06	0.06	0.03	334.7	14.5	86.00	1.30	1.4e-02	2.8e-04	4.68	0.25			
3063-1587-1	HD 149026 b	6179	15	4.37	0.04	0.32	PASTEL	2.87589	2.5e-06	0.00	...	43.3	1.2	84.55	0.58	2.9e-03	8.7e-05	6.80	0.52			
3065-1195-1	HAT-P-2 b	6412	1	4.16	0.02	0.06	PASTEL	5.633347	6.1e-06	0.52	0.00	983.9	17.2	86.72	1.00	5.2e-03	6.1e-04	9.72	0.76			
3086-152-1	HAT-P-14 b	6600	90	4.25	0.03	0.11	EXO	4.62767	5.0e-06	0.11	0.01	219.0	3.3	83.50	0.30	6.5e-03	2.4e-04	8.90	0.36			
3120-1368-1	Kepler-454 b	5701	34	4.37	0.06	0.27	EXO	10.57000	7.5e-08	0.00	...	2.0	0.4	87.09	0.20	4.2e-04	4.5e-05	18.29	1.10			
3131-1199-1	Kepler-37 b	5417	75	4.57	0.01	-0.32	EXO	13.36731	7.1e-05	0.00	...	0.9	1.1	88.63	0.41	1.2e-05	2.3e-06	28.68	1.26			
3134-218-1	Kepler-93 b	5669	75	4.47	0.03	-0.18	PASTEL	4.72674	9.7e-07	0.00	...	1.6	0.3	89.18	0.04	2.2e-04	1.8e-06	12.50	0.01			
3140-349-1	KOI-12 b	6820	120	4.34	0.15	0.09	EXO	17.85523	9.0e-07	0.72	...	800.0	...	88.95	0.20	8.2e-03	1.5e-05	20.00	1.50			
3147-188-1	Kepler-78 b	5089	50	4.60	0.10	-0.14	EXO	0.35501	6.0e-08	2.0	0.3	79.00	12.50	2.0e-04	3.8e-05	2.66	0.33			
3239-392-1	HAT-P-6 b	6570	80	4.22	0.03	-0.13	EXO	3.85298	5.0e-06	0.00	...	115.5	4.2	85.51	0.35	8.7e-03	9.9e-05	7.73	0.34			
3281-800-1	HAT-P-32 b	6207	88	4.33	0.01	-0.04	EXO	2.15001	1.0e-06	0.00	0.00	122.8	23.2	88.90	0.40	2.3e-02	1.2e-04	6.06	0.13			
3293-1539-1	HAT-P-29 b	6087	88	4.34	0.06	0.21	EXO	5.72319	4.9e-05	0.09	0.05	78.3	5.9	87.10	0.60	8.6e-03	5.2e-04	11.74	1.02			
3413-5-1	XO-2 b	5340	80	4.45	0.02	0.45	EXO	2.61586	5.0e-06	0.00	...	85.0	8.0	88.90	0.68	1.1e-02	1.8e-04	8.18	0.26			
3416-543-1	HAT-P-13 b	5653	90	4.13	0.04	0.41	EXO	2.91625	1.0e-05	0.01	0.00	106.0	0.7	83.40	0.60	7.1e-03	2.2e-04	5.90	0.33			
3431-46-1	HD 80606 b	5561	24	4.42	0.02	0.35	PASTEL	111.43670	4.0e-04	0.93	0.00	472.0	5.0	89.29	0.02	1.1e-02	3.8e-04	98.38	7.32			
3441-925-1	HAT-P-22 b	5302	80	4.36	0.04	0.24	EXO	3.21222	9.0e-06	0.02	0.01	313.3	4.2	86.90	0.55	1.1e-02	3.6e-03	8.58	0.39			
3466-819-1	HAT-P-3 b	5185	80	4.56	0.03	0.27	EXO	2.89970	5.4e-05	0.00	...	89.1	2.0	87.24	0.69	1.2e-02	5.2e-04	10.05	0.50			
3525-76-1	WASP-58 b	5800	150	4.27	0.09	-0.45	EXO	5.01718	1.1e-05	0.00	...	110.1	4.1	87.40	1.50	1.4e-02	1.0e-03	10.35	1.21			

Table 5 *continued*

Table 5 (continued)

Tycho	Name	T_{eff}	$\sigma_{T_{\text{eff}}}$	$\log g$	$\sigma_{\log g}$	[Fe/H]	$\sigma_{\text{[Fe/H]}}$	Source ^a	P_{orb}	$\sigma_{P_{\text{orb}}}$	e	σ_e	K_{RV}	$\sigma_{K_{\text{RV}}}$	i	σ_i	δ_{tr}	$\sigma_{\delta_{\text{tr}}}$	a/R_{\star}	AU/R_{\odot}	σ_a/R_{\star}	AU/R_{\odot}
		K	K	[g/s]	[g/s]			d	d	d			m s ⁻¹	m s ⁻¹	deg.	deg.						
3546-413-1	Kepler-14 b	6395	60	3.99	0.03	0.12		EXO	6.79012	4.3e-06	0.04	0.02	682.9	7.1	90.00	1.40	3.2e-03	1.5e-04	8.49	0.43		
3547-1402-1	HAT-P-7 b	6389	17	4.07	0.06	0.26		EXO	2.20474	1.7e-05	0.00	0.02	211.8	2.6	83.11	0.03	6.0e-03	4.7e-06	4.13	0.15		
3549-2811-1	TyES-2 b	5850	50	4.43	0.02	-0.15		EXO	2.47073	1.0e-05	0.00		181.3	2.6	83.57	0.14	1.6e-02	2.3e-04	7.64	0.30		
3551-189-1	Kepler-68 b	5793	74	4.28	0.06	0.12		EXO	5.39876	4.0e-06	0.00		2.1	0.6	87.60	0.90	2.9e-04	1.6e-04	10.71	0.24		
3561-2092-1	HAT-P-11 b	4708	84	4.37	0.22	0.29		PASTEL	4.88782	7.1e-06	0.20	0.05	11.6	1.2	88.50	0.60	3.3e-03	1.0e-04	15.10	0.47		
3607-1028-1	HAT-P-40 b	6080	100	3.93	0.02	0.22		EXO	4.45724	1.0e-05	0.00		58.1	2.9	88.30	0.90	6.5e-03	2.3e-04	5.94	0.40		
3727-1064-1	XO-3 b	6429	50	3.95	0.06	-0.18		EXO	3.19154	1.4e-04	0.29	0.00	1488.0	10.0	79.32	1.36	8.9e-03	7.8e-04	4.95	0.18		
3733-1994-1	XO-4 b	6397	70	4.18	0.03	-0.04		PASTEL	4.12508	4.0e-06	0.00		168.6	6.2	88.80	0.60	7.8e-03	1.2e-04	7.68	0.11		
3925-739-1	WASP-48 b	5920	150	4.03	0.03	-0.12		EXO	2.14363	3.0e-06	0.00		136.0	11.3	80.09	0.62	9.6e-03	2.0e-04	4.25	0.18		
4321-1320-1	HD 17156 b	6040	24	4.20	0.06	0.19		PASTEL	21.21663	4.5e-04	0.68	0.00	279.8	0.1	87.82	0.17	5.3e-03	8.7e-05	23.34	0.43		
4697-201-1	WASP-77 A b	5365	160	4.33	0.08	-0.34		Ammons	1.36003	2.0e-06	0.00		321.9	3.9	89.40	0.55	1.7e-02	1.7e-04	5.43	0.12		
4762-714-1	WASP-35 b	5990	80	4.40	0.01	-0.15		EXO	3.16158	2.0e-06	0.00		94.8	7.1	87.96	0.28	1.5e-02	1.0e-04	8.53	0.21		
4799-1733-1	CoRoT-7 b	5275	75	4.50	0.10	0.05		EXO	0.85359	6.0e-09	0.00		3.1	0.7	80.10	0.30	3.5e-04	1.1e-05	4.26	0.21		
4927-1063-1	WASP-106 b	6055	136	4.23	0.02	-0.09		EXO	9.28971	1.0e-05	0.00		165.3	4.3	89.49	0.50	6.4e-03	1.8e-04	13.79	0.44		
4967-678-1	WASP-54 b	6100	100	4.00	0.03	-0.27		EXO	3.69364	5.8e-06	0.07	0.03	73.0	2.0	84.97	0.61	8.6e-03	2.0e-04	5.88	0.29		
5162-1142-1	WASP-74 b	5990	110	4.39	0.07	0.39		EXO	2.13775	1.0e-06	0.00		114.1	1.4	79.81	0.24	9.6e-03	1.4e-04	4.86	0.20		
5200-1560-1	WASP-69 b	4700	50	4.50	0.15	0.15		EXO	3.86814	1.7e-06	0.00		38.1	2.4	86.71	0.20	1.8e-02	4.2e-04	12.00	0.46		
5290-462-1	WASP-50 b	5400	100	4.54	0.02	-0.12		EXO	1.95510	5.1e-06	0.01	0.01	256.6	4.4	84.00	18.00	2.0e-02	3.5e-04	7.53	0.35		
5782-970-1	WASP-70 A b	5700	80	4.26	0.09	-0.01		EXO	3.71302	4.7e-06	0.00		72.3	2.0	87.12	0.94	9.7e-03	2.4e-04	8.61	0.56		
5811-835-1	K2-39 b	4881	20	3.44	0.07	0.32		EXO	4.60543	4.6e-04	0.00		14.4	2.6	80.39	4.19	3.7e-04	3.4e-05	3.41	0.42		
5839-876-1	WASP-26 b	6034	31	4.44	0.06	0.16		PASTEL	2.75660	1.0e-05	0.00		135.5	0.0	82.50	0.50	1.0e-02	4.0e-04	6.43	0.31		
5889-271-1	WASP-78 b	6100	150	4.10	0.20	-0.35		EXO	2.17518	4.8e-06	0.00		113.8	9.1	83.20	1.95	6.5e-03	1.0e-04	3.54	0.21		
5936-2086-1	WASP-49 b	5690	150	4.50	0.10	-0.23		EXO	2.78174	5.6e-06	0.00		56.8	2.4	84.89	0.19	1.4e-02	3.8e-04	8.37	0.37		
6087-1053-1	WASP-31 b	6362	102	4.31	0.02	-0.20		EXO	3.40591	5.0e-06	0.00		58.2	3.5	84.54	0.27	1.6e-02	3.2e-04	8.03	0.25		
6107-663-1	WASP-83 b	5480	110	4.34	0.08	0.29		EXO	4.97125	1.5e-05	0.00		32.9	3.1	88.90	0.70	1.0e-02	4.0e-04	12.12	0.66		
6125-113-1	WASP-55 b	5900	100	4.30	0.10	-0.20		EXO	4.46563	4.0e-06	0.00		70.0	4.0	89.60	0.20	1.6e-02	3.0e-04	10.83	0.31		
6147-229-1	WASP-16 b	5700	150	4.49	0.04	0.01		EXO	3.11860	1.4e-05	0.00		116.7	2.2	85.22	0.35	1.2e-02	4.5e-04	9.52	0.57		
6307-1388-1	WASP-67 b	5200	100	4.35	0.15	-0.07		EXO	4.61442	1.0e-05	0.00		56.0	4.0	85.80	0.35	1.8e-02	9.0e-04	12.83	0.63		
6336-204-1	WASP-68 b	5910	60	4.17	0.11	0.22		EXO	5.08430	1.5e-05	0.00		97.9	1.9	88.10	1.30	5.7e-03	3.4e-04	7.93	0.42		
6413-439-1	WASP-20 b	5950	100	4.23	0.02	-0.01		EXO	4.89963	3.4e-06	0.00		32.8	1.7	85.57	0.22	1.2e-02	2.2e-04	9.29	0.33		
6446-326-1	WASP-22 b	6000	100	4.50	0.20	-0.05		EXO	3.53269	1.0e-05	0.02	0.01	70.0	1.7	89.20	0.50	1.0e-02	4.0e-04	8.94	0.85		
6469-1972-1	WASP-61 b	6250	150	4.26	0.01	-0.10		EXO	3.85590	3.0e-06	0.00		233.0	0.0	89.35	0.56	8.8e-03	1.0e-04	8.15	0.24		
6507-2660-1	WASP-101 b	6380	120	4.31	0.08	0.20		EXO	3.558572	4.0e-06	0.00		54.0	4.0	85.00	0.20	1.3e-02	2.0e-04	8.45	0.30		
6636-340-1	WASP-34 b	5700	100	4.50	0.10	-0.02		EXO	4.31768	4.5e-06	0.04	0.01	72.1	1.2	85.20	0.20	1.3e-02	2.6e-04	12.07	1.58		
6706-861-1	WASP-25 b	5750	100	4.50	0.15	-0.05		EXO	3.76483	5.0e-06	0.00		75.5	5.3	88.00	0.50	1.9e-02	2.0e-04	11.10	0.52		
6779-268-1	K2-38 b	5757	60	4.35	0.08	0.28		EXO	4.01593	5.0e-04	...		4.6	1.1	87.28	2.48	1.6e-04	2.2e-05	10.10	1.96		

Table 5 continued

Table 5 (*continued*)

Tycho	Name	T_{eff}	$\sigma_{T_{\text{eff}}}$	$\log g$	$\sigma_{\log g}$	[Fe/H]	$\sigma_{\text{[Fe/H]}}$	Source ^a	P_{orb}	$\sigma_{P_{\text{orb}}}$	e	σ_e	K_{RV}	$\sigma_{K_{\text{RV}}}$	i	σ_i	δ_{tr}	$\sigma_{\delta_{\text{tr}}}$	a/R_{\star}	AU/R_{\odot}	σ_a/R_{\star}	AU/R_{\odot}
6787-1927-1	WASP-17 b	6550	100	4.20	0.20	-0.25	EXO	3.73543	7.6e-06	0.00	...	59.2	2.9	86.63	0.42	1.7e-02	1.8e-04	8.97	0.62			
6926-454-1	HATS-3 b	6351	76	4.22	0.01	-0.16	EXO	3.54785	5.0e-06	0.00	...	125.7	15.7	86.20	0.30	1.0e-02	1.2e-04	7.45	0.20			
6972-75-1	WASP-6 b	5450	100	4.60	0.20	-0.20	EXO	3.36101	2.8e-06	0.05	0.02	74.3	1.5	88.47	0.56	2.1e-02	2.2e-04	10.62	0.41			
6996-583-1	WASP-45 b	5140	200	4.45	0.07	0.00	EXO	3.12609	3.5e-06	0.00	...	148.3	4.1	84.47	0.67	1.5e-02	7.1e-04	9.25	0.80			
7011-487-1	WASP-72 b	6250	100	4.09	0.05	-0.06	EXO	2.21673	1.5e-06	0.00	...	181.3	4.7	86.80	2.55	3.7e-03	3.0e-04	4.61	0.35			
7038-834-1	WASP-79 b	6600	100	4.20	0.15	0.03	EXO	3.66238	5.1e-06	0.00	...	88.2	7.8	85.40	0.60	1.1e-02	5.1e-04	7.03	0.36			
7193-1804-1	WASP-66 b	6600	150	4.30	0.20	-0.31	EXO	4.08605	7.0e-06	0.00	...	246.0	11.0	85.90	0.90	6.7e-03	1.0e-04	6.73	0.37			
7247-587-1	WASP-41 b	5545	33	4.53	0.05	0.06	EXO	3.05240	9.0e-07	0.00	0.01	138.0	2.0	89.40	0.30	1.9e-02	1.0e-04	9.96	0.42			
7283-1162-1	WASP-15 b	6300	100	4.35	0.15	-0.17	EXO	3.75210	1.0e-05	0.00	...	63.4	1.2	85.96	0.35	9.7e-03	1.2e-04	7.29	0.38			
7466-1400-1	WASP-94 A b	6170	80	4.27	0.07	0.26	EXO	3.95019	3.7e-06	0.00	0.06	45.4	2.8	88.70	0.70	1.2e-02	1.6e-04	8.44	0.84			
7522-505-1	WASP-8 b	5600	80	4.50	0.10	0.17	EXO	8.15872	1.5e-05	0.31	0.00	222.2	0.7	88.55	0.16	1.3e-02	3.2e-04	18.28	0.91			
7612-556-1	WASP-63 b	5550	100	4.01	0.03	0.08	EXO	4.37808	6.0e-06	0.00	...	39.0	3.0	87.80	1.30	6.1e-03	1.7e-04	6.59	0.30			
7963-1570-1	WASP-7 b	6400	100	4.36	0.03	0.00	EXO	4.95466	4.9e-05	0.00	...	97.0	13.0	89.60	0.65	5.8e-03	2.0e-04	10.54	0.48			
8015-1020-1	WASP-29 b	4800	150	4.50	0.20	0.11	EXO	3.92273	4.0e-06	0.03	0.04	35.6	2.7	88.80	0.70	1.0e-02	4.0e-04	12.18	0.69			
8017-108-1	WASP-4 b	5500	150	4.45	0.02	0.00	EXO	1.33823	2.2e-06	0.00	...	240.0	3.0	89.47	0.38	2.3e-02	5.8e-05	5.43	0.16			
8040-72-1	WASP-18 b	6431	48	4.47	0.13	0.13	PASTEL	0.94145	8.2e-07	0.01	0.00	1818.3	1.9	80.60	1.20	9.2e-03	1.6e-04	3.57	0.19			
8055-876-1	WASP-117 b	6040	90	4.28	0.16	-0.11	EXO	10.02165	5.5e-04	0.30	0.02	25.2	0.7	89.14	0.30	8.0e-03	5.2e-04	17.43	0.98			
8056-948-1	WASP-99 b	6150	100	4.30	0.10	0.21	EXO	5.75251	4.0e-05	0.00	...	242.2	1.7	88.80	1.10	4.1e-03	2.0e-04	8.77	0.47			
8146-86-1	KELT-15 b	6003	54	4.17	0.03	0.05	EXO	3.32944	1.6e-05	0.00	...	110.0	26.0	88.30	1.45	1.0e-02	4.3e-04	6.70	0.25			
8378-64-1	KELT-10 b	5948	74	4.32	0.02	0.09	EXO	4.16627	6.3e-06	80.0	3.5	88.61	0.80	1.4e-02	3.1e-04	9.34	0.26			
8411-1384-1	WASP-88 b	6430	130	3.96	0.04	-0.08	EXO	4.95400	1.9e-05	0.00	...	52.4	6.6	88.00	1.45	7.0e-03	3.0e-04	6.67	0.31			
8442-960-1	WASP-95 b	5830	140	4.36	0.07	0.14	EXO	2.18467	1.4e-06	0.00	...	175.7	1.7	88.40	1.65	1.0e-02	3.0e-04	6.51	0.39			
8478-1241-1	WASP-97 b	5640	100	4.45	0.08	0.23	EXO	2.07276	1.0e-06	0.00	...	194.5	2.3	88.00	1.15	1.2e-02	2.0e-04	6.72	0.28			
8805-131-1	WASP-73 b	6030	120	3.93	0.05	0.14	EXO	4.08722	2.2e-04	0.00	...	196.3	4.1	87.40	2.10	3.3e-03	3.0e-04	5.75	0.39			
8884-719-1	WASP-100 b	6900	120	4.35	0.17	-0.03	EXO	2.84938	8.0e-06	0.00	...	213.0	8.0	82.60	2.15	7.6e-03	5.0e-04	4.93	0.75			
8900-874-1	WASP-62 b	6230	80	4.45	0.10	0.04	EXO	4.41195	3.0e-06	0.00	...	60.0	4.0	88.30	0.75	1.2e-02	2.0e-04	9.55	0.41			

^a Source for spectroscopic stellar parameters: EXO = [exoplanets.org](#); PASTEL = [Paunzen \(2015\)](#); SWEET = [Santos et al. \(2013\)](#); Ammons = [Ammons et al. \(2006\)](#); McDonald:2012 = [McDonald et al. \(2012\)](#); Wright:2003 = [Wright et al. \(2003\)](#).

Table 6. Sample of radial-velocity (non-transiting) planets used in this study.

Tycho	Name	T_{eff}	$\sigma_{T_{\text{eff}}}$	$\log g$	$\sigma_{\log g}$	[Fe/H]	Source ^a	P_{orb}	$\sigma_{P_{\text{orb}}}$	e	σ_e	K_{RV}	$\sigma_{K_{\text{RV}}}$	a	σ_a	AU
		K	K	[cgs]	[cgs]			d	d			m s ⁻¹	m s ⁻¹	AU	AU	
12-104-1	HD 5319 b	4900	25	3.35	0.09	0.05	PASTEL	641.00000	2.0e+00	0.02	0.03	31.6	1.2	1.67	0.04	
32-383-1	HD 10442 b	5034	44	3.50	0.06	0.11	EXO	1043.00000	9.0e+00	0.11	0.06	31.5	2.2	2.34	0.05	
90-645-1	HD 28678 b	4722	100	3.25	0.04	-0.16	McDonald:2012	387.10001	3.4e+00	0.17	0.07	33.5	2.2	1.32	0.04	
96-602-1	GJ 179 b	3370	100	4.83	...	0.30	EXO	2288.00000	5.9e+01	0.21	0.08	25.8	2.2	2.41	0.08	
107-1139-1	HD 33636 b	5964	22	4.56	0.04	-0.08	PASTEL	2127.69995	8.2e+00	0.48	0.01	164.2	2.0	3.27	0.06	
112-182-1	HD 34445 b	5879	16	4.21	0.03	0.18	PASTEL	1049.00000	1.1e+01	0.27	0.07	15.7	1.4	2.07	0.04	
116-1316-1	HD 38529 b	5610	17	3.89	0.03	0.35	PASTEL	14.31019	8.1e-04	0.24	0.03	57.0	1.2	0.13	0.00	
127-402-1	HD 37605 b	5340	36	4.32	0.04	0.29	PASTEL	55.01307	6.4e-04	0.68	0.00	203.0	0.7	0.28	0.05	
154-891-1	HD 46375 b	5259	12	4.45	0.04	0.24	PASTEL	3.02357	6.5e-05	0.06	0.03	33.7	0.7	0.04	0.00	
213-177-1	GJ 328 b	3900	100	4.50	...	0.00	EXO	4100.00000	3.0e+02	0.37	0.05	40.0	2.0	4.43	0.24	
219-1438-1	HD 74156 b	6050	18	4.26	0.03	0.11	PASTEL	51.63800	4.0e-03	0.63	0.01	108.0	4.0	0.29	0.00	
255-946-1	HD 95089 b	4955	18	3.34	0.03	0.01	PASTEL	507.00000	1.6e+01	0.16	0.09	23.5	1.9	1.39	0.05	
267-1200-1	HD 99492 b	4815	185	4.28	0.46	0.24	SWEET	17.04310	4.7e-03	0.25	0.09	9.8	1.0	0.12	0.00	
275-157-1	HD 102195 b	5301	6	4.49	0.02	0.04	PASTEL	4.11377	5.6e-04	0.00	...	63.0	2.0	0.05	0.00	
275-243-1	HD 102329 b	4745	71	2.96	0.16	0.05	EXO	778.09998	7.5e+00	0.21	0.04	84.8	3.2	1.81	0.07	
356-1276-1	omega Ser b	4744	28	2.84	0.12	-0.25	PASTEL	277.01999	5.1e-01	0.11	0.07	31.8	2.3	1.08	0.04	
386-86-1	HD 149143 b	6013	47	4.25	0.05	0.36	PASTEL	4.07200	7.0e-03	0.02	0.01	149.6	3.0	0.05	0.00	
426-1099-1	HD 153243 b	6104	19	4.55	...	0.05	PASTEL	12.62000	4.0e-03	0.02	0.02	91.1	2.1	0.11	0.00	
430-2613-1	HD 164509 b	6026	44	4.43	...	0.24	PASTEL	282.39999	3.8e+00	0.26	0.14	14.2	2.7	0.88	0.02	
457-495-1	HD 175541 b	5036	17	3.46	0.04	-0.09	PASTEL	297.29999	6.0e+00	0.33	0.20	14.0	2.0	0.96	0.02	
458-1450-1	HD 171028 b	5671	16	3.84	0.03	-0.48	EXO	550.00000	3.0e+00	0.59	0.01	60.6	1.0	1.32	0.03	
504-2358-1	HD 192699 b	5164	63	3.38	0.14	-0.25	PASTEL	345.53000	1.7e+00	0.13	0.05	49.3	2.9	1.12	0.02	
534-2537-1	HD 200964 b	5079	17	3.39	0.09	-0.17	PASTEL	613.79999	1.4e+00	0.04	0.03	34.5	2.1	1.64	0.03	
601-636-1	HD 1502 b	5011	27	3.30	0.10	-0.01	PASTEL	431.79999	3.1e+00	0.10	0.04	60.7	1.9	1.27	0.03	
604-1102-1	HD 4313 b	5005	10	3.45	0.08	0.11	PASTEL	356.00000	2.6e+00	0.04	0.04	46.9	1.9	1.13	0.02	
692-497-1	HD 31253 b	6130	22	4.18	0.06	0.17	PASTEL	466.00000	3.0e+00	0.30	0.20	12.0	2.0	1.26	0.02	
736-601-1	HD 45652 b	5232	48	4.20	0.07	0.29	PASTEL	43.60000	2.0e-01	0.38	0.06	33.1	2.5	0.23	0.00	
794-1622-1	bet Cnc b	4104	91	1.81	0.10	-0.17	PASTEL	605.20001	4.0e+00	0.08	0.02	133.0	8.8	1.67	0.03	
805-24-1	HD 73534 b	4973	14	3.74	0.01	0.22	PASTEL	1770.00000	4.0e+01	0.07	0.07	16.2	1.1	3.02	0.08	
813-2344-1	M 67 SAND 364 b	4284	9	2.20	0.06	-0.02	EXO	121.71000	3.1e-01	0.35	0.08	67.4	5.8	0.53	0.01	
817-1748-1	HD 75784 b	4917	44	3.56	0.06	0.25	EXO	5040.00000	3.4e+03	0.36	0.16	57.0	11.0	6.46	2.92	
843-568-1	HD 89307 b	5955	14	4.46	0.04	-0.13	PASTEL	2166.00000	3.8e+01	0.20	0.05	28.9	2.2	3.27	0.07	
869-1019-1	HD 106352 b	5874	10	4.36	0.02	-0.06	PASTEL	1531.00000	4.7e+00	0.48	0.01	138.8	2.0	2.61	0.04	
870-114-1	HD 102272 b	4790	40	2.58	0.00	-0.41	PASTEL	127.58000	3.0e-01	0.05	0.04	155.5	5.6	0.51	0.03	

Table 6 continued

Table 6 (*continued*)

Tycho	Name	T_{eff}	$\sigma_{T_{\text{eff}}}$	$\log g$	$\sigma_{\log g}$	[Fe/H]	Source ^a	P_{orb}	$\sigma_{P_{\text{orb}}}$	e	σ_e	K_{RV}	$\sigma_{K_{\text{RV}}}$	a	σ_a
		K	[cgs]	[cgs]			d	d	d			m s ⁻¹	m s ⁻¹	AU	AU
898-1042-1	70 Vir b	5531	11	3.97	0.02	-0.06	PASTEL	116.68840	4.4e+03	0.40	0.00	316.3	1.7	0.48	0.01
910-165-1	HD 128311 b	4966	32	4.52	0.05	0.07	PASTEL	454.20001	1.6e+00	0.34	0.05	46.5	4.5	1.09	0.02
983-872-1	HD 152581 b	5095	23	3.31	0.05	-0.30	PASTEL	689.00000	1.3e+01	0.00	0.11	36.6	1.8	1.49	0.07
1031-1530-1	HD 170469 b	5842	28	4.30	0.03	0.29	PASTEL	1145.00000	1.8e+01	0.11	0.08	12.0	1.9	2.24	0.05
1055-3415-1	HD 183263 b	5948	27	4.37	0.01	0.29	PASTEL	626.51599	1.1e+00	0.36	0.01	84.0	3.7	1.49	0.02
1058-3400-1	xi Aql b	4748	54	2.79	0.07	-0.24	PASTEL	136.75000	2.5e+01	0.00	...	65.4	1.7	0.54	0.04
1092-1778-1	HD 196885 b	6271	32	4.34	0.03	0.22	PASTEL	1333.00000	1.5e+01	0.48	0.06	53.9	3.7	2.54	0.05
1107-2709-1	18 Del b	5056	33	3.08	0.08	0.02	PASTEL	993.29999	3.2e+00	0.08	0.01	119.4	1.3	2.59	0.04
1117-615-1	BD +14 4559 b	4864	101	4.26	0.29	0.17	PASTEL	268.94000	9.9e-01	0.29	0.03	55.2	2.3	0.78	0.05
1162-750-1	HD 220773 b	5938	30	4.26	...	0.11	PASTEL	3724.69995	4.6e+02	0.51	0.10	20.0	3.0	4.94	0.42
1193-2072-1	HD 3651 b	5158	38	4.44	0.04	0.08	PASTEL	62.21800	1.5e-02	0.60	0.04	15.9	0.7	0.29	0.00
1194-26-1	HD 4203 b	5596	20	4.23	0.05	0.40	PASTEL	431.88000	8.5e-01	0.52	0.03	60.3	2.2	1.17	0.02
1195-588-1	HD 5891 b	4673	123	2.67	0.09	-0.37	Ammons	177.11000	3.2e-01	0.07	0.02	178.5	4.1	0.64	0.04
1211-1730-1	HD 10697 b	5608	16	4.04	0.02	0.15	PASTEL	1075.19995	1.5e+00	0.10	0.01	115.4	1.1	2.13	0.04
1231-1727-1	HIP 14810 b	5520	19	4.32	0.01	0.29	PASTEL	6.67386	1.9e-05	0.14	0.00	424.3	0.5	0.07	0.00
1250-4-1	HD 285507 b	4503	73	4.67	0.05	0.13	EXO	6.08810	1.8e-03	0.09	0.02	125.8	2.3	0.06	0.00
1252-844-1	HD 24040 b	5802	15	4.26	0.05	0.19	PASTEL	3668.00000	1.7e+02	0.04	0.06	47.4	2.7	4.92	0.21
1273-1104-1	epsilon Tau b	4914	25	2.73	0.04	0.16	PASTEL	594.90002	5.3e+00	0.15	0.02	95.9	1.8	1.94	0.03
1275-2034-1	GJ 176 b	3679	77	4.50	...	0.00	PASTEL	8.78320	5.4e-03	0.00	...	4.1	0.5	0.07	0.00
1310-2544-1	HD 37124 b	5548	18	4.47	0.03	-0.36	PASTEL	154.37801	8.9e-02	0.05	0.03	28.5	0.8	0.53	0.01
1398-321-1	Pr 201 b	6174	50	4.41	0.10	0.19	EXO	4.42640	7.0e-03	0.00	...	58.1	4.1	0.06	0.00
1408-143-1	HD 81040 b	5755	20	4.54	0.08	-0.03	PASTEL	1001.70001	7.0e+00	0.53	0.04	168.0	9.0	1.94	0.03
1422-614-1	TYC 1422-614-1 b	4806	45	2.85	0.18	-0.20	EXO	198.39999	4.2e-01	0.06	0.04	82.0	6.1	0.70	0.04
1422-790-1	BD +20 2457 b	4259	64	1.77	0.19	-0.79	EXO	379.63000	2.0e+00	0.15	0.03	322.4	9.6	1.05	0.07
1422-1130-1	HD 88133 b	5404	19	3.92	0.05	0.32	PASTEL	3.41587	5.9e-04	0.13	0.07	36.1	3.0	0.05	0.00
1440-2597-1	HD 100655 b	4891	46	2.79	0.11	0.07	PASTEL	157.57001	6.5e-01	0.09	0.05	35.2	2.3	0.68	0.04
1445-2560-1	11 Com b	4830	79	2.61	0.13	-0.34	EXO	326.03000	3.2e-01	0.23	0.00	302.8	2.6	1.18	0.06
1447-2345-1	HD 108863 b	4863	36	3.06	0.08	0.00	PASTEL	443.39999	4.2e+00	0.00	0.05	45.2	1.7	1.45	0.03
1454-315-1	HD 114762 b	5869	13	4.18	0.03	-0.72	PASTEL	83.91510	3.0e-03	0.34	0.00	612.5	3.5	0.36	0.01
1460-132-1	tau Boo b	6460	23	4.26	0.05	0.26	PASTEL	3.31243	1.9e-05	0.02	0.01	466.4	3.3	0.05	0.00
1481-485-1	HD 131496 b	4886	45	3.16	0.11	0.12	PASTEL	883.00000	2.9e+01	0.16	0.07	35.0	2.1	2.11	0.07
1496-1841-1	HD 142245 b	4922	13	3.65	0.05	0.17	PASTEL	1299.00000	4.8e+01	0.00	0.16	24.8	2.6	2.78	0.09
1601-1129-1	HD 231701 b	6167	56	4.31	0.06	0.00	PASTEL	141.60001	2.8e+00	0.10	0.08	39.0	3.5	0.56	0.01
1640-113-1	HD 195019 b	5751	21	4.18	0.02	0.05	PASTEL	18.20132	3.9e-04	0.01	0.00	271.5	1.5	0.14	0.00
1681-1751-1	HD 210702 b	4911	66	3.47	0.03	-0.01	PASTEL	354.29001	2.2e+00	0.04	0.04	37.5	2.2	1.17	0.02
1691-1788-1	HD 208527 b	4035	65	1.60	0.30	-0.09	EXO	875.50000	5.8e+00	0.08	0.04	155.4	3.2	2.10	0.18

Table 6 *continued*

Table 6 (*continued*)

Tycho	Name	T_{eff}	σT_{eff}	$\log g$	$\sigma_{\log g}$	[Fe/H]	$\sigma_{\text{[Fe/H]}}$	Source ^a	P_{orb}	σP_{orb}	e	σ_e	K_{RV}	σK_{RV}	a	σ_a
		K	[cgs]	[cgs]				d	d	d			m s ⁻¹	m s ⁻¹	AU	AU
1716-1182-1	HD 219828 b	5869	19	4.17	0.01	0.16	PASTEL	3.83350	1.3e-03	0.00	...	7.0	0.5	0.05	0.00	
1717-2193-1	51 Peg b	5762	10	4.31	0.03	0.18	PASTEL	4.23078	3.6e-05	0.01	0.01	55.9	0.7	0.05	0.00	
1754-192-1	HD 8574 b	6064	14	4.28	0.04	0.01	PASTEL	227.00000	2.0e-01	0.30	0.03	58.3	1.8	0.76	0.01	
1755-1637-1	HD 9446 b	5821	21	4.48	0.05	0.09	PASTEL	30.05200	2.7e-02	0.20	0.06	46.6	3.0	0.19	0.01	
1758-2416-1	alpha Ari b	4557	28	2.39	0.11	-0.23	PASTEL	380.00000	3.0e-01	0.25	0.03	41.1	0.8	1.13	0.06	
1761-192-1	HD 12661 b	5645	31	4.36	0.03	0.36	PASTEL	262.70862	8.3e-02	0.38	0.01	73.6	0.6	0.84	0.02	
1771-1397-1	30 Ari B b	6331	61	4.43	0.05	0.19	PASTEL	335.10001	2.5e+00	0.29	0.09	272.0	24.0	0.99	0.02	
1853-1187-1	HD 32963 b	5727	32	4.41	0.03	0.11	PASTEL	2372.00000	2.6e+01	0.07	0.04	11.1	0.4	3.52	0.06	
1894-1961-1	HD 50554 b	6011	16	4.42	0.03	-0.01	PASTEL	1224.00000	1.2e+01	0.44	0.04	91.5	7.6	2.26	0.04	
1949-2012-1	55 Cnc b	5240	30	4.41	0.02	0.28	PASTEL	14.65100	1.0e-04	0.00	0.00	71.1	0.2	0.11	0.00	
1951-1006-1	HD 79498 b	5760	80	4.50	...	0.00	PASTEL	1966.09998	4.1e+01	0.59	0.02	26.0	1.0	3.13	0.07	
1964-1473-1	mu Leo b	4496	20	2.41	0.05	0.26	PASTEL	357.79999	1.2e+00	0.09	0.06	52.0	5.4	1.13	0.03	
1989-2141-1	HD 108874 b	5600	37	4.44	0.03	0.26	PASTEL	394.48123	6.0e-01	0.13	0.02	37.3	1.1	1.04	0.02	
1994-2335-1	HD 116029 b	4819	54	2.98	0.12	0.09	PASTEL	670.00000	1.1e+01	0.00	0.10	36.6	3.1	1.65	0.05	
2031-1389-1	omicron CrB b	4760	27	2.69	0.01	-0.27	PASTEL	187.83000	5.4e-01	0.19	0.09	32.2	2.8	0.83	0.02	
2037-1826-1	epsilon CrB b	4332	12	2.34	...	-0.32	PASTEL	417.89999	5.0e-01	0.11	0.03	129.4	2.0	1.24	0.05	
2038-1873-1	HD 145457 b	4769	27	2.48	0.11	-0.25	PASTEL	176.30000	3.9e-01	0.11	0.04	70.6	3.1	0.76	0.04	
2063-479-1	GJ 649 b	3696	56	4.50	...	0.00	PASTEL	598.29999	4.2e+00	0.30	0.08	12.4	1.1	1.13	0.04	
2073-136-1	HD 156668 b	4835	14	4.19	0.01	-0.06	PASTEL	4.64550	1.1e-03	0.00	...	1.9	0.3	0.05	0.00	
2082-1290-1	HD 158038 b	4860	38	3.24	0.19	0.19	PASTEL	521.00000	6.9e+00	0.29	0.09	33.9	3.3	1.50	0.04	
2099-2717-1	HD 164922 b	5372	12	4.35	0.03	0.17	PASTEL	1155.00000	2.3e+01	0.05	0.09	7.3	1.2	2.10	0.04	
2126-1196-1	HD 177830 b	4901	37	3.64	0.07	0.42	PASTEL	410.10001	2.2e+00	0.10	0.05	32.6	1.0	1.14	0.03	
2148-1948-1	HD 188015 b	5727	26	4.40	0.06	0.29	PASTEL	461.20001	1.7e+00	0.14	0.03	37.6	1.2	1.19	0.03	
2150-5013-1	HD 185269 b	6048	15	4.03	0.03	0.13	PASTEL	6.83785	1.0e-03	0.30	0.04	90.7	4.4	0.08	0.00	
2153-1463-1	HD 190228 b	5289	17	3.82	0.04	-0.25	PASTEL	1136.09998	9.9e+00	0.53	0.03	91.4	3.0	2.60	0.05	
2153-2883-1	HD 190360 b	5552	11	4.32	0.03	0.24	PASTEL	2915.03687	2.9e+01	0.31	0.02	23.2	0.5	3.97	0.07	
2261-371-1	HD 1605 b	4757	50	3.40	0.07	0.21	EXO	577.90002	5.2e+00	0.08	0.06	19.8	1.0	1.49	0.04	
2285-553-1	HD 5608 b	4929	32	3.32	0.05	0.14	PASTEL	792.59998	7.7e+00	0.19	0.06	23.5	1.6	1.99	0.04	
2313-437-1	HD 13189 b	4175	33	1.62	0.13	-0.37	PASTEL	471.60001	6.0e+00	0.27	0.06	173.3	9.8	1.25	0.08	
2355-246-1	HD 22781 b	5027	50	4.60	0.02	-0.37	EXO	528.07001	1.4e-01	0.82	0.00	726.4	7.1	1.17	0.02	
2469-686-1	HD 67087 b	6340	2	4.50	...	0.00	PASTEL	352.20001	1.6e+00	0.17	0.07	73.6	4.2	1.08	0.02	
2488-663-1	HD 75898 b	6061	27	4.21	0.07	0.27	PASTEL	418.20001	5.7e+00	0.10	0.05	58.2	3.1	1.19	0.04	
2497-418-1	HD 82886 b	4953	123	3.40	0.06	-0.31	Ammons	705.00000	3.4e+01	0.07	0.17	28.7	2.1	1.58	0.08	
2506-894-1	HD 87883 b	4915	73	4.47	0.05	0.05	PASTEL	2754.00000	8.7e+01	0.53	0.12	34.7	4.5	3.58	0.10	
2524-2128-1	HIP 57274 b	4510	136	4.11	0.46	0.01	PASTEL	8.13520	4.0e-03	0.19	0.10	4.6	0.5	0.07	0.00	
2576-2228-1	rho CrB b	5805	12	4.25	0.03	-0.22	PASTEL	39.84490	6.3e-03	0.06	0.03	64.9	2.4	0.23	0.00	

Table 6 *continued*

Table 6 (*continued*)

Tycho	Name	T_{eff}	$\sigma_{T_{\text{eff}}}$	$\log g$	$\sigma_{\log g}$	[Fe/H]	Source ^a	P_{orb}	$\sigma_{P_{\text{orb}}}$	e	σ_e	K_{RV}	$\sigma_{K_{\text{RV}}}$	a	σ_a
		K	[cgs]	[cgs]	[cgs]		d	d	d			m s ⁻¹	m s ⁻¹	AU	AU
2578-1609-1	kappa CrB b	4816	15	3.26	0.03	0.09	PASTEL	1300.00000	1.5e+01	0.12	0.05	27.3	1.3	2.72	0.05
2595-1464-1	HD 155358 b	5905	13	4.22	0.03	-0.60	PASTEL	194.30000	3.0e-01	0.17	0.03	32.0	2.0	0.63	0.02
2648-2151-1	HD 178911 B b	5588	115	4.46	0.20	0.24	PASTEL	71.48400	2.0e-02	0.11	0.00	343.3	1.0	0.34	0.01
2649-1153-1	HD 173416 b	4780	3	2.39	0.04	-0.13	PASTEL	323.60001	2.2e+00	0.21	0.04	51.8	2.0	1.16	0.06
2653-91-1	HD 180314 b	4924	25	2.96	0.04	0.14	PASTEL	396.03000	6.2e-01	0.26	0.01	340.8	3.3	1.46	0.06
2664-550-1	HD 187123 b	5809	19	4.37	0.02	0.11	PASTEL	3.096558	7.8e-06	0.01	0.01	69.4	0.4	0.04	0.00
2794-157-1	GJ 15 A b	3567	11	4.90	0.17	-0.32	EXO	11.44330	1.6e-03	0.00	...	2.9	0.3	0.07	0.00
2822-2210-1	upsilon And b	6150	11	4.15	0.02	0.06	PASTEL	4.61714	5.6e-05	0.01	0.01	68.2	1.3	0.06	0.00
2840-1669-1	HD 16175 b	5981	17	4.18	0.03	0.30	PASTEL	990.00000	2.0e+01	0.60	0.11	94.0	11.0	2.12	0.07
2842-200-1	HD 13331 b	5867	25	4.36	0.04	0.05	PASTEL	4218.00000	3.9e+02	0.02	0.04	23.3	1.4	5.15	0.33
2845-2243-1	HD 16760 b	5568	80	4.50	...	0.00	PASTEL	465.10001	2.3e+00	0.07	0.01	408.0	7.0	1.09	0.02
2867-1318-1	HD 23596 b	6040	29	4.23	0.05	0.28	PASTEL	1561.00000	1.2e+01	0.27	0.01	127.0	2.0	2.77	0.05
2927-323-1	HD 45550 b	5574	19	4.21	0.08	0.29	PASTEL	963.59998	3.4e+00	0.78	0.01	58.0	1.7	1.94	0.04
2930-2105-1	HD 43691 b	6206	25	4.15	0.07	0.27	PASTEL	36.96000	2.0e-02	0.14	0.02	124.0	2.0	0.24	0.00
2937-1747-1	HD 40979 b	6165	25	4.43	0.04	0.20	PASTEL	264.14999	2.3e-01	0.25	0.01	119.4	2.2	0.85	0.01
2946-426-1	HD 49674 b	5602	21	4.44	0.04	0.32	PASTEL	4.94737	9.8e-04	0.09	0.09	12.0	0.9	0.06	0.00
3004-578-1	HD 89744 b	6245	18	4.03	0.04	0.21	PASTEL	256.78000	5.0e-02	0.67	0.01	271.6	4.0	0.90	0.02
3009-2703-1	47 UMa b	5874	11	4.30	0.02	0.01	PASTEL	1078.00000	2.0e+00	0.03	0.01	48.4	0.9	2.10	0.04
3011-791-1	HD 95127 b	4218	30	1.78	0.30	-0.18	EXO	482.00000	5.0e+00	0.11	0.10	116.0	12.5	1.28	0.08
3012-667-1	HD 96127 b	3943	23	2.06	0.09	-0.24	SWEET	647.29999	1.7e+01	0.30	0.10	104.8	10.6	1.42	0.13
3015-1137-1	HD 99706 b	4891	35	3.07	0.08	0.02	PASTEL	868.00000	3.7e+01	0.37	0.10	22.4	2.4	2.13	0.08
3048-172-1	HD 136418 b	4989	10	3.45	0.03	-0.11	PASTEL	464.29999	3.2e+00	0.25	0.04	44.7	1.9	1.29	0.03
3050-1243-1	HD 132563 B b	5985	100	4.27	0.05	-0.19	SWEET	1544.00000	3.4e+01	0.22	0.09	26.7	2.2	2.62	0.06
3067-576-1	14 Her b	5338	25	4.45	0.02	0.41	PASTEL	1773.40002	2.5e+00	0.37	0.00	90.0	0.5	2.93	0.08
3161-126-1	HD 197037 b	6137	20	4.37	...	-0.16	PASTEL	1035.69995	1.3e+01	0.22	0.07	15.5	1.0	2.07	0.04
3227-413-1	HD 216536 b	4639	45	2.36	0.21	-0.17	EXO	148.60001	7.0e-01	0.38	0.11	50.0	6.0	0.61	0.06
3231-323-1	14 And b	4667	27	2.53	0.06	-0.30	PASTEL	185.84000	2.3e-01	0.00	...	100.0	1.3	0.82	0.02
3304-101-1	HD 17092 b	4326	148	3.00	0.12	0.18	Ammons	359.89999	2.4e+00	0.17	0.05	82.4	3.2	1.31	0.06
3304-323-1	BD +48 738 b	4411	158	2.62	0.26	-0.09	Ammons	392.60001	5.5e+00	0.20	0.10	31.9	2.6	1.11	0.08
3413-210-1	XO-2S b	5399	55	4.43	0.08	0.39	EXO	18.15700	3.4e-02	0.18	0.04	20.6	0.9	0.13	0.00
3425-1596-1	HD 81688 b	4846	28	2.60	0.10	-0.25	PASTEL	184.02000	1.8e-01	0.00	...	58.6	1.0	0.81	0.01
3501-1373-1	HD 154345 b	5468	14	4.43	0.04	-0.11	PASTEL	3341.55884	9.3e+01	0.04	0.05	14.0	0.7	4.21	0.10
3565-1525-1	16 Cyg B b	5750	8	4.36	0.01	0.06	PASTEL	798.50000	1.0e+00	0.68	0.02	50.5	1.6	1.66	0.03
3646-2286-1	HD 222155 b	5701	44	3.99	0.03	-0.18	PASTEL	3999.00000	5.0e+02	0.16	0.22	24.2	5.6	5.14	0.46
3658-583-1	HD 2952 b	4844	20	2.67	0.07	0.00	EXO	311.60001	1.8e+00	0.13	0.09	26.3	3.6	1.23	0.02
3777-2071-1	6 Lyn b	5022	28	3.15	0.13	-0.10	PASTEL	874.77399	1.2e+01	0.06	0.03	31.5	1.2	2.19	0.06

Table 6 *continued*

Table 6 (*continued*)

Tycho	Name	T_{eff}	σT_{eff}	$\log g$	$\sigma_{\log g}$	[Fe/H]	Source ^a	P_{orb}	σP_{orb}	e	σ_e	K_{RV}	σK_{RV}	a	σ_a
		K	[cgs]	[cgs]	[cgs]		d	d	d			m s ⁻¹	m s ⁻¹	AU	AU
3839-846-1	HD 102956 b	4994	15	3.35	0.04	0.13	PASTEL	6.49480	4.0e-04	0.05	0.03	73.4	1.9	0.08	0.00
3850-458-1	HD 118203 b	5864	25	4.08	0.05	0.23	PASTEL	6.13350	6.0e-04	0.31	0.01	217.0	3.0	0.07	0.00
3861-267-1	HD 132406 b	5783	38	4.20	0.06	0.14	PASTEL	974.00000	3.9e+01	0.34	0.09	115.0	26.0	1.98	0.06
3869-494-1	HD 139357 b	4599	4	2.59	0.05	0.26	PASTEL	1125.69995	9.0e+00	0.10	0.02	161.2	3.2	2.35	0.14
3875-1620-1	iota Dra b	4557	29	2.84	0.06	0.12	PASTEL	511.09799	8.9e-02	0.71	0.00	307.6	2.3	1.31	0.06
3903-2143-1	HD 167042 b	4877	71	3.52	0.01	0.01	PASTEL	420.76999	3.3e+00	0.09	0.05	32.2	1.3	1.29	0.02
3910-257-1	HD 163607 b	5572	13	4.05	...	0.22	PASTEL	75.29000	2.0e-02	0.73	0.02	51.1	1.4	0.36	0.01
4006-19-1	HD 240237 b	3926	100	1.67	0.01	-0.25	McDonald:2012	745.70001	1.4e+01	0.40	0.10	91.5	12.8	1.92	0.16
4006-980-1	HD 240210 b	3850	100	2.30	0.05	-0.18	Wright:2003	501.75000	2.3e+00	0.15	0.02	161.9	3.5	1.33	0.09
4054-322-1	HD 13908 b	6243	51	4.11	...	0.01	PASTEL	19.38200	6.0e-03	0.05	0.02	55.3	1.2	0.15	0.00
4126-818-1	HD 6898 b	5932	23	4.40	0.03	0.35	PASTEL	6.27711	2.1e-04	0.12	0.01	184.7	3.7	0.07	0.00
4127-2431-1	omicron UMa b	5183	22	2.55	0.08	-0.07	PASTEL	1630.00000	3.5e+01	0.13	0.06	33.6	2.1	3.95	0.09
4130-2355-1	4 UMa b	4457	19	2.23	0.09	-0.22	PASTEL	269.29999	2.0e+00	0.43	0.02	215.6	7.1	0.88	0.04
4166-541-1	HD 113337 b	6607	62	4.20	...	0.07	PASTEL	324.00000	2.0e+00	0.46	0.04	75.6	3.7	1.03	0.03
4202-656-1	HD 156279 b	5453	40	4.46	0.03	0.14	EXO	131.05000	5.4e-01	0.71	0.02	578.0	20.0	0.49	0.01
4215-406-1	HIP 91258 b	5519	70	4.53	0.12	0.23	EXO	5.05050	1.5e-03	0.02	0.01	130.9	1.7	0.06	0.00
4222-2311-1	42 Dra b	4407	35	2.15	0.12	-0.43	PASTEL	479.10001	6.2e+00	0.38	0.06	110.5	7.0	1.17	0.05
4283-211-1	HD 220074 b	3787	110	1.30	0.50	-0.25	EXO	672.09998	3.7e+00	0.14	0.05	230.8	5.0	1.60	0.13
4322-1310-1	HD 11755 b	4312	5	1.67	0.03	-0.74	EXO	433.70001	3.2e+00	0.19	0.10	191.3	10.2	1.09	0.04
4339-2274-1	HD 24064 b	4052	22	1.44	0.11	-0.49	EXO	535.59998	3.0e+00	0.35	0.08	251.0	9.3	1.29	0.04
4346-320-1	HD 32518 b	4661	53	2.41	0.12	-0.10	PASTEL	157.53999	3.8e-01	0.01	0.02	115.8	4.7	0.60	0.03
4400-99-1	HD 109246 b	5844	21	4.46	0.19	0.10	EXO	68.27000	1.3e-01	0.12	0.04	38.2	1.6	0.33	0.01
4414-2315-1	11 UMi b	4213	46	1.93	0.07	-0.02	PASTEL	516.21997	3.2e+00	0.08	0.03	189.7	7.2	1.53	0.07
4416-1739-1	bet UMi b	4030	100	1.85	0.01	-0.26	PASTEL	522.29999	2.7e+00	0.19	0.02	126.1	8.1	1.42	0.07
4417-267-1	8 UMi b	4847	7	2.57	0.03	-0.03	EXO	93.40000	4.5e+00	0.06	0.09	46.1	4.0	0.49	0.02
4428-1943-1	GJ 687 b	3340	97	4.82	0.03	0.15	PASTEL	38.14000	1.5e-02	0.04	0.08	6.4	0.8	0.17	0.01
4494-1346-1	HD 7924 b	5131	14	4.46	0.03	-0.21	PASTEL	5.39792	2.5e-04	0.06	0.05	3.6	0.2	0.06	0.00
4532-2096-1	HD 33564 b	6415	51	4.33	0.11	0.16	PASTEL	388.00000	3.0e+00	0.34	0.02	232.0	5.0	1.12	0.02
4550-2113-1	HD 104985 b	4740	62	2.47	0.13	-0.35	PASTEL	199.50500	8.5e-02	0.09	0.01	166.8	1.3	0.68	0.06
4561-2319-1	HD 120084 b	4886	3	2.68	0.11	0.09	PASTEL	2082.00000	2.9e+01	0.66	0.12	53.0	22.0	4.27	1.35
4606-3584-1	gamma Cep b	4809	42	3.23	0.08	0.09	PASTEL	905.57397	3.1e+00	0.12	0.05	27.5	1.5	1.98	0.07
4620-542-1	HD 12648 b	4835	7	2.18	0.03	-0.57	EXO	133.60001	5.0e-01	0.04	0.08	102.0	8.4	0.54	0.02
4671-94-1	HD 2638 b	5186	8	4.38	0.04	0.13	PASTEL	3.44420	2.0e-04	0.00	...	67.4	0.4	0.04	0.00
4683-883-1	HD 7449 b	6047	15	4.52	0.01	-0.10	PASTEL	1275.00000	1.3e+01	0.82	0.06	41.6	15.2	2.34	0.04
4698-1302-1	75 Cet b	4848	22	2.81	0.04	-0.00	PASTEL	691.90002	3.6e+00	0.12	0.05	38.3	2.0	1.98	0.06
4701-1094-1	81 Cet b	4871	14	2.71	0.05	0.01	PASTEL	952.70001	8.8e+00	0.21	0.03	62.8	1.5	2.28	0.09

Table 6 *continued*

Table 6 (*continued*)

Tycho	Name	T_{eff}	σT_{eff}	$\log g$	$\sigma_{\log g}$	[Fe/H]	$\sigma_{\text{[Fe/H]}}$	Source ^a	P_{orb}	σP_{orb}	e	σ_e	K_{RV}	σK_{RV}	a	σ_a
		K	K	[cgs]	[cgs]			d	d	d			m s ⁻¹	m s ⁻¹	AU	AU
4701-1095-1	HD 16141 b	5757	9	4.14	0.02	0.13	PASTEL	75.52300	5.5e-02	0.25	0.05	12.0	0.9	0.36	0.01	
4708-1423-1	HD 19994 b	6151	17	4.18	0.03	0.20	PASTEL	466.20001	1.7e+00	0.27	0.01	29.3	2.1	1.31	0.02	
4748-1630-1	HD 30562 b	5882	10	4.07	0.02	0.20	PASTEL	1117.00000	2.7e+01	0.76	0.05	33.7	2.2	2.34	0.06	
4757-731-1	HD 290327 b	5505	63	4.41	0.10	-0.14	PASTEL	2443.00000	1.6e+02	0.08	0.05	41.3	2.9	3.43	0.16	
4822-3681-1	HD 52265 b	6117	10	4.32	0.02	0.22	PASTEL	119.29000	8.6e-02	0.32	0.06	42.1	3.1	0.50	0.01	
4846-68-1	HD 66428 b	5716	20	4.33	0.03	0.27	PASTEL	1973.00000	3.1e+01	0.47	0.03	48.3	2.7	3.14	0.07	
4862-360-1	HD 72659 b	5932	19	4.27	0.03	-0.02	PASTEL	3658.00000	3.2e+01	0.22	0.03	41.0	1.3	4.75	0.08	
4899-942-1	HD 86081 b	6018	18	4.18	0.03	0.20	PASTEL	2.13750	2.0e-04	0.01	0.00	207.7	0.8	0.03	0.00	
4905-1374-1	24 Sex b	5019	18	3.33	0.07	-0.05	PASTEL	455.20001	3.2e+00	0.18	0.03	33.2	1.6	1.41	0.02	
4913-618-1	HD 9278 b	5738	15	4.41	0.03	0.30	PASTEL	325.81000	2.6e-01	0.33	0.01	106.0	1.7	0.95	0.02	
4923-464-1	HD 99109 b	5282	32	4.34	0.05	0.35	PASTEL	439.29999	5.6e+00	0.09	0.12	14.1	2.2	1.11	0.02	
4924-460-1	HD 96063 b	5125	15	3.63	0.05	-0.19	PASTEL	361.10001	9.9e+00	0.00	0.14	25.9	3.5	1.11	0.03	
4933-678-1	HD 100777 b	5533	3	4.32	0.01	0.25	PASTEL	383.70001	1.2e+00	0.36	0.02	34.9	0.8	1.03	0.03	
4943-39-1	HD 107148 b	5777	8	4.38	0.03	0.29	PASTEL	48.05600	5.7e-02	0.05	0.11	10.9	2.0	0.27	0.01	
4958-894-1	HD 114783 b	5113	21	4.49	0.04	0.12	PASTEL	493.70001	1.8e+00	0.14	0.03	31.9	0.9	1.16	0.02	
4983-226-1	HD 126614 A b	5568	23	4.30	0.06	0.54	PASTEL	1244.00000	1.7e+01	0.41	0.10	7.3	0.7	2.37	0.04	
4986-302-1	HD 130322 b	5385	10	4.45	0.02	0.03	PASTEL	10.70850	3.0e-04	0.01	0.02	108.3	2.0	0.09	0.00	
5002-997-1	HD 136118 b	6176	25	4.24	0.05	-0.05	PASTEL	1187.30005	2.4e+00	0.34	0.01	210.7	2.5	2.33	0.04	
5133-750-1	HD 179079 b	5730	26	4.16	0.03	0.25	PASTEL	14.47600	1.1e-02	0.12	0.09	6.6	0.6	0.12	0.00	
5146-2250-1	HIP 97233 b	5020	150	3.26	...	0.29	PASTEL	1058.80005	6.7e+00	0.61	0.03	320.1	18.4	2.54	0.05	
5161-868-1	HD 192263 b	4976	18	4.51	0.05	0.03	PASTEL	24.35560	4.6e-03	0.05	0.04	51.9	2.6	0.15	0.00	
5221-210-1	HD 206610 b	4890	71	3.34	0.12	0.16	PASTEL	610.00000	1.3e+01	0.23	0.06	40.7	1.9	1.54	0.05	
5227-1521-1	GJ 849 b	3241	150	4.80	0.14	0.24	PASTEL	1882.00000	2.5e+02	0.04	0.02	22.0	4.0	2.35	0.22	
5235-1468-1	HD 217107 b	5622	17	4.34	0.02	0.36	PASTEL	7.12682	3.9e-05	0.13	0.01	139.2	0.9	0.08	0.00	
5242-229-1	HD 218566 b	4730	100	4.46	0.18	0.28	Wright:2003	225.70000	4.0e-01	0.30	0.10	8.3	0.7	0.69	0.01	
5242-591-1	HD 217786 b	6014	32	4.35	...	-0.14	PASTEL	1319.00000	4.0e+00	0.40	0.05	261.0	20.0	2.38	0.04	
5258-491-1	HD 222582 b	5790	14	4.38	0.02	0.01	PASTEL	572.38000	6.1e-01	0.73	0.01	276.3	7.0	1.34	0.02	
5261-789-1	HD 1461 b	5737	24	4.35	0.01	0.21	PASTEL	5.77270	2.5e-03	0.14	0.19	2.7	0.6	0.06	0.00	
5262-825-1	HD 1690 b	4374	31	2.04	0.03	-0.27	PASTEL	533.00000	1.7e+00	0.64	0.04	190.0	29.0	1.36	0.09	
5273-16-1	HD 6718 b	5801	41	4.51	0.08	-0.03	PASTEL	2496.00000	1.8e+02	0.10	0.08	24.1	1.5	3.55	0.18	
5278-2314-1	HD 11964 b	5309	41	3.94	0.05	0.10	PASTEL	1944.58984	2.6e+01	0.04	0.04	9.4	0.4	3.13	0.06	
5296-1533-1	epsilon Eri b	5091	11	4.53	0.02	-0.10	PASTEL	2500.00000	3.5e+02	0.25	0.23	18.6	2.9	3.38	0.32	
5317-733-1	HD 28185 b	5662	11	4.42	0.02	0.23	PASTEL	379.00000	2.0e+00	0.05	0.03	163.5	3.0	1.02	0.02	
5342-401-1	HD 33844 b	4861	100	3.24	0.08	0.27	EXO	551.40002	7.8e+00	0.15	0.07	33.5	2.0	1.60	0.06	
5342-891-1	HD 33142 b	5009	15	3.49	0.07	0.00	PASTEL	326.60001	3.9e+00	0.12	0.17	30.4	2.5	1.09	0.02	
5347-367-1	HD 38801 b	5277	27	3.90	0.03	0.19	PASTEL	696.29999	2.7e+00	0.00	...	200.0	3.9	1.65	0.03	

Table 6 *continued*

Table 6 (*continued*)

Tycho	Name	T_{eff}	σT_{eff}	$\log g$	$\sigma_{\log g}$	[Fe/H]	Source ^a	P_{orb}	σP_{orb}	e	σ_e	K_{RV}	σK_{RV}	a	σ_a
		K	K	[cgs]	[cgs]		d	d	d			m s ⁻¹	m s ⁻¹	AU	AU
5367-701-1	HD 44219 b	5792	53	4.20	...	0.04	PASTEL	472.29999	5.7e+00	0.61	0.08	19.4	3.0	1.19	0.02
5409-2156-1	NGC 2423 3 b	4545	71	2.20	0.20	-0.08	EXO	714.29999	5.3e+00	0.21	0.07	137.6	9.1	1.66	0.12
5435-2991-1	HD 69830 b	5423	10	4.49	0.03	-0.03	PASTEL	8.66700	3.0e-03	0.10	0.04	3.5	0.2	0.08	0.00
5469-1000-1	HD 82943 b	5979	8	4.43	0.02	0.27	PASTEL	442.39999	5.1e+00	0.20	0.07	39.8	2.0	1.19	0.02
5480-20-1	BD -08 2823 b	4816	114	4.43	0.22	-0.06	PASTEL	5.60000	2.0e-02	0.15	0.15	6.5	0.1	0.06	0.00
5503-946-1	BD -10 3166 b	5393	44	4.69	0.06	0.38	EXO	3.48777	1.1e-04	0.02	0.02	60.9	1.4	0.04	0.00
5504-418-1	HD 96167 b	5807	31	4.13	0.02	0.34	PASTEL	498.89999	1.0e+00	0.71	0.04	20.8	1.5	1.35	0.04
5519-1520-1	HD 106270 b	5528	69	4.50	...	0.00	PASTEL	2890.00000	3.9e+02	0.40	0.05	142.1	6.9	4.38	0.40
5521-1086-1	HD 103774 b	6556	89	4.81	...	0.29	PASTEL	5.88810	5.0e-04	0.09	0.04	34.3	1.8	0.07	0.00
5594-103-1	GJ 581 b	3442	54	4.50	...	0.00	PASTEL	5.36865	9.0e-05	0.03	0.01	12.6	0.2	0.04	0.00
5639-555-1	HD 148427 b	5025	4	3.48	0.06	0.08	PASTEL	331.50000	3.0e+00	0.16	0.08	27.7	2.0	1.04	0.02
5681-1576-1	HD 168443 b	5569	18	4.13	0.03	0.08	PASTEL	58.11247	3.0e-04	0.53	0.02	475.1	0.9	0.29	0.00
5685-2670-1	HD 168746 b	5570	12	4.39	0.02	-0.08	PASTEL	6.40400	1.4e-03	0.11	0.08	28.6	1.7	0.07	0.00
5803-1956-1	HD 210277 b	5538	14	4.38	0.02	0.22	PASTEL	442.19000	5.0e-01	0.48	0.02	38.9	0.8	1.13	0.02
5819-1255-1	GJ 876 b	3129	19	4.50	...	0.00	PASTEL	61.11660	8.6e-03	0.03	0.00	214.0	0.4	0.21	0.01
5840-482-1	HIP 2247 b	4665	120	4.19	0.26	0.01	PASTEL	655.59998	6.0e-01	0.54	0.00	173.3	1.7	1.34	0.02
5842-736-1	HD 1666 b	6360	84	4.50	...	0.00	PASTEL	270.00000	8.5e-01	0.63	0.03	199.4	7.2	0.94	0.02
5853-449-1	HIP 5158 b	4813	171	4.32	0.35	0.17	PASTEL	345.72000	5.4e+00	0.52	0.08	57.0	11.0	0.89	0.02
5858-2028-1	HD 11506 b	6183	17	4.43	0.01	0.34	PASTEL	1405.00000	4.5e+01	0.30	0.10	80.0	3.0	2.60	0.09
5870-602-1	HD 18742 b	5021	14	3.31	0.02	-0.14	PASTEL	772.00000	1.1e+01	0.12	0.06	44.3	3.8	1.98	0.07
5956-2621-1	7 CMa b	4786	27	3.03	0.11	0.10	PASTEL	763.00000	1.7e+01	0.14	0.06	44.9	4.0	1.80	0.06
5991-217-1	HD 60532 b	6218	26	3.91	0.06	-0.17	PASTEL	201.30000	6.0e-01	0.28	0.03	29.3	1.4	0.76	0.02
6045-1121-1	HD 86264 b	6388	53	4.25	0.09	0.29	PASTEL	1475.00000	5.5e+01	0.70	0.20	132.0	17.0	2.84	0.09
6083-1275-1	HD 95872 b	5312	100	4.43	0.15	0.41	EXO	4375.00000	1.7e+02	0.06	0.04	59.0	4.0	5.15	0.16
6100-1491-1	HD 104067 b	4937	25	4.49	0.09	0.00	PASTEL	55.80600	4.9e-02	0.00	...	11.6	0.8	0.26	0.00
6116-1517-1	61 Vir b	5551	11	4.39	0.02	-0.01	PASTEL	4.21500	6.0e-04	0.12	0.11	2.1	0.2	0.05	0.00
6143-1636-1	HD 125612 b	5931	29	4.45	0.02	0.24	PASTEL	559.40485	1.3e+00	0.46	0.01	79.8	2.2	1.37	0.03
6191-172-1	HD 141937 b	5870	9	4.45	0.02	0.11	PASTEL	653.21997	1.2e+00	0.41	0.01	234.5	6.4	1.50	0.03
6209-1322-1	HIP 79431 b	3191	39	4.50	...	0.40	EXO	111.70000	7.0e-01	0.29	0.02	149.5	2.5	0.36	0.01
6242-339-1	HD 156846 b	6090	31	4.02	0.04	0.15	PASTEL	359.51001	9.0e-02	0.85	0.00	464.3	3.0	1.12	0.02
6244-136-1	HD 155233 b	4960	148	3.17	...	0.08	PASTEL	885.00090	6.3e+01	0.03	0.10	32.2	8.7	2.07	0.13
6359-848-1	HD 202206 b	5760	12	4.51	0.04	0.34	PASTEL	255.87000	6.0e-02	0.44	0.00	564.8	1.3	0.81	0.02
6373-214-1	HD 204941 b	5026	29	4.42	0.06	-0.19	PASTEL	1733.00000	7.4e+01	0.37	0.08	5.9	0.7	2.55	0.08
6373-682-1	HD 204313 b	5783	29	4.37	0.01	0.16	PASTEL	1920.09998	2.5e+01	0.23	0.04	57.0	3.0	3.07	0.06
6385-788-1	HD 212771 b	5069	16	3.51	0.01	-0.15	PASTEL	373.29999	3.4e+00	0.11	0.06	58.2	7.8	1.16	0.02
6411-109-1	HD 224693 b	6103	82	4.21	0.01	0.25	PASTEL	26.73000	2.0e-02	0.05	0.03	40.2	2.0	0.19	0.00

Table 6 *continued*

Table 6 (*continued*)

Tycho	Name	T_{eff}	σT_{eff}	$\log g$	$\sigma_{\log g}$	[Fe/H]	Source ^a	P_{orb}	σP_{orb}	e	σ_e	K_{RV}	σK_{RV}	a	σ_a
		K	K	[cgs]	[cgs]			d	d			m s ⁻¹	m s ⁻¹	AU	AU
6421-1078-1	HD 4732 b	4989	15	3.46	0.04	0.15	PASTEL	360.20001	1.4e+00	0.13	0.06	47.3	3.5	1.19	0.04
6423-1832-1	HD 4208 b	5629	15	4.46	0.02	-0.26	PASTEL	828.00000	8.1e+00	0.05	0.04	19.1	0.7	1.65	0.03
6434-494-1	HIP 12961 b	3901	175	4.65	0.09	-0.14	PASTEL	57.43500	4.2e-02	0.17	0.03	24.7	0.9	0.25	0.01
6445-136-1	HD 20782 b	5790	15	4.38	0.03	-0.06	PASTEL	591.90002	2.8e+00	0.97	0.01	185.3	49.7	1.37	0.02
6466-1769-1	HD 30856 b	4971	28	3.31	0.08	-0.14	PASTEL	912.00000	4.1e+01	0.12	0.18	31.9	2.7	2.04	0.07
6481-1002-1	HD 33283 b	6108	53	4.12	0.05	0.34	PASTEL	18.17900	7.0e-03	0.48	0.05	25.2	2.0	0.15	0.00
6516-711-1	HD 47186 b	5657	9	4.36	0.02	0.24	PASTEL	4.08450	2.0e-04	0.04	0.02	9.1	0.2	0.05	0.00
6517-2108-1	HD 43197 b	5473	24	4.30	...	0.36	PASTEL	327.79999	1.2e+00	0.83	0.03	32.4	7.1	0.92	0.02
6589-761-1	HD 77338 b	5341	31	4.60	0.10	0.32	PASTEL	5.73610	1.5e-03	0.09	0.22	6.0	1.7	0.06	0.00
6631-431-1	HD 90156 b	5611	7	4.52	0.04	-0.23	PASTEL	49.77000	7.0e-02	0.31	0.10	3.7	0.2	0.25	0.00
6649-807-1	HD 98219 b	4946	25	3.50	0.07	-0.02	PASTEL	436.89999	4.5e+00	0.00	0.10	41.2	1.9	1.32	0.03
6766-877-1	HD 134987 b	5736	17	4.31	0.02	0.28	PASTEL	258.17999	7.0e-02	0.23	0.00	49.5	0.2	0.81	0.02
6801-585-1	HD 145377 b	6014	20	4.47	0.05	0.11	PASTEL	103.95000	1.3e-01	0.31	0.02	242.7	4.6	0.45	0.01
6854-175-1	HD 164604 b	4717	68	4.32	...	0.12	PASTEL	606.40002	9.0e+00	0.24	0.14	77.0	32.0	1.30	0.03
6866-1721-1	HD 171238 b	5410	20	4.50	...	0.00	PASTEL	1523.00000	4.3e+01	0.40	0.06	52.2	1.8	2.54	0.06
6869-1277-1	HD 169830 b	6314	13	4.14	0.03	0.15	PASTEL	225.62000	2.2e-01	0.31	0.01	80.7	0.9	0.81	0.01
6875-192-1	HD 181342 b	5005	18	3.38	0.05	0.21	PASTEL	663.00000	2.9e+01	0.18	0.06	52.3	3.7	1.78	0.06
6875-222-1	HD 180902 b	4992	3	3.46	0.00	-0.01	PASTEL	479.00000	1.3e+01	0.09	0.10	30.7	3.7	1.38	0.04
6875-3273-1	HD 179949 b	6221	15	4.44	0.02	0.20	PASTEL	3.09251	3.2e-05	0.02	0.01	112.6	1.8	0.04	0.00
6914-1943-1	HD 192310 b	5067	16	4.47	0.02	0.01	PASTEL	74.72000	1.0e-01	0.13	0.04	3.0	0.1	0.32	0.01
6956-378-1	HD 207832 b	5761	32	4.48	0.02	0.14	PASTEL	161.97000	8.8e-01	0.13	0.12	22.1	2.0	0.57	0.02
6974-283-1	HD 246770 b	5399	18	4.37	0.04	0.27	PASTEL	118.45000	5.5e-01	0.37	0.06	30.9	1.9	0.46	0.01
7014-630-1	HD 16417 b	5807	35	4.18	0.03	0.10	PASTEL	17.24000	1.0e-02	0.20	0.09	5.0	0.4	0.14	0.00
7023-236-1	HD 20868 b	4802	146	4.26	0.30	0.05	PASTEL	380.85001	9.0e-02	0.75	0.00	100.3	0.4	0.95	0.02
7073-2172-1	HD 45364 b	5452	15	4.38	0.00	-0.17	PASTEL	226.92999	3.7e-01	0.17	0.02	7.2	0.1	0.68	0.01
7096-565-1	HD 50499 b	6043	10	4.32	0.02	0.63	PASTEL	2457.87158	3.8e+01	0.25	0.20	23.0	1.1	3.87	0.08
7136-2007-1	HD 73256 b	5460	26	4.41	0.02	0.25	PASTEL	2.54858	1.6e-04	0.03	0.02	269.0	8.0	0.04	0.00
7144-1553-1	HD 73267 b	5387	10	4.37	...	0.05	PASTEL	1260.00000	7.0e+00	0.26	0.01	64.3	0.5	2.20	0.04
7190-2048-1	HD 93083 b	5049	31	4.34	0.05	0.11	PASTEL	143.58000	6.0e-01	0.14	0.03	18.3	0.5	0.48	0.01
7220-1321-1	GJ 433 b	3461	150	4.81	0.14	-0.17	SWEET	7.37090	8.0e-04	0.08	0.08	3.1	0.2	0.06	0.00
7258-1542-1	HD 114386 b	4836	18	4.45	0.06	-0.05	PASTEL	937.70001	1.6e+01	0.23	0.03	34.3	1.6	1.73	0.03
7263-2071-1	HD 114729 b	5835	14	4.15	0.03	-0.28	PASTEL	1114.00000	1.5e+01	0.17	0.05	18.8	1.3	2.10	0.04
7272-1998-1	HD 117207 b	5662	11	4.33	0.03	0.24	PASTEL	2597.00000	4.1e+01	0.14	0.04	26.6	0.9	3.74	0.07
7287-1874-1	HIP 67851 b	4800	89	3.08	0.08	-0.05	PASTEL	88.80000	2.0e-01	0.09	0.05	46.8	2.0	0.46	0.02
7428-2738-1	HD 181720 b	5736	37	4.09	0.08	-0.62	PASTEL	956.00000	1.4e+01	0.26	0.06	8.4	0.4	1.85	0.04
7449-1245-1	HD 190647 b	5640	8	4.17	0.01	0.22	PASTEL	1038.09998	5.1e+00	0.18	0.02	36.4	1.2	2.07	0.06

Table 6 *continued*

Table 6 (*continued*)

Tycho	Name	T_{eff}	σT_{eff}	$\log g$	$\sigma_{\log g}$	[Fe/H]	$\sigma_{\text{[Fe/H]}}$	Source ^a	P_{orb}	σP_{orb}	e	σ_e	K_{RV}	σK_{RV}	a	σ_a
		K	K	[cgs]	[cgs]			d	d	d			m s ⁻¹	m s ⁻¹	AU	AU
7487-1980-1	HD 205739 b	6386	85	4.40	...	0.21	PASTEL	279.79999	1.0e-01	0.27	0.07	42.0	3.0	0.89	0.02	
7532-852-1	HD 4113 b	5663	31	4.30	...	0.20	PASTEL	526.62000	3.0e-01	0.90	0.00	97.1	3.8	1.27	0.02	
7533-1111-1	HD 6434 b	5769	14	4.38	0.05	-0.55	PASTEL	21.99800	9.0e-03	0.17	0.03	34.2	1.1	0.14	0.00	
7544-986-1	HD 8535 b	6176	18	4.42	...	0.04	PASTEL	1313.00000	2.8e+01	0.15	0.07	11.8	0.8	2.44	0.05	
7567-1183-1	HD 20794 b	5401	17	4.22	0.11	-0.40	EXO	18.31500	8.0e-03	0.00	...	0.8	0.1	0.12	0.00	
7665-696-1	HD 70642 b	5665	10	4.40	0.01	0.17	PASTEL	2068.00000	3.9e+01	0.03	0.04	30.4	1.3	3.18	0.07	
7670-3068-1	HD 73526 b	5601	24	4.12	0.05	0.22	PASTEL	188.30000	9.0e-01	0.19	0.05	102.0	5.0	0.65	0.01	
7683-1503-1	HD 75289 b	6117	16	4.37	0.03	0.26	PASTEL	3.50927	6.4e-05	0.03	0.03	54.9	1.8	0.05	0.00	
7704-39-1	HD 83443 b	5442	17	4.39	0.04	0.35	PASTEL	2.98570	5.7e-05	0.01	0.01	56.2	1.7	0.04	0.00	
7706-1752-1	HD 85512 b	4300	45	4.36	0.10	-0.26	SWEET	58.43000	1.3e-01	0.11	0.10	0.8	0.1	0.26	0.00	
7745-1381-1	HD 102365 b	5598	19	4.42	0.04	-0.33	PASTEL	122.10000	3.0e-01	0.34	0.14	2.4	0.3	0.46	0.01	
7762-1479-1	HD 109749 b	5858	26	4.31	0.00	0.27	PASTEL	5.24000	2.0e-03	0.00	...	28.3	0.6	0.06	0.00	
7774-1925-1	HD 114613 b	5697	17	3.94	0.03	0.16	PASTEL	3827.00000	1.0e+02	0.25	0.08	5.5	0.4	5.31	0.13	
7809-2461-1	HD 125595 b	4691	166	4.17	0.37	0.08	PASTEL	9.67370	3.9e-03	0.00	...	4.8	0.5	0.08	0.00	
7853-621-1	HD 147513 b	5863	14	4.53	0.01	0.04	PASTEL	528.40002	6.3e+00	0.26	0.05	29.3	1.8	1.31	0.02	
7863-1386-1	HD 143361 b	5507	10	4.36	...	0.22	PASTEL	1086.00000	9.0e+01	0.18	0.10	63.0	20.0	2.03	0.12	
7881-474-1	HD 153950 b	6124	81	4.32	0.06	-0.01	PASTEL	499.39999	3.6e+00	0.34	0.02	69.2	1.2	1.28	0.02	
7890-1378-1	HD 162020 b	4723	71	4.31	0.18	-0.10	SWEET	8.42820	5.0e-05	0.28	0.00	1813.0	4.0	0.08	0.00	
7896-3839-1	HD 159868 b	5566	20	4.00	0.03	-0.05	PASTEL	1178.40002	8.8e+00	0.01	0.02	38.3	1.1	2.30	0.04	
7979-47-1	HIP 105854 b	4420	100	2.98	0.08	0.28	Wright:2003	184.20000	5.0e-01	0.02	0.03	178.1	10.0	0.81	0.01	
7982-636-1	HD 208487 b	6158	21	4.51	0.04	0.07	PASTEL	130.08000	5.1e-01	0.24	0.16	19.7	3.6	0.52	0.01	
8025-341-1	HD 142 b	6247	28	4.33	0.06	0.07	PASTEL	350.29999	3.6e+00	0.26	0.18	33.9	4.7	1.04	0.02	
8031-1-1	HD 5388 b	6257	31	4.24	...	-0.28	PASTEL	777.00000	4.0e+00	0.40	0.02	41.7	1.6	1.76	0.03	
8048-1022-1	GJ 86 b	5182	11	4.63	0.02	-0.22	PASTEL	15.76491	3.9e-04	0.04	0.01	376.7	2.9	0.11	0.00	
8056-1164-1	iotा Hor b	6167	24	4.46	0.04	0.16	PASTEL	302.79999	2.3e+00	0.14	0.13	57.1	5.2	0.92	0.02	
8075-1657-1	HD 28254 b	5653	68	4.15	0.11	0.36	PASTEL	1116.00000	2.6e+01	0.81	0.04	37.3	3.0	2.15	0.05	
8108-493-1	HD 48265 b	5733	55	4.09	...	0.38	PASTEL	762.00000	5.0e+01	0.24	0.10	29.0	6.0	1.59	0.07	
8189-1278-1	HD 85539 b	5164	10	4.36	0.03	-0.08	PASTEL	788.00000	2.5e+01	0.41	0.12	3.8	0.3	1.52	0.04	
8224-925-1	HD 103197 b	5250	84	4.45	0.15	0.22	PASTEL	47.84000	3.0e-02	0.00	...	5.9	0.3	0.25	0.00	
8265-2722-1	HD 117618 b	5977	15	4.35	0.03	0.01	PASTEL	25.82700	1.9e-02	0.42	0.17	12.8	2.2	0.17	0.00	
8312-3251-1	HD 148156 b	6185	36	4.51	...	0.25	PASTEL	1027.00000	2.8e+01	0.52	0.06	17.5	1.0	2.13	0.05	
8317-525-1	HD 330075 b	5000	21	4.26	0.03	0.05	PASTEL	3.38773	8.0e-05	0.00	...	107.0	0.7	0.04	0.00	
8345-4656-1	HD 156411 b	5901	8	4.01	0.02	-0.12	PASTEL	842.20001	1.4e+01	0.22	0.08	14.0	0.8	1.88	0.04	
8346-37-1	GJ 674 b	3257	150	4.92	0.21	-0.25	SWEET	4.69380	7.0e-03	0.20	0.02	8.7	0.2	0.04	0.00	
8354-785-1	GJ 676 A b	3734	181	4.62	0.09	0.08	PASTEL	1056.80005	2.8e+00	0.33	0.01	129.3	1.2	1.82	0.06	
8355-436-1	mu Ara b	5747	17	4.25	0.02	0.28	PASTEL	643.25000	9.0e-01	0.13	0.02	37.8	0.4	1.53	0.03	

Table 6 *continued*

Table 6 (*continued*)

Tycho	Name	T_{eff}	σT_{eff}	$\log g$	$\sigma_{\log g}$	[Fe/H]	$\sigma_{\text{[Fe/H]}}$	Source ^a	P_{orb}	σP_{orb}	e	σ_e	K_{RV}	σK_{RV}	a	σ_a
		K	K	[cgs]	[cgs]			d	d	d			m s ⁻¹	m s ⁻¹	AU	AU
8431-60-1	GJ 832 b	3419	150	4.83	0.15	-0.09	PASTEL	3657.00000	1.0e+02	0.08	0.04	15.4	0.7	3.56	0.15	
8449-868-1	HD 213240 b	5979	19	4.27	0.03	0.15	PASTEL	882.70001	7.6e+00	0.42	0.01	96.6	2.0	1.89	0.03	
8450-1033-1	tau Gru b	5944	17	4.11	0.02	0.20	PASTEL	1311.00000	4.9e+01	0.07	0.07	19.6	1.5	2.52	0.09	
8468-177-1	HD 2039 b	5945	36	4.38	0.06	0.30	PASTEL	1120.00000	2.3e+01	0.71	0.05	153.0	22.0	2.20	0.06	
8475-527-1	HD 10647 b	6158	20	4.46	0.03	-0.03	PASTEL	1003.00000	5.6e+01	0.16	0.19	17.9	4.6	2.02	0.08	
8500-534-1	HD 23079 b	5974	10	4.43	0.02	-0.13	PASTEL	730.59998	5.7e+00	0.10	0.03	54.9	1.1	1.60	0.03	
8502-1934-1	GJ 163 b	3223	172	4.87	0.18	-0.02	PASTEL	8.63100	1.0e-03	0.11	0.04	6.2	0.3	0.06	0.00	
8508-1724-1	HD 27894 b	4895	23	4.36	0.06	0.30	PASTEL	17.99100	7.0e-03	0.05	0.01	58.1	0.5	0.12	0.00	
8508-2041-1	epsilon Ret b	4773	52	3.59	0.09	0.35	PASTEL	428.10001	1.1e+00	0.06	0.04	32.2	1.4	1.19	0.03	
8515-1843-1	HD 30177 b	5556	23	4.30	0.05	0.37	PASTEL	2770.00000	1.0e+02	0.19	0.03	146.8	2.8	3.81	0.13	
8553-2637-1	HD 63765 b	5449	11	4.41	0.00	-0.16	PASTEL	358.00000	1.0e+00	0.24	0.04	20.9	1.3	0.94	0.02	
8638-692-1	HD 101930 b	5108	27	4.33	0.05	0.15	PASTEL	70.46000	1.8e-01	0.11	0.02	18.1	0.4	0.30	0.01	
8642-742-1	HD 102117 b	5655	16	4.29	0.02	0.28	PASTEL	20.81330	6.4e-03	0.12	0.08	12.0	0.9	0.15	0.00	
8668-674-1	HD 121504 b	6027	24	4.59	0.06	0.15	PASTEL	63.33000	3.0e-02	0.03	0.01	55.8	0.9	0.33	0.01	
8735-1682-1	HD 154857 b	5589	18	4.01	0.01	-0.22	PASTEL	408.60001	5.0e-01	0.46	0.02	48.3	1.0	1.29	0.02	
8735-1768-1	HD 154672 b	5743	23	4.27	0.04	0.25	PASTEL	163.94000	1.0e-02	0.61	0.03	225.0	2.0	0.60	0.02	
8826-247-1	HD 215497 b	5110	108	4.40	0.21	0.20	PASTEL	3.93404	6.6e-04	0.16	0.09	3.0	0.3	0.05	0.00	
8838-463-1	HD 221287 b	6324	43	4.61	0.01	0.05	PASTEL	456.10001	6.5e+00	0.08	0.11	71.0	13.0	1.25	0.04	
8847-598-1	HD 4308 b	5686	16	4.39	0.05	-0.35	PASTEL	15.56000	2.0e-02	0.00	0.00	4.1	0.2	0.12	0.00	
8855-128-1	HD 7199 b	5371	28	4.35	0.05	0.32	PASTEL	615.00000	7.0e+00	0.19	0.16	7.8	0.6	1.36	0.02	
8867-913-1	HD 23127 b	5773	56	4.16	0.06	0.26	PASTEL	1214.00000	9.0e+00	0.44	0.07	27.5	1.0	2.32	0.06	
8874-376-1	HD 25171 b	6220	39	4.43	...	-0.11	PASTEL	1845.00000	1.7e+02	0.08	0.06	15.0	3.6	3.03	0.19	
8892-1247-1	HD 40307 b	4866	26	4.49	0.04	-0.30	PASTEL	4.31150	6.0e-04	0.00	...	2.0	0.1	0.05	0.00	
8915-2808-1	HD 65216 b	5645	20	4.49	0.02	-0.16	PASTEL	613.09998	1.1e+01	0.41	0.06	33.7	1.1	1.37	0.03	
8939-306-1	HD 76700 b	5644	33	4.16	0.07	0.31	PASTEL	3.97097	2.3e-04	0.09	0.08	27.6	1.7	0.05	0.00	
8975-2606-1	NGC 4349 127 b	4445	87	1.64	0.23	-0.25	EXO	677.79999	6.2e+00	0.19	0.07	188.0	13.0	1.68	0.15	
8983-384-1	HD 108147 b	6242	15	4.50	0.04	0.18	PASTEL	10.89850	4.5e-03	0.53	0.12	25.1	6.1	0.10	0.00	
9023-815-1	HD 142415 b	5940	28	4.44	0.04	0.13	PASTEL	386.29999	1.6e+00	0.50	...	51.3	2.3	1.06	0.02	
9037-233-1	HD 147018 b	5491	12	4.50	...	0.00	PASTEL	44.23600	8.0e-03	0.47	0.01	145.3	1.7	0.24	0.00	
9083-198-1	HD 181433 b	4918	15	4.45	0.04	0.38	PASTEL	9.37430	1.9e-03	0.40	0.06	2.9	0.2	0.08	0.00	
9100-354-1	HD 196050 b	5879	28	4.25	0.05	0.21	PASTEL	1378.00000	2.1e+01	0.23	0.04	49.7	2.0	2.51	0.05	
9143-238-1	HD 11977 b	4893	112	2.89	0.02	-0.15	PASTEL	711.00000	8.0e+00	0.40	0.07	105.0	8.0	2.06	0.04	
9175-83-1	HD 38283 b	5981	12	4.23	0.02	-0.18	PASTEL	363.20001	1.6e+00	0.41	0.16	10.0	0.8	1.02	0.02	
9236-2866-1	HD 108341 b	5184	44	4.45	...	0.04	PASTEL	1129.00000	7.0e+00	0.85	0.09	144.0	188.5	2.01	0.03	
9241-249-1	HD 111232 b	5512	24	4.45	0.01	-0.43	PASTEL	1143.00000	1.4e+01	0.20	0.01	159.3	2.3	1.97	0.04	
9270-1491-1	HD 131664 b	5892	40	4.45	0.04	0.30	PASTEL	1951.00000	4.1e+01	0.64	0.00	359.5	22.3	3.17	0.07	

Table 6 *continued*

Table 6 (*continued*)

Tycho	Name	T_{eff}	$\sigma_{T_{\text{eff}}}$	$\log g$	$\sigma_{\log g}$	[Fe/H]	Source ^a	P_{orb}	$\sigma_{P_{\text{orb}}}$	e	σ_e	K_{RV}	$\sigma_{K_{\text{RV}}}$	a	σ_a
		K	[cgs]	[cgs]			d	d				m s ⁻¹	m s ⁻¹	AU	AU
9296-423-1	HD 175167 b	5635	28	4.09	0.09	0.28	PASTEL	1290.00000	2.2e+01	0.54	0.09	161.0	55.0	2.40	0.05
9340-1818-1	HD 216437 b	5840	22	4.24	0.04	0.22	PASTEL	1353.00000	2.5e+01	0.32	0.03	39.0	1.0	2.49	0.05
9354-780-1	HD 1237 b	5520	8	4.53	0.03	0.11	PASTEL	133.71001	2.0e-01	0.51	0.02	167.0	4.0	0.49	0.01
9385-1045-1	HD 63454 b	4812	28	4.28	0.03	0.10	PASTEL	2.81805	7.1e-05	0.00	0.01	64.2	1.6	0.04	0.00
9386-2614-1	HD 39091 b	5951	24	4.37	0.04	0.08	PASTEL	2151.00000	8.5e+01	0.64	0.01	196.4	1.3	3.35	0.10
9437-1921-1	HD 137388 b	5181	29	4.39	0.03	0.19	PASTEL	330.00000	3.0e+00	0.36	0.12	7.9	0.9	0.89	0.02
9479-407-1	HD 212301 b	6239	24	4.50	0.04	0.18	PASTEL	2.24571	2.8e-04	0.00	...	59.5	0.7	0.03	0.00
9522-552-1	HD 142022 b	5421	77	4.35	0.00	0.19	PASTEL	1928.00000	4.6e+01	0.53	0.20	92.0	65.5	2.93	0.07

^a Source for spectroscopic stellar parameters: EXO = [exoplanets.org](#); PASTEL = [Paunzen \(2015\)](#); SWEET = [Santos et al. \(2013\)](#); Ammons = [Ammons et al. \(2006\)](#); McDonald:2012 = [McDonald et al. \(2012\)](#); Wright:2003 = [Wright et al. \(2003\)](#).

Table 7. Results.

Tycho	Name	$\chi^2_{\nu}^{\text{a}}$	A_V	σ_{A_V}	F_{bol}	$\sigma_{F_{\text{bol}}}$	Θ	σ_{Θ}	R_{\star}	$\sigma_{R_{\star}}$	ρ_{\star}	$\sigma_{\rho_{\star}}$	M_{\star}^{b}	$\sigma_{M_{\star}}$	R_p	σ_{R_p}	M_p^{c}	σ_{M_p}
		mag.	mag.	erg s ⁻¹ cm ⁻²	erg s ⁻¹ cm ⁻²	μas	μas	R_{\odot}	g cm ⁻³	g cm ⁻³	M_{\odot}	R_{Jup}	R_{Jup}	M_{Jup}	M_{Jup}	M_{Jup}		
2-1155-1	WASP-32 b	0.58	0.06	0.03	6.85e-10	1.54e-11	19.02	0.63	0.95	0.15	1.18	0.11	0.72	0.34	0.96	0.15	2.63	0.82
12-104-1	HD 5319 b	3.03	0.06	0.01	2.04e-08	4.24e-10	163.12	2.37	4.19	0.15	1.18	0.03	1.44	0.31	1.71	0.26
30-116-1	WASP-71 b	0.45	0.00	0.00	1.43e-09	2.26e-11	28.28	0.96	1.82	0.19	0.18	0.03	0.76	0.27	1.18	0.12	1.39	0.33
32-383-1	HD 10442 b	2.31	0.06	0.00	2.47e-08	5.31e-10	169.77	3.48	4.73	0.20	2.58	0.42	2.94	0.38
88-57-1	WASP-82 b	0.62	0.13	0.05	2.92e-09	6.08e-11	35.22	1.05	2.10	0.16	0.22	0.02	1.48	0.37	1.62	0.13	1.17	0.20
90-645-1	HD 28678 b	1.41	0.18	0.01	1.91e-08	6.19e-10	169.89	7.72	6.98	0.46	3.16	0.51	2.55	0.32
96-602-1	GJ 179 b	1.04	0.00	0.00	3.44e-09	9.64e-11	141.42	8.62
107-1139-1	HD 33636 b	0.65	0.00	0.00	4.28e-08	4.02e-10	159.28	1.41	1.01	0.03	1.34	0.14	11.09	0.81
112-182-1	HD 34445 b	2.10	0.00	0.00	3.21e-08	4.85e-10	141.88	1.36	1.38	0.02	1.14	0.09	0.82	0.09
116-1316-1	HD 38529 b	4.87	0.00	0.00	1.09e-07	2.62e-09	287.55	3.90
127-402-1	HD 37605 b	0.68	0.00	0.00	9.93e-09	9.78e-11	95.70	1.38	0.95	0.02	0.68	0.08	2.17	0.16
154-891-1	HD 46375 b	0.80	0.00	0.00	2.02e-08	2.46e-10	140.64	1.09
203-1079-1	HAT-P-35 b	1.26	0.00	0.00	3.05e-10	7.81e-12	12.88	0.41	3.82	5.25	0.59	0.11	23.56	97.10	3.55	4.87	7.52	20.66
208-722-1	HAT-P-30 b	1.14	0.00	0.00	1.86e-09	3.79e-11	29.76	0.88	1.31	0.98	0.13	1.55	0.51	1.44	0.15	0.83	0.18	
211-706-1	WASP-84 b	0.26	0.00	0.00	1.50e-09	1.55e-11	37.80	1.44
213-177-1	GJ 328 b	1.45	0.00	0.00	7.08e-09	3.16e-10	151.50	8.49
219-1438-1	HD 74156 b	1.16	0.00	0.00	2.39e-08	2.85e-10	115.71	0.99
255-946-1	HD 95089 b	5.46	0.03	0.01	2.32e-08	1.36e-09	169.98	5.14
267-1200-1	HD 99492 b	4.42	0.00	0.00	3.19e-08	1.04e-09	211.16	16.60	0.83	0.07	0.48	0.51	0.07	0.05
275-157-1	HD 102195 b	1.47	0.00	0.00	1.79e-08	4.76e-10	130.44	1.76	0.82	0.01	0.76	0.04	0.41	0.02
275-243-1	HD 102329 b	1.12	0.07	0.01	2.68e-08	6.20e-10	19.93	6.40	9.82	0.75	3.21	1.28	8.16	2.19
320-1027-1	HAT-P-26 b	1.88	0.00	0.01	6.93e-10	2.12e-11	27.96	1.06	0.87	0.05	2.37	0.65	1.12	0.36	0.63	0.04	0.07	0.02
339-329-1	WASP-24 b	0.63	0.08	0.05	6.90e-10	1.62e-11	19.49	0.68	1.42	0.16	0.71	0.06	1.43	0.50	1.38	0.16	1.24	0.29
356-1276-1	omega Ser b	2.60	0.00	0.00	2.73e-07	7.36e-09	636.45	11.46
386-86-1	HD 149143 b	2.79	0.00	0.00	1.81e-08	4.20e-10	101.96	2.01	1.63	0.04	1.73	0.21	1.69	0.14
426-1099-1	HD 159243 b	1.30	0.00	0.00	9.27e-09	1.30e-10	70.79	0.67	1.13	0.03	1.65
430-2613-1	HD 164509 b	4.25	0.00	0.00	1.52e-08	4.51e-10	93.12	1.94	1.08	0.03	1.14
457-495-1	HD 175541 b	2.46	0.00	0.00	2.01e-08	4.07e-10	152.91	1.87	4.47	0.18	2.12	0.26	0.72	0.12
458-1450-1	HD 171028 b	1.33	0.04	0.00	1.42e-08	1.59e-10	101.61	0.81	2.47	0.07	1.53	0.13	2.62	0.16
488-2442-1	HAT-P-41 b	0.78	0.13	0.08	1.24e-09	3.85e-11	23.61	0.83	2.05	0.50	0.42	0.04	2.56	1.90	2.05	0.50	1.19	0.60
504-2458-1	HD 192699 b	1.66	0.00	0.00	7.88e-08	1.34e-09	288.29	7.49	4.31	0.15	1.61	0.51	2.32	0.51
534-2537-1	HD 200964 b	5.90	0.00	0.00	8.23e-08	3.62e-09	304.65	7.00	4.69	0.20	1.97	0.44	2.27	0.37
585-774-1	HIP 116454 b	3.02	0.00	0.00	2.67e-09	6.09e-11	54.70	1.25	0.72	0.02	3.00	0.34	0.81	0.11	0.22	0.01	0.04	0.01
601-636-1	HD 1502 b	3.65	0.05	0.01	1.49e-08	4.54e-10	133.22	2.49

Table 7 *continued*

Table 7 (continued)

Tycho	Name	χ_{ν}^2 ^a	A_V	σ_{AV}	F_{bol}	$\sigma_{F_{bol}}$	Θ	σ_{Θ}	R_*	σ_{R_*}	ρ_*	σ_{ρ_*}	M_* ^b	σ_{M_*}	R_p	σ_{R_p}	M_p ^c	σ_{M_p}
		mag.	mag.	erg s ⁻¹ cm ⁻²	erg s ⁻¹ cm ⁻²	erg s ⁻¹ cm ⁻²	μ as	R_{\odot}	g cm ⁻³	g cm ⁻³	M_{\odot}	R_{Jup}	M_{Jup}					
604-1102-1	HD 4313 b	1.47	0.06	0.00	2.49e-08	3.07e-10	172.57	1.27	4.91	0.24	...	2.47	0.52	2.99	0.43	
692-497-1	HD 31253 b	1.74	0.00	0.00	3.68e-08	6.76e-10	139.87	1.64	1.75	0.04	...	1.70	0.25	0.62	0.12	
736-601-1	HD 45652 b	0.73	0.00	0.00	1.67e-08	2.80e-10	129.16	2.61	0.96	0.02	...	0.54	0.09	0.35	0.05	
774-1441-1	HAT-P-24 b	0.57	0.05	0.06	5.55e-10	1.14e-11	15.89	0.43	1.38	0.22	0.74	0.12	1.37	0.69	1.30	0.21	0.75	0.25
794-1622-1	bet Cnc b	2.18	0.00	0.00	2.02e-06	4.96e-08	239.84	107.39	
805-24-1	HD 73534 b	3.05	0.00	0.00	1.65e-08	4.24e-10	142.44	2.00	2.63	0.07	...	1.40	0.09	1.20	0.10	
813-2344-1	M 67 SAND 364 b	3.58	0.00	0.00	5.31e-09	1.55e-10	108.75	1.66	39.59	35.82	...	9.06	16.45	6.69	8.12	
817-1748-1	HD 75784 b	4.25	0.00	0.00	2.41e-08	6.53e-10	176.01	3.95	3.17	0.18	...	1.33	0.24	5.42	1.62	
843-568-1	HD 89307 b	1.03	0.00	0.00	4.25e-08	4.08e-10	159.15	1.07	1.10	0.01	...	1.27	0.12	2.11	0.21	
869-1019-1	HD 106252 b	0.67	0.00	0.00	2.93e-08	2.88e-10	135.97	0.83	1.10	0.02	...	1.01	0.05	6.93	0.27	
870-114-1	HD 102272 b	1.23	0.10	0.01	1.28e-08	3.25e-10	134.83	2.85	10.30	0.97	...	1.45	0.27	4.94	0.64	
898-1042-1	70 Vir b	1.47	0.00	0.00	2.72e-07	4.58e-09	467.31	4.39	1.84	0.03	...	1.14	0.08	7.62	0.34	
910-165-1	HD 128311 b	4.56	0.00	0.00	3.34e-08	8.26e-10	203.13	3.68	
950-1156-1	WASP-38 b	1.08	0.04	0.01	5.11e-09	1.59e-10	51.26	1.15	1.52	0.07	0.71	0.05	1.76	0.28	1.23	0.06	3.44	0.36
983-872-1	HD 152581 b	3.44	0.08	0.01	1.59e-08	5.58e-10	133.08	2.63	4.80	0.24	...	1.72	0.26	2.28	0.26	
1014-973-1	HAT-P-57 b	0.98	0.00	0.02	1.61e-09	2.85e-11	27.45	1.10	1.85	0.39	0.62	0.03	2.77	1.74	1.74	0.36	1.41	1.52
1031-1530-1	HD 170469 b	1.35	0.00	0.00	1.40e-08	1.47e-10	94.97	1.05	1.24	0.02	...	1.10	0.08	0.66	0.11	
1055-3415-1	HD 183263 b	1.02	0.00	0.00	1.88e-08	2.11e-10	106.10	1.15	1.23	0.02	...	1.31	0.07	3.95	0.22	
1058-3400-1	xi Aql b	3.25	0.00	0.00	4.38e-07	1.42e-08	803.61	22.53	
1092-1778-1	HD 196885 b	1.96	0.00	0.00	7.36e-08	1.15e-09	188.91	2.48	
1107-2709-1	18 Del b	1.12	0.00	0.00	1.94e-07	4.14e-09	471.86	8.01	
1117-615-1	BD +14 4559 b	0.71	0.00	0.00	4.82e-09	5.54e-11	80.39	3.37	0.86	0.04	...	0.49	0.33	1.04	0.47	
1162-750-1	HD 220773 b	0.67	0.00	0.00	3.91e-08	2.45e-10	153.61	1.70	1.65	0.03	...	1.80	
1183-2072-1	HD 3651 b	1.55	0.00	0.00	1.35e-07	2.60e-09	378.62	6.76	
1194-26-1	HD 4203 b	1.05	0.00	0.00	9.15e-09	1.10e-10	83.64	0.79	1.42	0.05	...	1.25	0.16	2.23	0.21	
1195-588-1	HD 5891 b	0.81	0.00	0.00	2.10e-08	2.42e-10	181.65	9.62	10.64	0.99	...	1.93	0.54	7.63	1.43	
1211-1730-1	HD 10697 b	2.61	0.00	0.00	8.27e-08	1.42e-09	250.51	2.63	
1231-1727-1	HIP 14810 b	2.90	0.00	0.00	1.12e-08	4.18e-10	95.01	1.90	1.04	0.03	...	0.81	0.04	3.38	0.12	
1242-608-1	BD+20 594 b	0.33	0.11	0.04	1.23e-09	1.25e-11	28.89	1.00	1.08	0.06	1.89	0.34	1.67	0.40	0.23	0.01	0.07	0.03
1250-4-1	HD 285507 b	0.75	0.00	0.00	2.84e-09	5.55e-11	72.02	2.44	0.69	0.02	...	0.82	0.12	0.98	0.10	
1252-844-1	HD 24040 b	2.28	0.00	0.00	2.63e-08	3.00e-10	131.83	1.04	1.30	0.02	...	1.11	0.12	3.86	0.36	
1273-1104-1	epsilon Tau b	2.14	0.00	0.00	1.22e-06	2.31e-08	1252.55	17.53	
1275-2034-1	GJ 176 b	2.15	0.00	0.00	1.27e-08	6.47e-10	227.65	11.17	0.46	0.02	...	0.24	
1310-2544-1	HD 37124 b	3.15	0.00	0.00	2.43e-08	3.16e-10	138.72	1.29	
1391-121-1	K2-34 b	1.40	0.00	0.00	6.47e-10	1.27e-11	18.54	0.34	1.22	0.25	0.50	0.06	0.64	0.41	1.07	0.22	1.11	0.47
1398-321-1	Pr 201 b	0.36	0.03	0.04	1.76e-09	2.60e-11	30.19	0.54	1.15	0.12	...	1.24	0.39	0.54	0.12	

Table 7 (continued)

Table 7 (*continued*)

Tycho	Name	$\chi_{\nu}^{2\text{a}}$	A_V	σ_{AV}	F_{bol}	$\sigma_{F_{\text{bol}}}$	Θ	σ_{Θ}	R_*	σ_{R_*}	ρ_*	σ_{ρ_*}	M_*^{b}	σ_{M_*}	R_p	σ_{R_p}	M_p^{c}	σ_{M_p}
1408-143-1	HD 81040 b	1.11	0.00	0.00	2.23e-08	3.23e-10	123.56	1.28	0.91	0.01	...	1.05	0.19	7.27	0.98	
1422-614-1	TYC 1422-614-1 b	2.26	0.00	0.00	3.13e-09	9.19e-11	66.38	1.59	10.83	22.96	55.59	78.55
1422-790-1	BD +20 2457 b	5.45	0.00	0.00	7.54e-09	4.17e-10	131.13	5.36	71.02	73.63	...	1.23	0.16	0.30	0.04	
1422-1130-1	HD 88133 b	3.06	0.00	0.00	1.81e-08	4.12e-10	126.29	1.70	2.01	0.04	...	2.28	0.69	1.61	0.34	
1440-2597-1	HD 100635 b	1.73	0.03	0.01	9.04e-08	2.60e-09	344.22	8.24	10.06	0.86	
1445-2560-1	11 Com b	5.16	0.00	0.00	4.07e-07	1.70e-08	748.85	29.16	
1447-2345-1	HD 108863 b	1.06	0.07	0.01	2.86e-08	5.24e-10	195.72	3.41	7.19	0.39	...	2.17	0.46	2.84	0.42	
1454-315-1	HD 114762 b	1.56	0.00	0.00	3.32e-08	5.20e-10	144.82	1.33	1.20	0.02	...	0.80	0.06	10.69	0.56	
1460-132-1	tau Boo b	1.58	0.00	0.00	3.99e-07	3.91e-09	414.46	3.65	
1481-185-1	HD 131496 b	3.21	0.03	0.01	2.65e-08	8.91e-10	186.84	4.67	5.54	0.24	...	1.62	0.43	2.24	0.42	
1482-882-1	WASP-14 b	0.93	0.01	0.01	3.40e-09	6.80e-11	38.10	1.24	1.40	0.08	0.83	0.14	1.62	0.39	1.38	0.08	8.84	1.40
1496-1841-1	HD 142245 b	4.22	0.04	0.01	3.65e-08	1.64e-09	215.88	4.99	4.63	0.16	...	3.50	0.47	3.07	0.42	
1601-1129-1	HD 231701 b	0.56	0.02	0.01	7.00e-09	8.64e-11	60.23	1.16	1.42	0.05	...	1.52	0.23	1.31	0.18	
1622-1261-1	HAT-P-34 b	0.74	0.01	0.03	1.87e-09	3.29e-11	28.54	0.82	1.73	0.29	1.15	0.32	4.26	2.47	1.35	0.23	7.01	2.75
1632-1396-1	HAT-P-23 b	1.34	0.01	0.02	3.50e-10	9.10e-12	14.70	0.44	0.96	0.20	0.92	0.18	0.58	0.38	1.09	0.23	1.34	0.59
1640-113-1	HD 195019 b	2.97	0.00	0.00	4.82e-08	8.15e-10	181.80	2.09	1.48	0.03	...	1.21	0.08	3.98	0.17	
1681-1751-1	HD 210702 b	2.06	0.00	0.00	1.33e-07	2.50e-09	413.71	11.86	
1688-1821-1	HD 209458 b	1.27	0.00	0.00	2.34e-08	3.63e-10	112.92	0.96	1.19	0.02	1.04	0.07	1.23	0.09	1.39	0.02	0.73	0.04
1691-1788-1	HD 208527 b	5.51	0.13	0.05	1.62e-07	1.80e-08	678.05	43.50	
1716-1182-1	HD 219828 b	1.95	0.00	0.00	1.64e-08	2.62e-10	101.74	1.08	1.56	0.04	...	1.31	0.08	0.06	0.01	
1717-2193-1	51 Peg b	0.85	0.00	0.00	1.79e-07	2.05e-09	349.06	2.38	
1754-192-1	HD 8574 b	0.92	0.00	0.00	3.79e-08	3.70e-10	145.04	0.98	1.38	0.02	...	1.34	0.12	2.03	0.14	
1755-1637-1	HD 9446 b	0.68	0.00	0.00	1.25e-08	1.38e-10	90.38	0.83	
1758-2416-1	alpha Ari b	4.51	0.00	0.00	5.83e-06	1.75e-07	3183.93	62.53	
1761-192-1	HD 12661 b	0.60	0.00	0.00	2.95e-08	1.51e-10	147.52	1.71	1.20	0.02	1.20	0.10	2.43	0.14
1771-1397-1	30 Ari B b	1.31	0.00	0.00	4.24e-08	7.74e-10	140.73	3.03	1.41	0.05	...	1.93	0.27	13.82	1.80	
1818-1428-1	K2-29 b	0.40	0.12	0.05	5.00e-10	1.48e-11	21.34	0.44	
1833-1187-1	HD 32963 b	1.54	0.00	0.00	2.46e-08	2.55e-10	131.02	1.61	
1891-1178-1	WASP-12 b	0.18	0.29	0.02	7.66e-10	6.75e-12	19.10	0.91	1.59	0.18	0.42	0.07	1.20	0.45	1.82	0.21	1.31	0.33
1894-1961-1	HD 50554 b	0.75	0.00	0.00	4.91e-08	4.23e-10	168.00	1.15	
1901-976-1	HAT-P-56 b	0.44	0.00	0.00	1.14e-09	1.14e-11	21.41	0.34	1.47	0.11	0.63	0.03	1.42	0.33	1.51	0.11	2.31	0.44
1949-2012-1	55 Cnc b	0.61	0.00	0.00	1.23e-07	1.22e-09	350.24	4.41	
1951-1006-1	HD 79498 b	1.11	0.00	0.00	1.65e-08	2.28e-10	105.93	3.04	
1964-1473-1	mu Leo b	3.97	0.00	0.00	1.08e-06	2.18e-08	1407.71	19.20	
1973-954-1	KELT-4 A b	1.68	0.00	0.00	2.73e-09	4.32e-11	37.14	0.95	
1981-1168-1	HD 97658 b	2.49	0.00	0.00	2.47e-08	7.69e-10	160.74	2.95	0.74	0.01	3.06	0.50	0.89	0.15	0.21	0.01	0.03	0.00

Table 7 *continued*

Table 7 (continued)

Tycho	Name	χ_{ν}^2 ^a	A_V	σ_{AV}	F_{bol}	$\sigma_{F_{bol}}$	Θ	σ_{Θ}	R_*	σ_{R_*}	ρ_*	σ_{ρ_*}	M_* ^b	σ_{M_*}	R_p	σ_{R_p}	M_p ^c	σ_{M_p}	
		mag.	mag.	erg s ⁻¹ cm ⁻²	erg s ⁻¹ cm ⁻²	erg s ⁻¹ cm ⁻²	mas	mas	R_{\odot}	g cm ⁻³	g cm ⁻³	M_{\odot}	R_{Jup}	R_{Jup}	M_{Jup}	M_{Jup}			
1984-2613-1	GJ 436 b	3.57	0.00	0.00	7.62e-09	4.40e-10	204.88	8.69	0.09	1.14	0.09	0.71	0.21	0.94	0.09	0.45	0.09
1986-1561-1	WASP-56 b	2.27	0.00	0.00	3.89e-10	1.32e-11	17.22	0.68	0.96	0.09	1.14	0.09	0.71	0.21	0.94	0.09	0.45	0.09	
1989-2141-1	HD 108874 b	2.12	0.00	0.00	8.86e-09	1.75e-10	82.20	1.36	1.05	0.02	1.10	0.09	1.42	0.09	
1994-2335-1	HD 116029 b	1.06	0.03	0.01	2.49e-08	6.03e-10	186.04	4.75	4.89	0.21	0.83	0.24	1.40	0.29	
2031-1389-1	omicron CrB b	1.47	0.00	0.00	2.12e-07	3.02e-09	55.683	7.71	
2037-1826-1	epsilon CrB b	3.81	0.00	0.00	9.12e-07	3.23e-08	1333.77	25.92	
2038-1873-1	HD 145457 b	1.44	0.04	0.01	8.34e-08	2.80e-09	347.71	7.23	10.52	0.41	1.23	0.34	2.23	0.42	
2041-1657-1	XO-1 b	0.77	0.00	0.04	1.02e-09	2.14e-11	26.48	0.74	0.88	0.05	1.79	0.22	0.88	0.19	1.14	0.07	0.83	0.13	
2063-479-1	GJ 649 b	2.99	0.00	0.00	1.26e-08	4.66e-10	225.46	8.03	0.50	0.02	0.29	
2073-136-1	HD 15668 b	4.17	0.00	0.00	1.51e-08	6.25e-10	143.79	3.10	
2082-1290-1	HD 158038 b	1.31	0.04	0.01	3.53e-08	9.67e-10	217.80	4.56	4.50	0.16	1.30	0.56	1.53	0.47	
2099-908-1	HAT-P-31 b	0.45	0.01	0.05	7.13e-10	1.20e-11	19.88	0.68	1.39	0.11	0.69	0.34	1.31	0.73	1.09	0.15	2.27	0.84	
2099-2717-1	HD 164922 b	1.84	0.00	0.00	4.61e-08	7.38e-10	203.78	1.92	0.97	0.01	0.76	0.06	0.31	0.05	
2109-49-1	KELT-8 b	2.85	0.12	0.06	1.55e-09	6.87e-11	32.60	0.95	1.46	0.08	0.37	0.07	0.81	0.21	1.62	0.10	0.66	0.12	
2126-1196-1	HD 177830 b	5.95	0.00	0.00	4.49e-08	2.09e-09	241.51	6.75	3.26	0.12	1.70	0.28	1.69	0.20	
2141-972-1	HD 189733 b	1.77	0.00	0.00	2.68e-08	3.94e-10	175.76	1.75	0.75	0.01	2.65	0.25	0.79	0.08	1.13	0.01	1.13	0.08	
2148-1948-1	HD 188015 b	1.11	0.00	0.00	1.38e-08	1.60e-10	98.06	1.06	
2150-5013-1	HD 185269 b	1.71	0.00	0.00	5.64e-08	8.84e-10	177.87	1.68	2.00	0.05	1.57	0.13	1.09	0.08	
2153-1463-1	HD 190228 b	2.13	0.00	0.00	3.62e-08	6.41e-10	186.35	2.09	
2153-2883-1	HD 190360 b	2.16	0.00	0.00	1.39e-07	5.04e-09	330.73	6.17	1.14	0.02	0.99	0.08	1.54	0.08	
2163-549-1	HAT-P-49 b	1.30	0.05	0.05	1.98e-09	5.48e-11	26.22	0.54	2.06	0.23	0.36	0.06	2.22	0.83	1.59	0.18	2.20	0.59	
2261-371-1	HD 1605 b	2.61	0.00	0.00	3.45e-08	7.41e-10	224.70	5.31	4.33	0.14	1.72	0.30	1.16	0.15	
2265-107-1	WASP-1 b	1.98	0.08	0.06	6.17e-10	2.26e-11	18.22	0.43	
2285-553-1	HD 5608 b	3.71	0.00	0.00	1.30e-07	5.18e-09	405.85	9.67	5.09	0.16	1.98	0.26	1.65	0.18	
2313-437-1	HD 13189 b	5.86	0.29	0.09	5.69e-08	6.41e-09	374.71	22.14	38.41	4.84	2.24	0.88	10.95	2.92	
2340-1714-1	WASP-11 b	0.79	0.03	0.04	6.85e-10	1.51e-11	31.12	1.34	0.89	0.08	2.80	0.42	1.42	0.43	1.11	0.10	0.79	0.17	
2355-246-1	HD 22781 b	2.03	0.00	0.00	1.01e-08	2.15e-10	108.86	2.46	
2353-852-1	KELT-7 b	0.91	0.08	0.01	1.04e-08	2.03e-10	60.95	0.61	1.81	0.07	0.42	0.04	1.76	0.25	1.60	0.06	1.39	0.22	
2420-899-1	KELT-2 A b	1.38	0.08	0.00	9.56e-09	1.44e-10	66.91	1.77	1.93	0.10	0.30	0.03	1.54	0.28	1.35	0.08	1.70	0.22	
2461-988-1	HAT-P-33 b	0.57	0.00	0.00	9.20e-10	1.39e-11	19.99	0.57	1.79	0.48	0.45	0.04	1.82	1.45	1.85	0.49	0.92	0.50	
2463-281-1	HAT-P-9 b	1.92	0.00	0.00	3.41e-10	6.68e-12	12.54	0.61	
2469-686-1	HD 67087 b	0.64	0.00	0.00	1.58e-08	8.37e-11	85.57	0.26	1.41	0.03	2.31	
2488-663-1	HD 75898 b	1.60	0.00	0.00	1.59e-08	3.15e-10	94.08	1.27	1.55	0.04	1.43	0.24	2.70	0.33	
2496-1114-1	WASP-13 b	0.58	0.00	0.00	1.69e-09	1.50e-11	31.78	0.76	1.37	0.15	0.40	0.04	0.72	0.25	1.22	0.14	0.36	0.09	
2497-418-1	HD 82886 b	0.63	0.00	0.00	2.93e-08	1.55e-10	191.12	9.52	5.26	0.31	2.53	0.46	2.33	0.33	
2506-894-1	HD 87883 b	2.05	0.00	0.00	3.18e-08	9.69e-10	202.24	6.78	0.79	0.03	0.66	0.09	1.54	0.26	

Table 7 (continued)

Table 7 (*continued*)

Tycho	Name	χ_{ν}^2 ^a	A_V	σ_{AV}	F_{bol}	$\sigma_{F_{\text{bol}}}$	Θ	σ_{Θ}	R_*	σ_{R_*}	ρ_*	σ_{ρ_*}	M_* ^b	σ_{M_*}	R_p	σ_{R_p}	M_p ^c	σ_{M_p}
2524-2128-1	HIP 57274 b	1.65	0.00	0.00	1.06e-08	2.41e-10	138.74	8.51	0.78	0.05	...	0.29	0.30	0.02	0.01	
2532-556-1	KELT-6 b	2.65	0.00	0.00	1.99e-09	4.89e-11	32.82	0.62	1.73	0.12	0.39	0.10	1.42	0.46	1.30	0.09	0.52	0.12
2569-1599-1	HAT-P-4 b	1.01	0.00	0.00	8.66e-10	1.30e-11	23.48	0.67
2576-2228-1	rho CrB b	7.00	0.00	0.00	1.90e-07	9.05e-09	354.10	8.58
2578-1609-1	kappa CrB b	2.53	0.00	0.00	3.96e-07	5.67e-09	743.27	7.17
2595-1464-1	HD 155358 b	0.95	0.00	0.00	3.45e-08	3.18e-10	145.94	0.95	1.38	0.02	1.15	0.08	0.99	0.08
2620-648-1	TyES-4 b	0.74	0.00	0.00	6.29e-10	1.29e-11	17.87	0.47	1.66	0.19	0.33	0.04	1.08	0.38	1.61	0.18	0.78	0.19
2634-1087-1	HAT-P-5 b	0.53	0.00	0.00	4.75e-10	5.03e-12	16.81	0.57	1.12	0.09	1.04	0.14	1.04	0.29	1.21	0.10	0.98	0.20
2636-195-1	WASP-3 b	0.68	0.01	0.03	1.65e-09	2.41e-11	27.19	0.87	1.44	0.12	0.77	0.16	1.62	0.53	1.42	0.17	2.43	0.53
2648-2151-1	HD 178911 B b	5.01	0.00	0.00	1.92e-08	7.16e-10	121.55	5.49	1.08	0.05	1.24	0.58	8.03	2.51
2649-1153-1	HD 173416 b	1.12	0.04	0.01	1.34e-07	4.20e-09	438.75	6.90
2652-1324-1	TyES-1 b	0.58	0.00	0.03	6.13e-10	9.18e-12	24.80	0.51	0.85	0.05	2.37	0.19	1.04	0.19	1.13	0.06	0.84	0.11
2653-91-1	HD 180314 b	2.34	0.04	0.01	7.62e-08	1.81e-09	311.74	4.90	8.13	0.30	2.20	0.27	20.13	1.66
2664-550-1	HD 187123 b	0.99	0.00	0.00	2.00e-08	2.09e-10	114.86	0.98
2717-417-1	HAT-P-17 b	0.56	0.00	0.00	1.97e-09	3.04e-11	44.15	1.39	0.87	0.04	2.08	0.19	0.99	0.15	1.05	0.04	0.58	0.06
2737-1152-1	HAT-P-8 b	1.49	0.09	0.01	2.19e-09	3.39e-11	33.32	0.90	1.57	0.15	0.46	0.07	1.27	0.41	1.40	0.13	1.28	0.27
2767-1746-1	WASP-60 b	2.31	0.13	0.00	4.03e-10	1.19e-11	15.80	0.59	1.17	0.15	1.03	0.36	1.19	0.61	0.88	0.12	0.55	0.19
2792-1700-1	HAT-P-16 b	0.53	0.10	0.04	1.24e-09	1.94e-11	25.41	0.69
2794-157-1	GJ 15 A b	6.42	0.00	0.00	4.82e-08	4.11e-09	472.89	20.36	0.36	0.02	0.38	0.15	0.02	0.00
2822-2210-1	upsilon And b	1.53	0.00	0.00	5.95e-07	6.96e-09	558.55	3.86
2831-594-1	WASP-33 b	2.17	0.00	0.01	1.42e-08	2.27e-10	61.20	1.29	1.55	0.05	0.70	0.06	1.85	0.25	1.60	0.06	1.17	1.16
2840-1669-1	HD 16175 b	0.91	0.00	0.00	3.20e-08	3.76e-10	136.92	1.15	1.72	0.03	1.63	0.14	5.10	0.81
2842-200-1	HD 13931 b	1.09	0.00	0.00	2.43e-08	2.33e-10	123.98	1.23	1.25	0.02	1.30	0.13	2.20	0.21
2845-2243-1	HD 16760 b	2.59	0.00	0.00	9.12e-09	2.08e-10	84.37	2.62
2867-1318-1	HD 23596 b	2.84	0.00	0.00	3.32e-08	6.99e-10	136.81	1.97	1.53	0.03	1.47	0.18	9.03	0.74
2883-1687-1	HAT-P-15 b	1.32	0.15	0.06	8.38e-10	2.43e-11	25.57	0.91	1.07	0.07	1.14	0.14	1.00	0.23	1.06	0.07	1.94	0.30
2927-323-1	HD 45350 b	1.53	0.00	0.00	1.97e-08	3.21e-10	123.59	1.34
2930-2105-1	HD 43691 b	2.22	0.00	0.00	1.61e-08	2.76e-10	90.10	1.09
2937-1747-1	HD 40979 b	0.51	0.00	0.00	5.30e-08	4.89e-10	165.91	1.58	1.21	0.02	1.45	0.15	4.67	0.34
2946-426-1	HD 49674 b	0.53	0.00	0.00	1.60e-08	9.47e-11	110.26	0.97	1.02	0.01	1.03	0.11	0.10	0.01
2996-683-1	KELT-3 b	1.10	0.00	0.00	2.98e-09	4.31e-11	37.63	0.65	1.70	0.12	0.56	0.08	1.96	0.50	1.56	0.11	1.94	0.33
3004-578-1	HD 89744 b	0.76	0.00	0.00	1.35e-07	2.17e-09	258.10	2.61
3009-2703-1	47 UMa b	0.93	0.00	0.00	2.58e-07	4.17e-09	402.83	3.63
3011-791-1	HD 95127 b	2.37	0.00	0.00	2.65e-08	7.70e-10	250.84	5.13	41.01	18.22	3.70	4.16	10.63	8.06
3012-667-1	HD 96127 b	5.53	0.00	0.00	6.37e-08	4.05e-09	444.77	15.05	51.10	22.81	...	10.94	10.02	20.96	12.99	...
3013-1229-1	HAT-P-21 b	1.63	0.00	0.00	5.67e-10	1.45e-11	20.89	0.66	1.21	0.17	1.00	0.23	1.24	0.60	1.11	0.16	4.87	1.57

Table 7 *continued*

Table 7 (continued)

Tycho	Name	χ_{ν}^2 ^a	A_V	σ_{AV}	F_{bol}	$\sigma_{F_{bol}}$	Θ	σ_{Θ}	R_*	σ_{R_*}	ρ_*	σ_{ρ_*}	M_* ^b	σ_{M_*}	R_p	σ_{R_p}	M_p ^c	σ_{M_p}
3015-1137-1	HD 99706 b	6.16	0.00	0.00	2.96e-08	1.54e-09	197.09	5.84	6.29	0.28	...	1.70	0.35	1.39	0.24	
3020-2221-1	HAT-P-36 b	0.86	0.00	0.00	3.30e-10	6.61e-12	16.11	0.60	1.00	0.09	1.10	0.18	0.78	0.25	1.15	0.10	1.53	0.32
3048-172-1	HD 136418 b	1.54	0.00	0.00	2.23e-08	4.04e-10	164.34	1.63	3.78	0.10	...	1.48	0.12	2.14	0.15	
3050-1243-1	HD 132563 B b	10.49	0.00	0.00	8.29e-09	6.55e-10	69.64	3.60	
3063-1587-1	HD 149026 b	1.94	0.00	0.00	1.41e-08	2.28e-10	85.33	0.82	1.41	0.03	0.72	0.16	1.42	0.33	0.74	0.02	0.38	0.06
3065-1195-1	HAT-P-2 b	1.58	0.00	0.00	8.55e-09	1.72e-10	61.61	0.62	1.71	0.06	0.55	0.13	1.93	0.49	1.20	0.08	11.43	1.94
3067-576-1	14 Her b	3.73	0.00	0.00	6.39e-08	1.29e-09	243.04	3.39	0.93	0.01	...	0.90	0.04	4.66	0.15	
3086-152-1	HAT-P-14 b	1.55	0.11	0.03	2.84e-09	8.57e-11	33.53	1.04	1.82	0.15	0.62	0.08	2.65	0.73	1.42	0.12	3.44	0.63
3120-1368-1	Kepler-454 b	0.17	0.01	0.04	6.68e-10	4.44e-12	21.78	0.28	1.05	0.07	1.04	0.19	0.85	0.22	0.21	0.02	0.02	0.00
3131-1199-1	Kepler-37 b	8.55	0.00	0.00	3.60e-09	1.49e-10	56.04	1.94	0.79	0.03	2.50	0.33	0.87	0.15	0.03	0.00	0.01	0.01
3134-218-1	Kepler-93 b	0.47	0.04	0.01	2.92e-09	3.09e-11	46.08	1.27	0.98	0.04	1.65	0.01	1.09	0.14	0.14	0.01	0.01	0.00
3140-349-1	KOI-12 b	1.34	0.30	0.02	9.06e-10	1.78e-11	17.72	0.65	1.75	0.51	0.47	0.11	1.82	1.64	1.54	0.45	5.32	6.11
3147-188-1	Kepler-78 b	0.17	0.08	0.03	6.94e-10	4.24e-12	27.86	0.56	0.75	0.03	2.84	1.05	0.84	0.32	0.10	0.01	0.01	0.00
3161-126-1	HD 197037 b	0.91	0.00	0.00	5.14e-08	8.10e-10	164.88	1.71	1.18	0.02	1.19	
3227-413-1	HD 216536 b	1.88	0.25	0.01	9.49e-09	2.54e-10	123.98	2.94	9.83	1.28	0.81	0.44	1.05	0.40
3231-323-1	14 And b	3.00	0.00	0.00	2.78e-07	5.51e-09	663.23	10.19	
3239-392-1	HAT-P-6 b	1.04	0.03	0.05	1.83e-09	4.72e-11	27.12	0.75	1.62	0.17	0.59	0.08	1.79	0.60	1.48	0.15	1.32	0.30
3281-800-1	HAT-P-32 b	0.33	0.07	0.02	8.72e-10	9.13e-12	21.00	0.61	1.19	0.10	0.91	0.06	1.09	0.28	1.75	0.14	0.83	0.21
3293-1539-1	HAT-P-29 b	4.77	0.35	0.01	6.16e-10	1.89e-11	18.35	0.61	1.30	0.14	0.93	0.24	1.45	0.60	1.17	0.13	0.88	0.25
3304-101-1	HD 17092 b	3.09	0.05	0.06	3.67e-08	2.17e-09	280.39	20.92	13.58	1.27	6.73	2.24	10.13	2.29
3304-323-1	BD +48 738 b	1.60	0.40	0.01	1.42e-08	4.57e-10	167.95	12.33	
3413-5-1	XO-2 b	3.52	0.08	0.04	1.04e-09	5.21e-11	30.99	1.21	
3413-210-1	XO-2S b	2.04	0.12	0.06	1.09e-09	4.23e-11	31.06	0.88	1.00	0.04	0.98	0.20	0.26	0.04
3416-543-1	HAT-P-13 b	0.70	0.00	0.00	1.63e-09	3.13e-11	34.58	1.15	
3425-1596-1	HD 81688 b	1.66	0.00	0.00	2.25e-07	3.59e-09	55.65	8.03	
3431-46-1	HD 80606 b	1.71	0.00	0.00	6.98e-09	1.32e-10	73.99	0.97	1.04	0.02	1.45	0.32	1.15	0.27	1.07	0.03	4.38	0.74
3441-925-1	HAT-P-22 b	5.47	0.00	0.00	3.99e-09	1.25e-10	61.53	2.09	1.11	0.05	1.16	0.16	1.13	0.22	1.15	0.19	2.47	0.32
3466-819-1	HAT-P-3 b	0.68	0.03	0.01	8.26e-10	1.73e-11	29.29	0.95	0.87	0.06	2.28	0.34	1.06	0.28	0.54	0.07	0.65	0.11
3501-1373-1	HD 154345 b	0.95	0.00	0.00	5.56e-08	9.58e-10	215.91	2.18	0.85	0.01	0.71	0.07	0.82	0.07
3525-76-1	WASP-58 b	1.23	0.00	0.00	5.46e-10	1.14e-11	19.03	1.00	1.22	0.11	0.83	0.29	1.06	0.47	1.43	0.14	0.97	0.28
3546-413-1	Kepler-44 b	1.72	0.00	0.00	3.67e-10	8.68e-12	12.83	0.28	
3547-1402-1	HAT-P-7 b	1.10	0.14	0.04	1.72e-09	5.00e-11	27.85	0.43	2.00	0.28	0.27	0.03	1.56	0.68	1.51	0.21	1.84	0.53
3549-2811-1	TrES-2 b	3.38	0.13	0.01	7.84e-10	2.02e-11	22.41	0.48	1.12	0.07	1.38	0.16	1.36	0.30	1.36	0.08	1.49	0.22
3551-189-1	Kepler-68 b	2.26	0.04	0.01	2.41e-09	6.76e-11	40.06	1.17	1.28	0.06	0.80	0.05	1.19	0.18	0.21	0.06	0.02	0.01
3561-2092-1	HAT-P-11 b	2.21	0.00	0.00	5.86e-09	2.07e-10	94.63	3.77	0.77	0.03	2.73	0.26	0.88	0.14	0.43	0.02	0.09	0.01
3565-1525-1	16 Cyg B b	2.45	0.00	0.00	9.03e-08	1.83e-09	248.82	2.64	1.13	0.01	...	1.08	0.04	1.78	0.08	

Table 7 (continued)

Table 7 (*continued*)

Tycho	Name	$\chi_{\nu}^{2\text{a}}$	A_V	σ_{AV}	F_{bol}	$\sigma_{F_{\text{bol}}}$	Θ	σ_{Θ}	R_*	σ_{R_*}	ρ_*	σ_{ρ_*}	M_*^{b}	σ_{M_*}	R_p	σ_{R_p}	M_p^{c}	σ_{M_p}
3607-1028-1	HAT-P-40 b	0.54	0.25	0.06	7.90e-10	1.60e-11	20.82	0.72	1.94	0.22	0.20	0.04	1.03	0.40	1.52	0.17	0.48	0.13
3646-22986-1	HD 222155 b	0.93	0.00	0.00	4.00e-08	4.25e-10	168.49	2.80	1.85	0.04	1.21	0.10	2.12	0.50
3658-583-1	HD 2952 b	0.60	0.08	0.04	1.51e-07	6.42e-09	453.47	10.56	10.76	0.58	0.22	0.02	0.58	0.14	1.41	0.12	1.37	0.26
3727-1064-1	XO-3 b	1.21	0.00	0.01	2.86e-09	7.47e-11	35.45	0.72	1.54	0.11	0.22	0.02	1.97	0.38	7.29	1.19
3777-2071-1	6 Lyn b	2.72	0.00	0.00	1.38e-07	3.11e-09	402.86	6.43
3793-1994-1	XO-4 b	0.97	0.00	0.00	1.54e-09	3.33e-11	26.28	0.64	1.45	0.09	0.50	0.02	1.10	0.22	1.25	0.08	1.42	0.19
3839-846-1	HD 102956 b	5.36	0.00	0.00	2.31e-08	6.36e-10	166.81	2.53	4.41	0.15	1.59	0.18	0.92	0.07
3850-458-1	HD 118203 b	6.79	0.00	0.00	1.74e-08	6.50e-10	105.21	2.16	2.06	0.06	1.84	0.24	2.79	0.25
3861-267-1	HD 132406 b	1.44	0.00	0.00	1.17e-08	2.15e-10	88.61	1.43	1.34	0.04	1.03	0.15	5.38	1.31
3869-494-1	HD 139357 b	1.61	0.00	0.00	1.50e-07	3.24e-09	501.15	5.49
3875-1620-1	ιota Dra b	7.50	0.00	0.00	1.74e-06	6.73e-08	1739.51	40.53
3903-2143-1	HD 167042 b	0.85	0.00	0.00	1.35e-07	1.46e-09	422.98	12.53
3910-257-1	HD 163607 b	3.03	0.00	0.00	1.77e-08	3.64e-10	117.43	1.33	1.69	0.03	1.17
3925-739-1	WASP-48 b	2.77	0.00	0.01	5.57e-10	1.51e-11	18.44	0.97	1.58	0.21	0.32	0.04	0.88	0.36	1.50	0.20	0.80	0.23
4006-19-1	HD 240237 b	11.61	0.31	0.05	4.54e-08	4.50e-09	378.45	26.90	71.23	17.07	8.76	4.21	15.89	5.58
4006-980-1	HD 240210 b	6.54	0.12	0.04	3.73e-08	2.59e-09	356.81	22.30
4054-522-1	HD 13908 b	1.96	0.00	0.00	2.62e-08	4.06e-10	113.68	2.09	1.95	0.06	1.79
4126-818-1	HD 68988 b	1.43	0.00	0.00	1.40e-08	2.05e-10	92.03	1.02	1.19	0.02	1.28	0.09	1.97	0.10
4127-2431-1	οmicron UMa b	7.38	0.00	0.00	1.34e-06	5.27e-08	1178.36	25.32
4130-2355-1	4 UMa b	3.48	0.05	0.08	5.80e-07	5.91e-08	1050.13	54.34
4166-541-1	HD 113337 b	1.14	0.00	0.00	1.02e-07	1.08e-09	20.39	3.91
4202-656-1	HD 156279 b	2.56	0.00	0.00	1.73e-08	6.00e-10	121.28	2.76	0.95	0.02	0.95	0.08	9.88	0.69
4215-406-1	HIP 91258 b	1.63	0.00	0.00	1.01e-08	2.20e-10	90.17	2.50	0.89	0.03	0.97	0.28	1.09	0.21
4222-2311-1	42 Dra b	5.36	0.00	0.00	4.56e-07	1.82e-08	952.00	24.36
4283-211-1	HD 220074 b	12.09	0.20	0.09	2.34e-07	3.36e-08	923.70	86.92	54.92	8.76	2.20	2.62	16.64	13.26
4321-1320-1	HD 17156 b	1.04	0.00	0.00	1.45e-08	2.12e-10	90.38	0.99	1.55	0.04	0.53	0.03	1.41	0.12	1.10	0.03	3.51	0.21
4322-1310-1	HD 11755 b	1.15	0.14	0.11	8.86e-08	1.01e-08	438.50	24.95	20.58	2.27	0.72	0.17	5.63	0.92
4339-2274-1	HD 24064 b	7.05	0.32	0.09	1.38e-07	1.61e-08	619.67	36.93	40.00	4.20	1.61	0.53	12.89	2.89
4346-320-1	HD 32518 b	1.63	0.20	0.13	1.16e-07	1.56e-08	429.29	30.50
4400-99-1	HD 109246 b	3.14	0.00	0.00	8.28e-09	1.70e-10	72.98	0.91	1.07	0.02	1.20	0.53	0.86	0.25
4414-2315-1	11 UMi b	5.91	0.00	0.00	4.50e-07	2.49e-08	1035.45	36.73	29.79	2.84	2.78	0.69	14.74	2.50
4416-1799-1	bet UMi b	2.02	0.00	0.00	8.48e-06	1.87e-07	4910.83	249.69
4417-267-1	8 UMi b	8.07	0.02	0.03	6.37e-08	5.38e-09	294.33	12.47	10.30	0.57	1.44	0.19	1.31	0.16
4428-1943-1	GJ 687 b	5.14	0.00	0.00	3.24e-08	2.32e-09	441.80	30.24	0.43	0.03	0.45	0.07	0.06	0.01
4494-1346-1	HD 7924 b	0.86	0.00	0.00	4.22e-08	6.19e-10	213.63	2.01	0.78	0.01	0.65	0.05	0.02	0.00
4532-2096-1	HD 33564 b	0.65	0.00	0.00	2.38e-07	0.00e+00	325.01	5.26

Table 7 *continued*

Table 7 (continued)

Tycho	Name	χ_{ν}^2 ^a	A_V	σ_{AV}	F_{bol}	$\sigma_{F_{\text{bol}}}$	Θ	σ_{Θ}	R_*	σ_{R_*}	ρ_*	σ_{ρ_*}	M_* ^b	σ_{M_*}	R_p	σ_{R_p}	M_p ^c	σ_{M_p}
		mag.	mag.	erg s ⁻¹ cm ⁻²	erg s ⁻¹ cm ⁻²	erg s ⁻¹ cm ⁻²	mas	mas	R_{\odot}	g cm ⁻³	g cm ⁻³	M_{\odot}	R_{Jup}	R_{Jup}	M_{Jup}	M_{Jup}		
4550-2113-1	HD 104985 b	4.91	0.00	0.00	1.56e-07	4.34e-09	481.22	14.31	
4561-2319-1	HD 120084 b	0.62	0.00	0.00	1.42e-07	2.34e-09	432.02	3.61	
4606-3584-1	gamma Cep b	2.86	0.00	0.00	1.66e-06	3.06e-08	1525.31	30.65	
4620-342-1	HD 12648 b	0.58	0.01	0.01	5.54e-08	8.55e-10	275.72	2.31	11.02	0.48	...	0.67	0.07	1.96	0.22	
4671-94-1	HD 2638 b	4.19	0.00	0.00	5.82e-09	2.97e-10	77.68	2.00	0.94	0.03	...	0.77	0.09	0.42	0.03	
4683-883-1	HD 7449 b	1.87	0.00	0.00	2.67e-08	4.30e-10	122.48	1.19	0.97	0.02	...	1.14	0.05	1.38	0.53	
4697-201-1	WASP-77 A b	2.35	0.00	0.00	2.77e-09	1.16e-10	50.11	3.17	1.09	0.07	1.64	0.11	1.49	0.32	1.38	0.09	2.29	0.33
4698-1302-1	75 Cet b	1.49	0.00	0.00	2.32e-07	3.28e-09	561.73	6.70	
4701-1094-1	81 Cet b	1.64	0.10	0.03	1.90e-07	8.55e-09	503.49	11.84	
4701-1095-1	HD 16141 b	1.36	0.00	0.00	5.01e-08	5.72e-10	184.90	1.21	1.48	0.02	...	1.11	0.06	0.26	0.02	
4708-1423-1	HD 19994 b	0.49	0.00	0.00	2.41e-07	1.47e-09	355.43	2.45	
4748-1630-1	HD 30562 b	1.37	0.00	0.00	1.28e-07	1.48e-09	283.67	1.90	1.61	0.03	...	1.12	0.07	1.22	0.14	
4757-731-1	HD 290327 b	0.67	0.00	0.00	7.31e-09	1.38e-10	77.27	1.91	0.95	0.03	...	0.84	0.20	2.43	0.42	
4762-714-1	WASP-35 b	0.36	0.09	0.00	1.15e-09	1.77e-11	25.88	0.72	1.08	0.06	1.17	0.09	1.05	0.19	1.30	0.07	0.71	0.10
4799-1733-1	CoRoT-7 b	1.21	0.03	0.00	6.11e-10	1.37e-11	24.34	0.75	0.83	0.04	2.00	0.29	0.82	0.17	0.15	0.01	0.01	0.00
4822-3681-1	HD 52265 b	1.18	0.00	0.00	7.87e-08	1.13e-09	205.37	1.64	1.32	0.02	...	1.32	0.07	1.16	0.10	
4846-68-1	HD 66428 b	1.11	0.00	0.00	1.37e-08	1.63e-10	98.30	0.91	1.13	0.02	...	1.00	0.07	2.64	0.20	
4862-360-1	HD 72659 b	0.75	0.00	0.00	2.82e-08	2.94e-10	130.75	1.10	1.46	0.02	...	1.43	0.11	3.85	0.23	
4899-942-1	HD 86081 b	0.98	0.00	0.00	8.87e-09	1.65e-10	71.24	0.80	1.58	0.04	...	1.39	0.11	1.64	0.09	
4905-1374-1	24 Sex b	3.35	0.00	0.00	8.28e-08	1.63e-09	312.93	3.85	
4913-618-1	HD 92788 b	0.92	0.00	0.00	3.23e-08	4.91e-10	149.51	1.40	1.11	0.01	...	1.15	0.08	3.71	0.17	
4923-464-1	HD 99109 b	0.71	0.00	0.00	7.13e-09	9.83e-11	82.87	1.19	0.98	0.02	...	0.76	0.10	0.44	0.08	
4924-460-1	HD 96063 b	2.78	0.07	0.02	1.76e-08	6.79e-10	138.48	2.79	
4927-1063-1	WASP-106 b	0.74	0.01	0.01	6.65e-10	1.12e-11	19.26	0.88	1.31	0.38	0.57	0.06	0.93	0.80	1.02	0.30	1.62	0.94
4933-678-1	HD 100777 b	1.09	0.00	0.00	1.21e-08	2.95e-10	98.33	1.21	1.04	0.02	...	0.83	0.04	1.03	0.04	
4943-39-1	HD 107148 b	0.84	0.00	0.00	1.66e-08	9.37e-11	105.82	0.49	
4958-894-1	HD 114783 b	3.28	0.00	0.00	2.91e-08	6.80e-10	178.81	2.60	
4967-678-1	WASP-54 b	0.42	0.04	0.03	1.92e-09	3.65e-11	32.28	1.10	1.76	0.19	0.28	0.04	1.08	0.38	1.58	0.17	0.59	0.14
4983-226-1	HD 126614 A b	2.73	0.00	0.00	8.77e-09	3.60e-10	82.75	1.84	1.32	0.05	...	1.26	0.20	0.41	0.06	
4986-302-1	HD 130322 b	0.51	0.00	0.00	1.77e-08	1.53e-10	125.54	0.74	
5002-997-1	HD 136118 b	1.10	0.00	0.00	4.53e-08	9.97e-10	152.88	2.12	1.71	0.03	...	1.84	0.23	15.49	1.33	
5133-750-1	HD 179079 b	1.98	0.00	0.00	1.80e-08	3.14e-10	111.84	1.44	1.70	0.04	...	1.53	0.14	0.10	0.01	
5146-2250-1	HIP 97233 b	2.68	0.03	0.01	3.77e-08	1.03e-09	211.19	12.99	4.52	0.31	...	1.35	
5161-868-1	HD 192263 b	1.73	0.00	0.00	2.52e-08	3.76e-10	175.72	1.86	0.74	0.01	...	0.66	0.08	0.56	0.05	
5162-1142-1	WASP-74 b	2.73	0.07	0.00	3.68e-09	9.40e-11	46.29	1.80	1.42	0.10	0.48	0.06	0.98	0.24	1.36	0.10	0.72	0.12
5200-1560-1	WASP-69 b	0.71	0.00	0.00	4.09e-09	6.37e-11	79.30	1.81	0.86	0.03	2.18	0.25	0.98	0.14	1.11	0.04	0.29	0.03

Table 7 (continued)

Table 7 (*continued*)

Tycho	Name	χ_{ν}^2 ^a	A_V	σ_{AV}	F_{bol}	$\sigma_{F_{\text{bol}}}$	Θ	σ_{Θ}	R_*	σ_{R_*}	ρ_*	σ_{ρ_*}	M_* ^b	σ_{M_*}	R_p	σ_{R_p}	M_p ^c	σ_{M_p}
5221-210-1	HD 206610 b	2.19	0.06	0.01	1.65e-08	6.08e-10	147.08	5.08	4.92	0.30	...	1.93	0.59	2.56	0.53	
5227-1521-1	GJ 849 b	1.79	0.00	0.00	1.15e-08	4.73e-10	280.12	26.56	0.53	0.05	...	0.65	0.24	1.00	0.31	
5235-1468-1	HD 217107 b	2.80	0.00	0.00	8.91e-08	1.49e-09	258.69	2.71	1.11	0.01	...	1.00	0.05	1.30	0.05	
5242-229-1	HD 218566 b	5.71	0.00	0.00	1.27e-08	4.88e-10	137.92	6.41	0.85	0.04	...	0.76	0.32	0.20	0.06	
5242-591-1	HD 217786 b	1.48	0.00	0.00	2.07e-08	3.51e-10	109.06	1.51	1.32	0.03	...	1.43	
5258-491-1	HD 222582 b	1.19	0.00	0.00	2.29e-08	2.24e-10	123.69	0.87	1.13	0.02	...	1.12	0.06	8.37	0.40	
5261-789-1	HD 1461 b	1.92	0.00	0.00	6.84e-08	9.99e-10	217.69	2.48	
5262-825-1	HD 1690 b	6.77	0.07	0.03	1.09e-08	9.58e-10	149.58	6.90	21.66	6.18	...	1.86	1.06	8.79	3.63	
5273-16-1	HD 6718 b	1.04	0.00	0.00	1.15e-08	1.24e-10	87.32	1.34	0.95	0.02	...	1.08	0.21	1.68	0.24	
5278-2314-1	HD 11964 b	3.14	0.00	0.00	7.71e-08	1.24e-09	269.79	4.79	
5290-462-1	WASP-50 b	1.56	0.00	0.00	5.77e-10	1.33e-11	22.57	0.88	0.89	0.07	2.12	0.30	1.06	0.29	1.22	0.09	1.65	0.29
5296-1533-1	epsilon Eri b	1.46	0.00	0.00	9.71e-07	1.40e-08	1040.95	8.91	
5317-733-1	HD 28185 b	0.79	0.00	0.00	2.05e-08	1.14e-10	122.42	0.68	1.03	0.01	1.02	0.06	5.90	0.24
5342-401-1	HD 33844 b	0.88	0.03	0.00	4.19e-08	4.07e-10	237.20	9.83	5.39	0.28	...	1.84	0.39	2.01	0.31	
5342-891-1	HD 33142 b	0.80	0.03	0.00	2.13e-08	2.14e-10	159.44	1.25	3.97	0.14	...	1.78	0.31	1.50	0.22	
5347-367-1	HD 38801 b	2.77	0.00	0.00	1.52e-08	4.80e-10	121.22	2.28	2.38	0.07	...	1.64	0.15	12.12	0.79	
5367-701-1	HD 44219 b	1.40	0.00	0.00	2.26e-08	3.34e-10	122.80	2.44	1.39	0.03	...	1.12	
5409-2156-1	NGC 2423 3 b	1.15	0.45	0.09	5.01e-09	1.84e-10	93.81	3.40	19.17	4.96	...	2.12	1.47	9.78	4.56	
5435-2991-1	HD 69830 b	1.42	0.00	0.00	1.17e-07	2.16e-09	318.20	3.19	
5469-1000-1	HD 82943 b	1.14	0.00	0.00	6.39e-08	6.66e-10	193.68	1.16	
5480-20-1	BD -08 2823 b	2.17	0.00	0.00	4.67e-09	1.84e-10	80.67	4.15	0.71	0.04	...	0.50	0.26	0.04	0.01	
5503-946-1	BD -10 3166 b	3.18	0.00	0.00	3.01e-09	1.27e-10	51.68	1.38	0.91	0.04	...	1.47	0.24	0.59	0.07	
5504-418-1	HD 96167 b	1.48	0.00	0.00	1.54e-08	2.91e-10	100.67	1.45	1.85	0.05	...	1.67	0.13	0.80	0.08	
5519-1520-1	HD 106270 b	1.25	0.00	0.00	2.60e-08	3.89e-10	144.50	3.78	
5521-1086-1	HD 103774 b	1.54	0.00	0.00	3.60e-08	5.47e-10	120.95	3.42	1.47	0.05	...	5.07	
5594-1093-1	GJ 581 b	0.61	0.00	0.00	9.49e-09	2.88e-10	225.25	7.85	
5639-555-1	HD 148427 b	2.16	0.00	0.00	5.51e-08	9.07e-10	254.58	2.14	3.86	0.12	...	1.64	0.27	1.30	0.17	
5681-1576-1	HD 168443 b	0.89	0.00	0.00	4.77e-08	4.66e-10	192.88	1.58	
5685-2670-1	HD 168746 b	1.66	0.00	0.00	1.88e-08	2.35e-10	121.04	0.93	1.09	0.02	...	1.07	0.06	0.27	0.02	
5782-970-1	WASP-70 A b	2.30	0.08	0.03	1.06e-09	3.14e-11	27.49	0.87	
5803-1956-1	HD 210277 b	0.78	0.00	0.00	6.82e-08	7.84e-10	233.17	1.82	1.07	0.01	...	1.01	0.05	1.29	0.05	
5811-835-1	K2-39 b	3.38	0.08	0.01	1.62e-09	3.62e-11	46.33	0.64	2.97	0.04	0.01	0.66	0.56	0.15	0.09	0.05	...	
5819-1255-1	GJ 876 b	1.70	0.00	0.00	1.82e-08	6.84e-10	377.30	8.44	0.38	0.01	...	0.17	
5839-376-1	WASP-26 b	0.95	0.00	0.03	1.01e-09	2.43e-11	23.88	0.38	1.22	0.15	0.66	0.09	0.86	0.34	1.21	0.15	0.85	
5840-482-1	HIP 2247 b	3.78	0.00	0.00	6.21e-09	3.07e-10	99.18	5.66	0.74	0.04	...	0.31	0.19	2.85	1.16	
5842-736-1	HD 1666 b	0.42	0.03	0.00	1.44e-08	1.44e-10	81.27	2.20	2.06	0.08	...	4.90	

Table 7 *continued*

Table 7 (continued)

Tycho	Name	χ_{ν}^2 ^a	A_V	σ_{AV}	F_{bol}	$\sigma_{F_{\text{bol}}}$	Θ	σ_{Θ}	R_*	σ_{R_*}	ρ_*	σ_{ρ_*}	M_* ^b	σ_{M_*}	R_p	σ_{R_p}	M_p ^c	σ_{M_p}
5853-449-1	HIP 5158 b	1.71	0.00	0.00	3.44e-09	9.19e-11	69.40	5.02	0.75	0.06	...	0.43	0.35	0.96	0.56	
5858-2028-1	HD 11506 b	1.91	0.00	0.00	2.57e-08	3.87e-10	114.88	1.10	1.24	0.02	...	1.51	0.06	5.54	0.29	
5870-602-1	HD 18742 b	3.79	0.03	0.01	2.46e-08	7.53e-10	170.30	2.78	5.88	0.23	...	2.58	0.24	3.73	0.39	
5889-271-1	WASP-78 b	0.94	0.00	0.01	3.19e-10	7.97e-12	13.14	0.67	2.46	0.58	0.18	0.03	1.87	1.36	1.93	0.45	1.11	0.54
5936-2086-1	WASP-49 b	1.83	0.07	0.01	7.89e-10	2.17e-11	24.54	1.36	0.97	0.09	1.43	0.19	0.92	0.30	1.11	0.11	0.37	0.08
5956-2621-1	7 CMa b	9.27	0.00	0.00	8.44e-07	2.93e-08	1098.30	23.02	
5991-217-1	HD 60532 b	1.37	0.00	0.00	4.36e-07	4.71e-09	467.58	4.69	
6045-1121-1	HD 86264 b	2.04	0.00	0.00	2.79e-08	4.67e-10	112.16	2.12	
6083-1275-1	HD 95872 b	0.80	0.00	0.00	3.55e-09	6.22e-11	57.81	2.23	0.84	0.04	0.70	0.25	3.74	0.93
6087-1053-1	WASP-31 b	0.89	0.10	0.04	4.84e-10	1.25e-11	15.18	0.53	
6100-1491-1	HD 104067 b	3.84	0.00	0.00	2.26e-08	8.03e-10	168.74	3.46	0.74	0.02	0.62	0.13	0.16	0.02
6107-663-1	WASP-83 b	0.41	0.00	0.05	4.07e-10	4.60e-12	18.41	0.75	
6116-1517-1	61 Vir b	3.17	0.00	0.00	3.35e-07	1.13e-08	514.69	8.90	
6125-113-1	WASP-55 b	0.23	0.13	0.00	5.12e-10	3.08e-12	17.81	0.61	1.09	0.11	1.20	0.10	1.11	0.35	1.33	0.13	0.61	0.13
6143-1696-1	HD 125612 b	1.11	0.00	0.00	1.26e-08	1.86e-10	87.39	1.10	1.07	0.02	1.19	0.07	3.23	0.15
6147-229-1	WASP-16 b	2.32	0.10	0.00	9.23e-10	2.15e-11	25.61	1.38	1.14	0.09	1.68	0.30	1.78	0.54	1.22	0.10	1.24	0.25
6191-172-1	HD 141937 b	1.33	0.00	0.00	3.38e-08	4.79e-10	146.12	1.15	1.03	0.01	...	1.09	0.05	9.69	0.40	
6209-1322-1	HIP 79431 b	2.53	0.00	0.00	4.13e-09	2.11e-10	172.90	6.11	0.54	0.02	0.34	
6242-339-1	HD 156846 b	1.99	0.00	0.00	6.38e-08	7.69e-10	186.51	2.24	1.90	0.04	1.38	0.14	10.67	0.74
6244-136-1	HD 155233 b	6.66	0.00	0.00	5.98e-08	3.43e-09	272.37	18.13	
6307-1388-1	WASP-67 b	4.01	0.10	0.01	4.43e-10	1.57e-11	21.31	0.90	0.88	0.08	1.88	0.28	0.91	0.28	1.15	0.11	0.43	0.09
6336-204-1	WASP-68 b	0.80	0.13	0.04	1.89e-09	2.45e-11	34.09	0.73	1.79	0.19	0.36	0.06	1.49	0.53	1.32	0.14	1.08	0.25
6359-848-1	HD 202206 b	1.10	0.00	0.00	1.63e-08	2.57e-10	105.43	0.95	1.03	0.02	1.27	0.12	18.63	1.15
6373-214-1	HD 204941 b	1.17	0.00	0.00	1.35e-08	3.48e-10	126.03	2.20	0.78	0.01	0.58	0.08	0.23	0.03
6373-682-1	HD 204313 b	0.70	0.00	0.00	1.72e-08	2.52e-10	107.41	1.35	1.10	0.02	1.03	0.04	3.46	0.21
6385-788-1	HD 212771 b	3.49	0.01	0.01	3.16e-08	1.14e-09	189.40	3.64	4.55	0.15	2.41	0.18	3.69	0.52
6411-109-1	HD 224633 b	4.07	0.00	0.00	1.33e-08	4.09e-10	84.77	2.66	
6413-439-1	WASP-20 b	1.86	0.00	0.00	1.29e-09	2.89e-11	27.81	0.99	
6421-1078-1	HD 4732 b	1.63	0.00	0.00	1.45e-07	2.03e-09	418.87	3.91	
6423-1832-1	HD 4208 b	0.71	0.00	0.00	2.13e-08	2.13e-10	126.15	0.95	0.92	0.01	0.90	0.04	0.82	0.04
6434-494-1	HIP 12661 b	1.26	0.00	0.00	5.19e-09	1.51e-10	129.73	11.80	0.65	0.06	0.69	0.19	0.36	0.07
6445-136-1	HD 20782 b	0.51	0.00	0.00	3.09e-08	1.51e-10	143.71	0.90	1.11	0.01	1.07	0.07	1.95	0.59
6446-326-1	WASP-22 b	0.87	0.08	0.02	5.64e-10	1.16e-11	18.07	0.64	1.24	0.13	1.08	0.31	1.46	0.63	1.23	0.14	0.67	0.19
6466-1769-1	HD 30856 b	1.64	0.03	0.00	2.26e-08	4.31e-10	166.74	2.49	4.73	0.17	1.65	0.31	2.11	0.32
6469-1972-1	WASP-61 b	0.79	0.00	0.01	3.46e-10	6.86e-12	13.05	0.64	1.55	0.24	0.69	0.06	1.82	0.85	1.41	0.22	2.68	0.84
6481-1002-1	HD 33283 b	1.98	0.00	0.00	1.56e-08	1.98e-10	91.65	1.71	1.74	0.05	...	1.47	0.18	0.37	0.04	

Table 7 continued

Table 7 (*continued*)

Tycho	Name	χ_{ν}^2 ^a	A_V	σ_{AV}	F_{bol}	$\sigma_{F_{\text{bol}}}$	Θ	σ_{Θ}	R_*	σ_{R_*}	ρ_*	σ_{ρ_*}	M_* ^b	σ_{M_*}	R_p	σ_{R_p}	M_p ^c	σ_{M_p}
6507-2660-1	WASP-101 b	0.44	0.05	0.04	2.10e-09	3.25e-11	30.81	1.19	1.31	0.08	0.89	0.09	1.41	0.30	1.43	0.09	0.51	0.08
6516-711-1	HD 47186 b	0.89	0.00	0.00	2.44e-08	2.46e-10	133.78	0.82	1.08	0.01	...	0.96	0.05	...	0.05	...	0.07	0.00
6517-2108-1	HD 43197 b	0.97	0.00	0.00	7.29e-09	7.80e-11	78.09	0.81	1.03	0.02	...	0.77
6589-761-1	HD 77338 b	0.73	0.00	0.00	1.06e-08	1.56e-10	98.64	1.40	0.97	0.02	...	1.37	0.32	0.06	0.02
6631-431-1	HD 90156 b	0.68	0.00	0.00	4.82e-08	4.80e-10	191.03	1.08
6636-540-1	WASP-34 b	0.50	0.04	0.00	1.99e-09	2.07e-11	37.59	1.33	0.91	0.08	1.78	0.70	0.96	0.45	1.00	0.08	0.56	0.17
6649-807-1	HD 98219 b	1.43	0.00	0.00	1.95e-08	3.16e-10	156.54	2.06	3.85	0.15	1.71	0.31	2.20	0.28
6706-861-1	WASP-25 b	1.93	0.14	0.00	5.45e-10	1.23e-11	19.35	0.71	0.80	0.08	1.82	0.25	0.67	0.22	1.07	0.10	0.44	0.10
6766-877-1	HD 134987 b	2.52	0.00	0.00	6.79e-08	1.07e-09	216.81	2.19	1.22	0.03	...	1.10	0.07	1.61	0.07	...
6779-268-1	K2-38 b	0.64	0.13	0.04	1.09e-09	2.31e-11	27.23	0.64	1.38	0.21	1.21	0.70	2.24	1.67	0.17	0.03	0.06	0.03
6787-1927-1	WASP-17 b	0.43	0.04	0.06	7.76e-10	1.47e-11	177.79	0.57	1.49	0.19	0.98	0.20	2.28	0.99	1.87	0.24	0.78	0.23
6801-585-1	HD 145377 b	1.45	0.00	0.00	1.51e-08	1.66e-10	92.96	0.82	1.05	0.02	...	1.20	0.14	6.02	0.48	...
6854-175-1	HD 164604 b	2.57	0.00	0.00	4.95e-09	1.40e-10	86.62	2.81	0.72	0.02	...	0.39
6866-1721-1	HD 171238 b	0.71	0.00	0.00	1.03e-08	1.01e-10	94.98	0.86
6869-1277-1	HD 169830 b	0.81	0.00	0.00	1.13e-07	5.70e-10	230.56	1.28
6875-192-1	HD 181342 b	5.01	0.03	0.01	3.26e-08	1.44e-09	197.37	4.59	5.09	0.20	2.25	0.31	3.79	0.44
6875-222-1	HD 180902 b	1.18	0.03	0.00	2.62e-08	5.69e-10	177.80	1.95	3.78	0.11	...	1.52	0.09	1.56	0.20	...
6875-3273-1	HD 17949 b	2.07	0.00	0.00	8.08e-08	1.19e-09	201.21	1.79
6914-1943-1	HD 192310 b	9.61	0.00	0.00	1.48e-07	5.43e-09	410.30	7.99
6926-454-1	HATS-3 b	0.91	0.00	0.06	4.70e-10	1.21e-11	14.73	0.40	1.00	0.20	0.62	0.05	0.44	0.26	0.99	0.19	0.55	0.23
6936-378-1	HD 207832 b	1.34	0.00	0.00	8.45e-09	1.26e-10	75.88	1.03	0.96	0.02	1.02	0.06	0.60	0.06
6972-75-1	WASP-6 b	2.87	0.07	0.01	3.99e-10	1.36e-11	18.42	0.75	0.73	0.07	2.01	0.23	0.55	0.17	1.03	0.10	0.37	0.08
6974-283-1	HD 216770 b	5.29	0.00	0.00	1.58e-08	4.35e-10	118.09	1.82	0.93	0.02	...	0.74	0.07	0.57	0.05	...
6996-583-1	WASP-45 b	3.97	0.00	0.00	3.64e-10	1.23e-11	19.79	1.58	0.96	0.10	1.53	0.40	0.95	0.39	1.14	0.13	1.04	0.29
7011-487-1	WASP-72 b	0.54	0.07	0.00	1.17e-09	1.06e-11	24.00	0.78	2.18	0.29	0.38	0.08	2.78	1.28	2.29	0.18	2.30	0.70
7014-630-1	HD 16417 b	2.66	0.00	0.00	1.28e-07	1.42e-09	290.73	3.89
7023-236-1	HD 20868 b	1.97	0.00	0.00	3.84e-09	1.41e-10	73.59	4.68	0.76	0.05	...	0.39	0.27	1.25	0.59	...
7038-834-1	WASP-79 b	1.06	0.00	0.01	2.37e-09	4.55e-11	30.60	0.97	1.60	0.14	0.49	0.08	1.43	0.43	1.67	0.15	0.85	0.18
7073-2172-1	HD 45364 b	0.45	0.00	0.00	1.69e-08	1.38e-10	119.64	0.83
7096-565-1	HD 50499 b	0.88	0.00	0.00	3.43e-08	3.99e-10	138.97	0.95
7136-2907-1	HD 73256 b	1.47	0.00	0.00	1.71e-08	2.60e-10	119.99	1.51	0.93	0.01	...	0.81	0.04	1.57	0.07	...
7144-1553-1	HD 73267 b	1.19	0.00	0.00	8.11e-09	1.04e-10	84.98	0.65
7190-2048-1	HD 93083 b	5.28	0.00	0.00	1.47e-08	5.42e-10	130.24	2.91
7193-1804-1	WASP-66 b	0.48	0.22	0.03	6.79e-10	1.23e-11	16.39	0.76	1.76	0.35	0.34	0.06	1.33	0.83	1.40	0.28	2.35	0.98
7220-1321-1	GJ 433 b	1.19	0.00	0.00	1.24e-08	3.72e-10	25.09	0.50	0.04	...	0.59	0.22	0.02	0.01
7247-587-1	WASP-41 b	4.46	0.08	0.01	7.62e-10	3.33e-11	24.59	0.61	0.83	0.04	2.01	0.26	0.81	0.15	1.10	0.05	0.85	0.11

Table 7 *continued*

Table 7 (continued)

Tycho	Name	χ_{ν}^2 ^a	A_V	σ_{AV}	F_{bol}	$\sigma_{F_{\text{bol}}}$	Θ	σ_{Θ}	R_*	σ_{R_*}	ρ_*	σ_{ρ_*}	M_* ^b	σ_{M_*}	R_p	σ_{R_p}	M_p ^c	σ_{M_p}
7258-1542-1	HD 114386 b	2.96	0.00	0.00	1.16e-08	4.94e-10	126.10	2.85	0.76	0.02	...	0.60	0.09	1.14	0.13	
7263-2071-1	HD 114729 b	2.15	0.00	0.00	5.68e-08	8.72e-10	191.69	1.76	1.55	0.02	...	1.24	0.08	1.09	0.09	
7272-1998-1	HD 117207 b	0.92	0.00	0.00	3.46e-08	2.03e-10	158.80	0.91	1.11	0.01	...	0.96	0.08	1.73	0.11	
7283-1162-1	WASP-15 b	0.48	0.03	0.03	1.17e-09	1.83e-11	23.63	0.77	1.48	0.38	0.52	0.08	1.18	0.93	1.41	0.36	0.54	0.29
7287-1874-1	HIP 67851 b	1.87	0.00	0.00	1.11e-07	1.59e-09	396.25	15.08	
7428-2738-1	HD 181720 b	2.83	0.00	0.00	2.04e-08	2.43e-10	118.98	1.71	1.50	0.07	...	1.03	0.20	0.40	0.06	
7449-1245-1	HD 190647 b	0.90	0.00	0.00	2.11e-08	2.28e-10	125.15	0.77	1.45	0.02	...	1.14	0.04	1.94	0.08	
7466-1400-1	WASP-94 A b	0.19	0.00	0.01	2.32e-09	2.29e-11	34.67	0.92	1.48	0.12	0.73	0.22	1.67	0.64	1.58	0.13	0.50	0.13
7487-1980-1	HD 205739 b	1.79	0.03	0.00	1.00e-08	1.61e-10	67.27	1.88	1.35	0.05	...	1.66	
7522-505-1	WASP-8 b	3.15	0.00	0.00	3.76e-09	1.38e-10	53.56	1.82	1.03	0.04	1.74	0.26	1.34	0.26	1.13	0.05	2.54	0.33
7532-852-1	HD 4113 b	1.13	0.00	0.00	1.92e-08	2.00e-10	118.34	1.47	1.06	0.02	...	0.82	
7533-1111-1	HD 6434 b	1.58	0.00	0.00	2.23e-08	2.30e-10	122.84	0.87	1.12	0.01	1.10	0.13	0.49	0.04
7544-986-1	HD 8535 b	1.23	0.00	0.00	2.22e-08	2.56e-10	106.93	0.90	1.27	0.02	...	1.55	
7567-1183-1	HD 20794 b	1.99	0.00	0.00	5.57e-07	8.29e-09	700.70	6.93	
7612-556-1	WASP-63 b	1.43	0.11	0.04	1.07e-09	2.93e-11	29.15	1.13	1.86	0.19	0.28	0.04	1.28	0.42	1.41	0.14	0.37	0.09
7665-696-1	HD 70642 b	3.40	0.00	0.00	3.61e-08	6.85e-10	162.27	1.66	1.02	0.01	0.96	0.03	1.85	0.09
7670-3068-1	HD 73526 b	0.52	0.03	0.01	7.35e-09	8.16e-11	74.82	0.77	1.53	0.03	1.14	0.15	3.08	0.31
7683-1503-1	HD 75289 b	2.36	0.00	0.00	7.33e-08	1.10e-09	198.18	1.84	1.23	0.02	1.29	0.10	0.49	0.03
7704-39-1	HD 83443 b	7.18	0.00	0.00	1.37e-08	4.91e-10	108.26	2.06	0.94	0.02	0.79	0.07	0.34	0.02
7706-1752-1	HD 85512 b	4.96	0.00	0.00	3.92e-08	1.47e-09	293.21	8.26	0.71	0.02	0.43	0.10	0.01	0.00
7745-1381-1	HD 102365 b	0.85	0.00	0.00	3.07e-07	1.79e-09	484.08	3.87	
7762-1479-1	HD 109749 b	0.72	0.00	0.00	1.42e-08	1.47e-10	95.01	0.99	1.28	0.03	1.23	0.05	0.28	0.01
7774-1925-1	HD 114613 b	2.59	0.00	0.00	3.00e-07	4.85e-09	461.84	4.73	
7809-2461-1	HD 125355 b	2.67	0.00	0.00	9.55e-09	3.48e-10	121.67	8.89	0.74	0.05	0.29	0.25	0.02	0.01
7853-621-1	HD 147513 b	1.24	0.00	0.00	1.87e-07	2.08e-09	344.37	2.53	
7863-1386-1	HD 143361 b	0.63	0.00	0.00	5.82e-09	5.13e-11	68.89	0.39	1.02	0.02	0.87	
7881-474-1	HD 153950 b	3.83	0.00	0.00	2.87e-08	4.88e-10	123.75	3.46	1.28	0.04	1.25	0.18	2.95	0.29
7890-1378-1	HD 162020 b	3.90	0.00	0.00	8.64e-09	2.35e-10	114.13	3.77	0.75	0.03	0.42	0.18	9.84	2.75
7896-3839-1	HD 159868 b	1.91	0.00	0.00	3.52e-08	6.01e-10	165.76	1.88	1.97	0.04	1.42	0.12	2.51	0.16
7963-1570-1	WASP-7 b	0.60	0.00	0.00	4.02e-09	6.26e-11	42.39	1.37	1.44	0.07	0.90	0.12	1.91	0.39	1.07	0.06	1.25	0.23
7979-47-1	HIP 105854 b	5.40	0.00	0.00	2.30e-07	6.54e-09	672.35	31.89	
7982-636-1	HD 208487 b	1.26	0.00	0.00	2.69e-08	3.93e-10	118.41	1.21	
8015-1020-1	WASP-29 b	0.56	0.01	0.01	1.25e-09	2.11e-11	42.05	2.65	0.79	0.07	2.22	0.38	0.77	0.25	0.77	0.07	0.23	0.05
8017-108-1	WASP-4 b	1.74	0.00	0.00	2.80e-10	1.93e-09	259.40	3.03	
8025-341-1	HD 142 b	1.19	0.00	0.00	1.37e-07	1.93e-09	259.40	1.79	1.86	0.04	2.19	
8031-1-1	HD 5388 b	0.76	0.00	0.00	5.44e-08	3.25e-10	163.20	1.79	1.86	0.04	

Table 7 (continued)

Table 7 (*continued*)

Tycho	Name	χ_{ν}^2 ^a	A_V	σ_{AV}	F_{bol}	$\sigma_{F_{\text{bol}}}$	Θ	σ_{Θ}	R_*	σ_{R_*}	ρ_*	σ_{ρ_*}	M_* ^b	σ_{M_*}	R_p	σ_{R_p}	M_p ^c	σ_{M_p}
8040-72-1	WASP-18 b	0.48	0.00	0.00	5.10e-09	6.31e-11	47.28	0.77	1.29	0.05	0.97	0.15	1.46	0.29	1.20	0.05	11.44	1.51
8048-1022-1	GJ 86 b	3.06	0.00	0.00	9.85e-08	2.93e-09	320.07	4.96	0.77	0.01	...	0.93	0.06	4.42	0.20	
8055-876-1	WASP-117 b	0.52	0.00	0.01	2.34e-09	2.34e-11	36.31	1.10	1.22	0.06	1.00	0.17	1.29	0.30	1.06	0.07	0.30	0.05
8056-948-1	WASP-99 b	0.59	0.06	0.01	4.65e-09	5.60e-11	49.39	1.63	1.64	0.09	0.39	0.06	1.21	0.28	1.02	0.06	2.43	0.37
8056-1164-1	iota Hor b	1.03	0.00	0.00	1.77e-07	1.63e-09	302.68	2.77	1.13	0.02	...	1.34	0.13	2.27	0.25	
8075-1657-1	HD 28254 b	2.15	0.00	0.00	2.29e-08	4.45e-10	129.78	3.37	
8108-493-1	HD 48265 b	1.56	0.00	0.00	1.64e-08	1.94e-10	106.65	2.16	2.06	0.06	1.90	
8146-86-1	KELT-15 b	0.20	0.02	0.01	8.71e-10	8.25e-12	22.43	0.42	1.78	0.21	0.51	0.06	2.06	0.75	1.74	0.20	1.31	0.43
8189-1278-1	HD 85390 b	1.57	0.00	0.00	1.19e-08	1.94e-10	112.12	1.02	0.80	0.01	...	0.54	0.04	0.11	0.01	
8224-925-1	HD 103197 b	2.95	0.00	0.00	5.38e-09	1.97e-10	72.88	2.69	0.88	0.03	...	0.80	0.28	0.09	0.02	
8265-2722-1	HD 117618 b	0.79	0.00	0.00	3.62e-08	3.69e-10	145.78	1.05	1.20	0.01	1.17	0.09	0.19	0.04
8312-3251-1	HD 148156 b	0.98	0.00	0.00	2.18e-08	2.64e-10	105.64	1.42	1.30	0.03	1.99	
8317-325-1	HD 330075 b	0.96	0.00	0.00	6.14e-09	9.87e-11	85.83	1.02	0.84	0.01	...	0.47	0.04	0.48	0.02	
8345-4656-1	HD 156411 b	1.16	0.00	0.00	5.84e-08	7.03e-10	190.02	1.26	
8346-37-1	GJ 674 b	3.38	0.00	0.00	2.39e-08	1.27e-09	399.60	38.32	
8354-785-1	GJ 676 A b	4.85	0.00	0.00	1.07e-08	6.19e-10	203.01	20.55	0.69	0.07	...	0.73	0.21	4.96	0.96	
8355-136-1	mu Ara b	2.95	0.00	0.00	2.34e-07	3.79e-09	401.18	4.09	
8378-64-1	KELT-10 b	0.44	0.00	0.01	1.34e-09	1.87e-11	28.37	0.74	0.94	0.42	1.46	0.21	0.42	0.14	
8411-1384-1	WASP-88 b	1.08	0.12	0.01	6.86e-10	1.35e-11	17.35	0.72	1.80	0.26	0.23	0.03	0.94	0.42	1.23	0.09	1.44	0.28
8431-60-1	GJ 832 b	7.62	0.00	0.00	3.82e-08	1.92e-09	457.89	41.80	
8442-960-1	WASP-95 b	0.87	0.00	0.00	2.56e-09	4.43e-11	40.80	1.99	1.23	0.09	0.09	0.20	1.46	0.42	1.23	0.09	1.44	0.28
8449-868-1	HD 213240 b	2.03	0.00	0.00	4.92e-08	5.23e-10	169.93	1.45	1.51	0.02	1.57	0.12	5.58	0.31
8450-1093-1	tau Gru b	1.95	0.00	0.00	9.95e-08	1.66e-09	244.44	2.54	
8468-177-1	HD 2039 b	1.13	0.03	0.01	6.79e-09	8.34e-11	63.88	0.88	1.19	0.03	1.23	0.19	6.29	1.16
8475-527-1	HD 10647 b	0.59	0.00	0.00	1.62e-07	1.49e-09	290.60	2.38	
8478-1241-1	WASP-97 b	0.36	0.02	0.02	1.59e-09	2.50e-11	34.30	1.25	1.08	0.06	1.34	0.17	1.18	0.24	1.14	0.06	1.36	0.19
8500-534-1	HD 23079 b	1.57	0.00	0.00	3.85e-08	5.49e-10	150.64	1.21	1.07	0.01	1.12	0.06	2.61	0.11
8502-1934-1	GJ 163 b	5.66	0.00	0.00	3.03e-09	1.51e-10	145.20	15.91	
8508-1724-1	HD 27894 b	1.23	0.00	0.00	6.31e-09	1.14e-10	90.84	1.21	
8508-2041-1	epsilon Ret b	3.52	0.00	0.00	5.63e-07	1.13e-08	901.71	21.75	
8515-1843-1	HD 30177 b	1.39	0.00	0.00	1.20e-08	1.65e-10	97.18	1.06	1.13	0.04	0.93	0.12	9.46	0.84
8533-2637-1	HD 63765 b	0.82	0.00	0.00	1.66e-08	2.15e-10	118.74	0.94	0.83	0.01	0.65	0.01	0.53	0.03
8638-692-1	HD 101930 b	1.84	0.00	0.00	1.62e-08	4.81e-10	133.53	2.47	0.86	0.02	0.57	0.07	0.25	0.02
8642-742-1	HD 102117 b	0.86	0.00	0.00	2.85e-08	3.10e-10	144.59	1.17	1.23	0.02	1.06	0.07	0.17	0.01
8668-674-1	HD 121504 b	0.88	0.00	0.00	2.55e-08	2.74e-10	120.36	1.19	1.07	0.02	1.62	0.21	1.51	0.13
8735-1682-1	HD 154857 b	1.57	0.00	0.00	3.62e-08	4.47e-10	166.75	1.52	2.30	0.06	1.96	0.12	2.45	0.11

Table 7 *continued*

Table 7 (continued)

Tycho	Name	$\chi^2_{\nu}^{\text{a}}$	A_V	σ_{AV}	F_{bol}	$\sigma_{F_{\text{bol}}}$	Θ	σ_{Θ}	R_*	σ_{R_*}	ρ_*	σ_{ρ_*}	M_*^{b}	σ_{M_*}	R_p	σ_{R_p}	M_p^{c}	σ_{M_p}
8735-1768-1	HD 154672 b	1.22	0.00	0.00	1.42e-08	1.49e-10	98.92	0.95	1.32	0.02	...	1.18	0.12	5.37	0.39	
8805-131-1	WASP-73 b	0.65	0.03	0.04	1.87e-09	3.81e-11	32.62	1.34	2.55	0.21	0.04	2.52	1.22	1.42	0.22	2.86	0.92	
8826-247-1	HD 215497 b	4.74	0.00	0.00	8.68e-09	4.31e-10	97.76	4.79	0.85	0.04	...	0.67	0.33	...	0.02	0.01		
8838-463-1	HD 221287 b	2.20	0.00	0.00	1.97e-08	3.09e-10	96.23	1.55	
8847-598-1	HD 4308 b	2.44	0.00	0.00	6.49e-08	8.06e-10	215.79	1.84	1.02	0.01	...	0.93	0.10	...	0.05	0.00		
8855-128-1	HD 7199 b	3.09	0.00	0.00	1.74e-08	3.77e-10	125.11	1.90	0.97	0.02	...	0.77	0.09	...	0.27	0.03		
8867-913-1	HD 23127 b	1.26	0.00	0.00	9.94e-09	1.14e-10	81.94	1.68	1.64	0.05	...	1.42	0.20	1.64	0.18	
8874-376-1	HD 25171 b	1.32	0.00	0.00	2.09e-08	3.51e-10	102.24	1.58	1.25	0.03	...	1.53	
8884-719-1	WASP-100 b	1.20	0.10	0.00	1.47e-09	2.11e-11	22.07	0.79	1.57	0.16	0.28	0.13	0.77	0.42	1.33	0.14	1.26	0.45
8892-1247-1	HD 40307 b	3.02	0.00	0.00	4.70e-08	9.74e-10	250.83	3.80	
8900-874-1	WASP-62 b	0.17	0.01	0.01	2.22e-09	1.98e-11	33.24	0.87	1.23	0.08	0.85	0.11	1.11	0.25	1.32	0.08	0.52	0.08
8915-2808-1	HD 65216 b	1.44	0.00	0.00	1.84e-08	1.85e-10	116.54	1.04	0.88	0.01	...	0.88	0.04	1.18	0.06	
8939-306-1	HD 76700 b	0.93	0.00	0.00	1.51e-08	1.66e-10	105.50	1.37	0.03	0.99	0.17	0.21	0.03	
8975-2606-1	NGC 4349 127 b	1.95	1.40	0.05	5.60e-09	2.29e-10	103.73	4.59	19.98	6.23	0.64	0.52	5.90	3.24
8983-384-1	HD 108147 b	0.92	0.00	0.00	4.16e-08	3.77e-10	143.44	0.95	
9023-815-1	HD 142415 b	1.79	0.00	0.00	3.04e-08	4.08e-10	135.29	1.60	1.04	0.02	...	1.07	0.10	1.67	0.12	
9037-233-1	HD 147018 b	1.11	0.00	0.00	1.35e-08	1.86e-10	105.59	0.87	0.92	0.01	...	0.97	
9038-198-1	HD 181433 b	4.31	0.00	0.00	1.44e-08	3.80e-10	135.95	1.99	0.79	0.01	...	0.63	0.07	0.02	0.00	
9100-354-1	HD 196050 b	1.73	0.00	0.00	2.65e-08	4.21e-10	128.89	1.66	1.42	0.03	...	1.31	0.17	3.18	0.30	
9143-238-1	HD 11977 b	8.81	0.00	0.00	4.08e-07	1.86e-08	73.04	37.55	
9175-83-1	HD 38283 b	0.51	0.00	0.00	5.70e-08	2.83e-10	182.77	0.99	1.49	0.01	...	1.37	0.07	0.40	0.04	
9236-2866-1	HD 108341 b	2.80	0.00	0.00	5.34e-09	1.35e-10	74.50	1.60	
9241-249-1	HD 111232 b	0.38	0.00	0.00	2.63e-08	1.37e-10	146.18	1.43	0.90	0.01	...	0.84	0.03	7.14	0.19	
9270-1491-1	HD 131664 b	1.32	0.00	0.00	1.48e-08	2.45e-10	96.11	1.57	1.08	0.02	...	1.19	0.11	19.12	1.70	
9296-423-1	HD 175167 b	3.42	0.00	0.00	1.73e-08	3.52e-10	113.52	1.61	1.75	0.04	...	1.37	0.29	8.97	3.32	
9340-1818-1	HD 216437 b	1.81	0.00	0.00	9.87e-08	1.04e-09	252.33	2.35	
9354-780-1	HD 1237 b	0.47	0.00	0.00	6.51e-08	3.25e-10	229.36	1.00	
9385-1045-1	HD 63454 b	1.14	0.00	0.00	6.34e-09	1.50e-10	94.20	1.57	0.77	0.01	...	0.42	0.03	0.25	0.01	
9386-2614-1	HD 39091 b	2.65	0.00	0.00	1.43e-07	2.86e-09	292.33	3.81	
9437-1921-1	HD 137388 b	0.82	0.00	0.00	9.85e-09	8.42e-11	101.25	1.24	0.88	0.01	...	0.68	0.05	0.20	0.02	
9479-407-1	HD 212301 b	2.23	0.00	0.00	2.06e-08	3.58e-10	100.88	1.19	1.16	0.02	...	1.55	0.16	0.51	0.04	
9522-552-1	HD 142022 b	1.72	0.00	0.00	2.30e-08	2.18e-10	141.33	4.10	1.04	0.03	...	0.90	0.05	4.44	3.17	

^a Reduced χ^2 of the SED fit.^b For transiting planet hosts, M_* is calculated from the direct observables ρ_* and R_* . For RV planet hosts, M_* is calculated from the direct observables $\log g$ and R_* .^c For RV planets, M_p is modulo $\sin i$.

APPENDIX

A. SPECTRAL ENERGY DISTRIBUTION MEASUREMENTS AND FITS FOR PLANET HOST SAMPLE

In Figure Set 14 we present the observed and fitted spectral energy distributions of the 498 planet host stars for which we were able to perform our SED fitting procedures, which includes the 358 planet host stars in our final study sample having *Gaia* DR1 parallaxes (Tables 5 and 6).

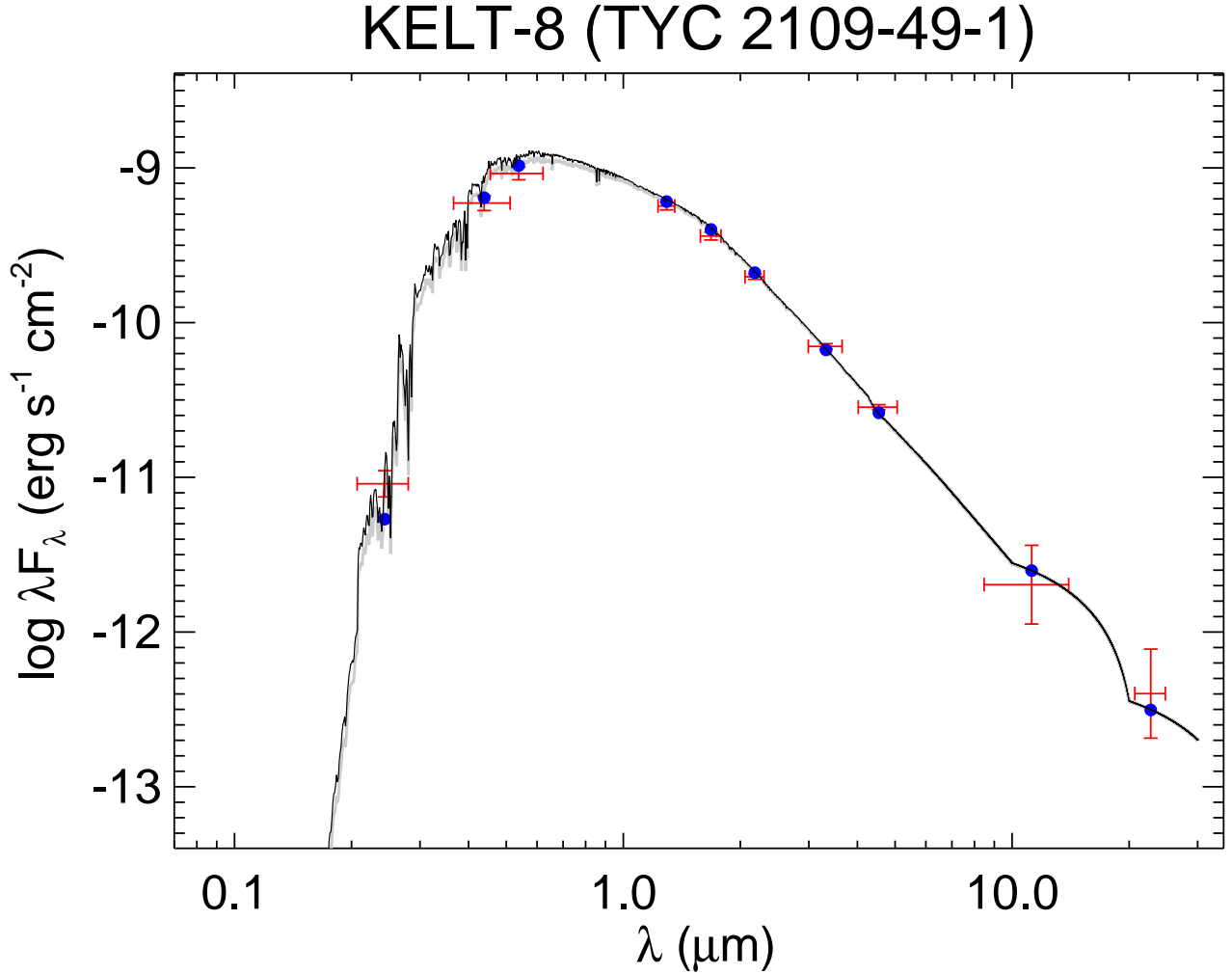


Figure 14. KELT-8 is shown as an example of the figure set. Each panel in the Figure Set is labeled at top by the *Tycho-2* ID and common name of the star, and shows the observed fluxes (in units of $\text{erg cm}^{-2} \text{s}^{-1}$) versus wavelength (in μm) as red error bars, where the vertical error bar represents the uncertainty in the measurement and the horizontal “error” bar represents the effective width of the passband. Also in each figure is the fitted SED model including extinction (light gray curve), on which is shown the model passband fluxes as blue dots. The corresponding un-extincted SED model is also shown (dark black curve); the reported F_{bol} is the sum over all wavelengths of this un-extincted model (see the text). The full figure set is displayed in Figures 15–97.

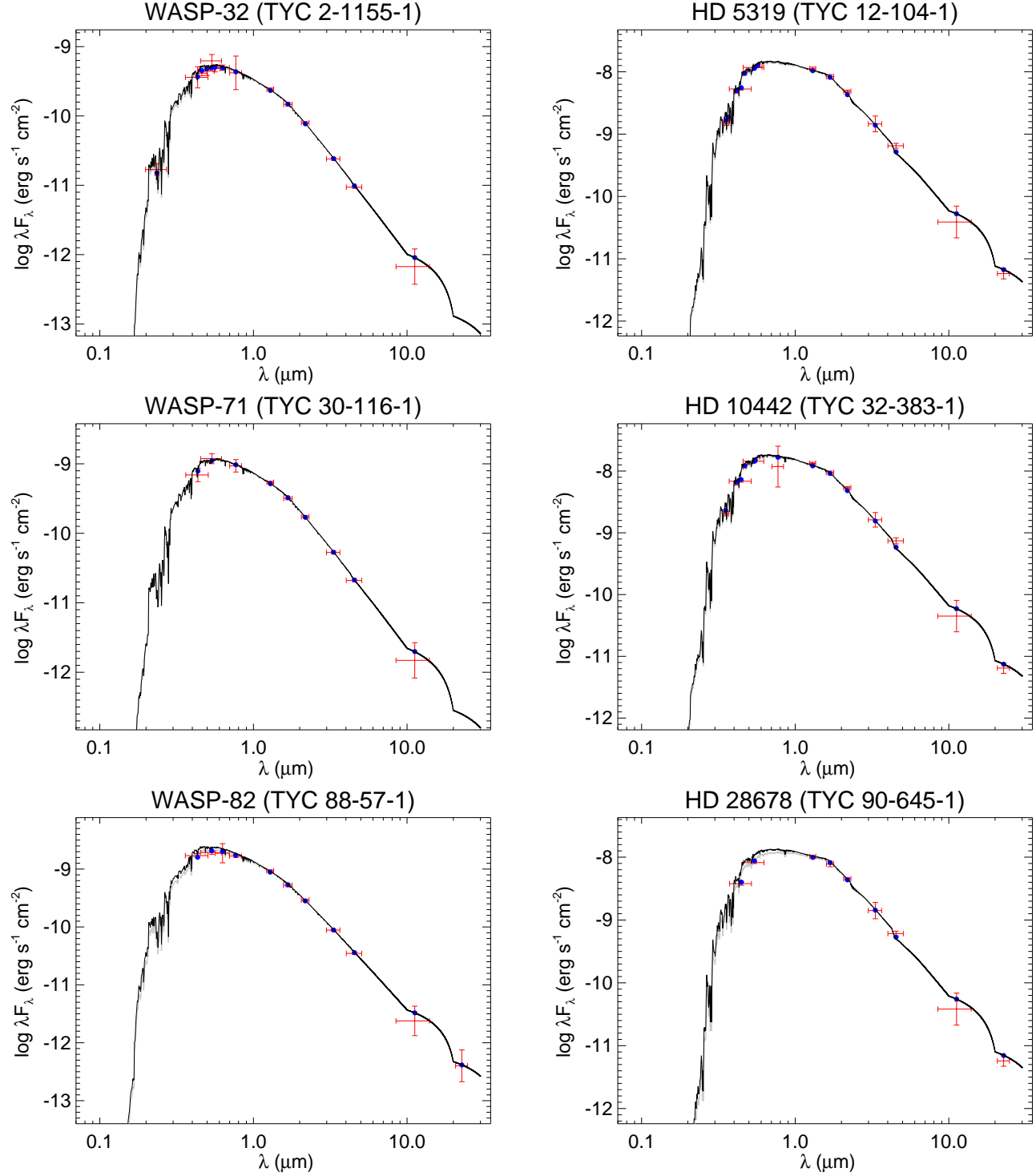


Figure 15. All labels, lines, symbols, and colors as in Figure 14.

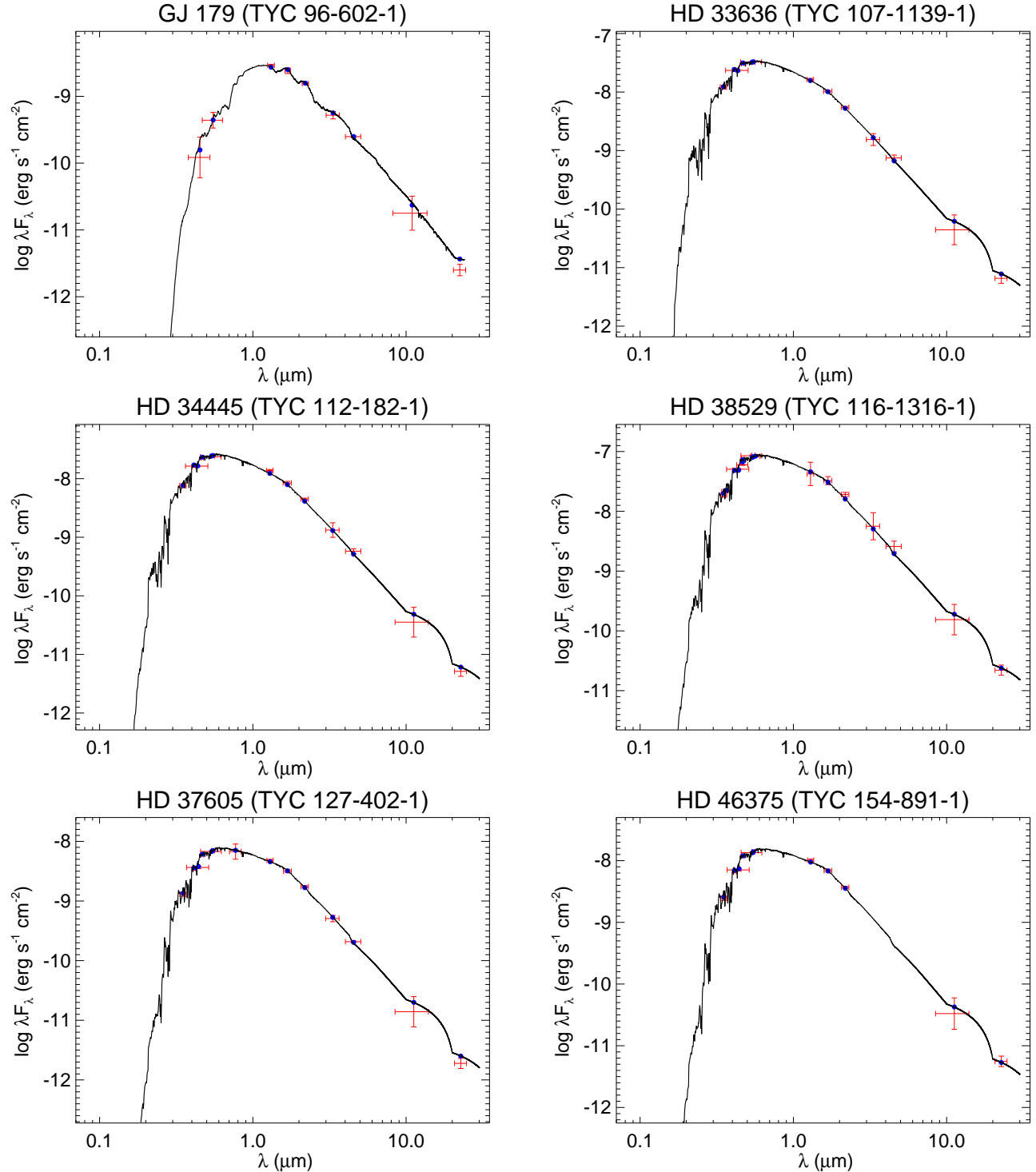


Figure 16. All labels, lines, symbols, and colors as in Figure 14.

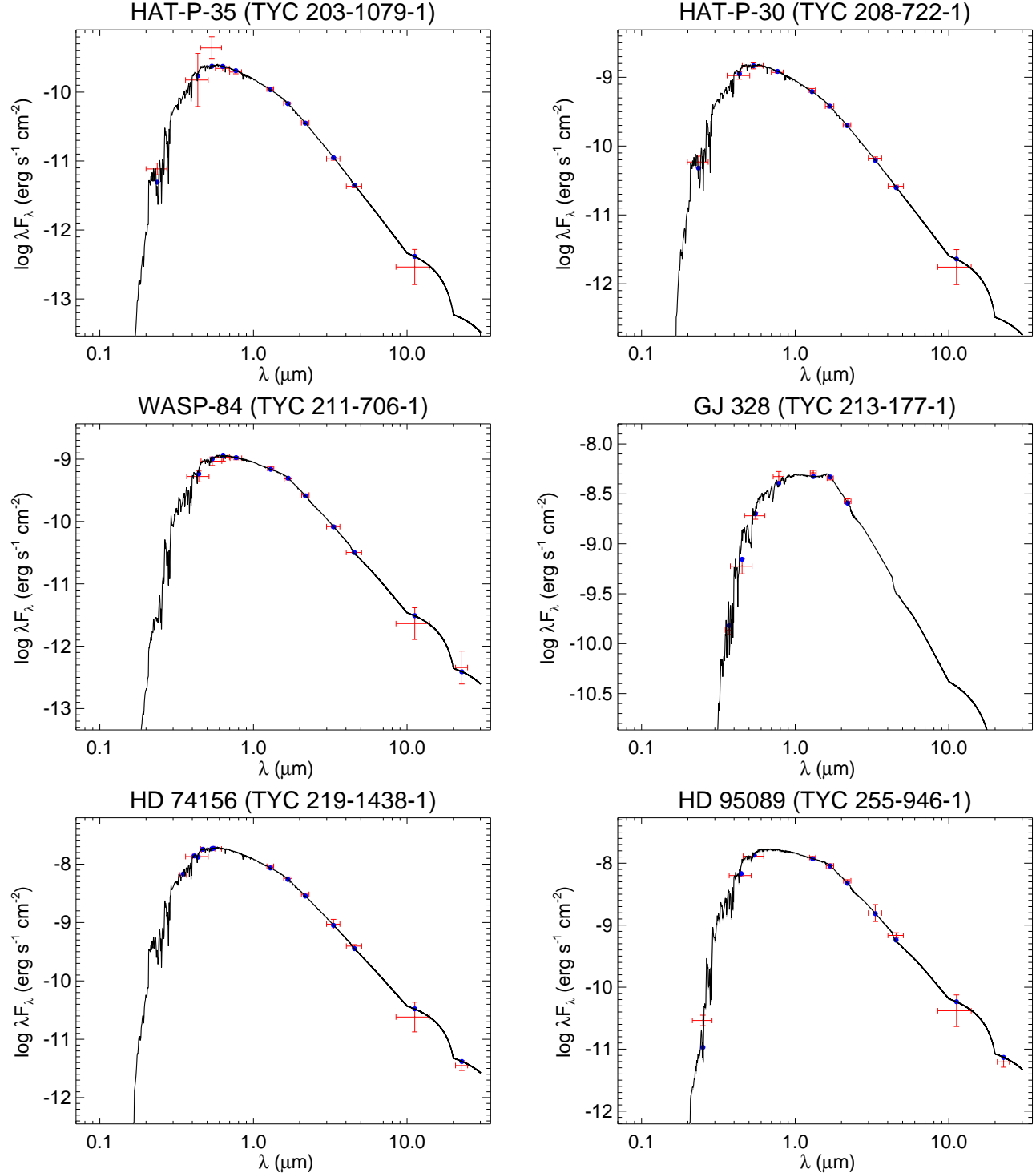


Figure 17. All labels, lines, symbols, and colors as in Figure 14.

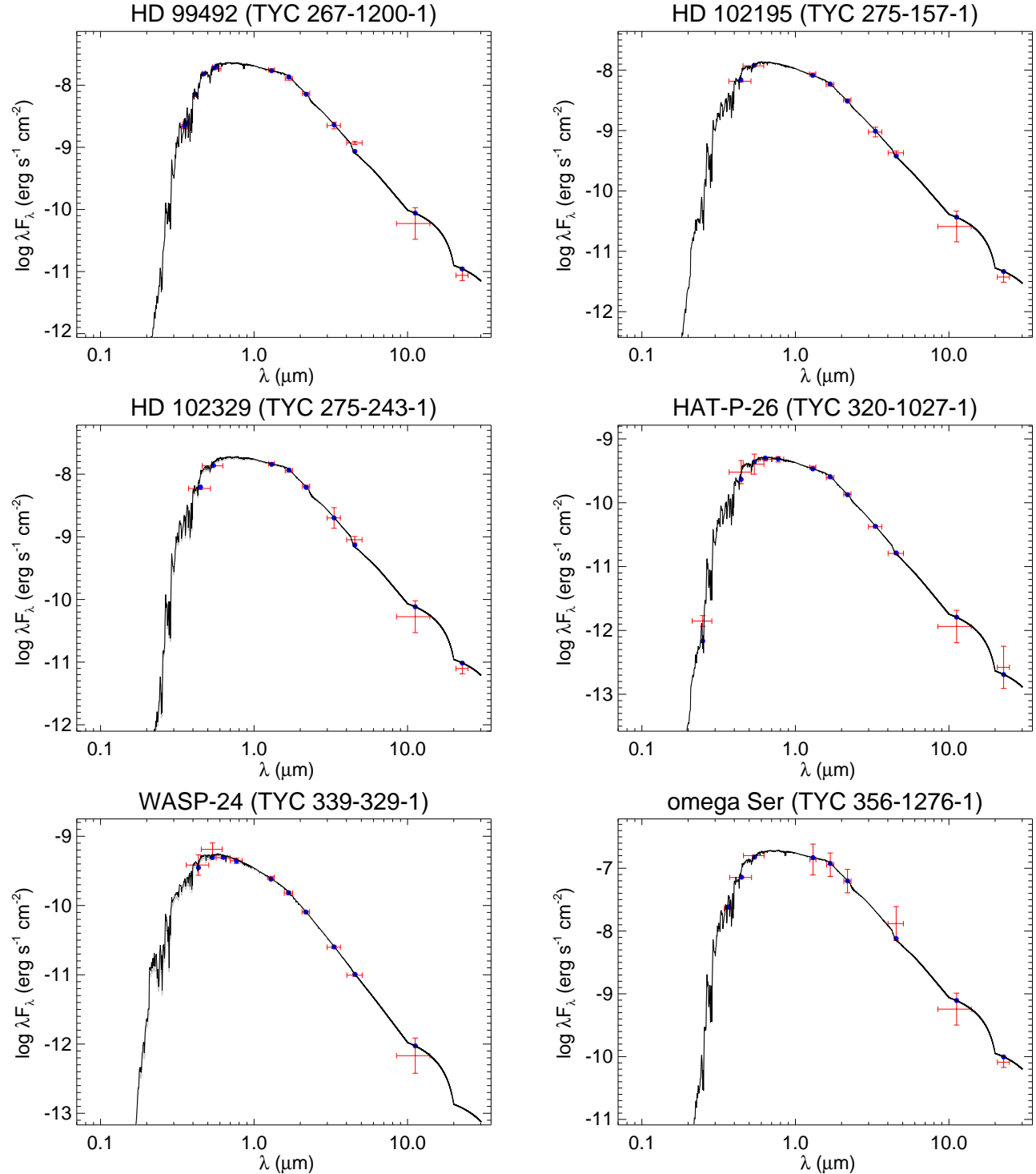


Figure 18. All labels, lines, symbols, and colors as in Figure 14.

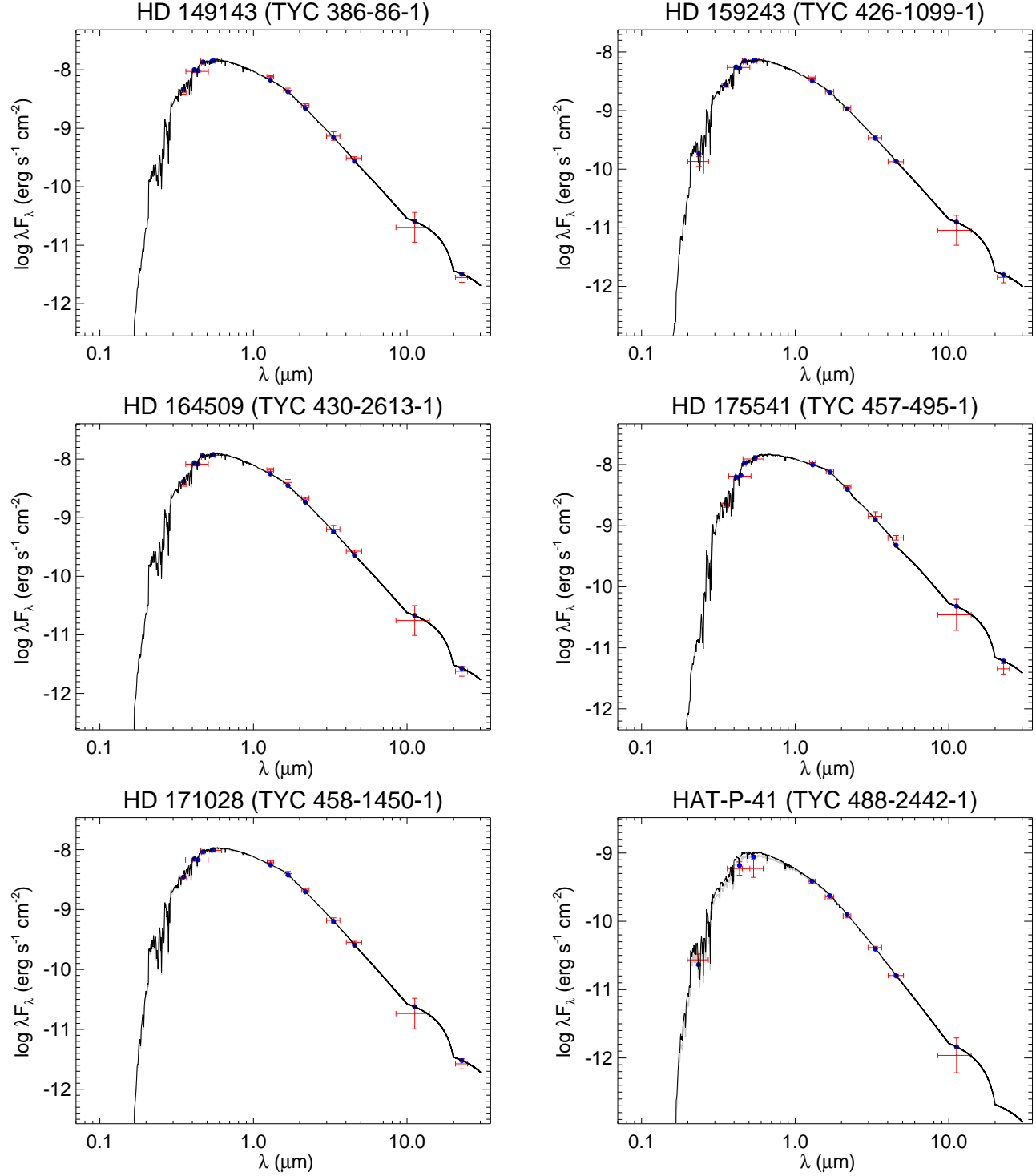


Figure 19. All labels, lines, symbols, and colors as in Figure 14.

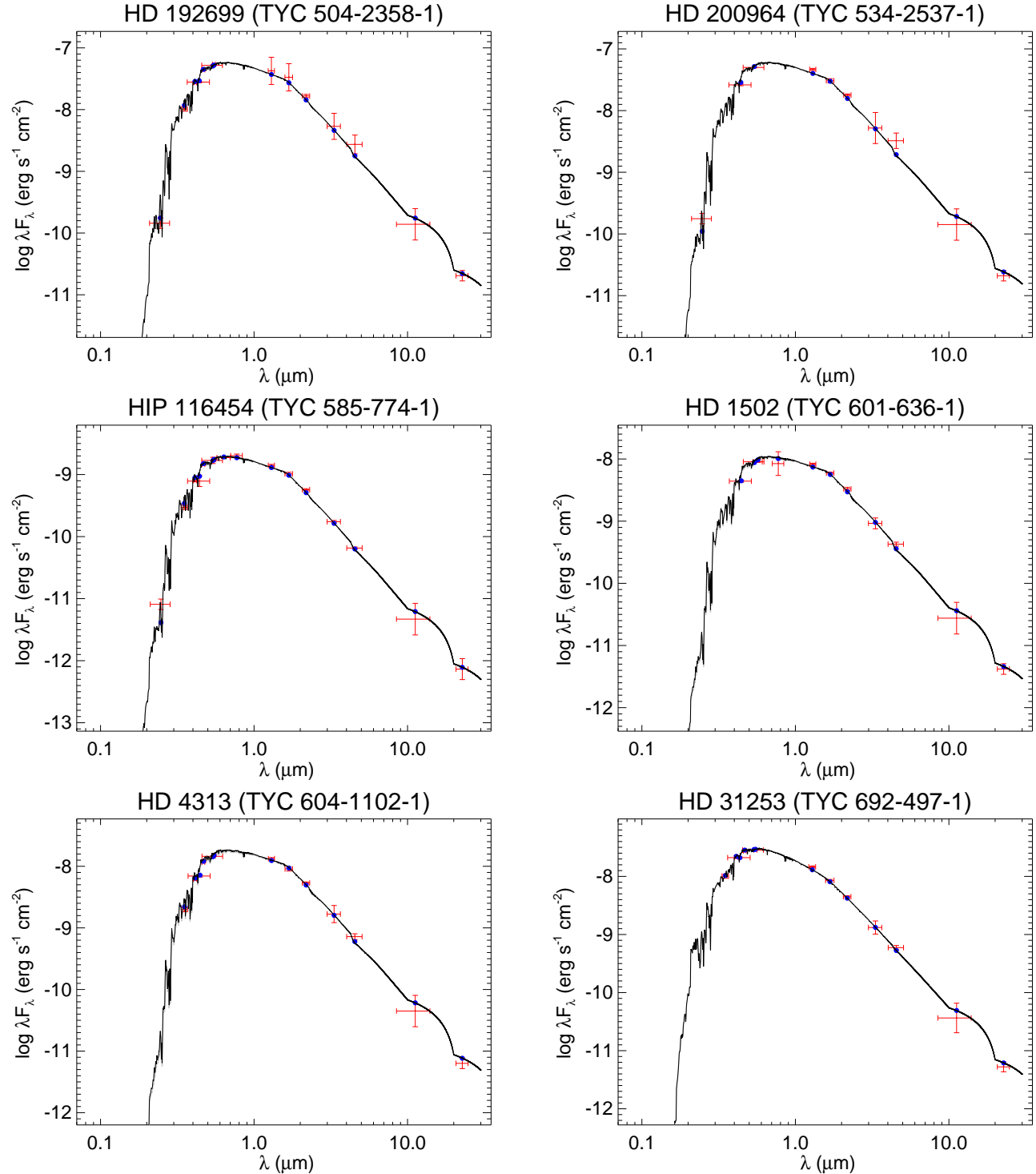


Figure 20. All labels, lines, symbols, and colors as in Figure 14.

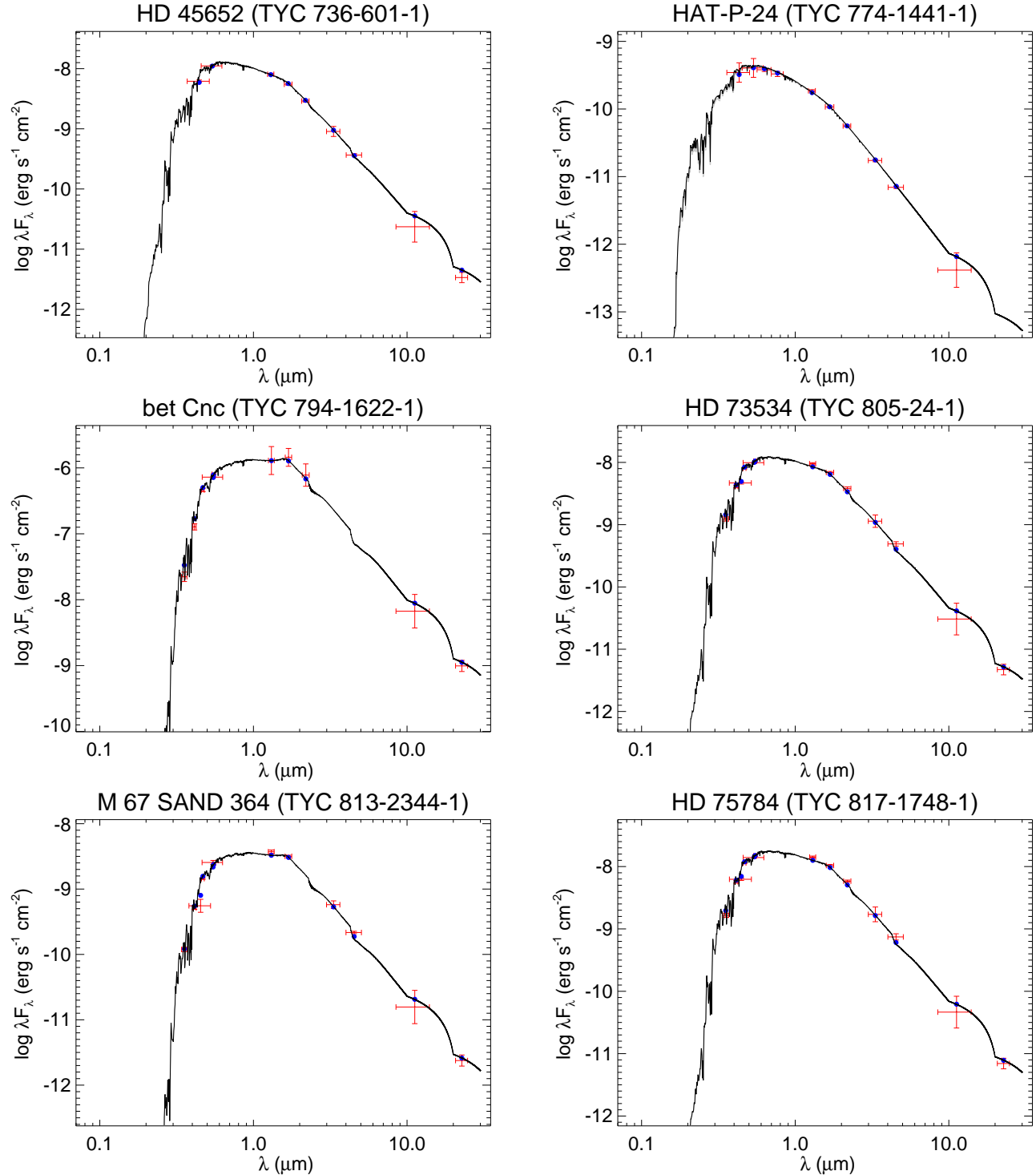


Figure 21. All labels, lines, symbols, and colors as in Figure 14.

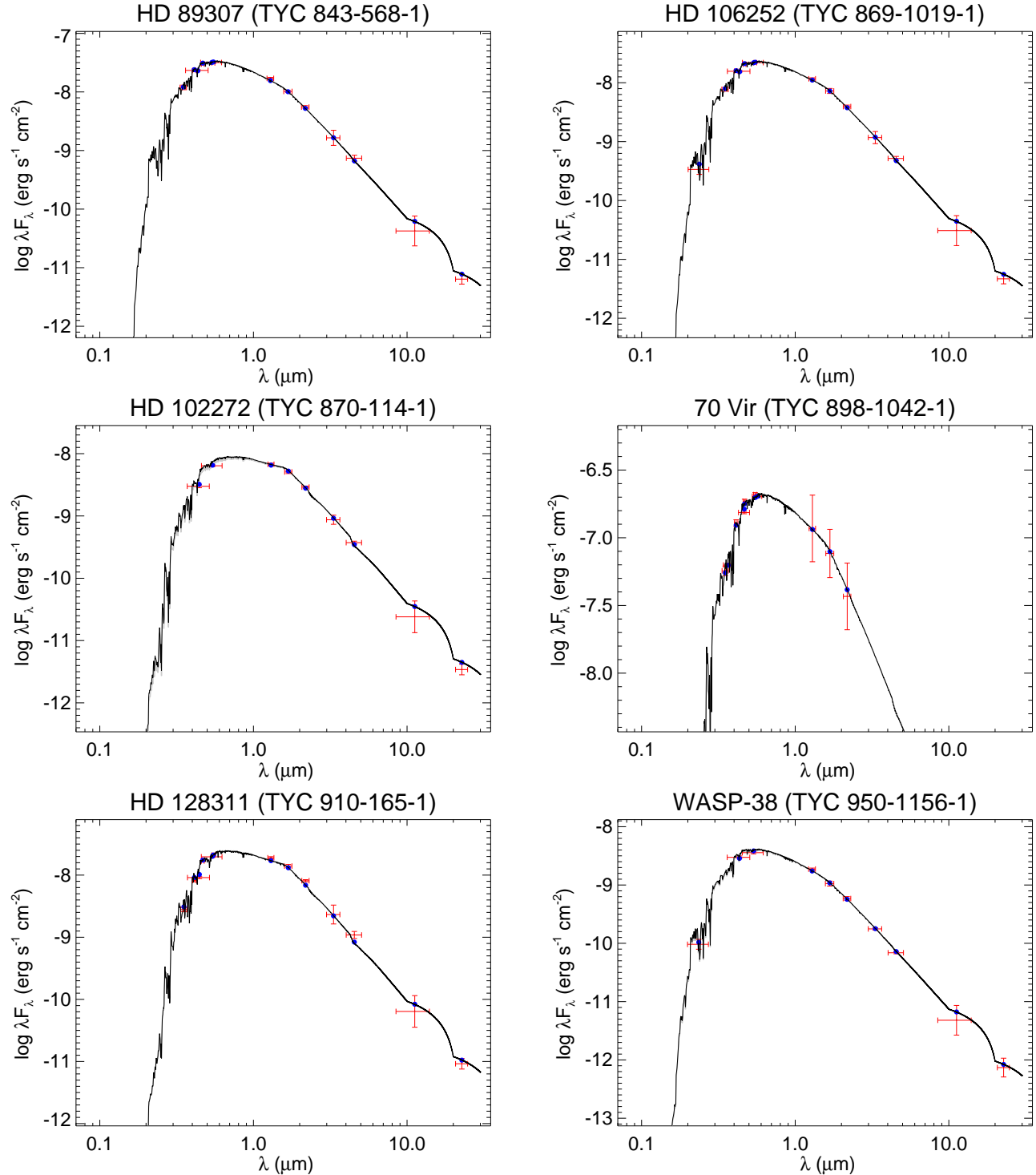


Figure 22. All labels, lines, symbols, and colors as in Figure 14.

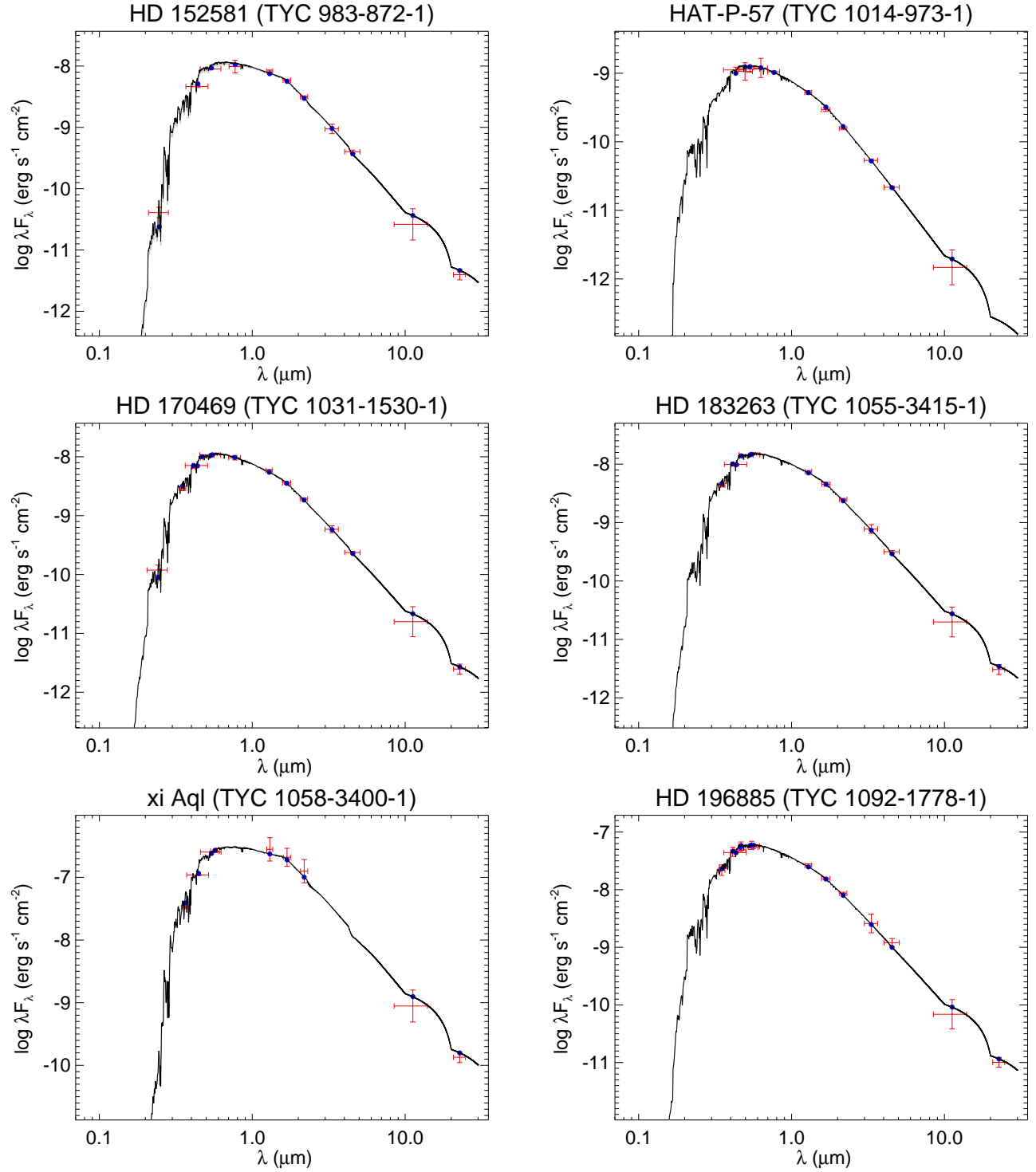


Figure 23. All labels, lines, symbols, and colors as in Figure 14.

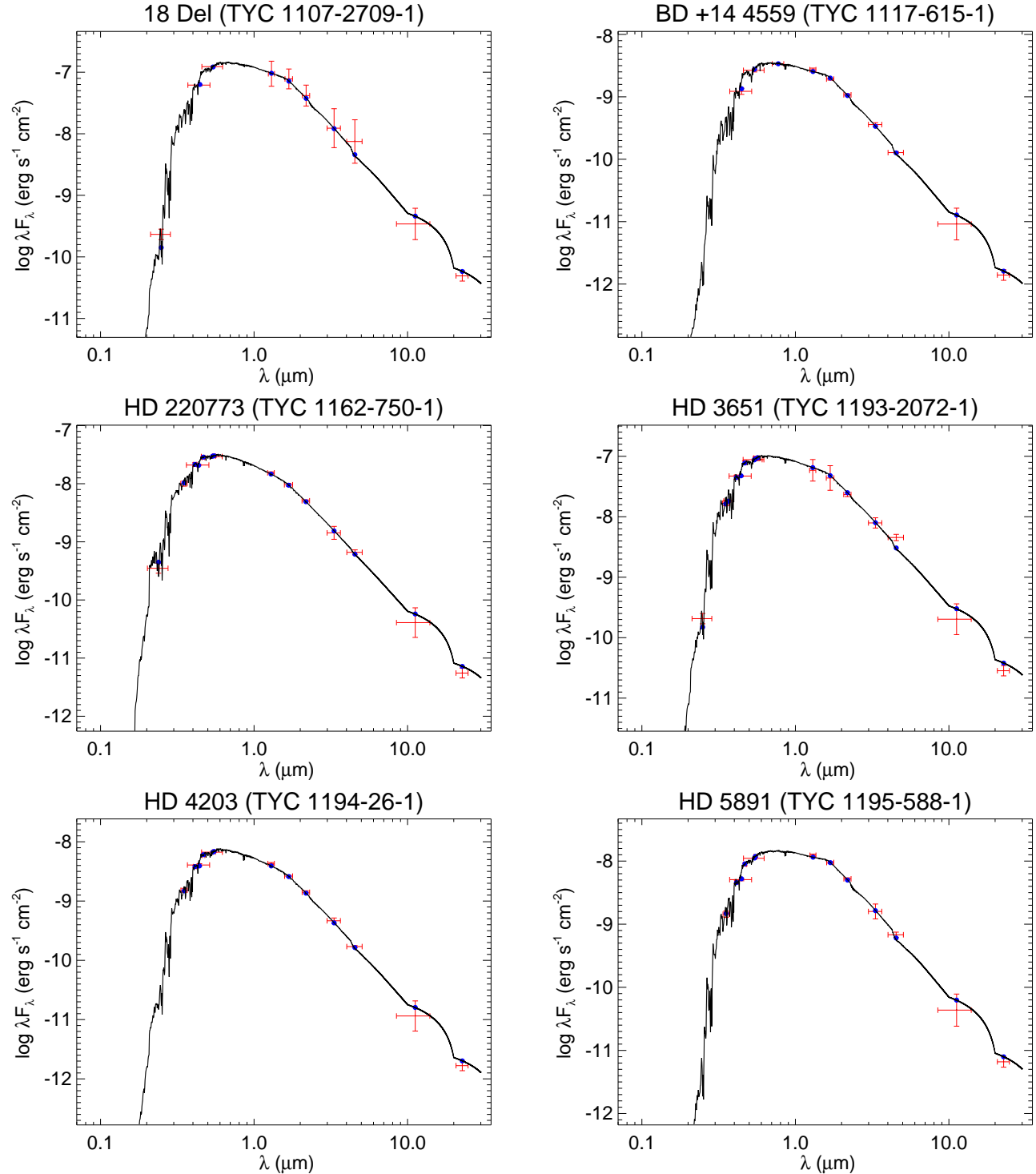


Figure 24. All labels, lines, symbols, and colors as in Figure 14.

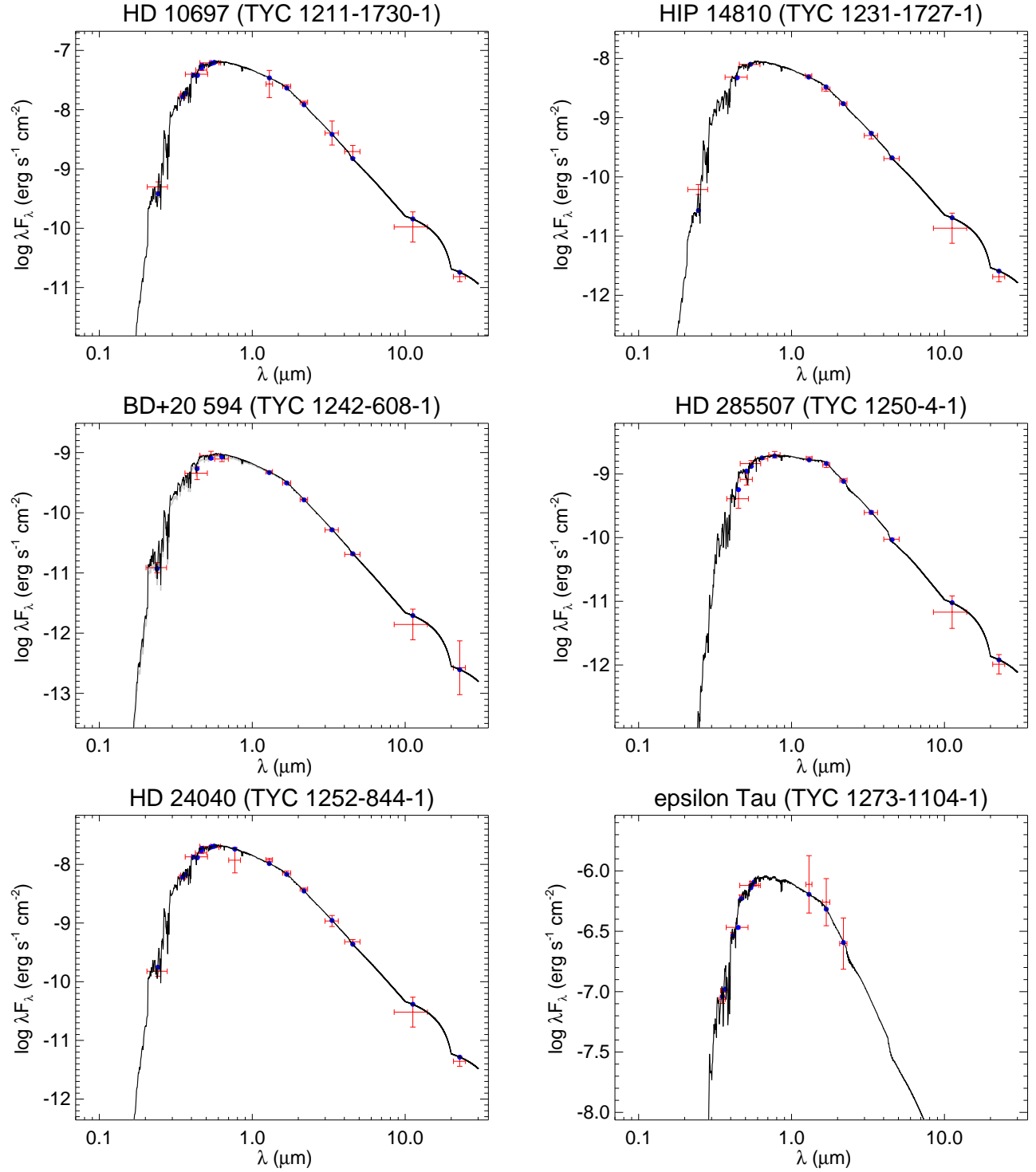


Figure 25. All labels, lines, symbols, and colors as in Figure 14.

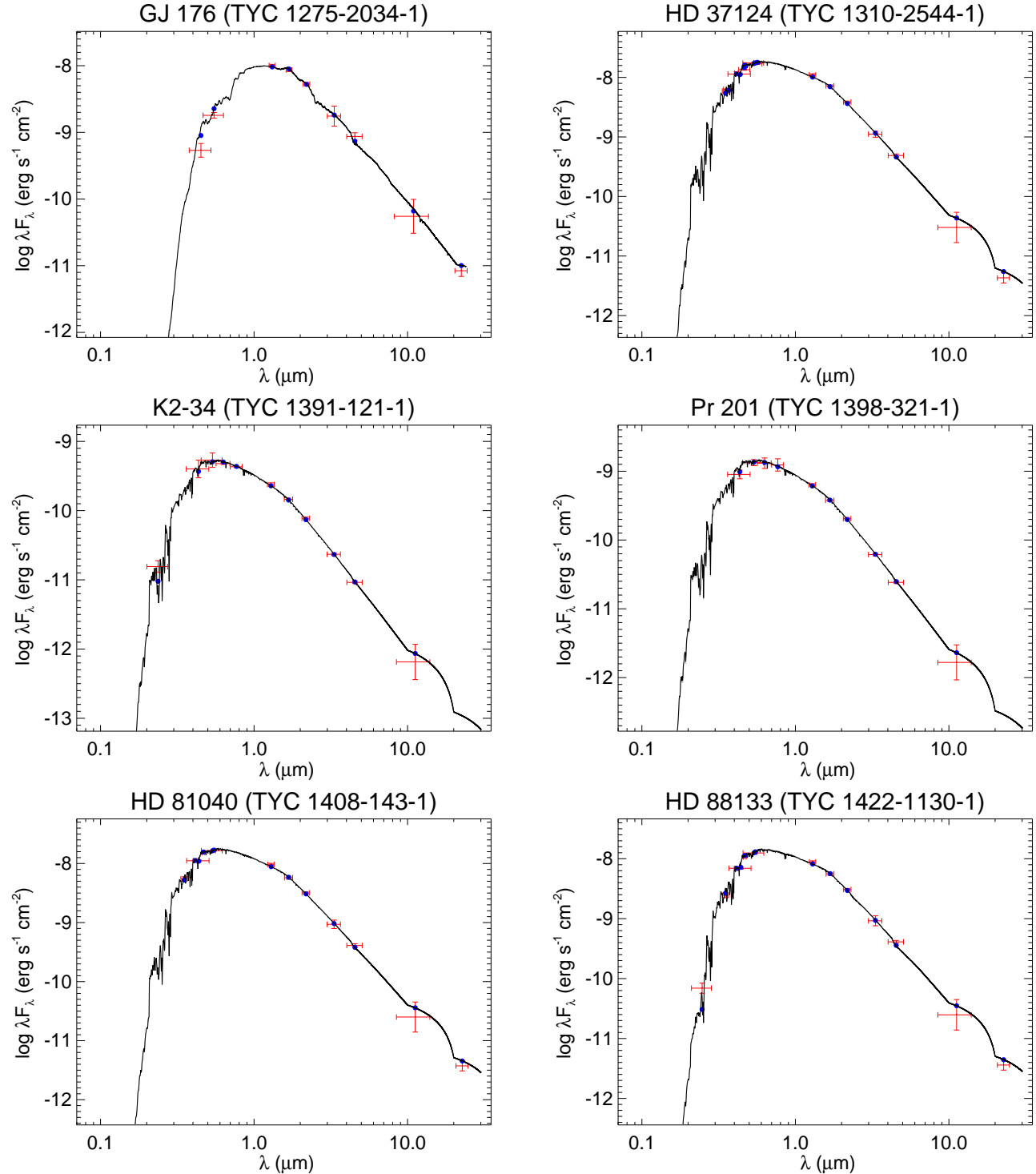


Figure 26. All labels, lines, symbols, and colors as in Figure 14.

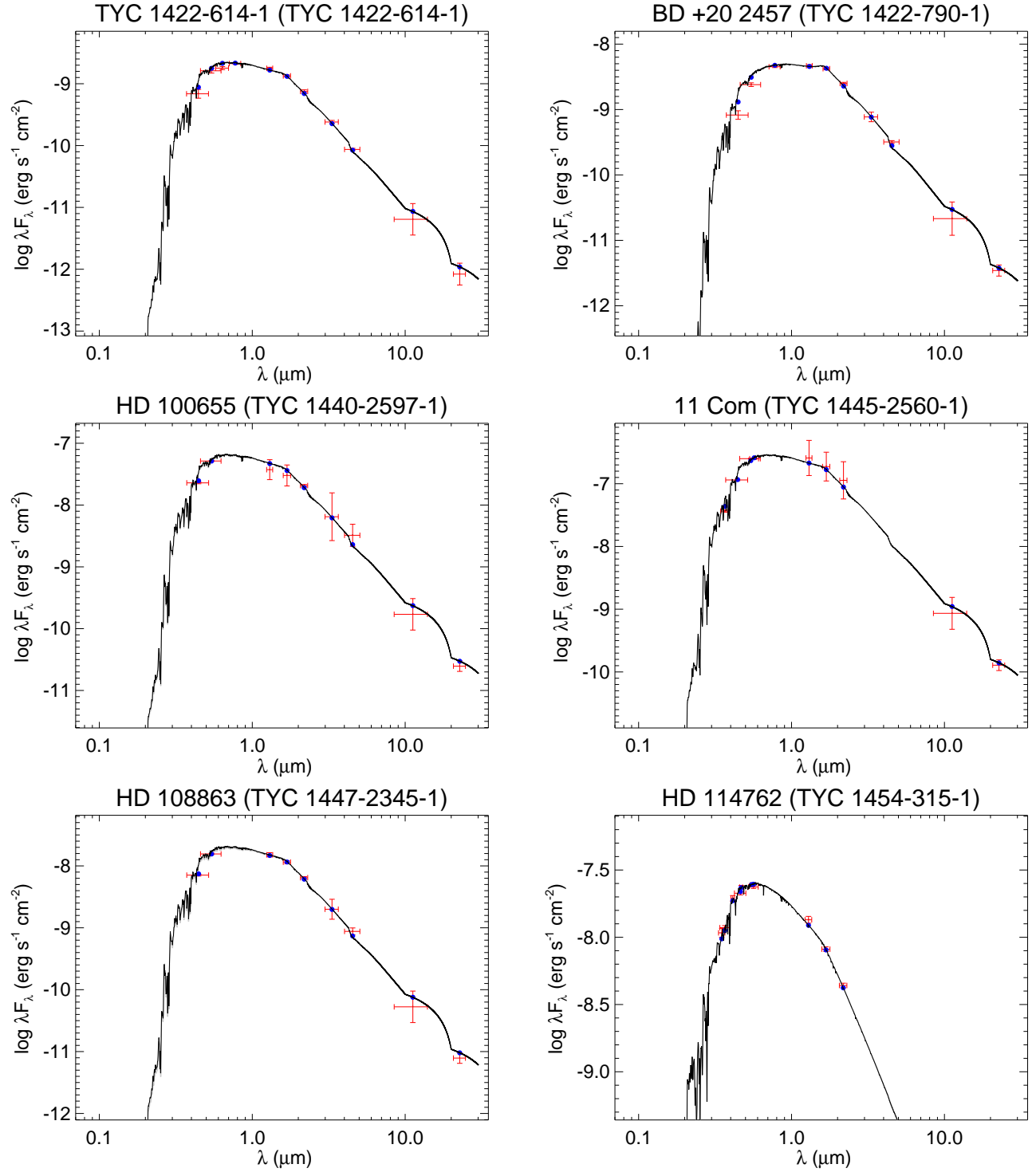


Figure 27. All labels, lines, symbols, and colors as in Figure 14.

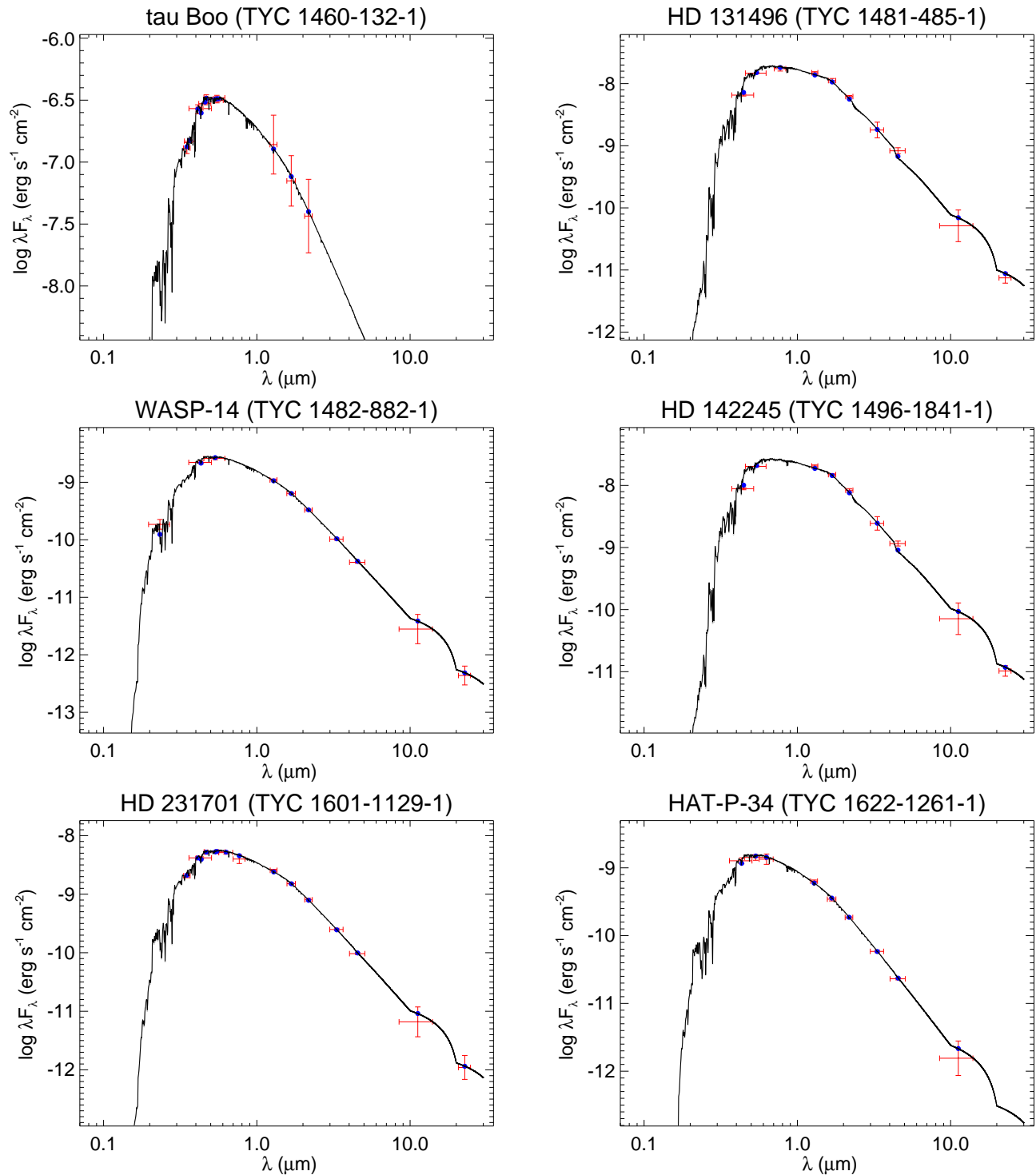


Figure 28. All labels, lines, symbols, and colors as in Figure 14.

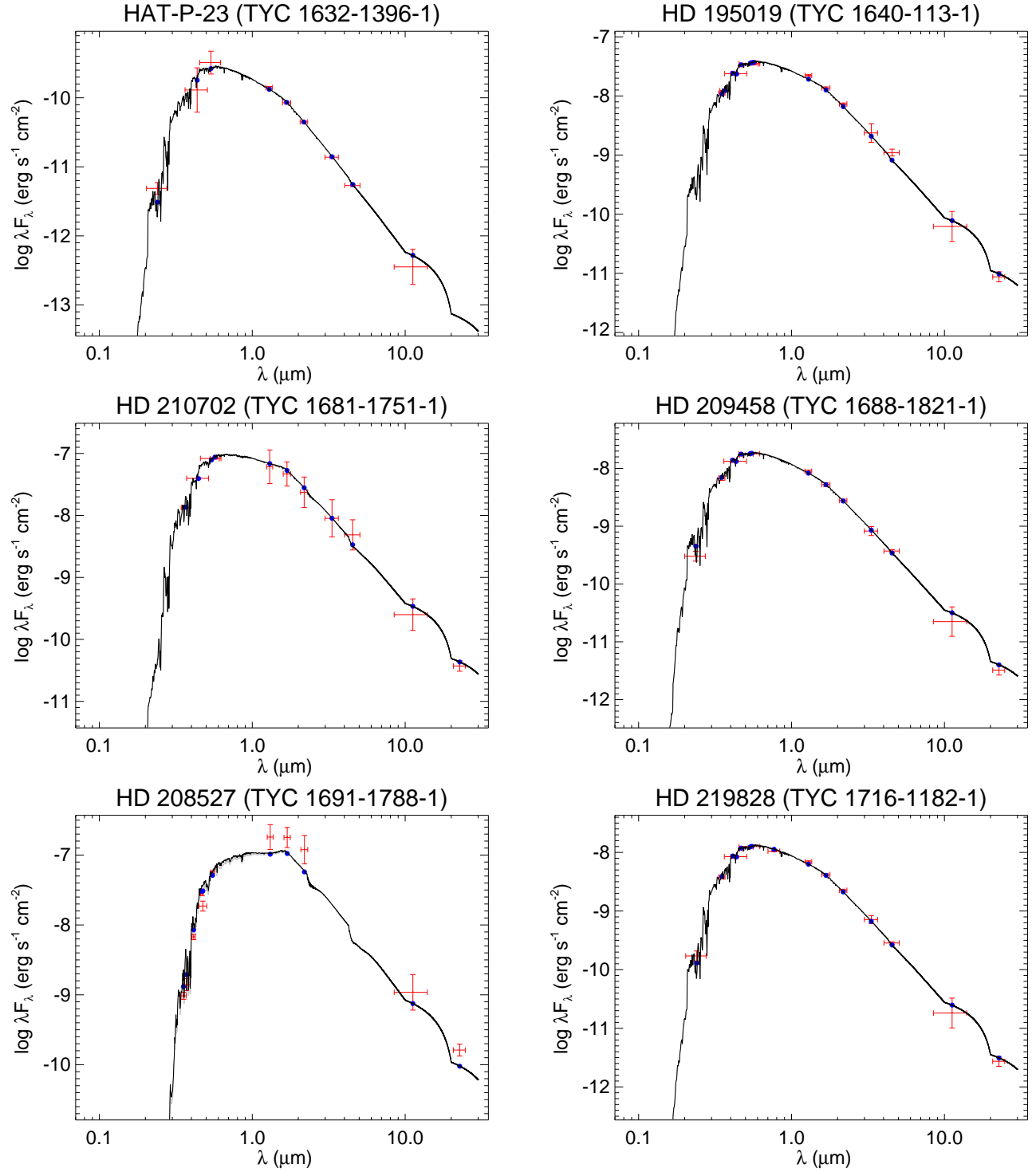


Figure 29. All labels, lines, symbols, and colors as in Figure 14.

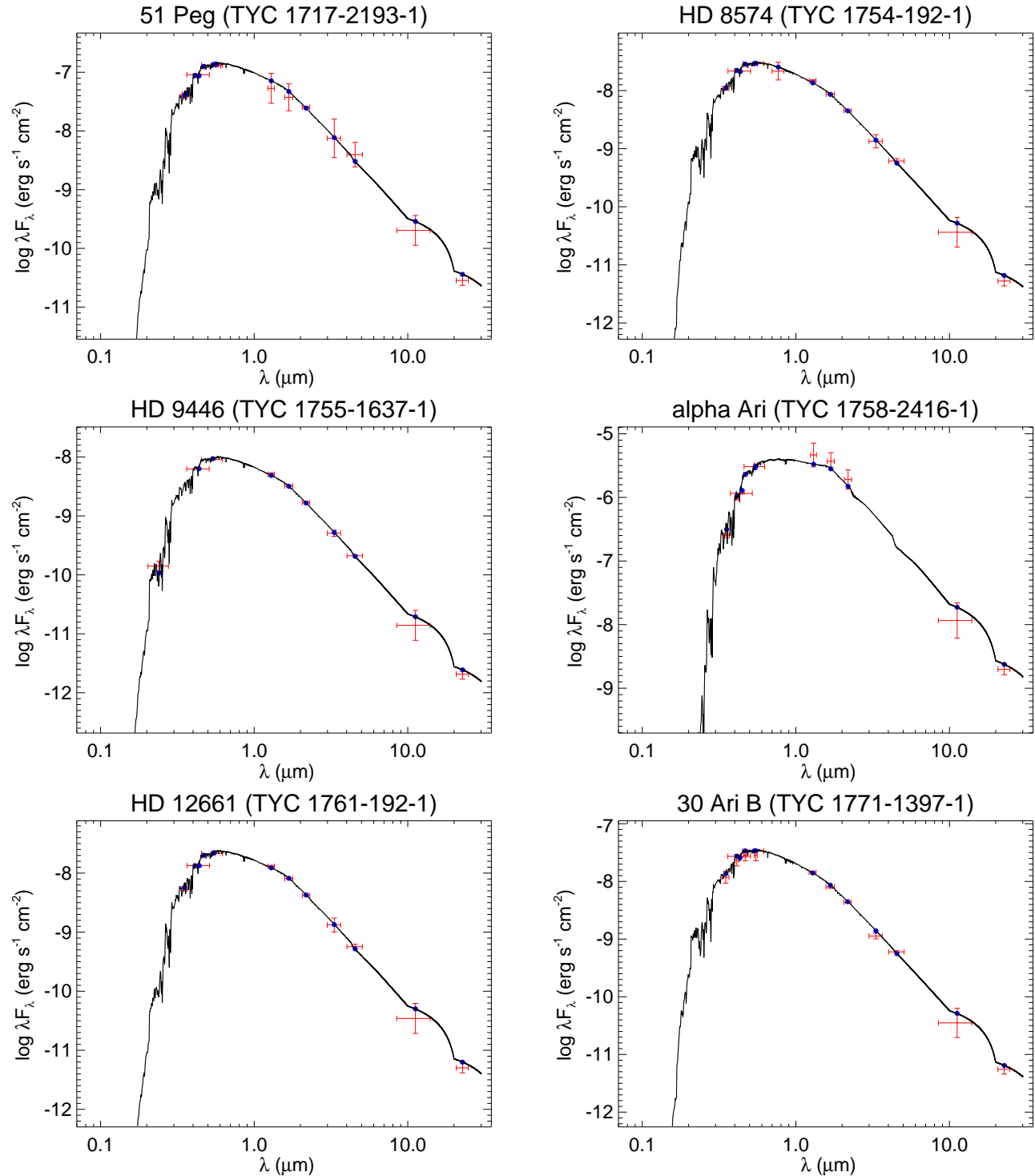


Figure 30. All labels, lines, symbols, and colors as in Figure 14.

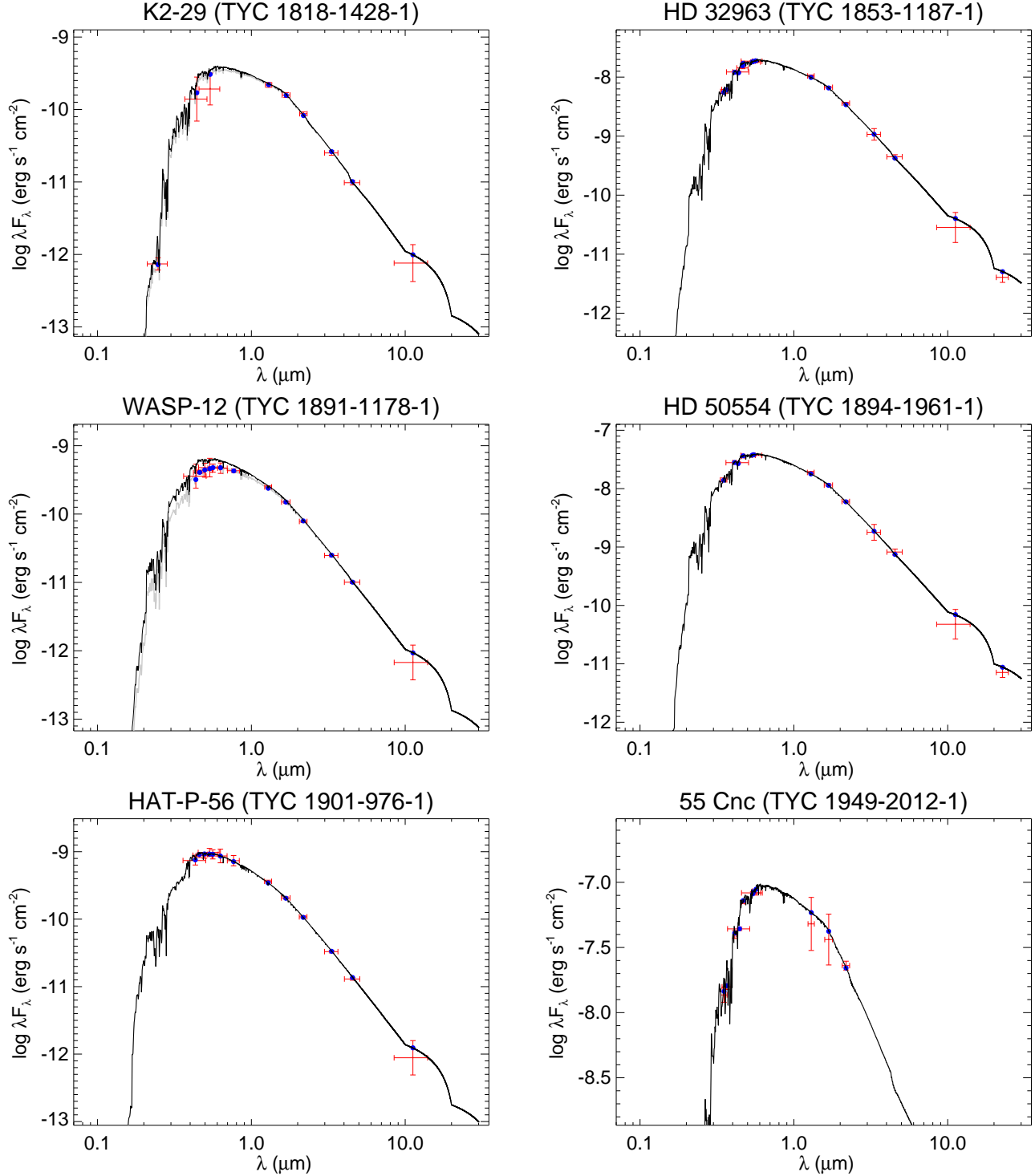


Figure 31. All labels, lines, symbols, and colors as in Figure 14.

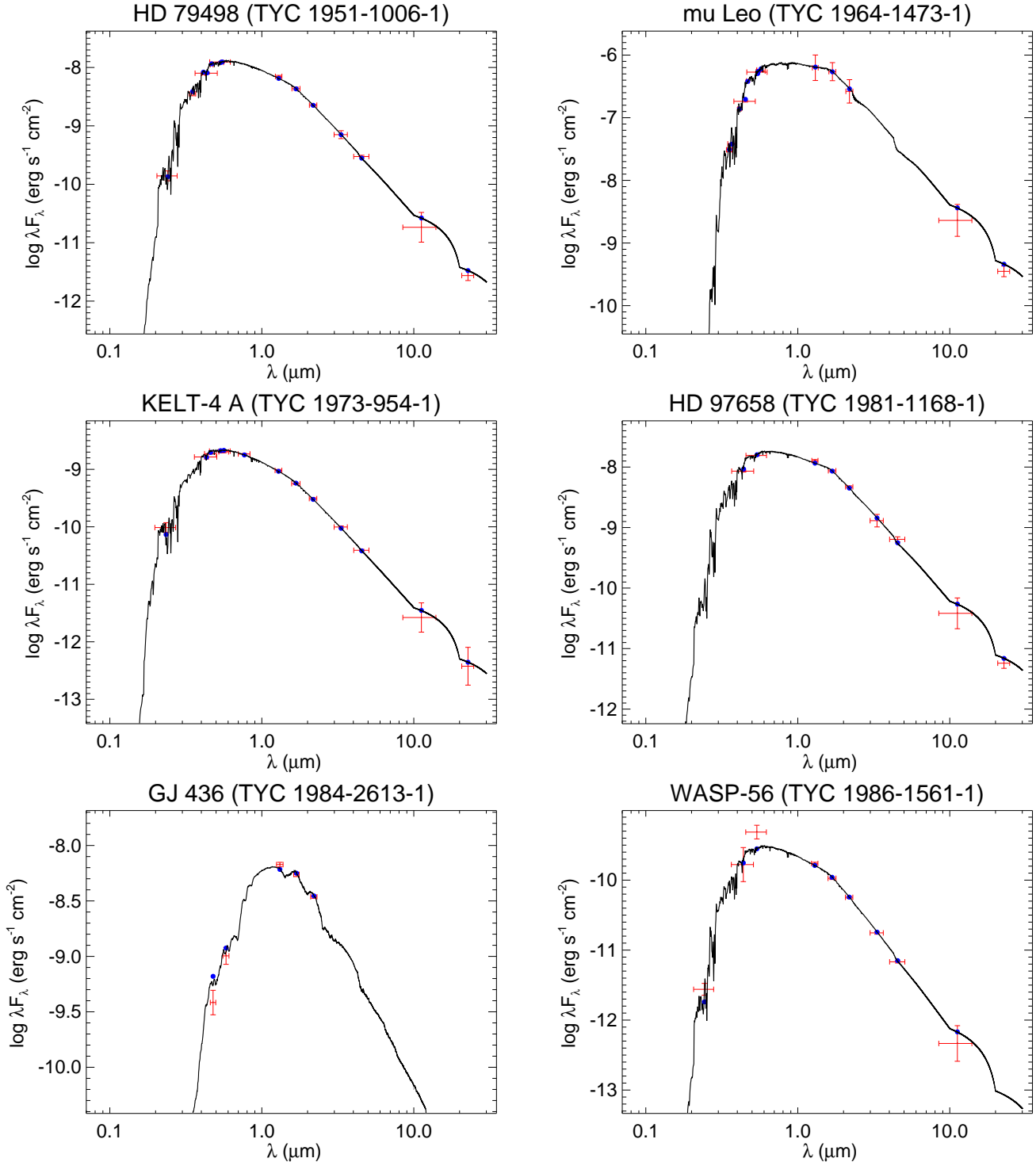


Figure 32. All labels, lines, symbols, and colors as in Figure 14.

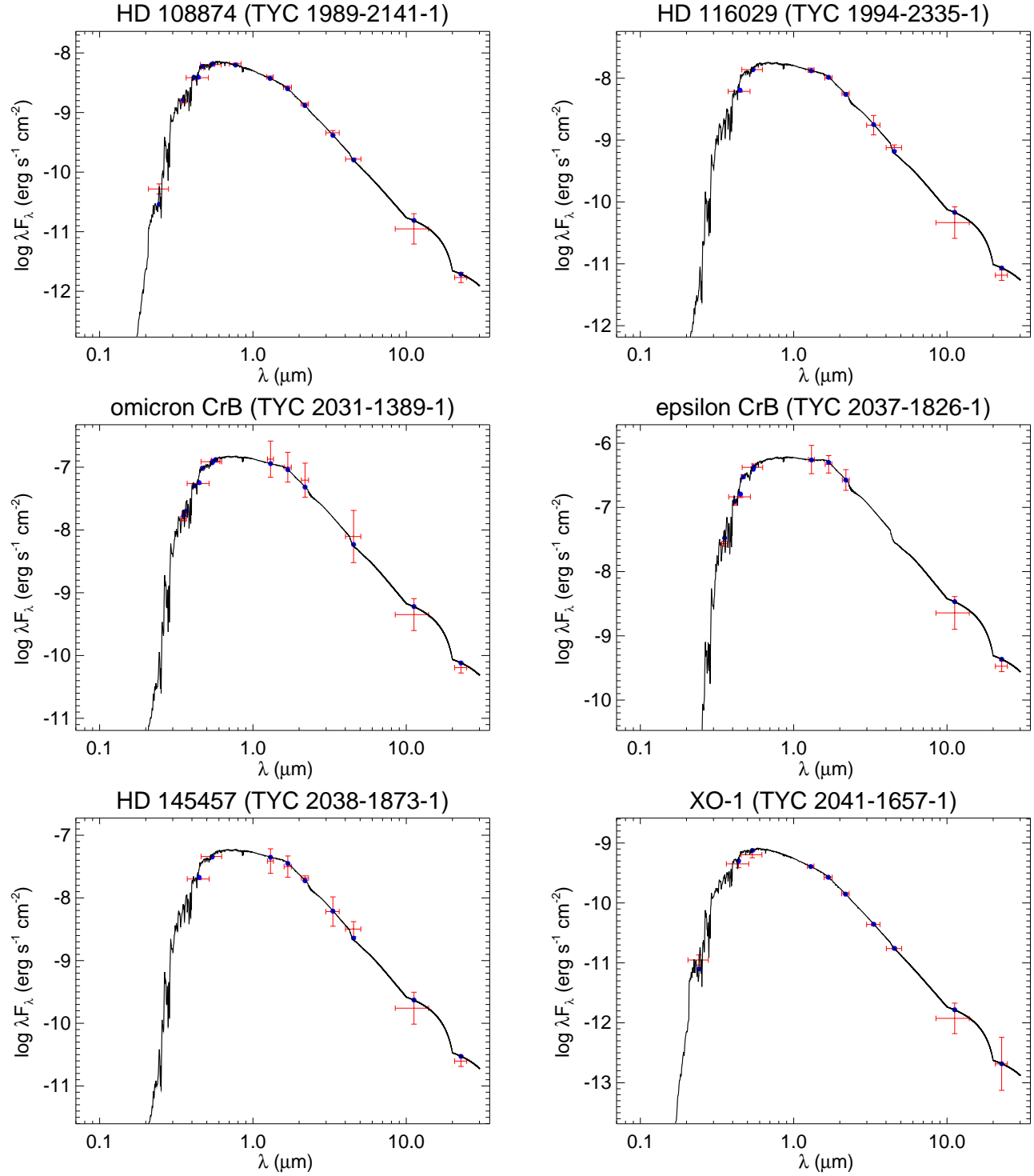


Figure 33. All labels, lines, symbols, and colors as in Figure 14.

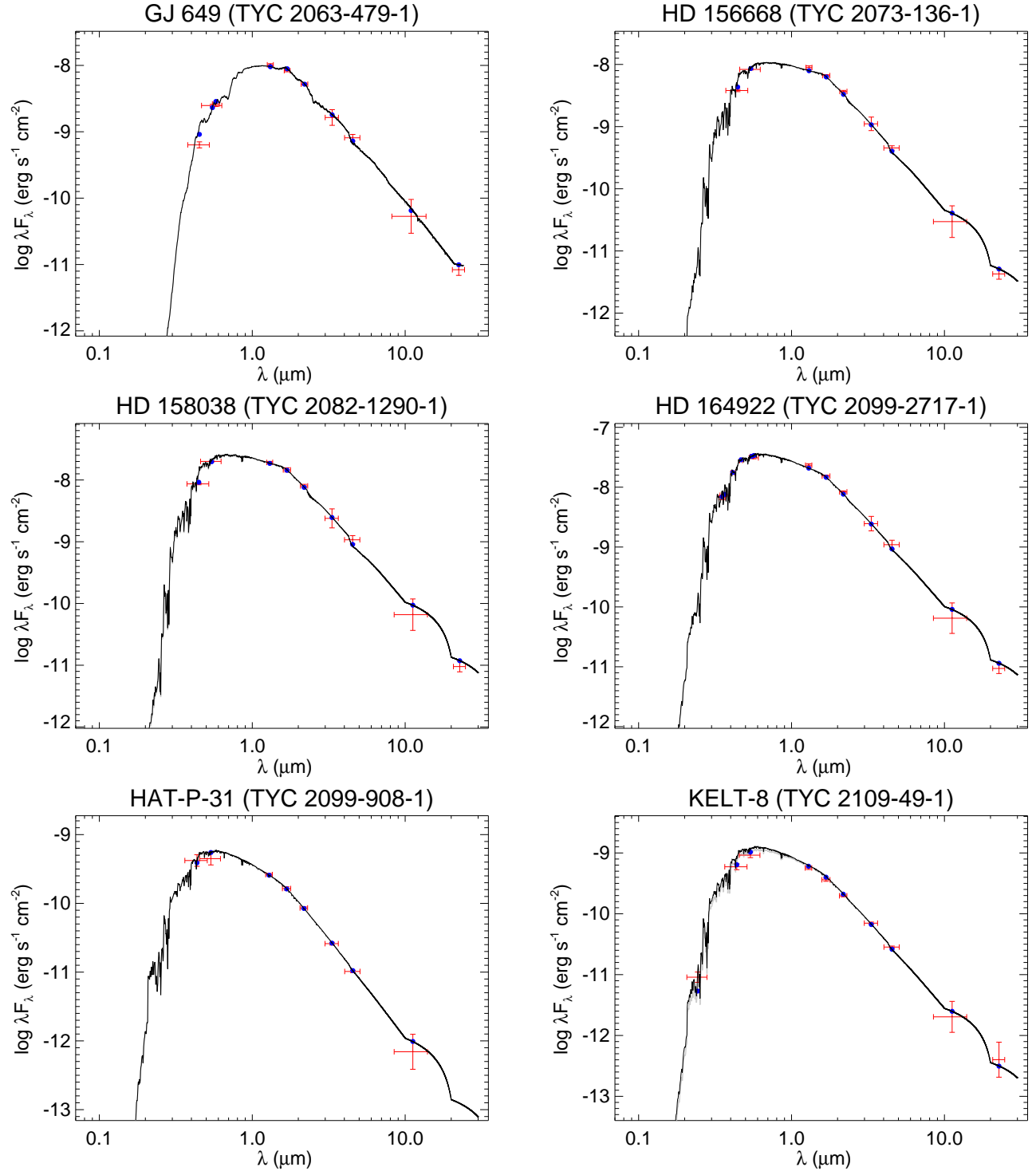


Figure 34. All labels, lines, symbols, and colors as in Figure 14.

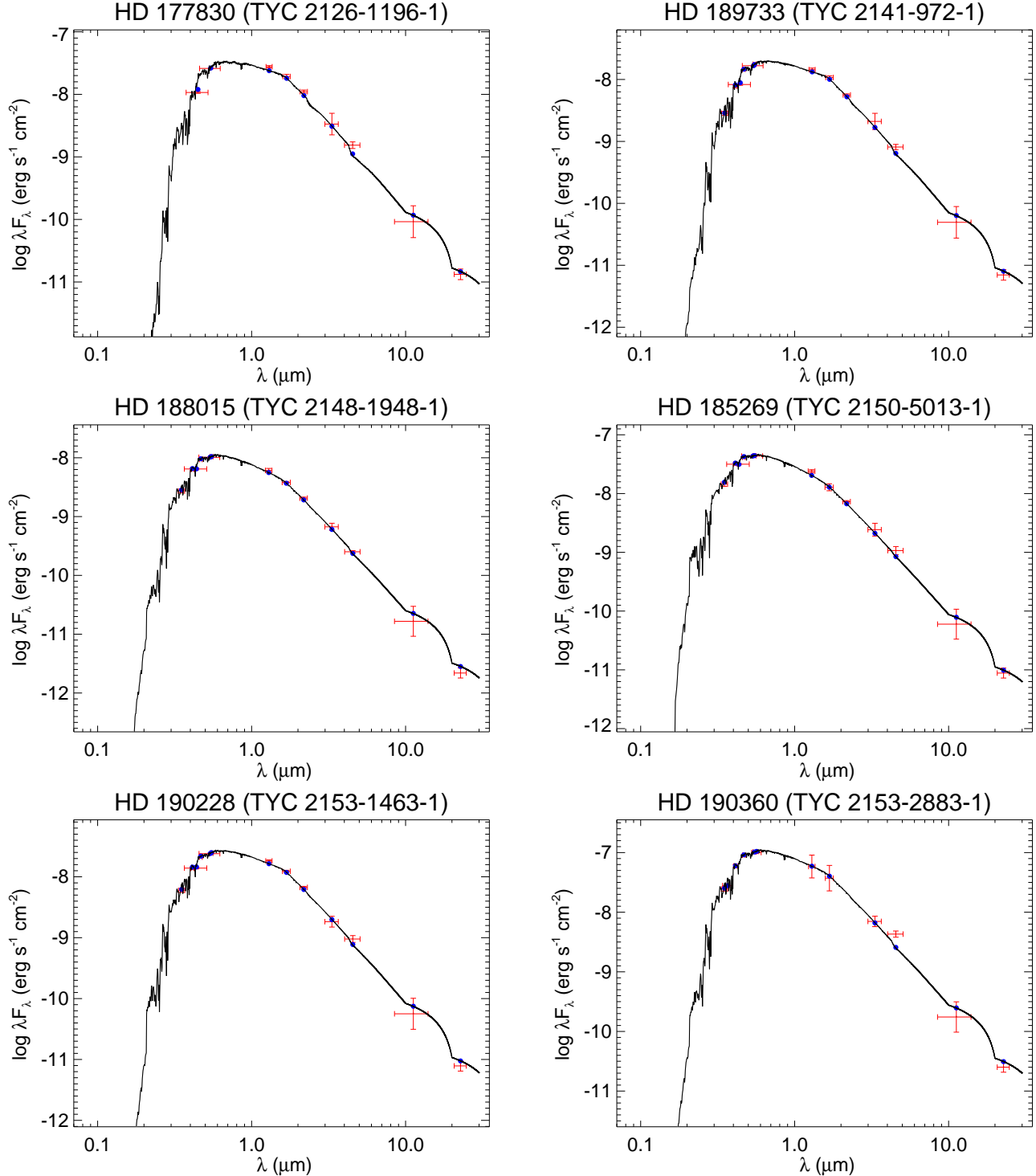


Figure 35. All labels, lines, symbols, and colors as in Figure 14.

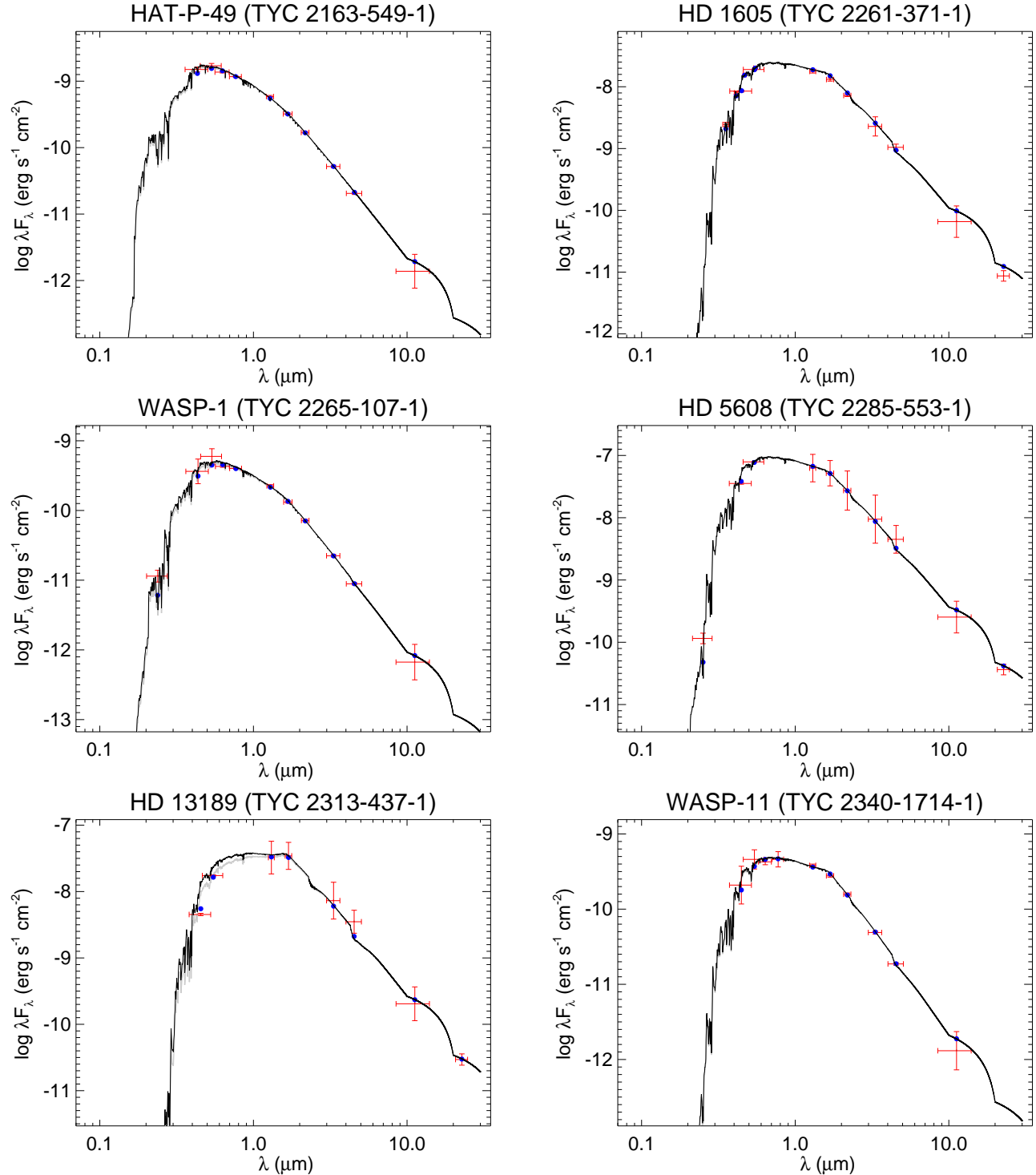


Figure 36. All labels, lines, symbols, and colors as in Figure 14.

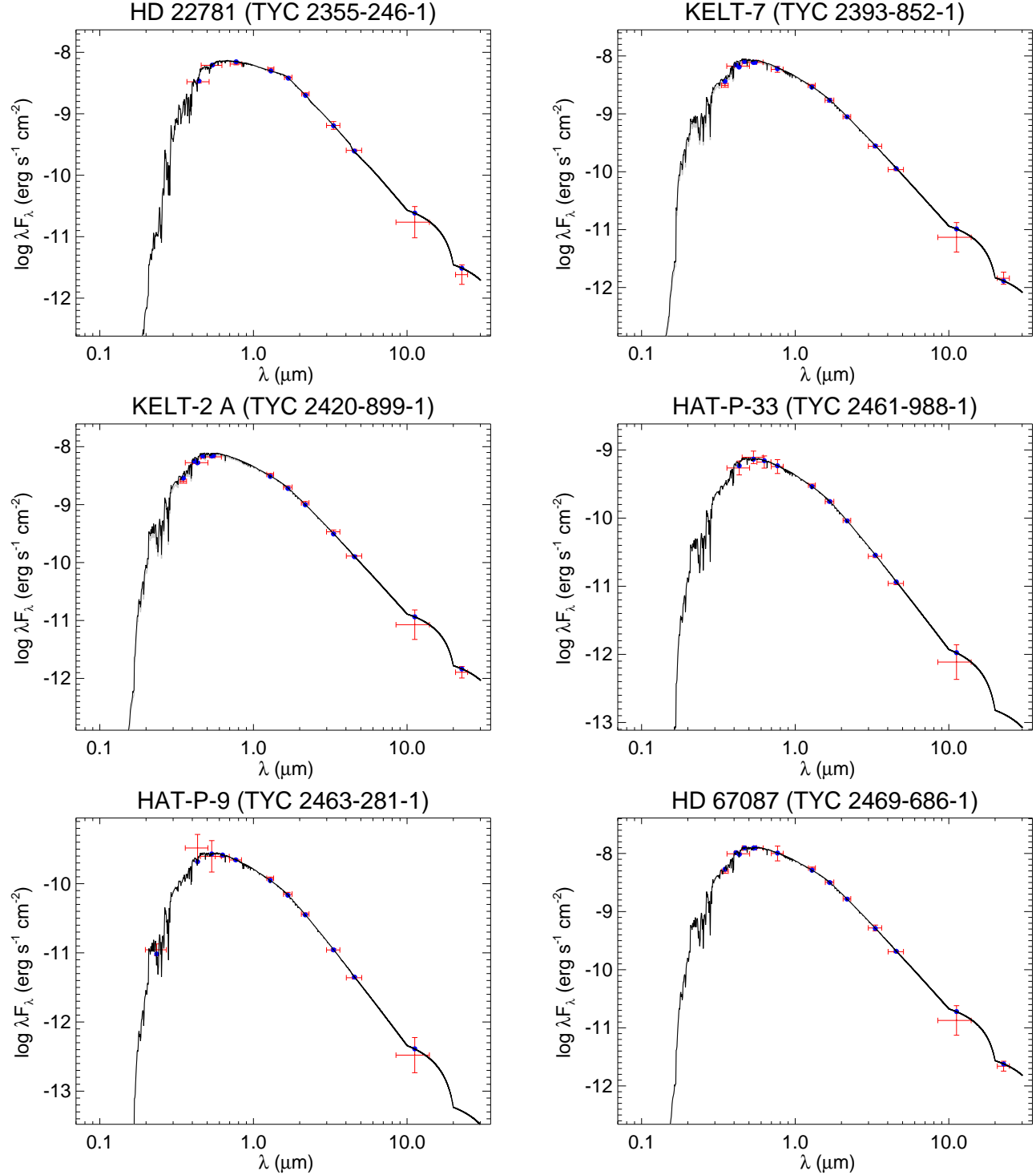


Figure 37. All labels, lines, symbols, and colors as in Figure 14.

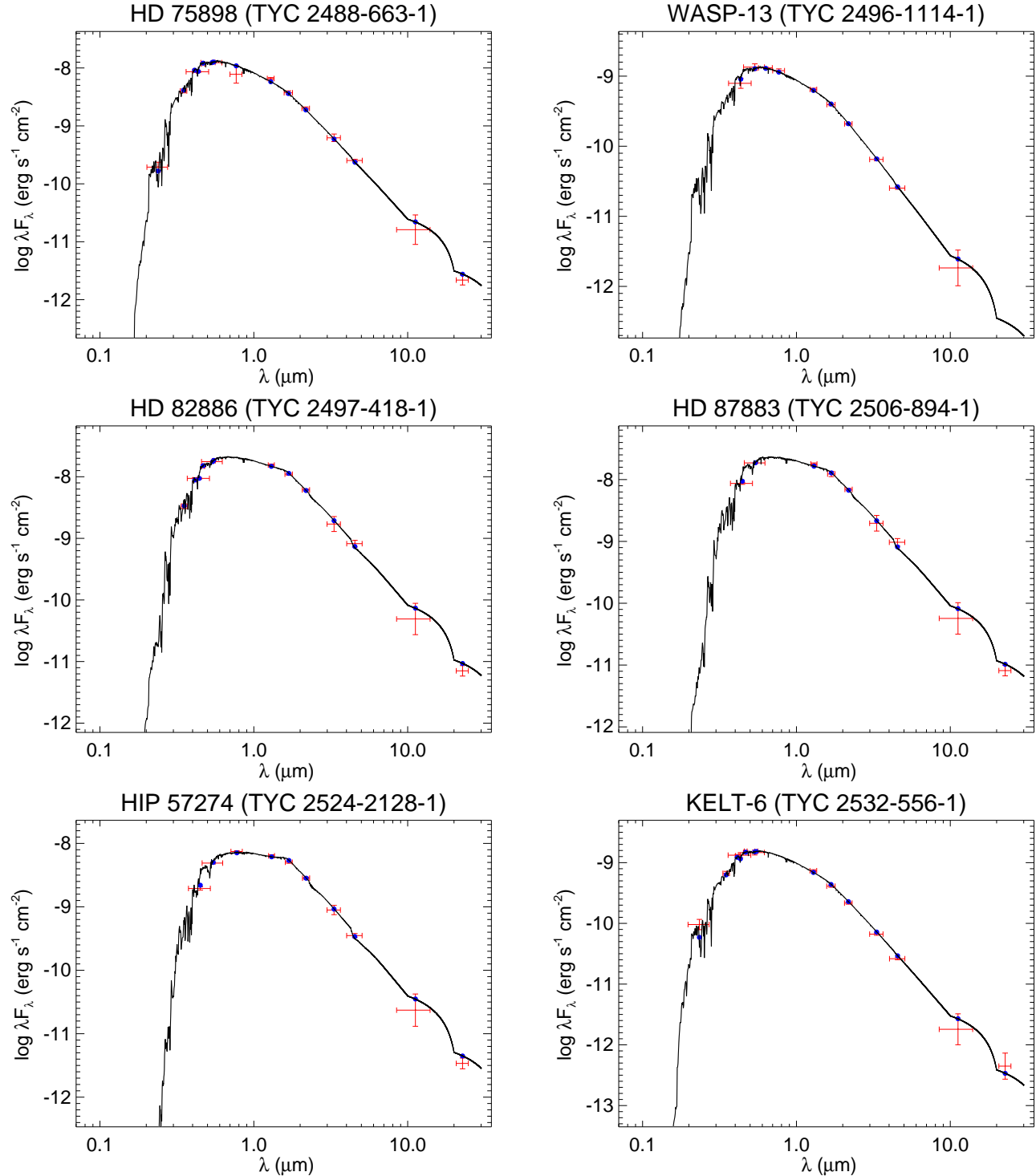


Figure 38. All labels, lines, symbols, and colors as in Figure 14.

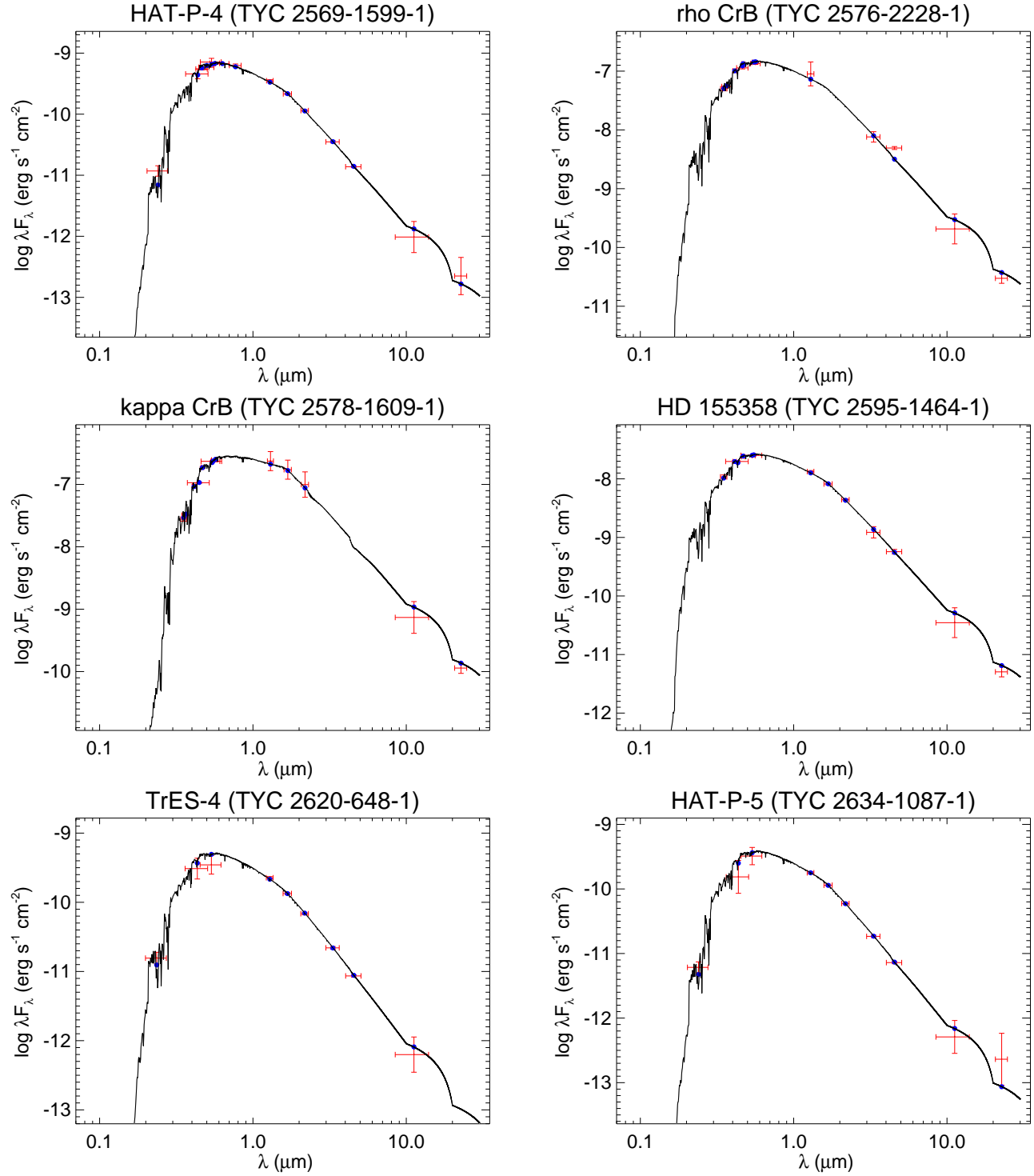


Figure 39. All labels, lines, symbols, and colors as in Figure 14.

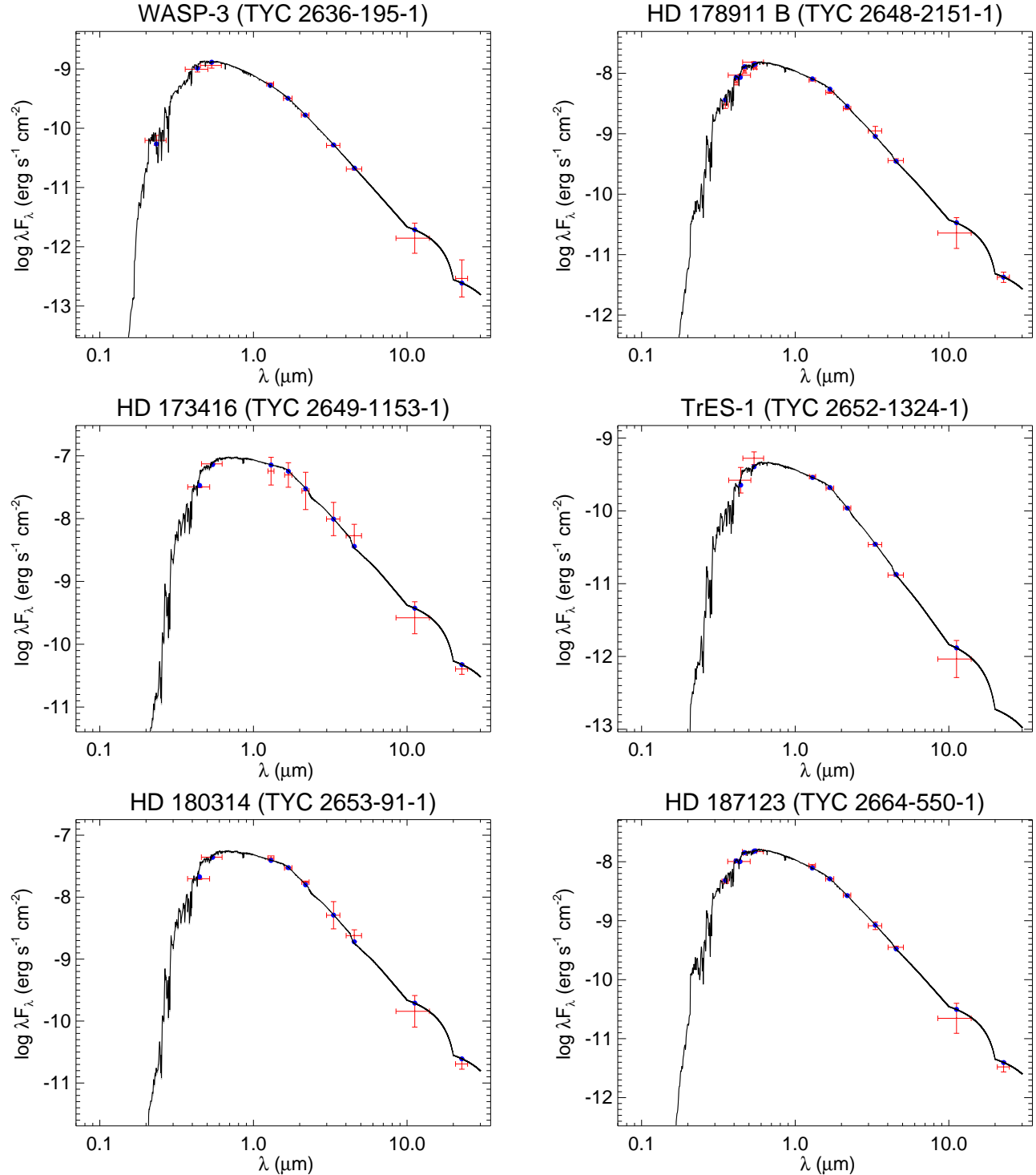


Figure 40. All labels, lines, symbols, and colors as in Figure 14.

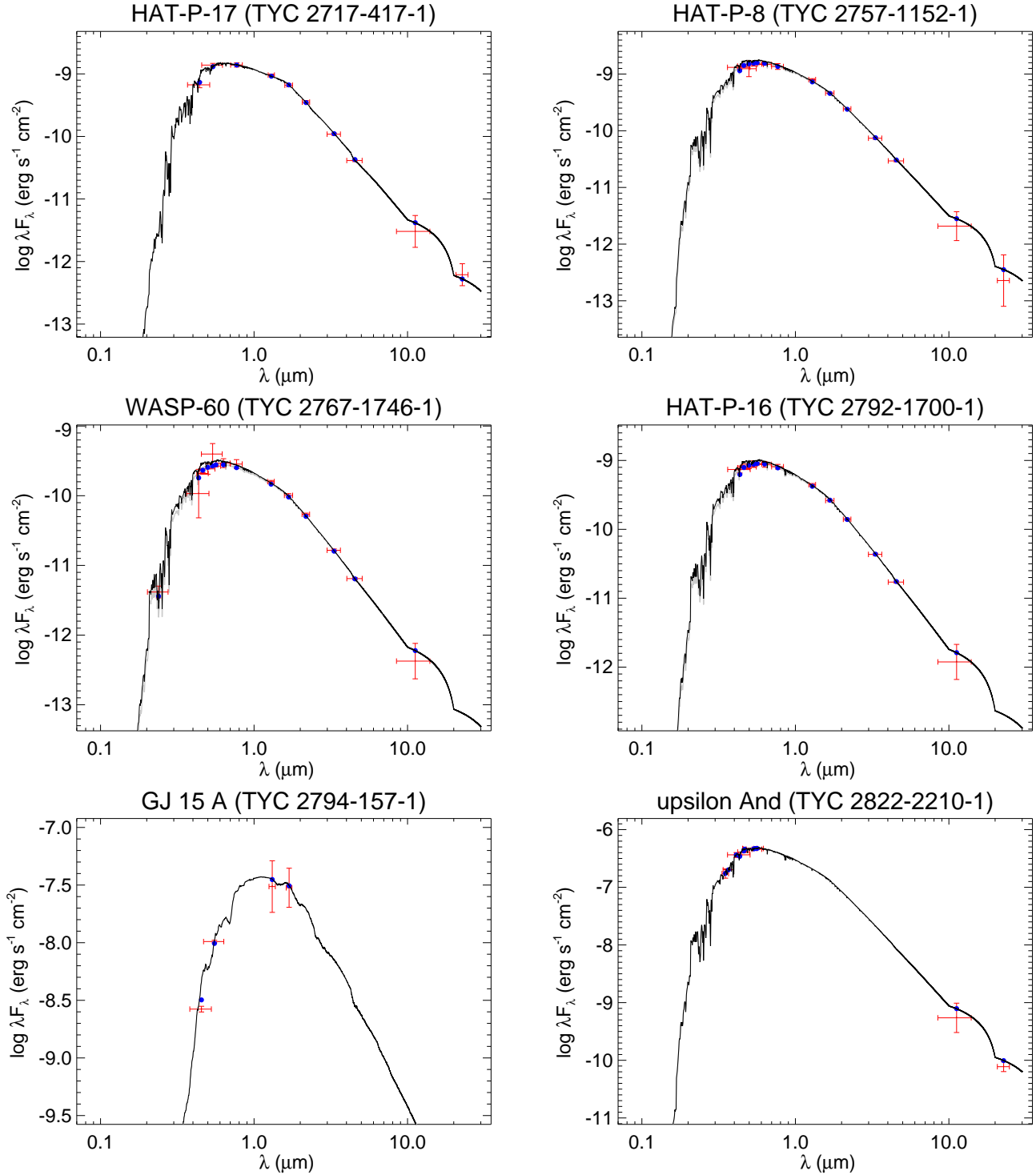


Figure 41. All labels, lines, symbols, and colors as in Figure 14.

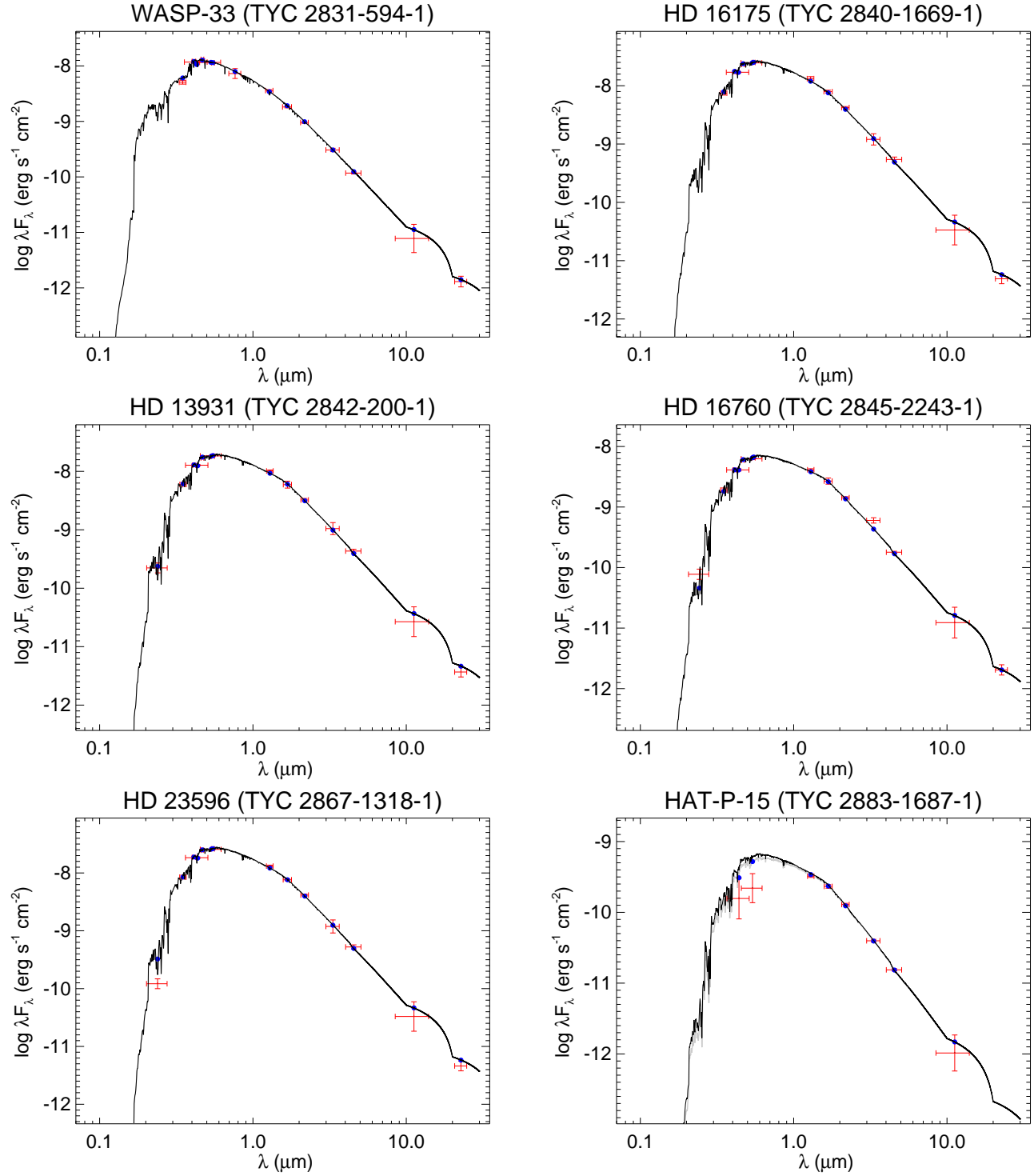


Figure 42. All labels, lines, symbols, and colors as in Figure 14.

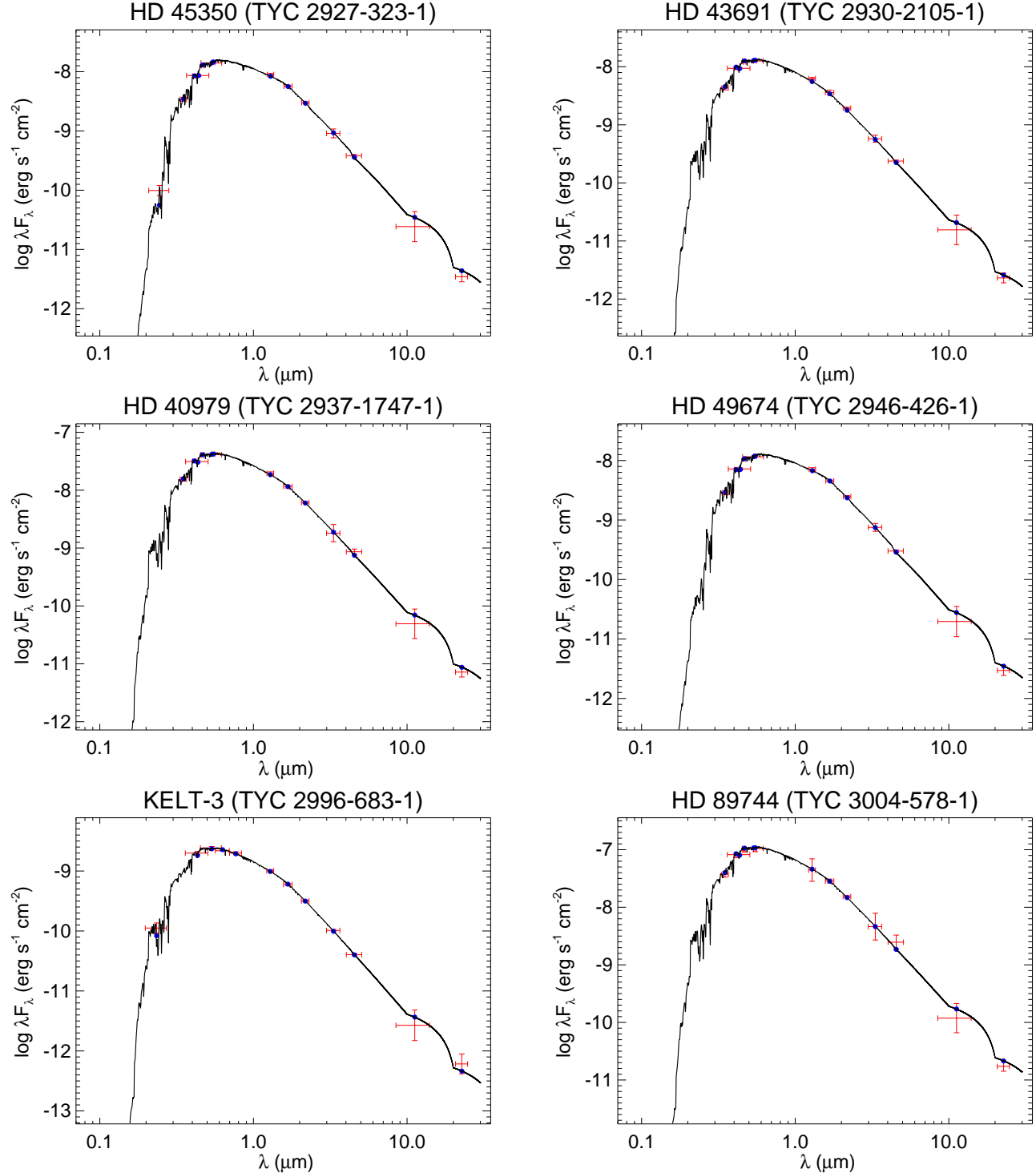


Figure 43. All labels, lines, symbols, and colors as in Figure 14.

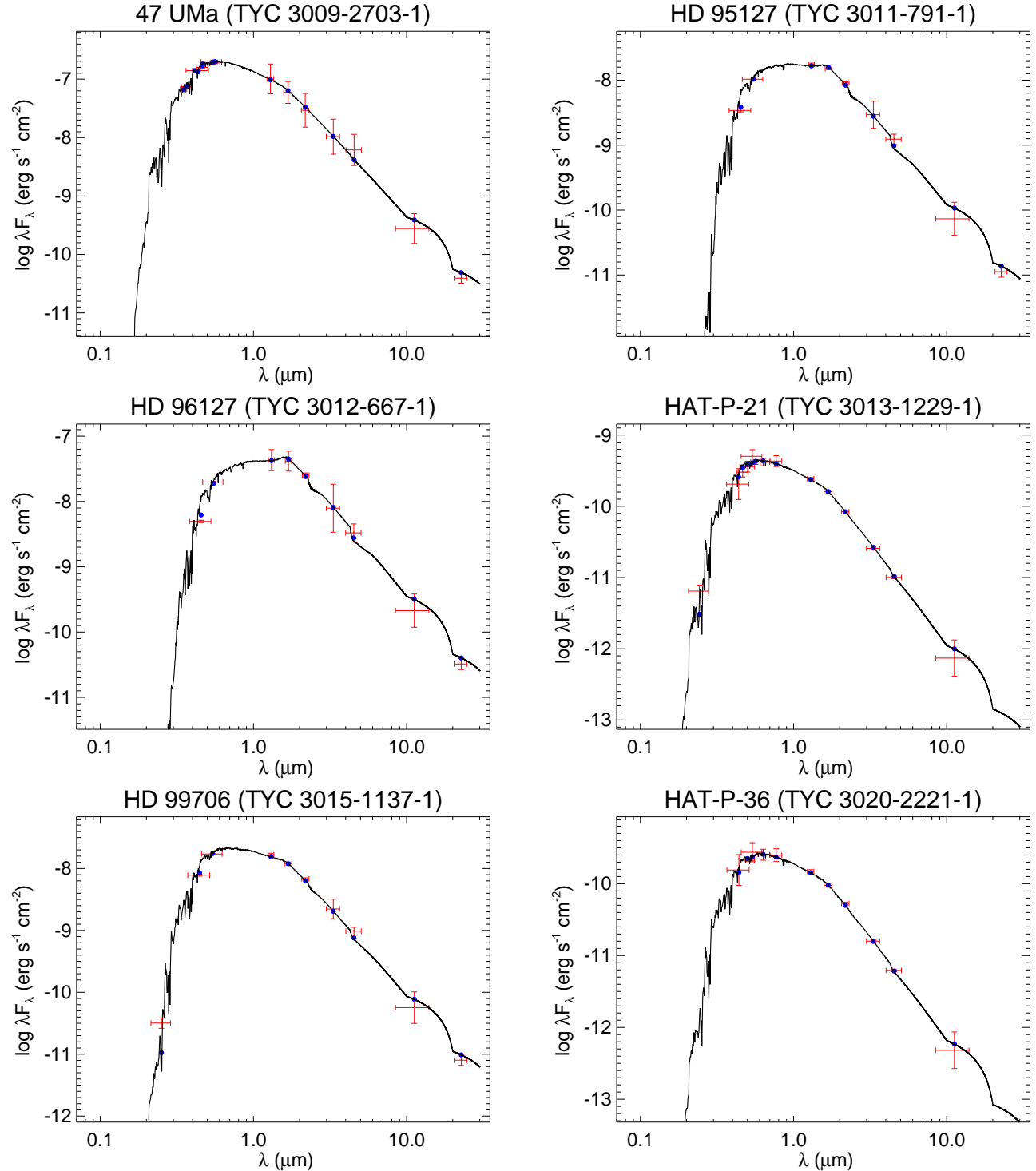


Figure 44. All labels, lines, symbols, and colors as in Figure 14.

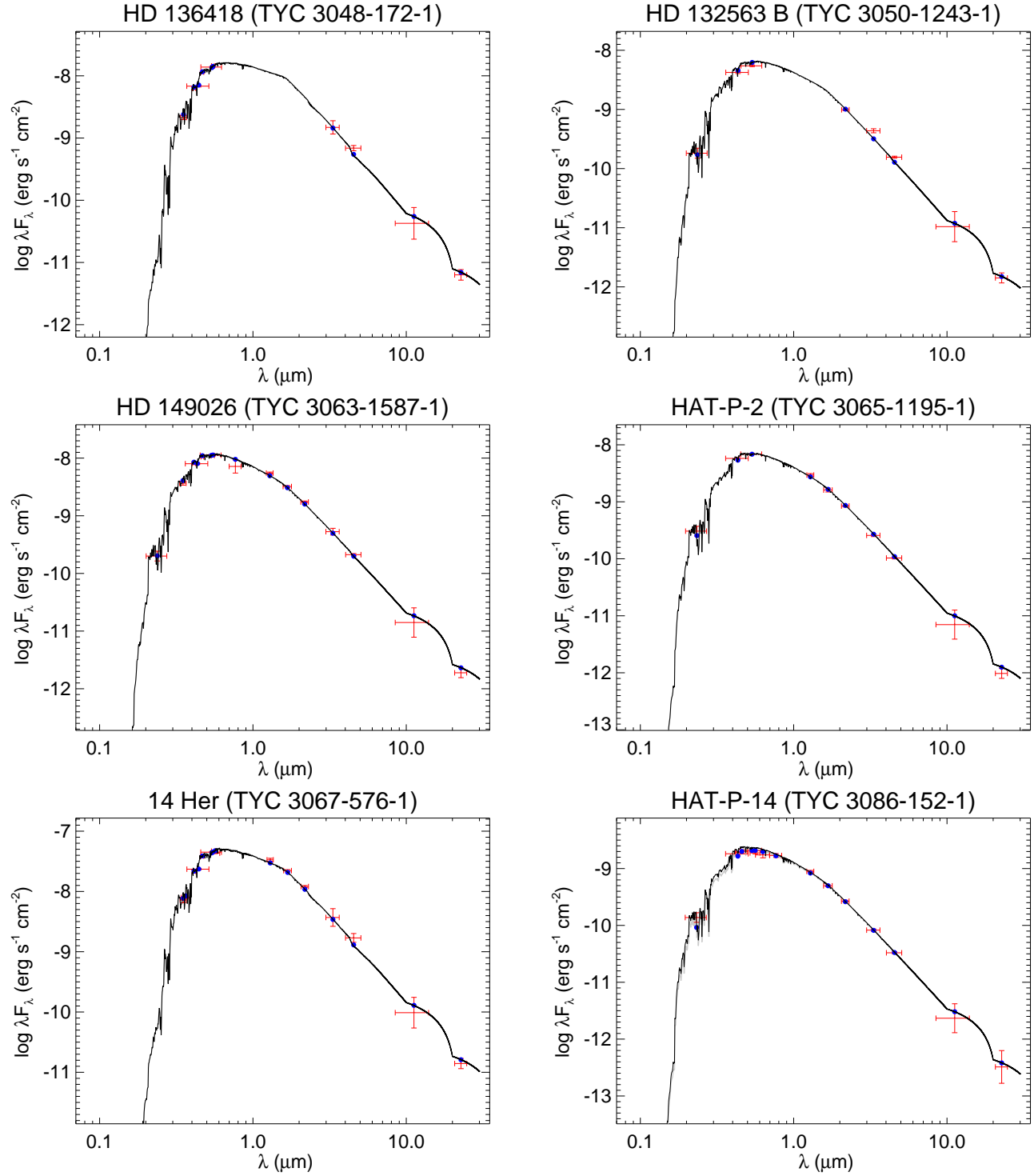


Figure 45. All labels, lines, symbols, and colors as in Figure 14.

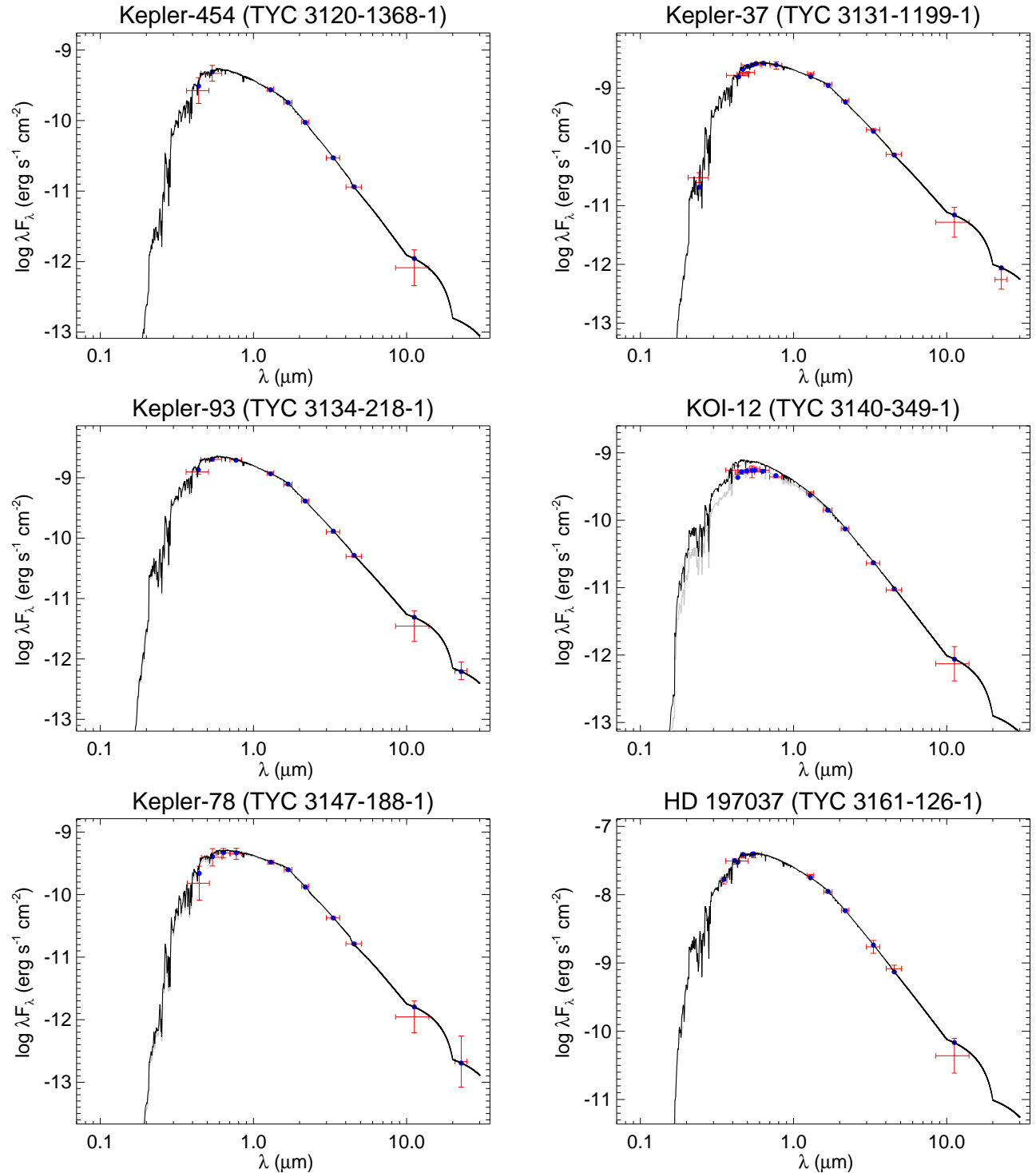


Figure 46. All labels, lines, symbols, and colors as in Figure 14.

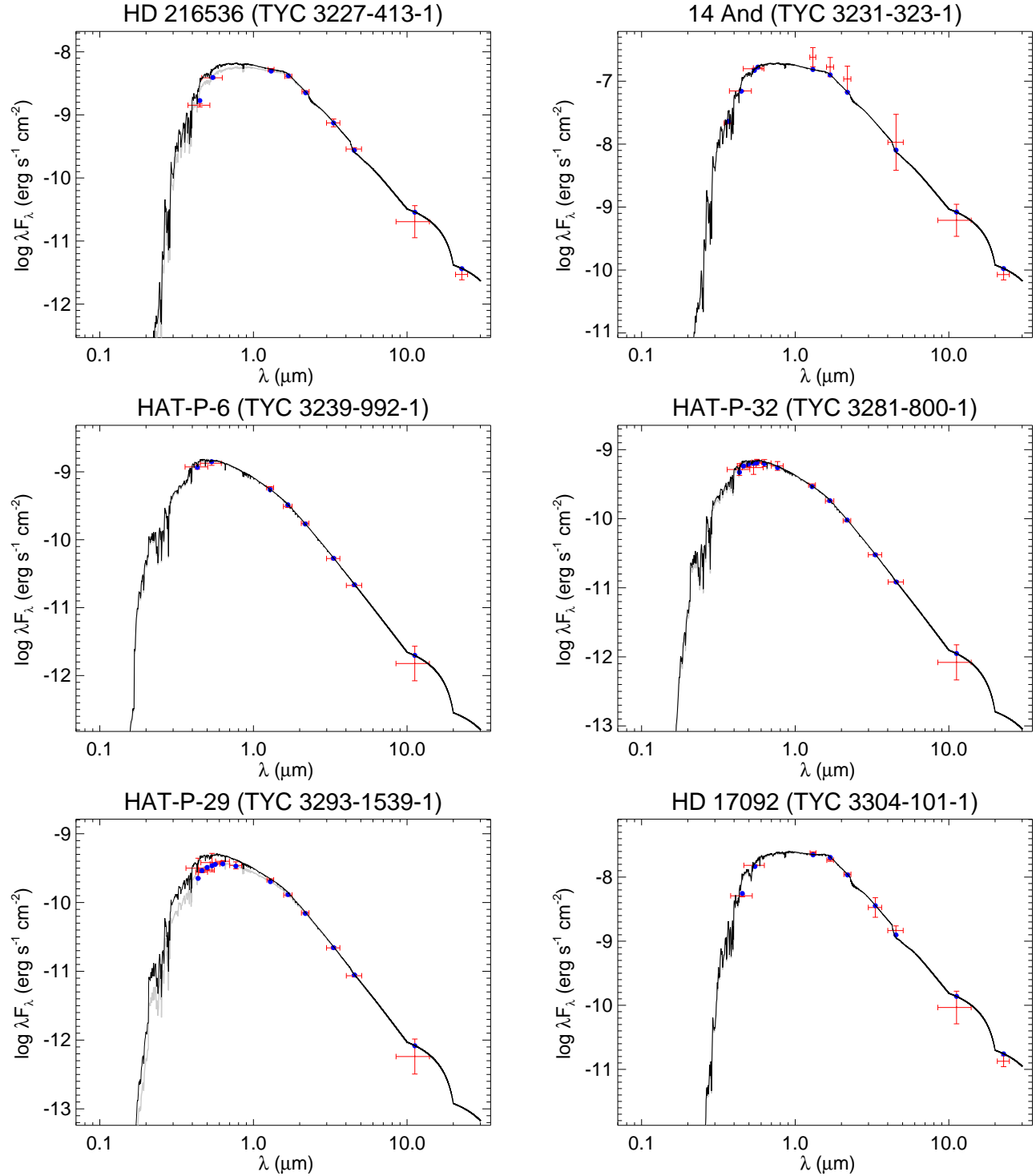


Figure 47. All labels, lines, symbols, and colors as in Figure 14.

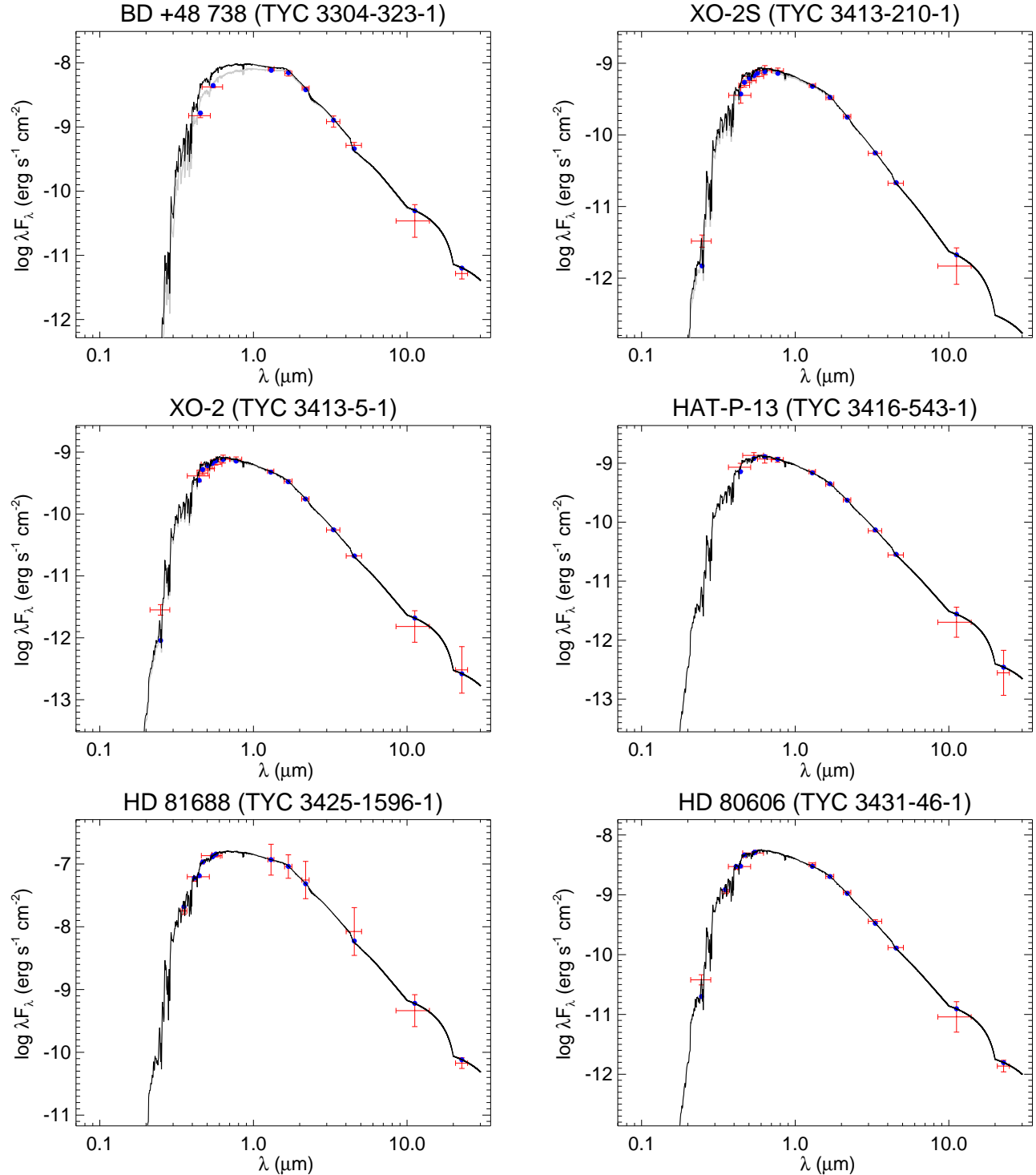


Figure 48. All labels, lines, symbols, and colors as in Figure 14.

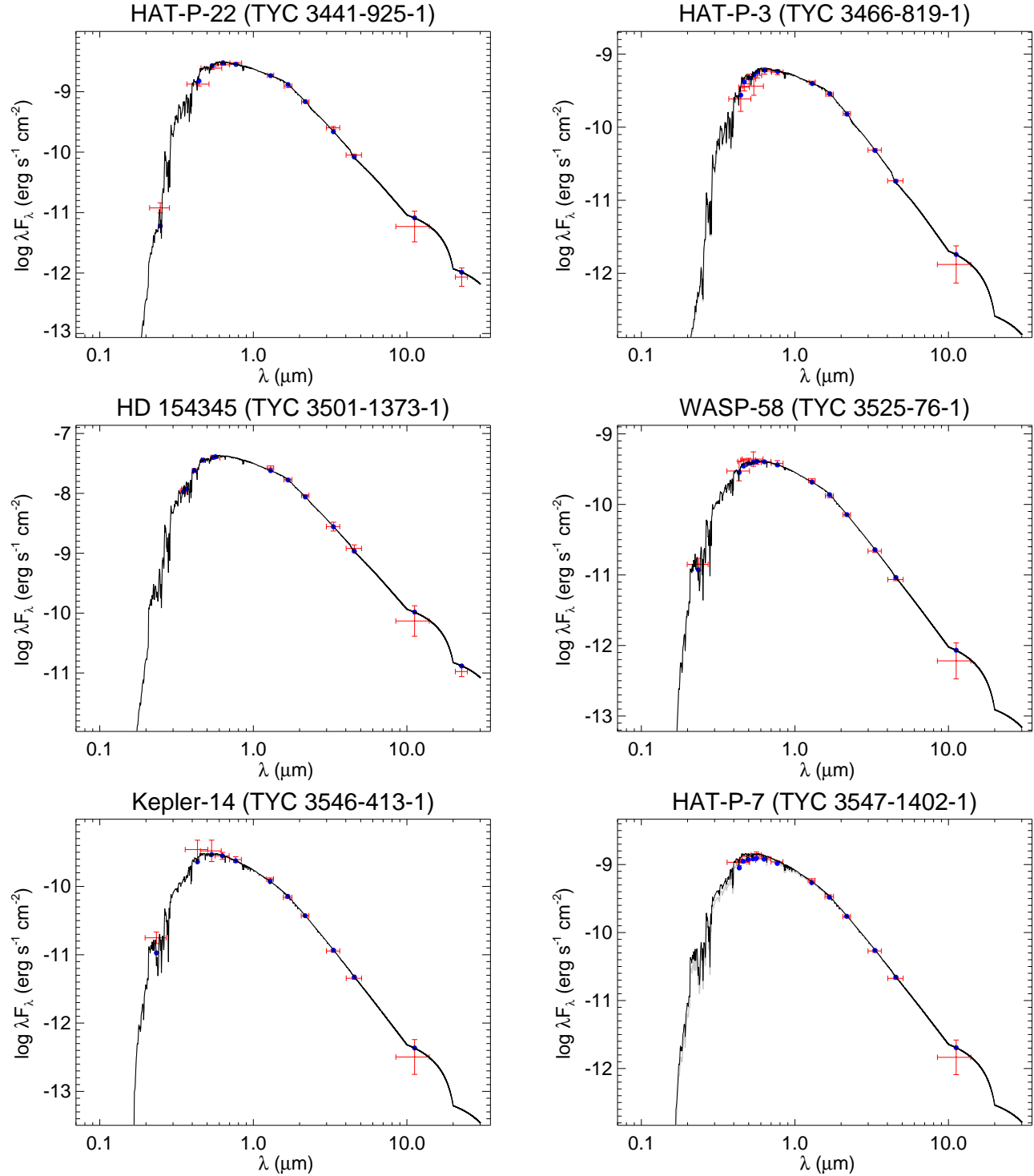


Figure 49. All labels, lines, symbols, and colors as in Figure 14.

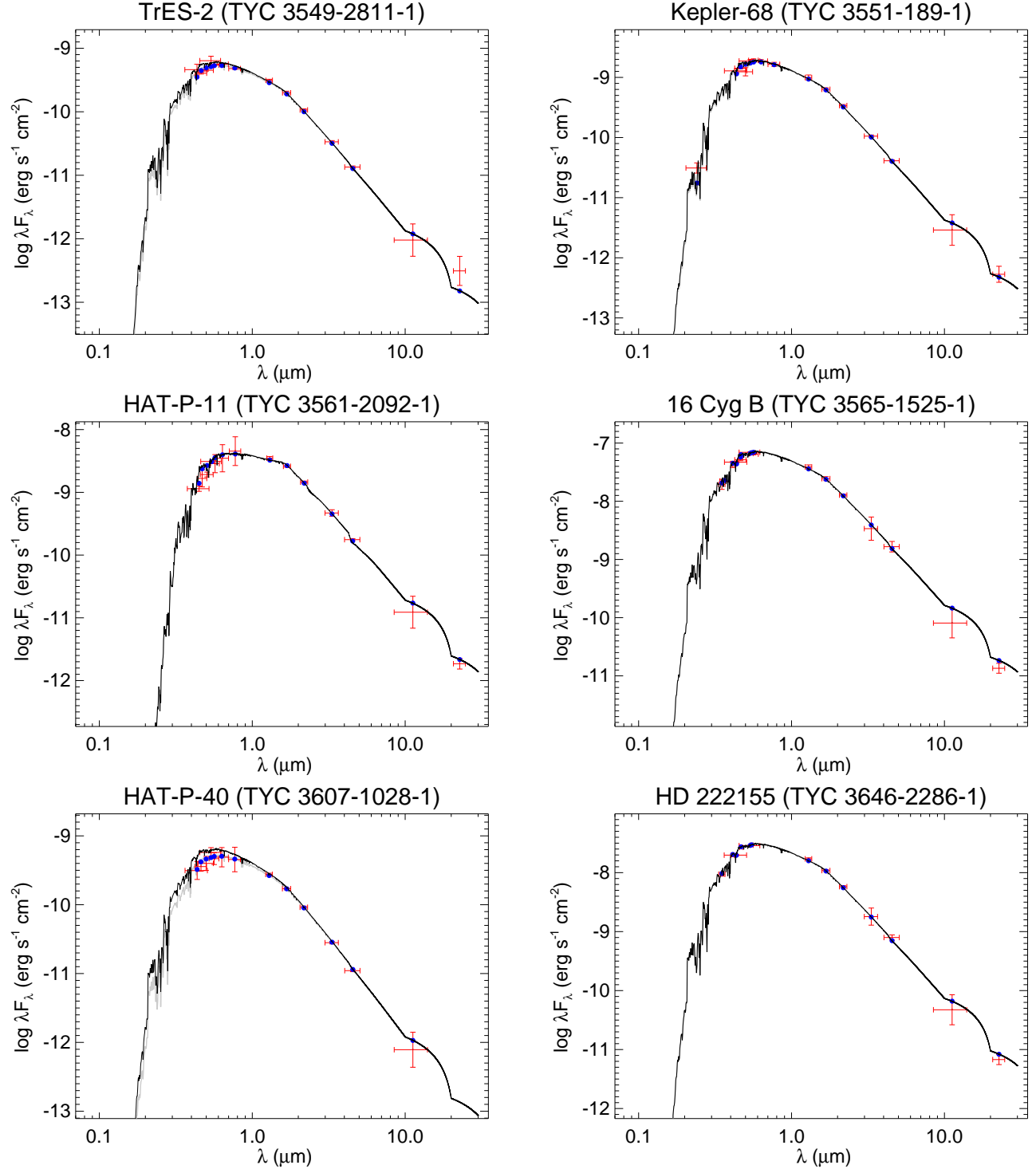


Figure 50. All labels, lines, symbols, and colors as in Figure 14.

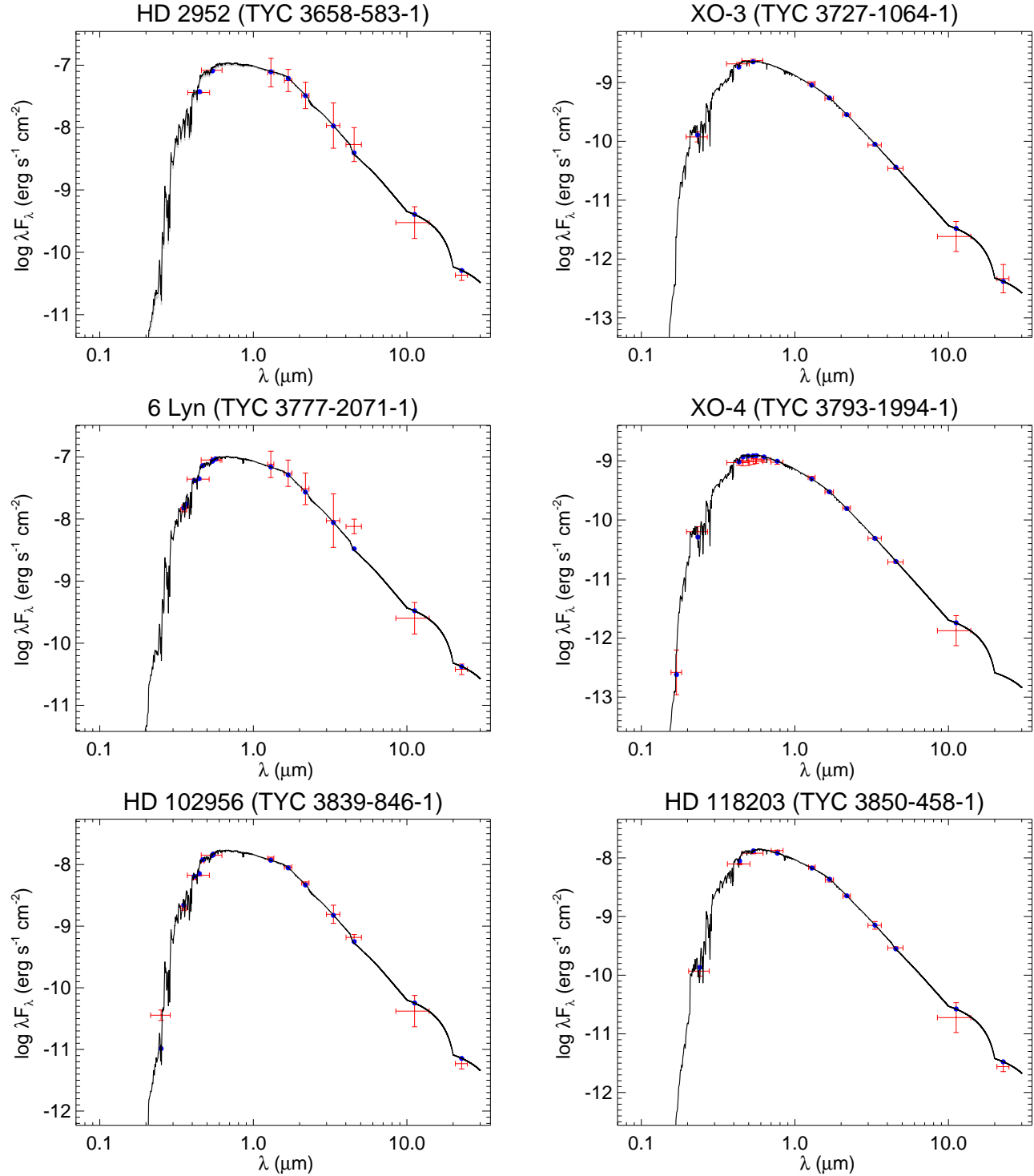


Figure 51. All labels, lines, symbols, and colors as in Figure 14.

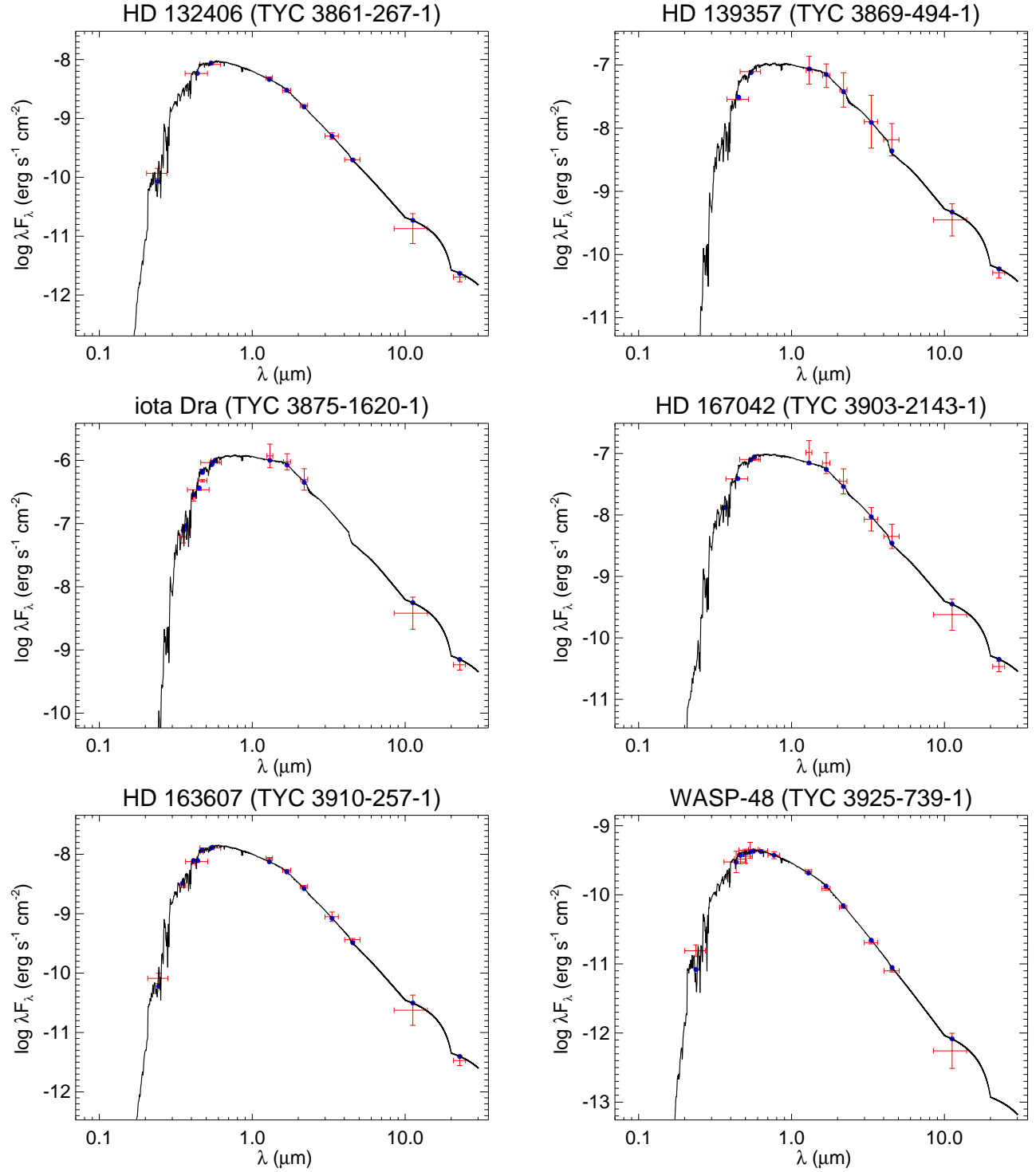


Figure 52. All labels, lines, symbols, and colors as in Figure 14.

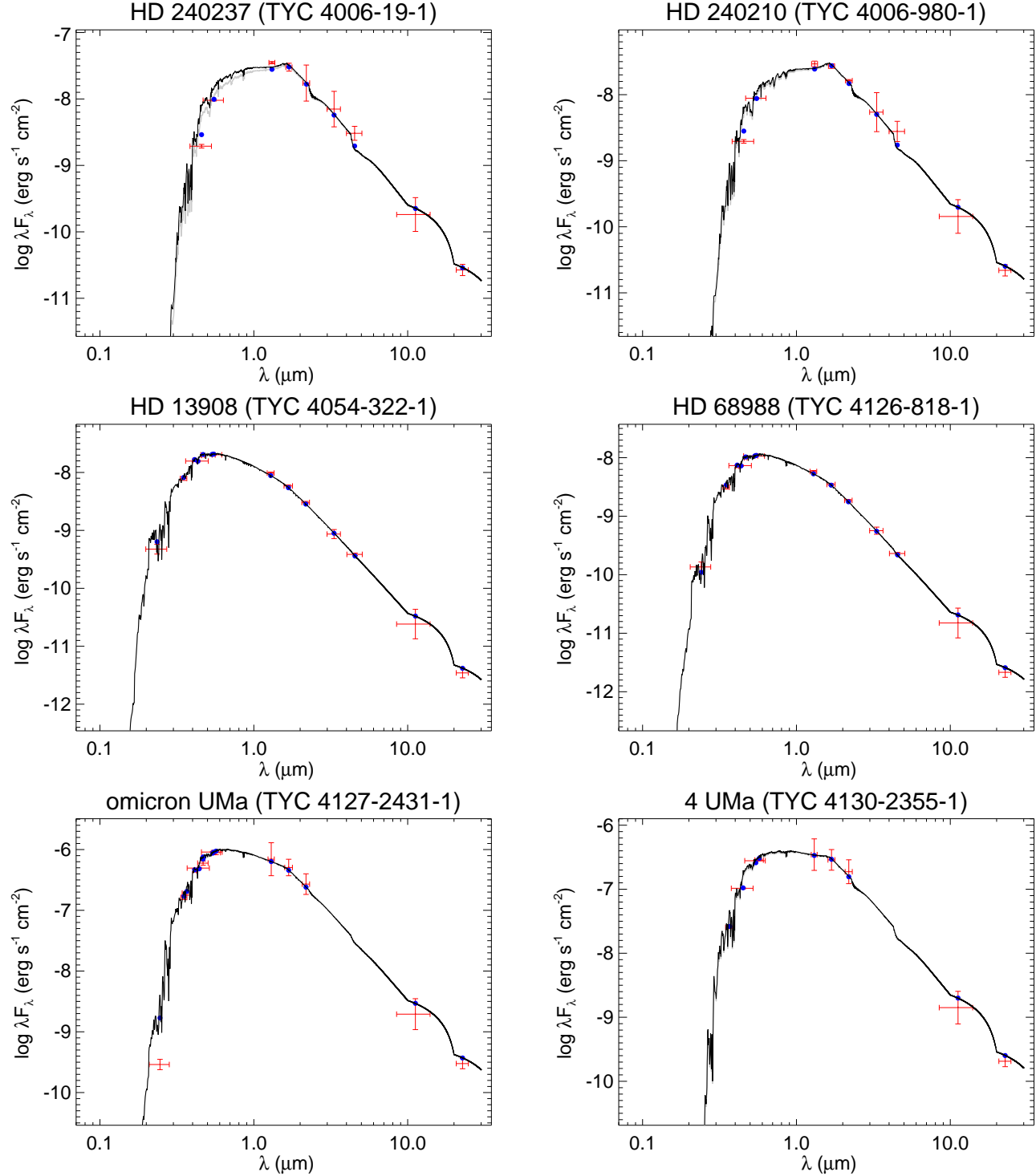


Figure 53. All labels, lines, symbols, and colors as in Figure 14.

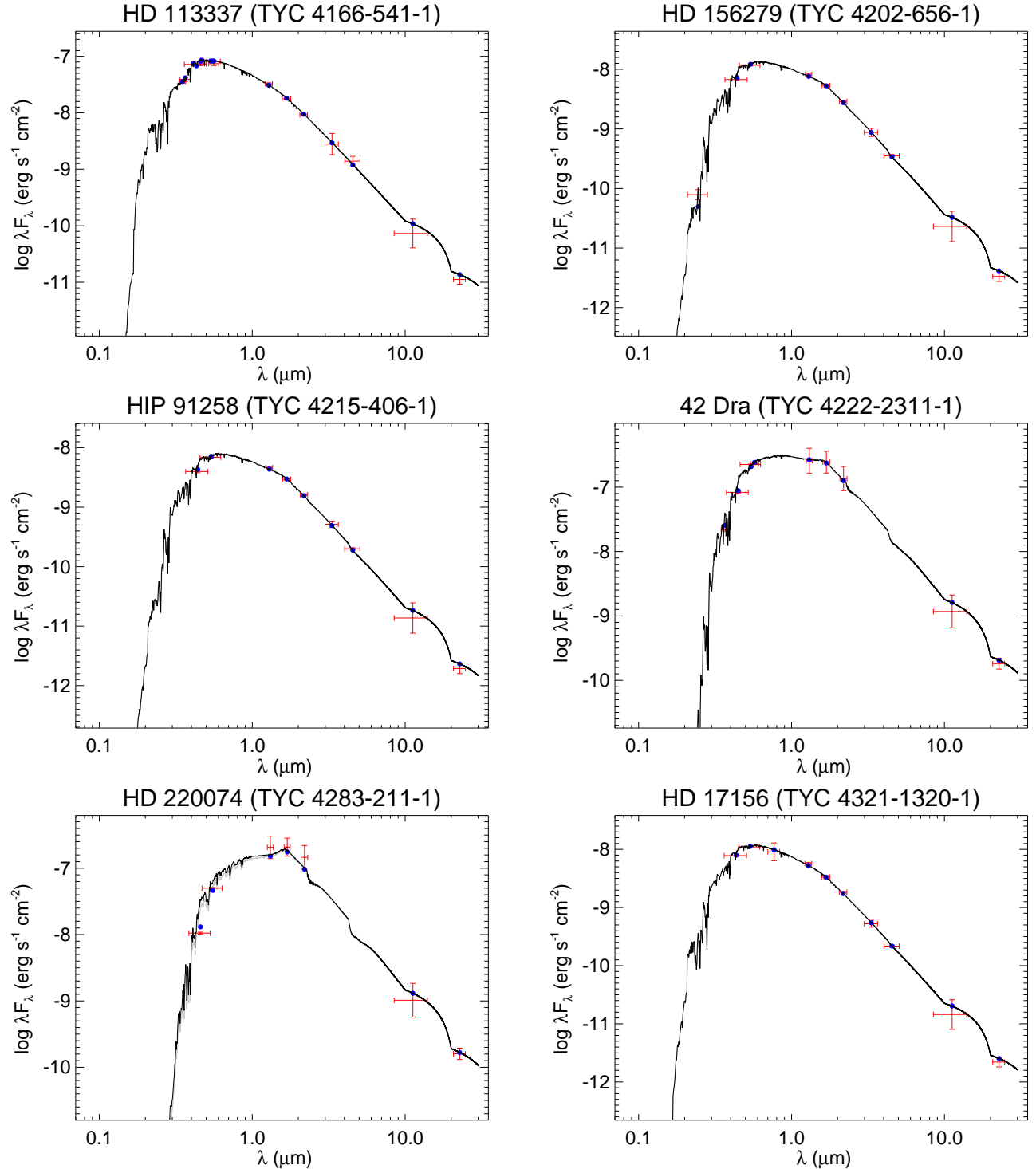


Figure 54. All labels, lines, symbols, and colors as in Figure 14.

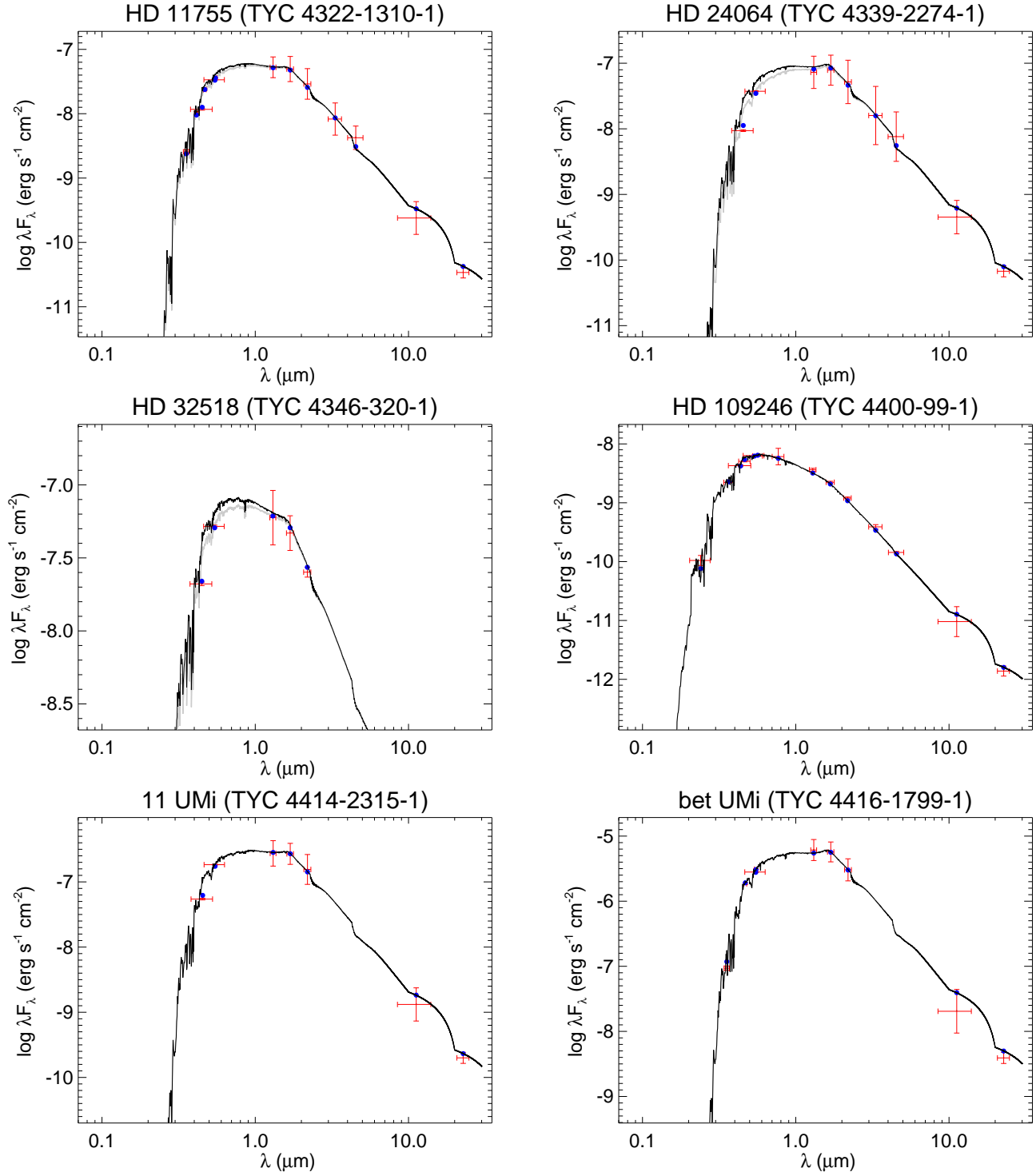


Figure 55. All labels, lines, symbols, and colors as in Figure 14.

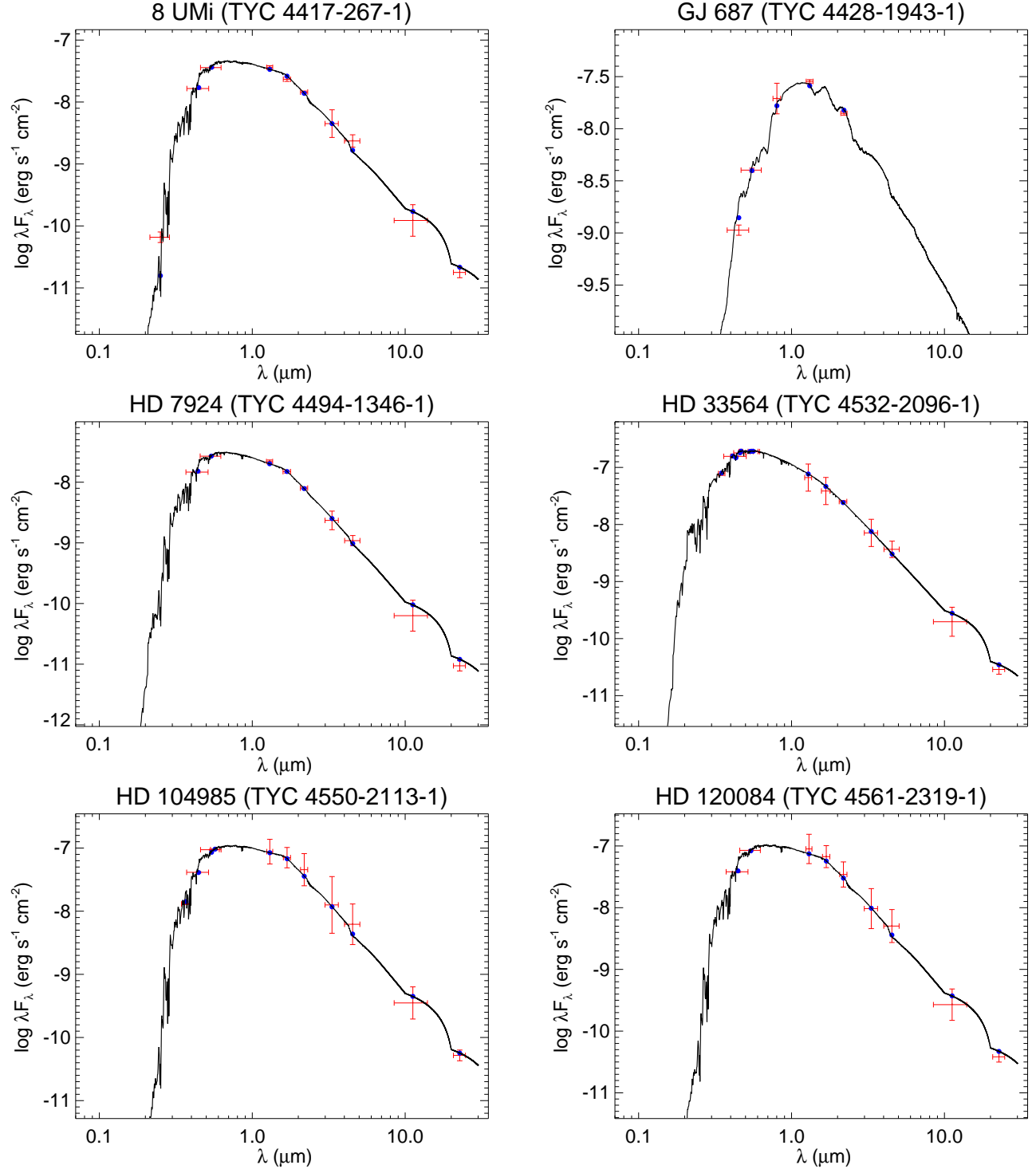


Figure 56. All labels, lines, symbols, and colors as in Figure 14.

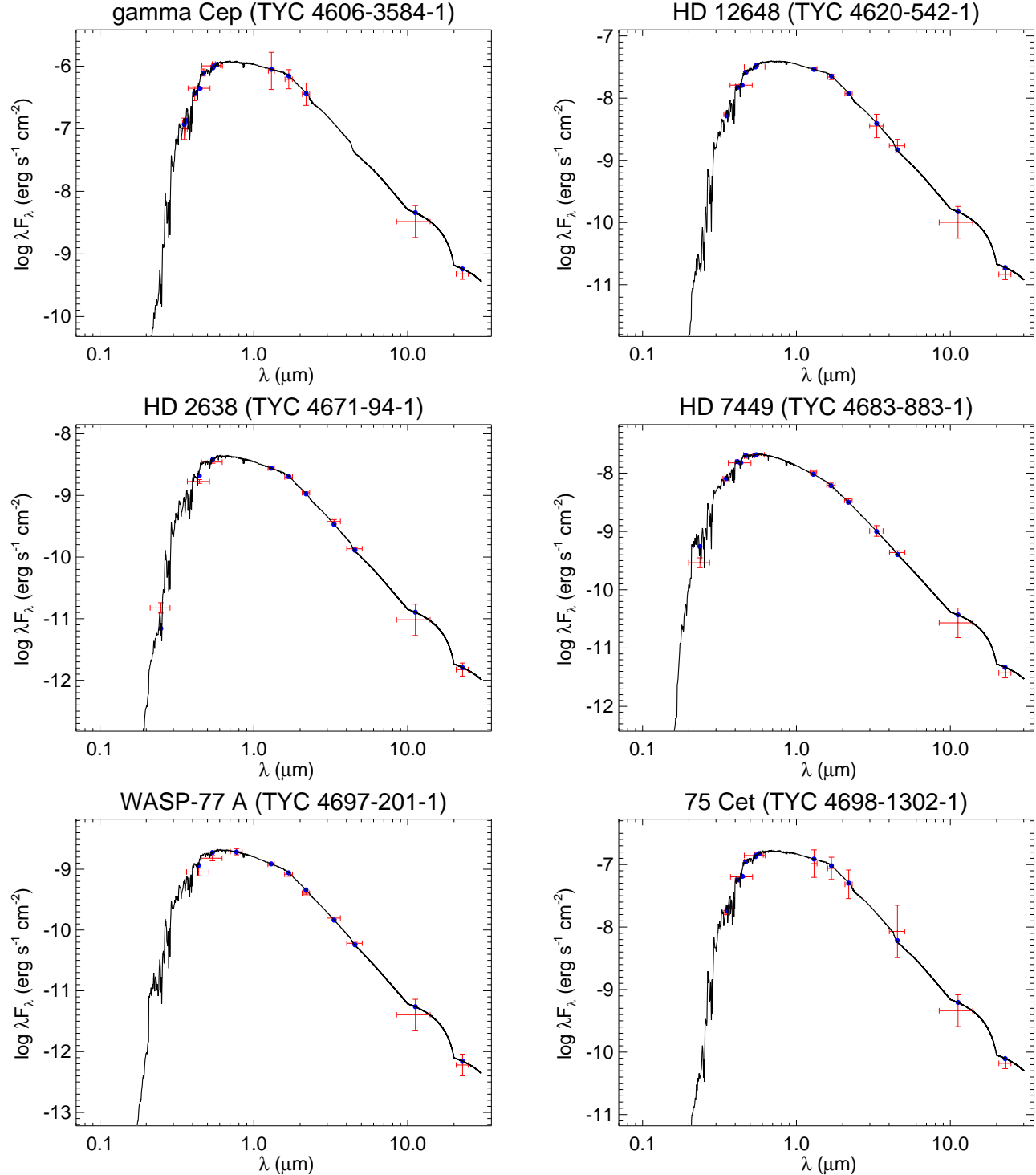


Figure 57. All labels, lines, symbols, and colors as in Figure 14.

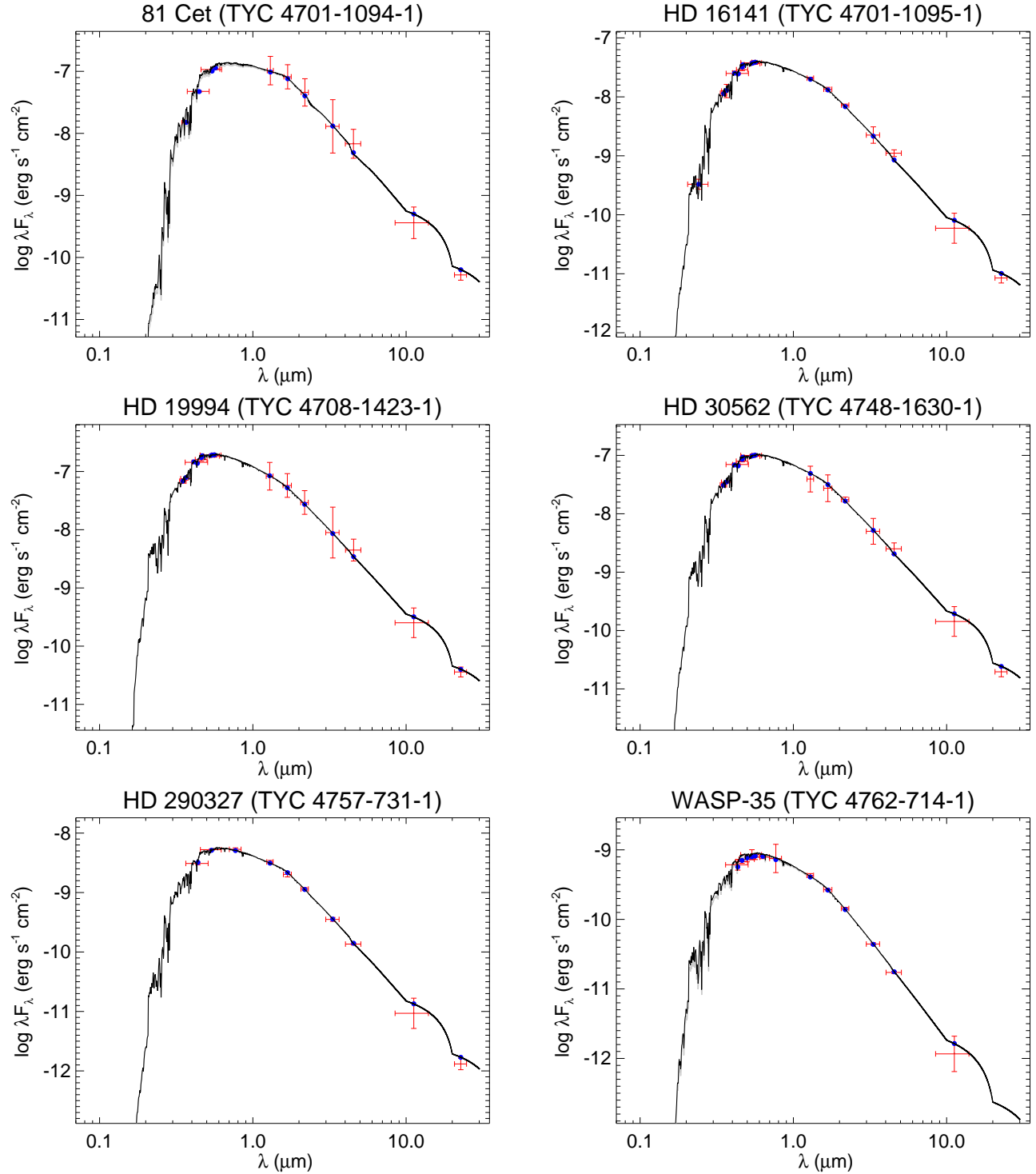


Figure 58. All labels, lines, symbols, and colors as in Figure 14.

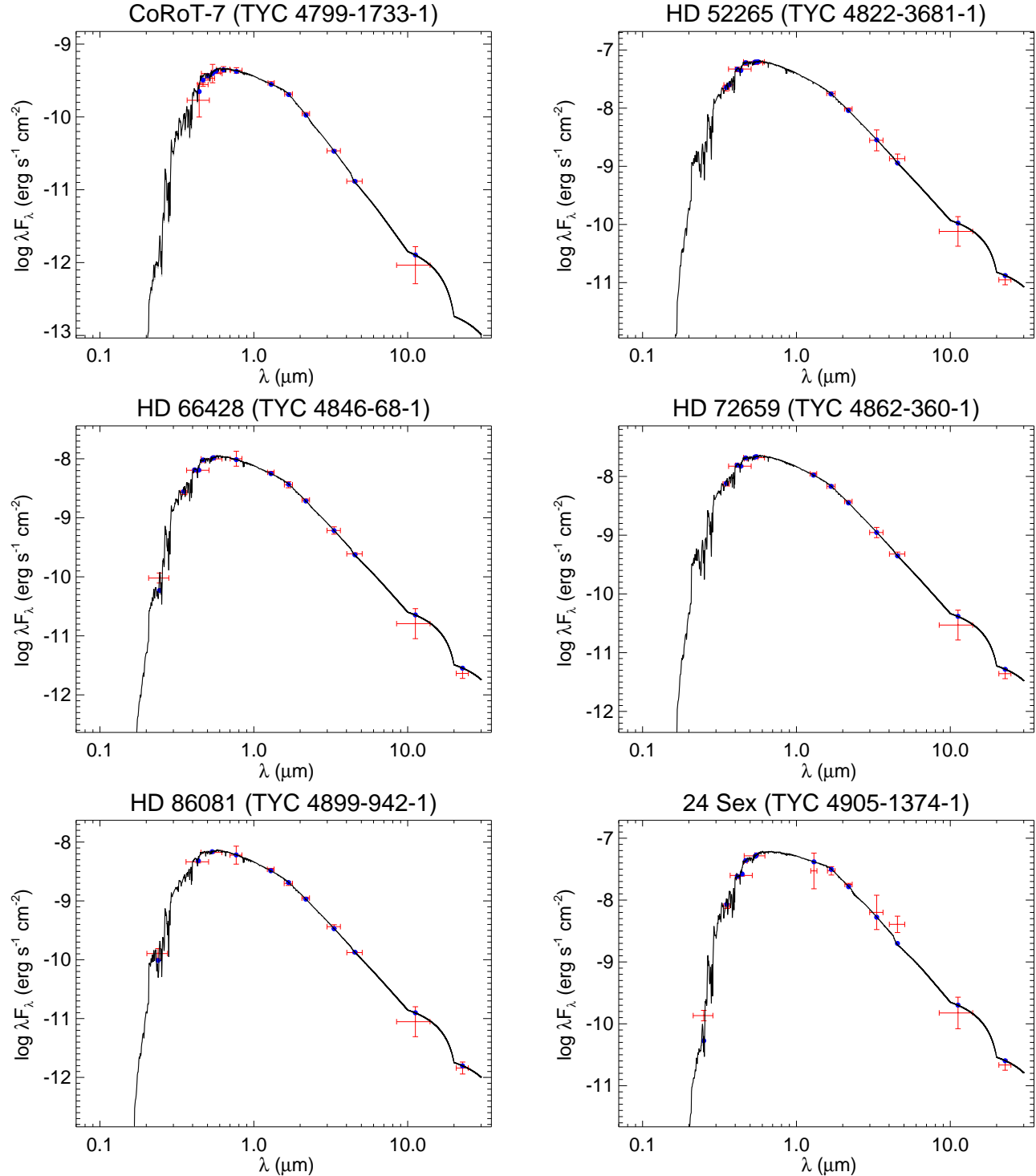


Figure 59. All labels, lines, symbols, and colors as in Figure 14.

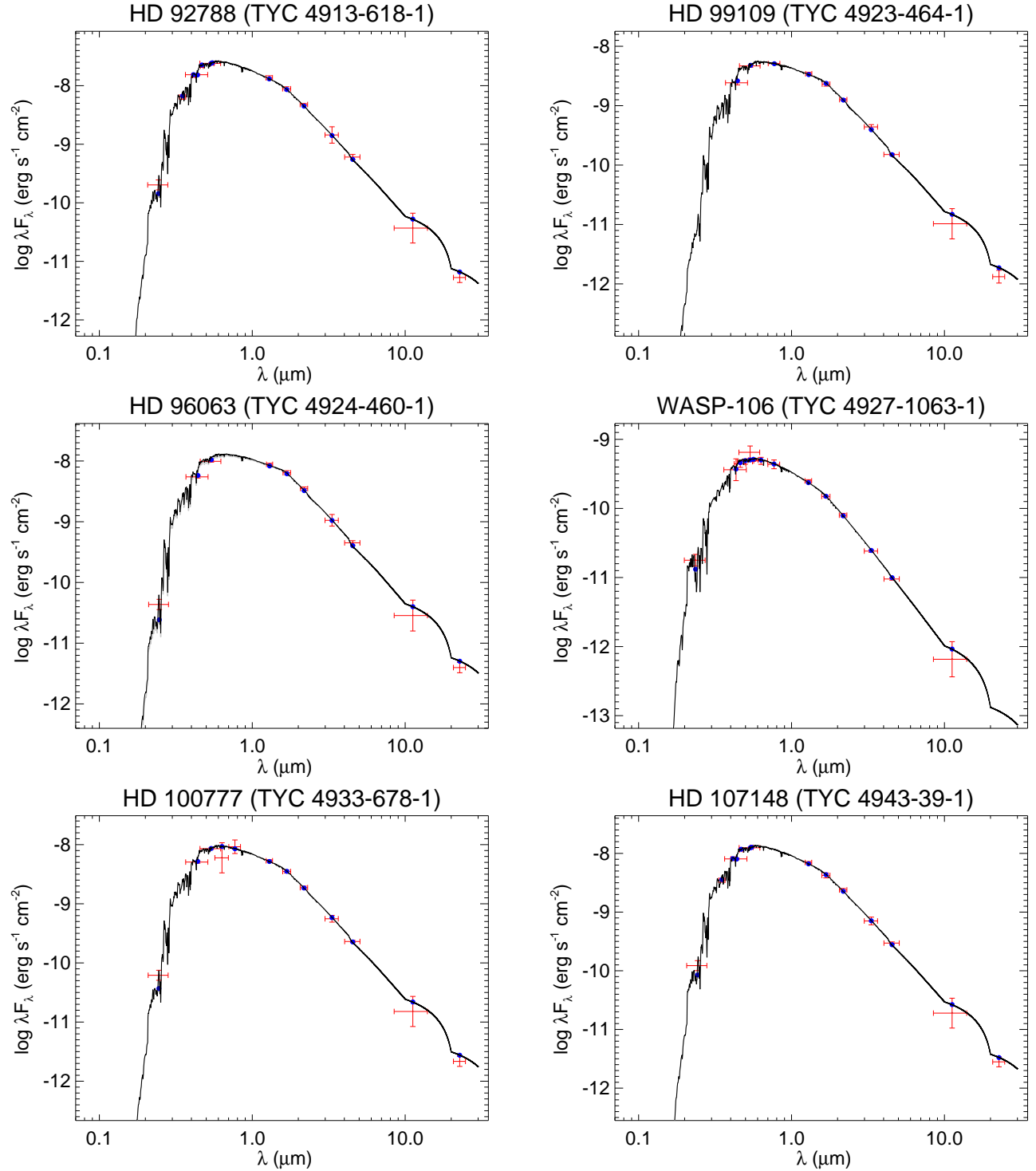


Figure 60. All labels, lines, symbols, and colors as in Figure 14.

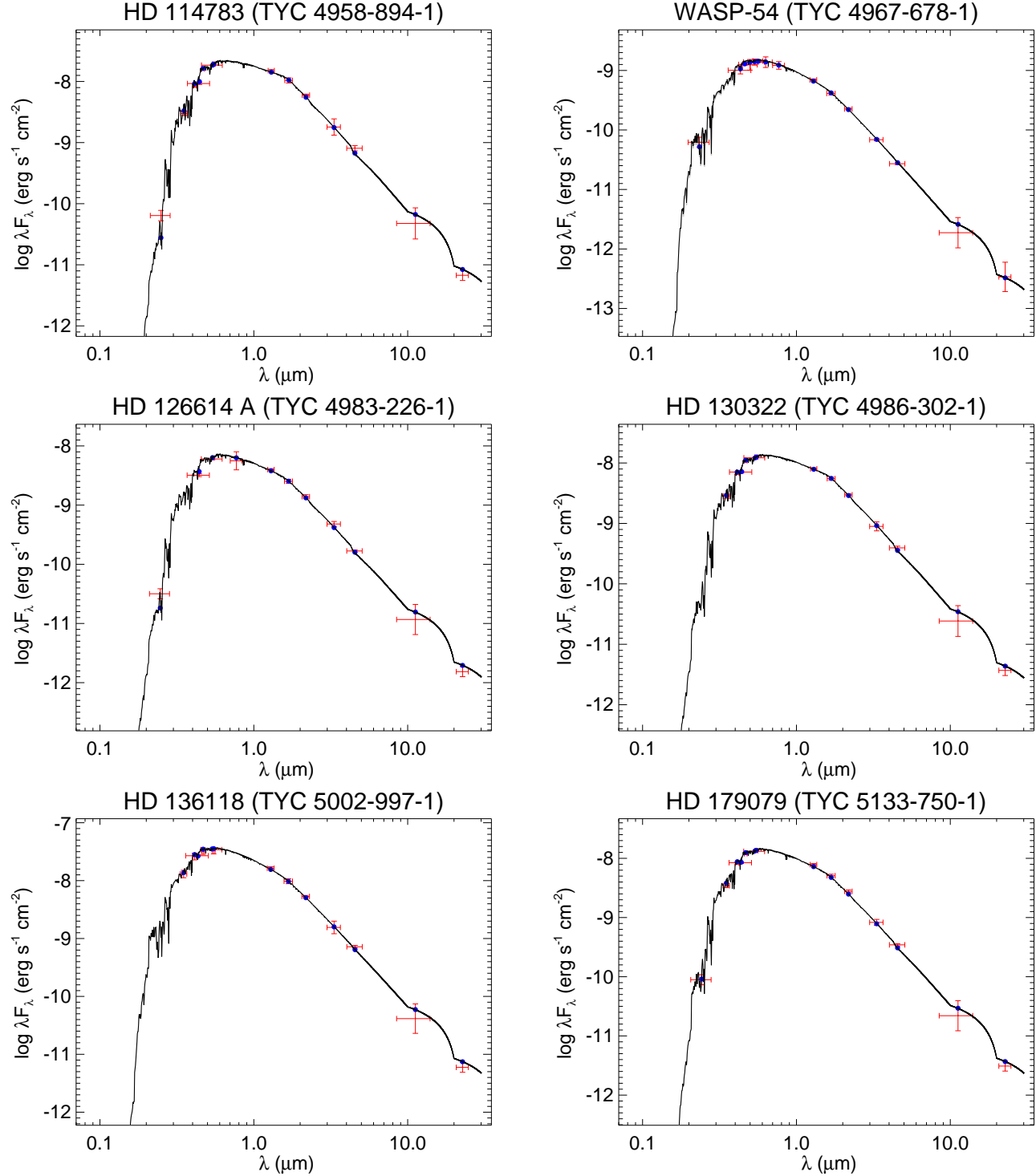


Figure 61. All labels, lines, symbols, and colors as in Figure 14.

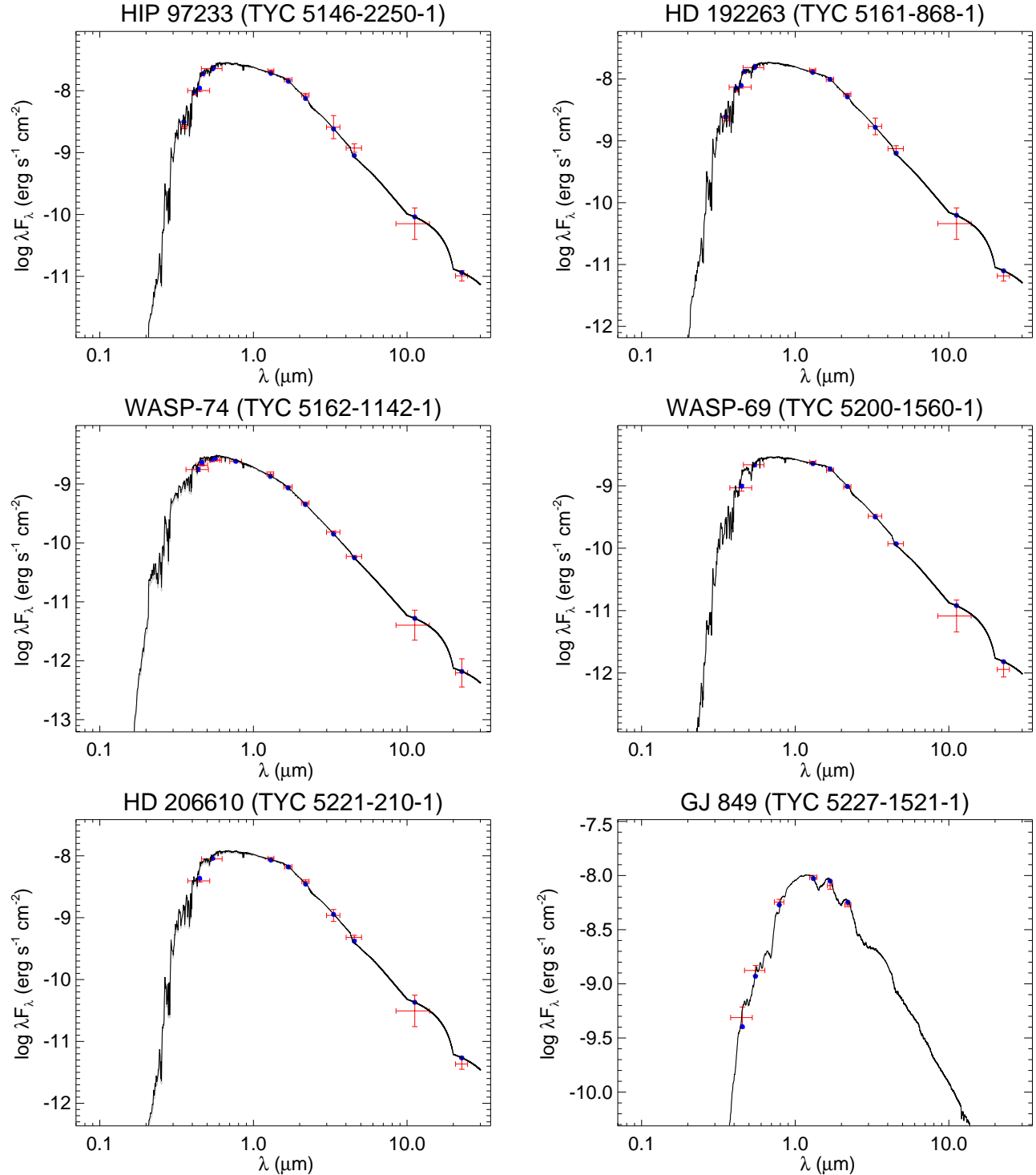


Figure 62. All labels, lines, symbols, and colors as in Figure 14.

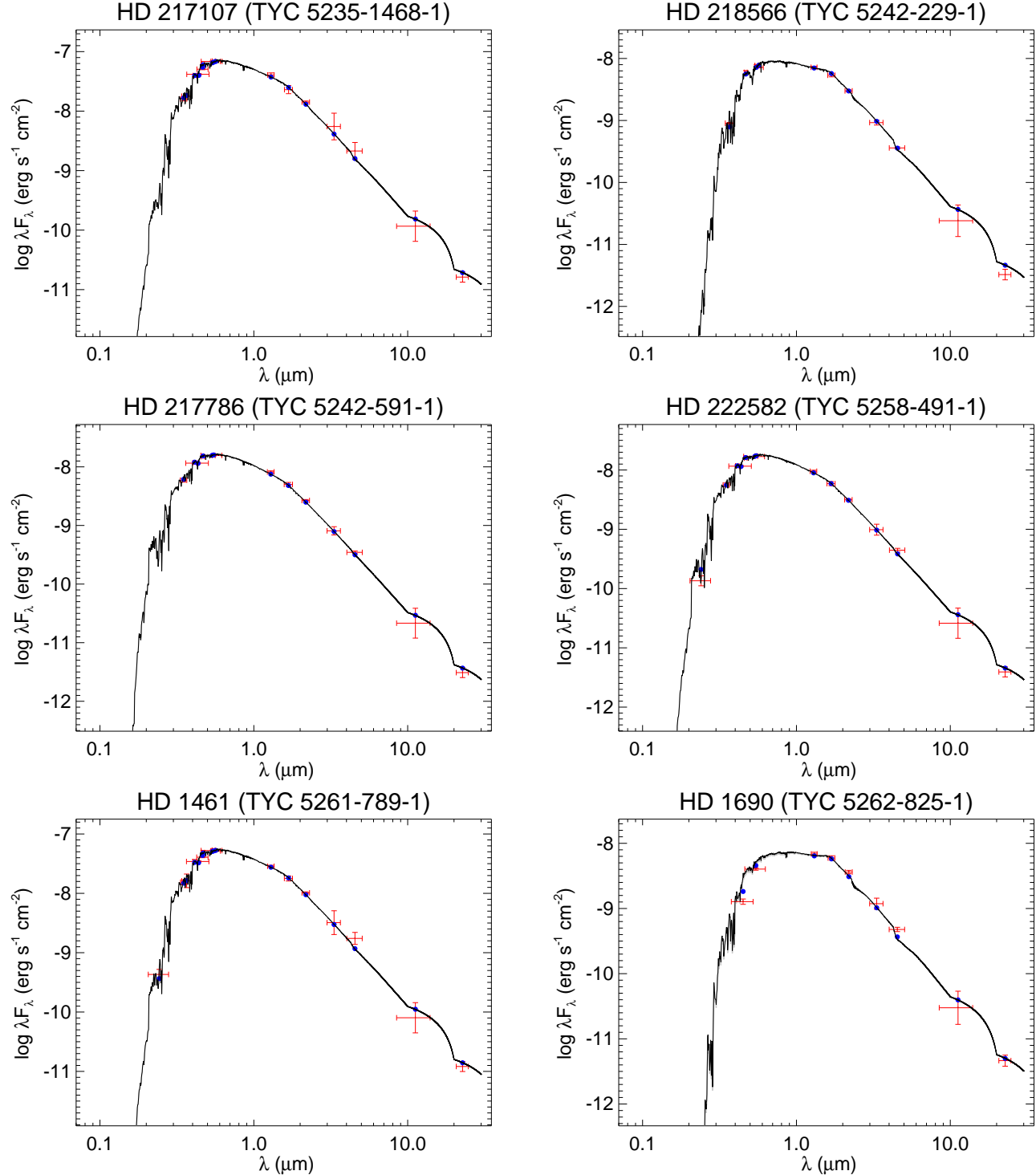


Figure 63. All labels, lines, symbols, and colors as in Figure 14.

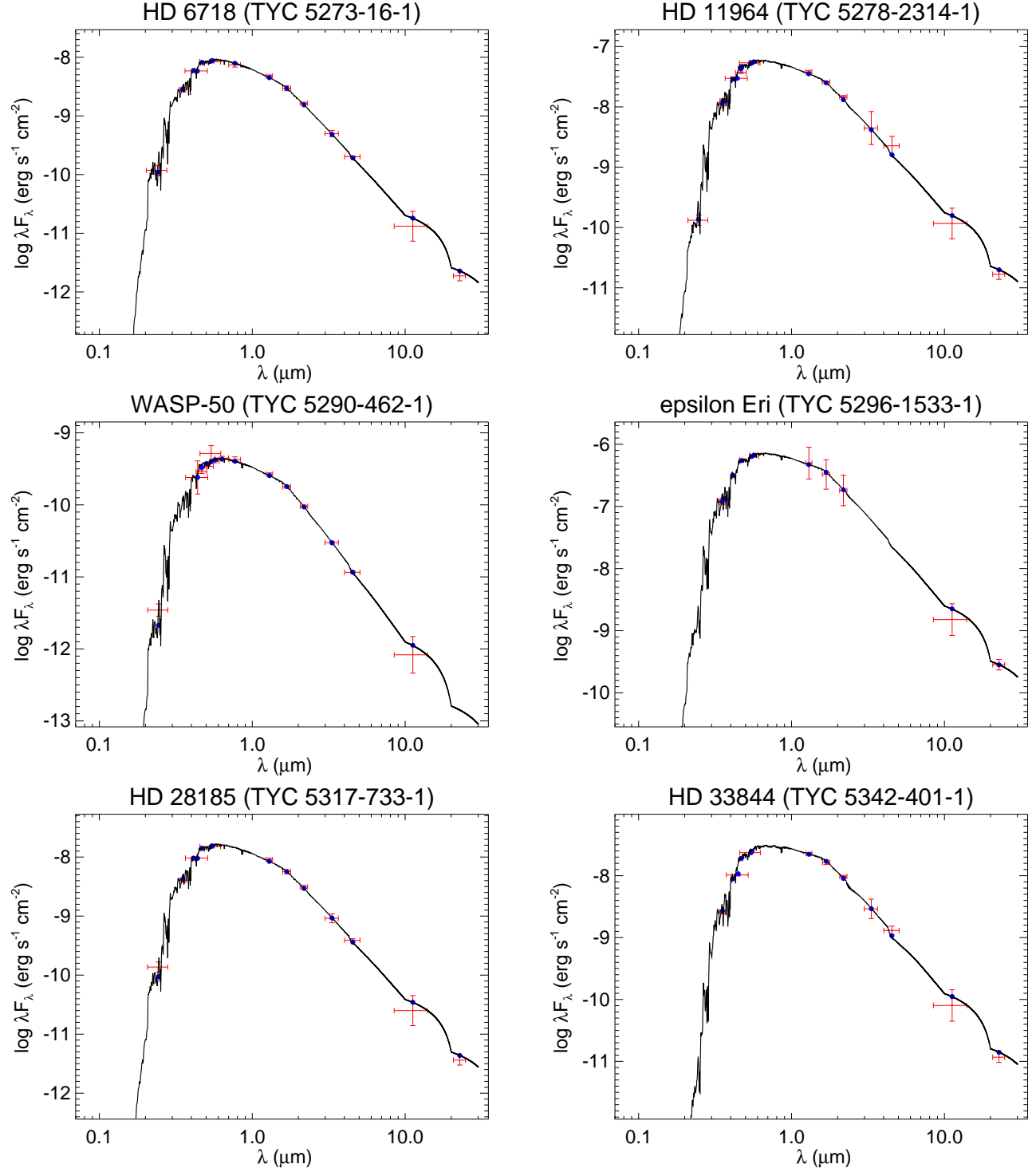


Figure 64. All labels, lines, symbols, and colors as in Figure 14.

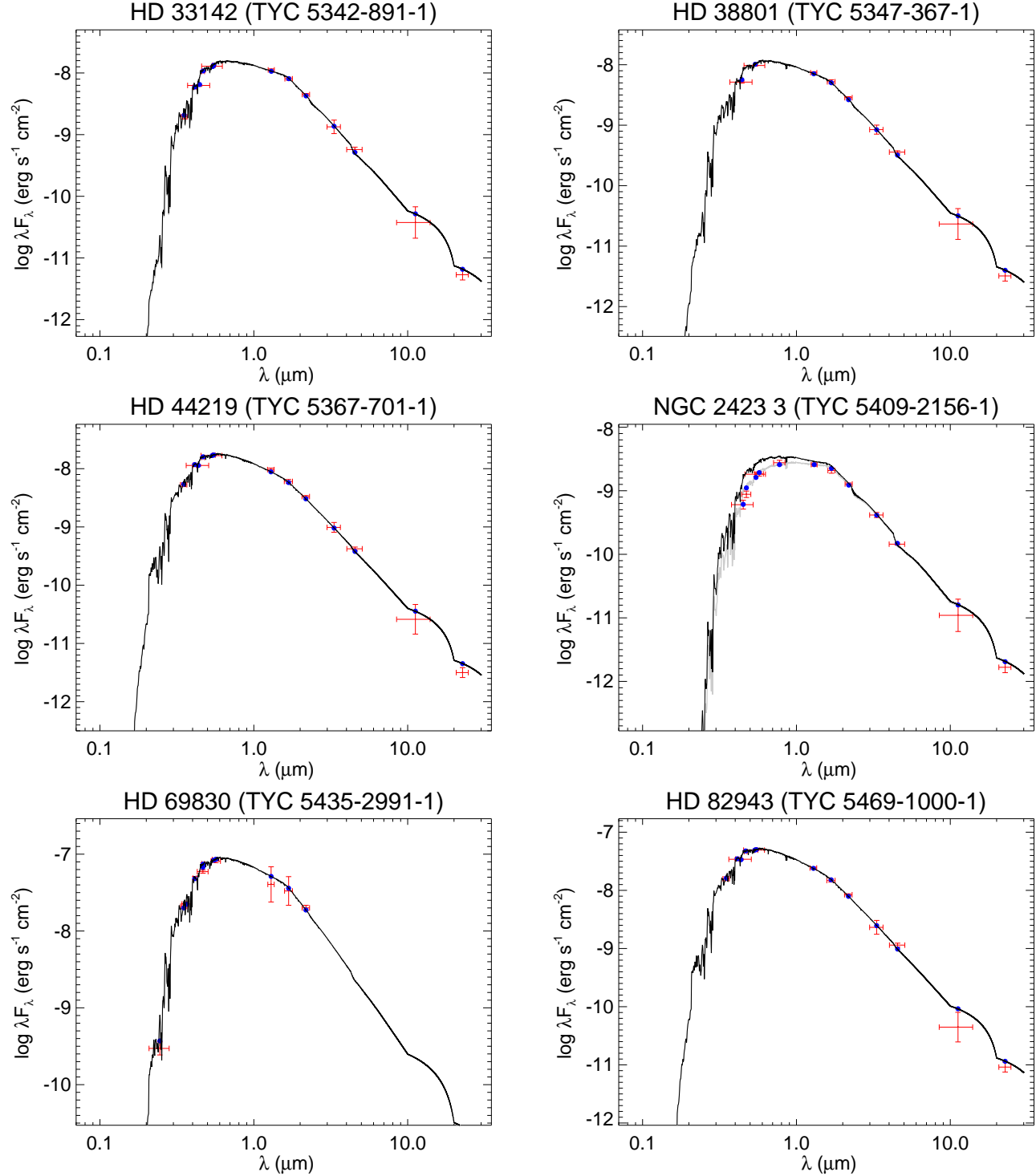


Figure 65. All labels, lines, symbols, and colors as in Figure 14.

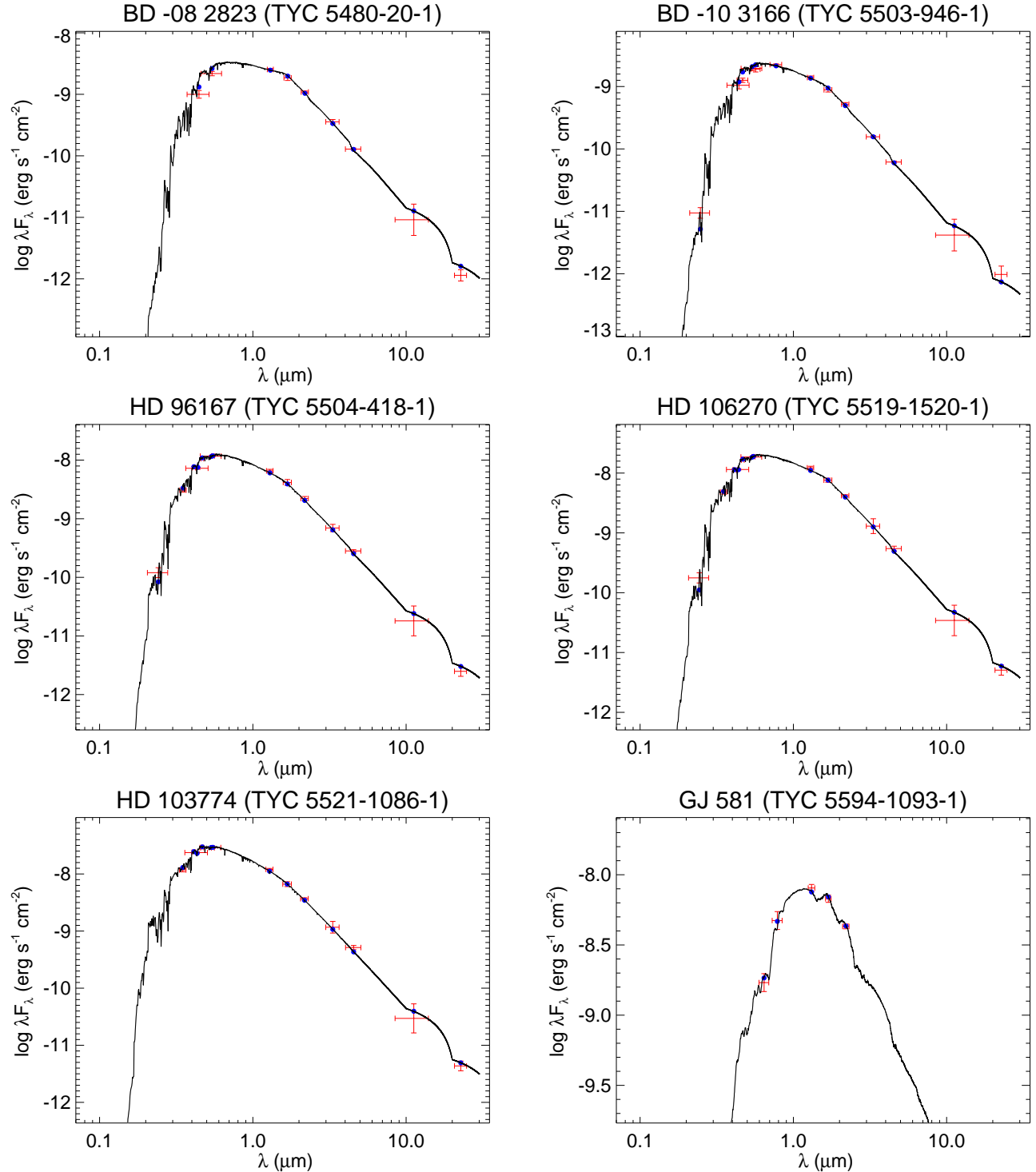


Figure 66. All labels, lines, symbols, and colors as in Figure 14.

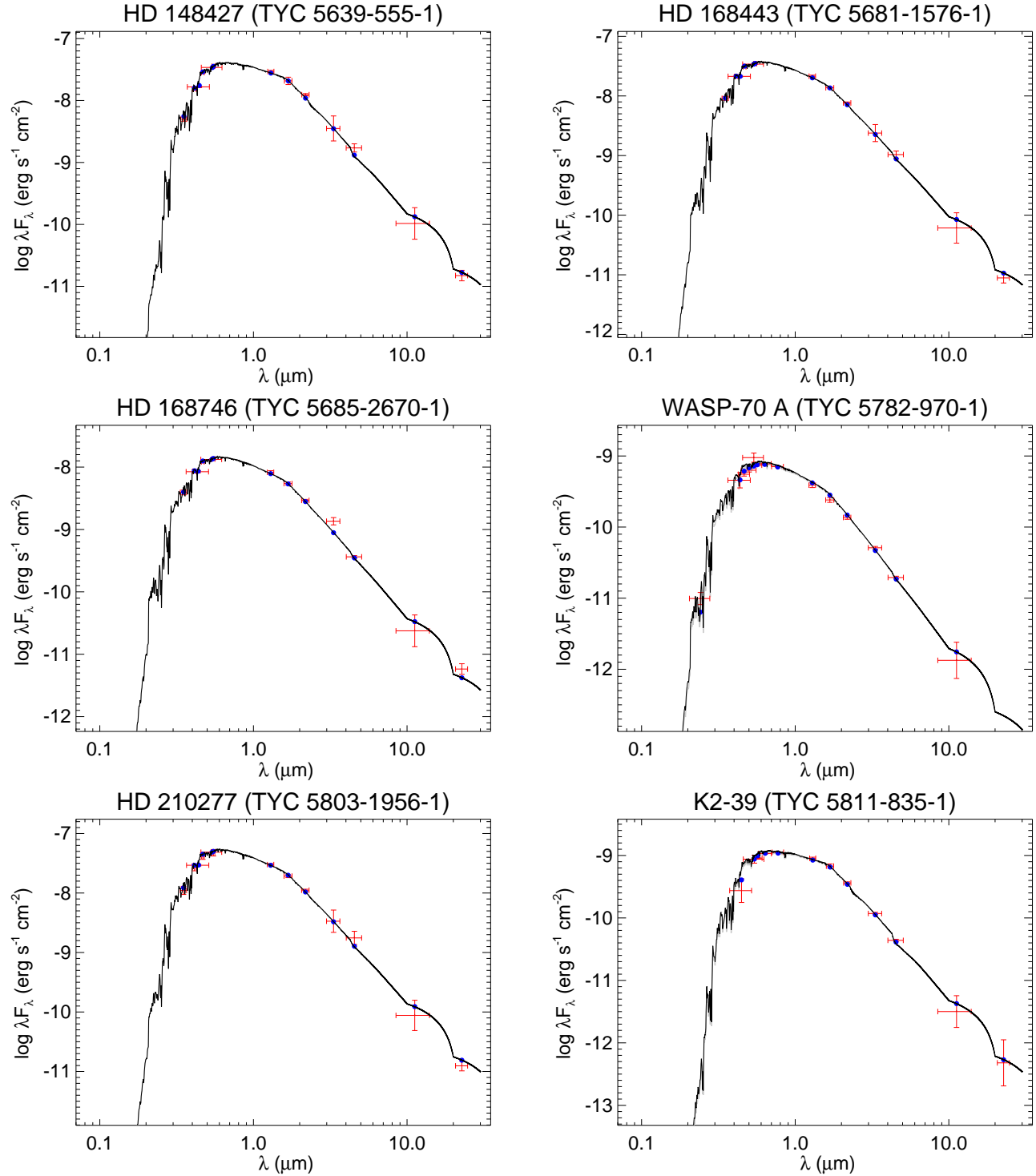


Figure 67. All labels, lines, symbols, and colors as in Figure 14.

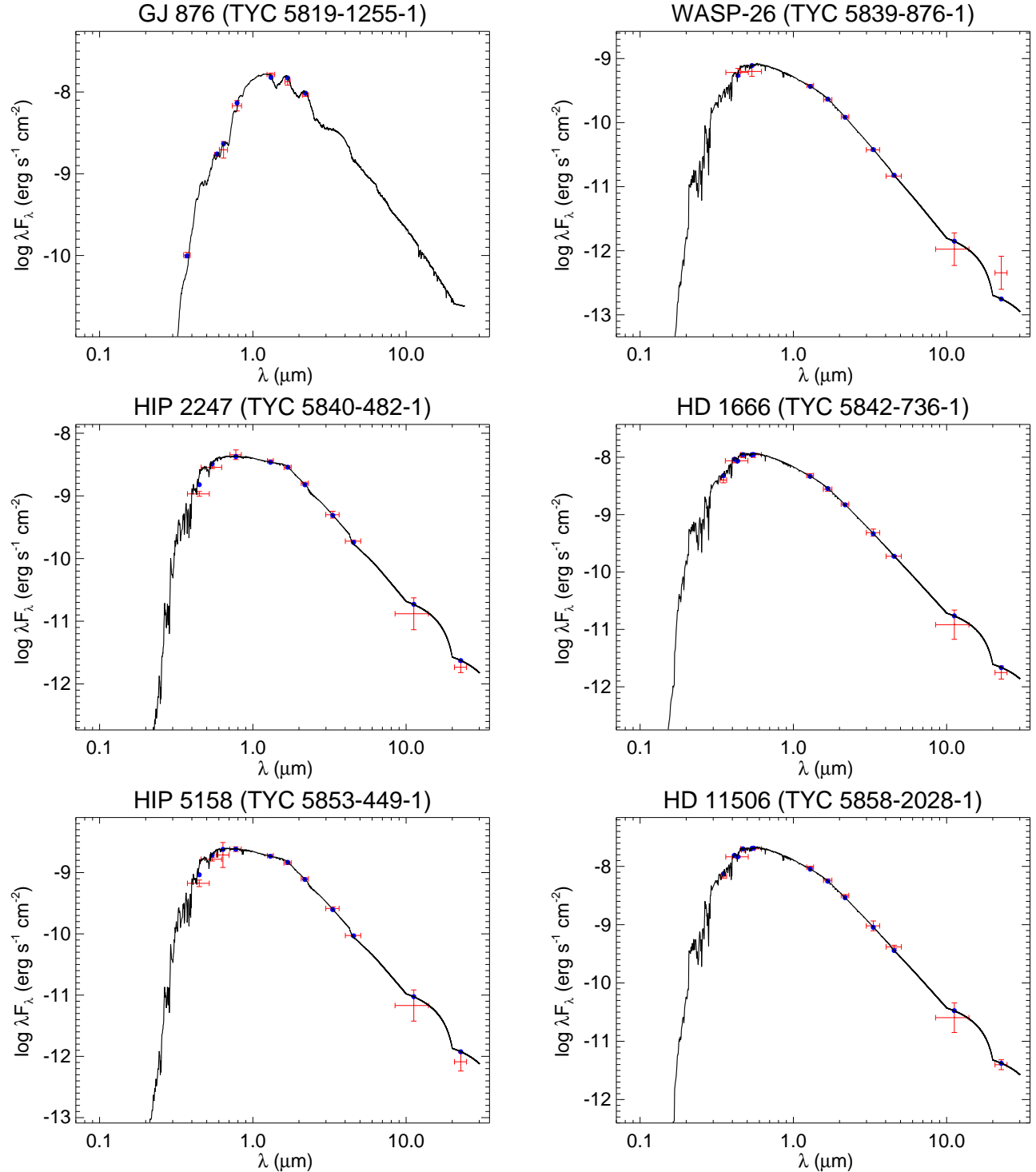


Figure 68. All labels, lines, symbols, and colors as in Figure 14.

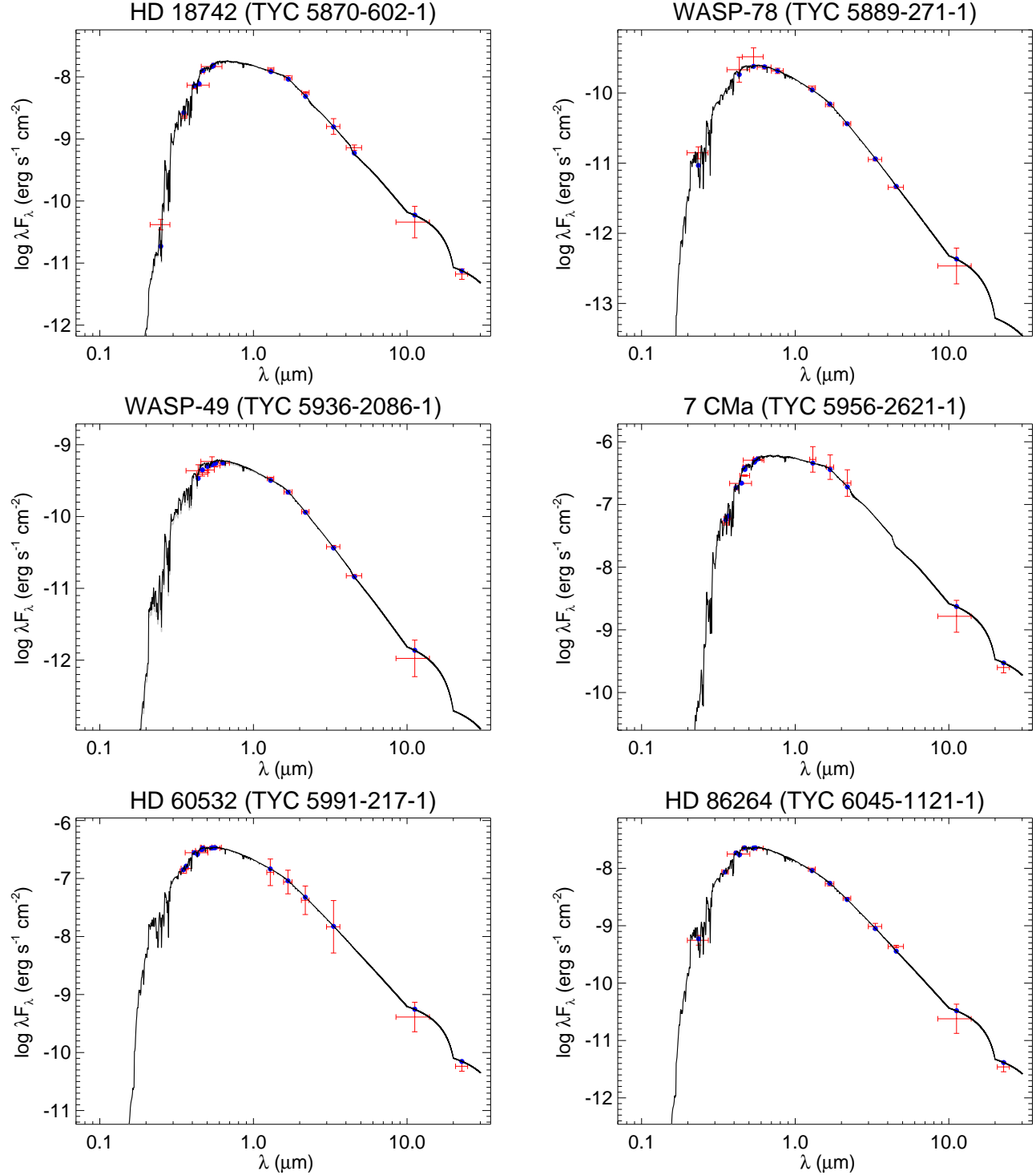


Figure 69. All labels, lines, symbols, and colors as in Figure 14.

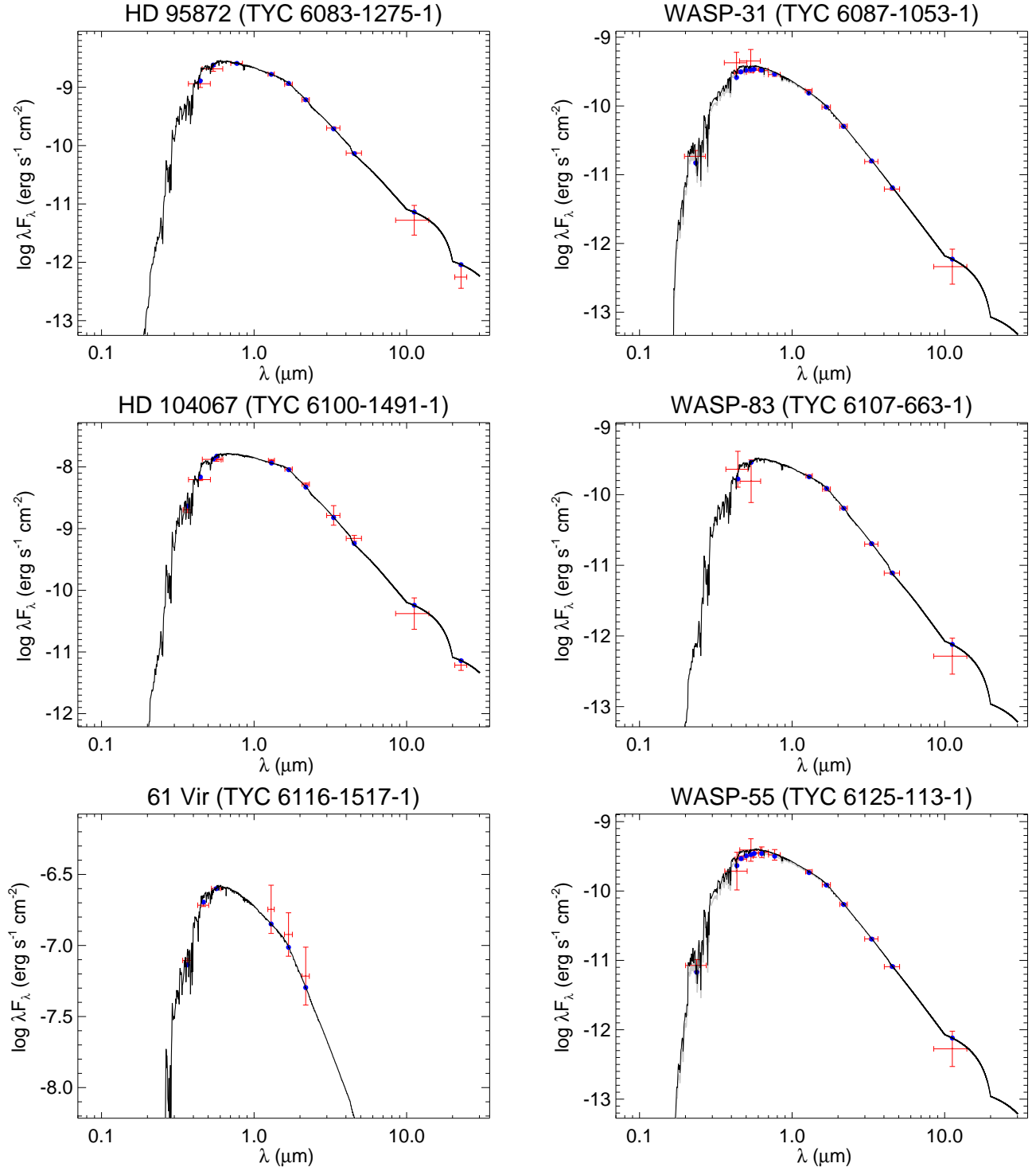


Figure 70. All labels, lines, symbols, and colors as in Figure 14.

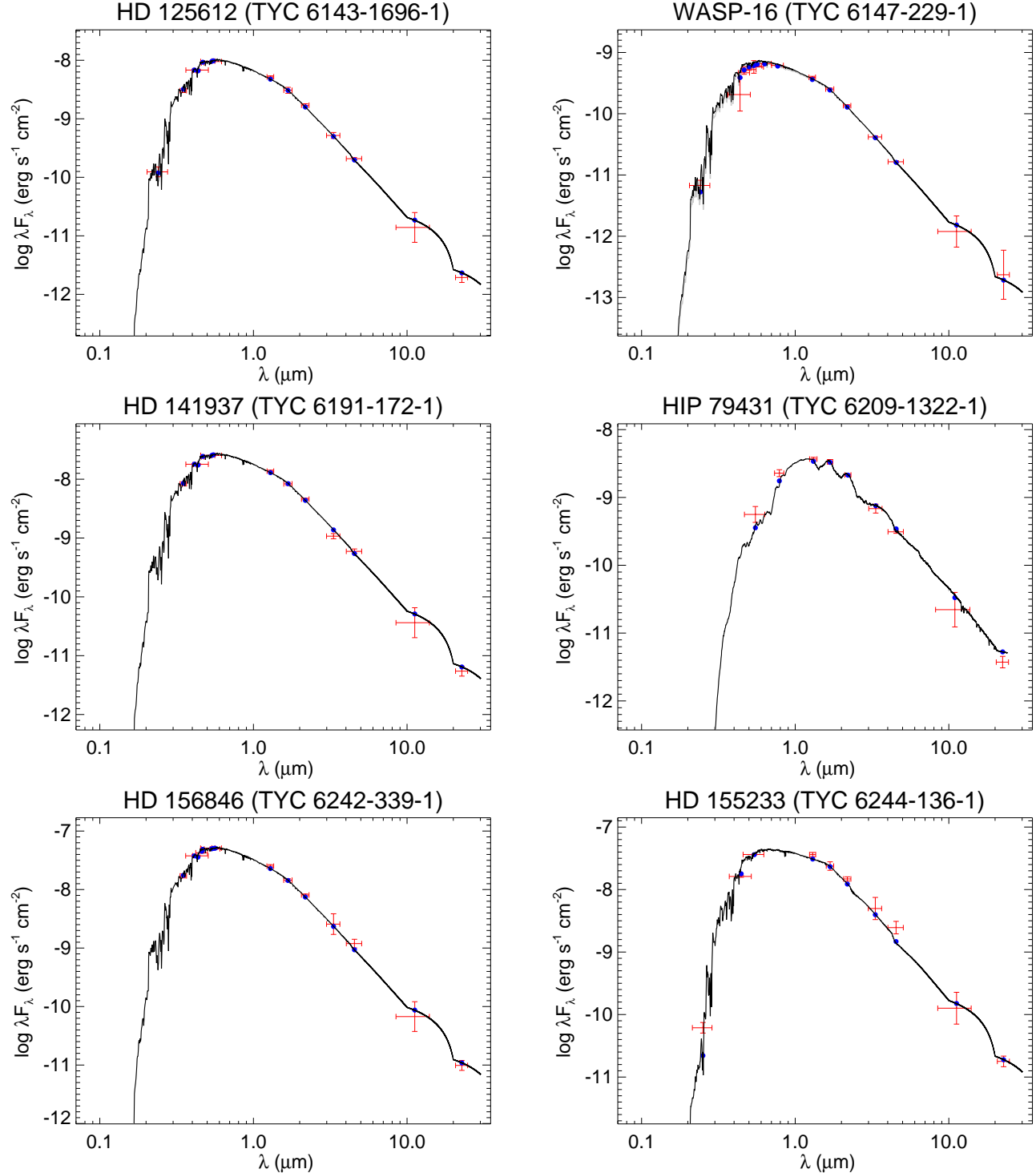


Figure 71. All labels, lines, symbols, and colors as in Figure 14.

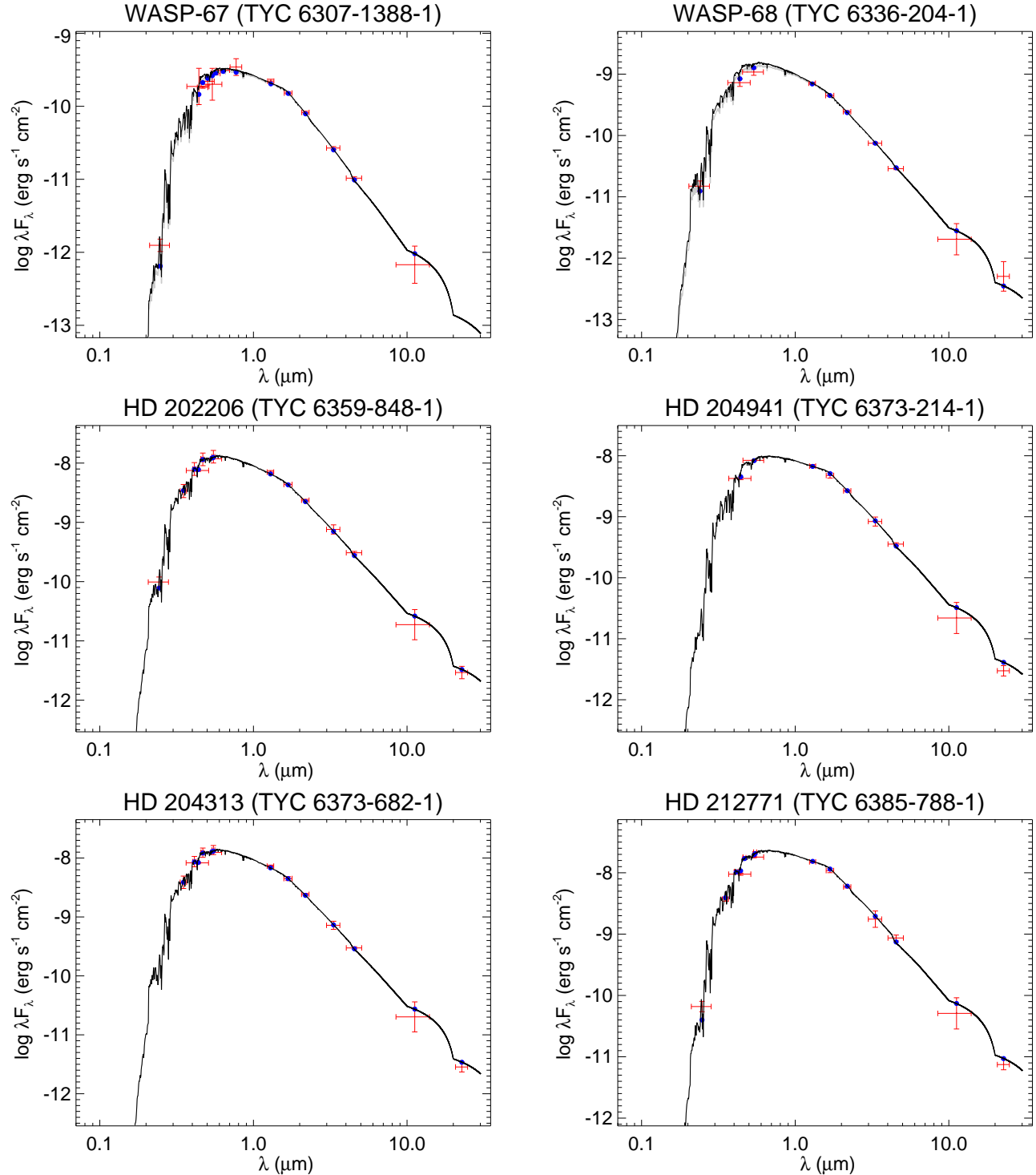


Figure 72. All labels, lines, symbols, and colors as in Figure 14.

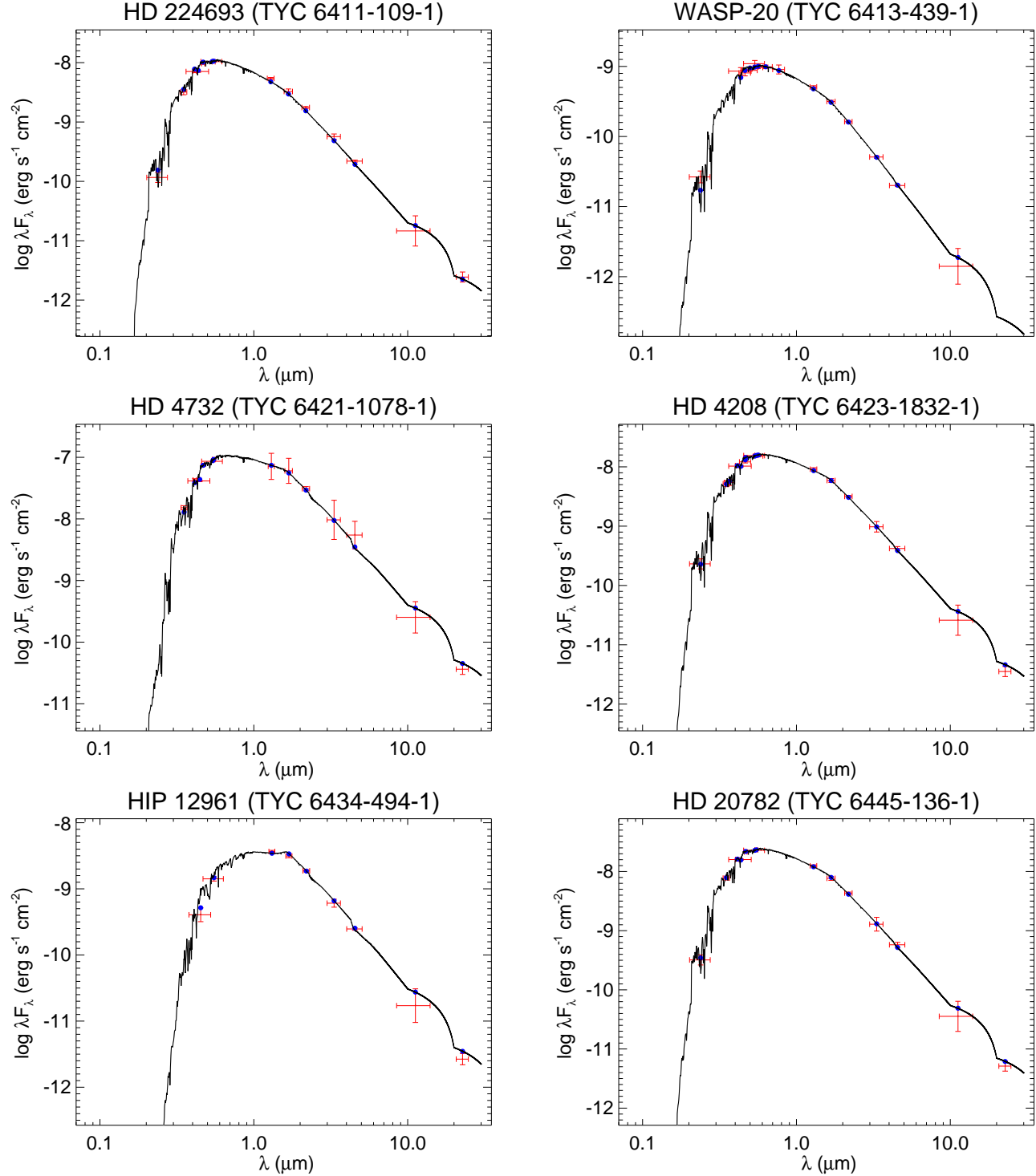


Figure 73. All labels, lines, symbols, and colors as in Figure 14.

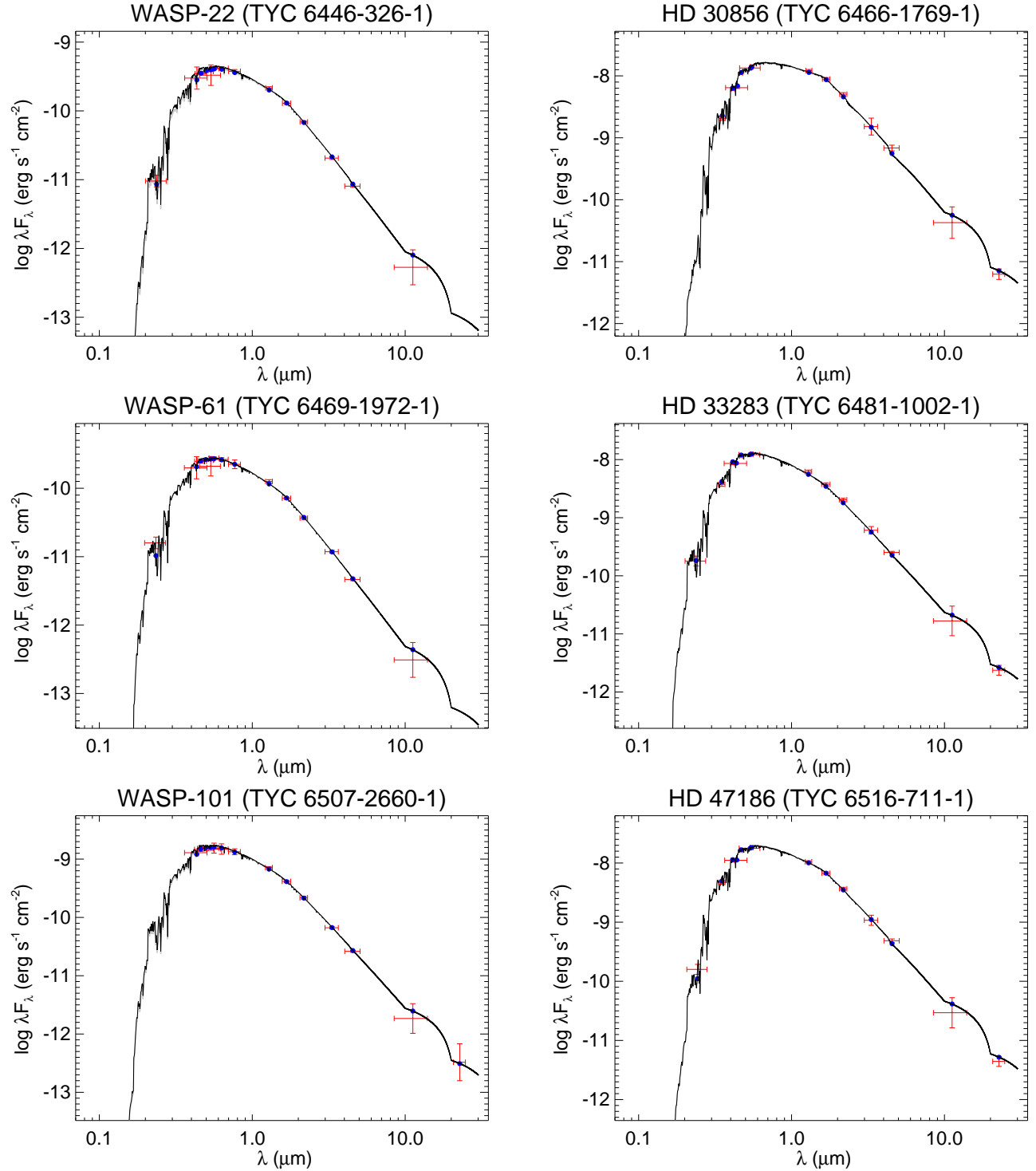


Figure 74. All labels, lines, symbols, and colors as in Figure 14.

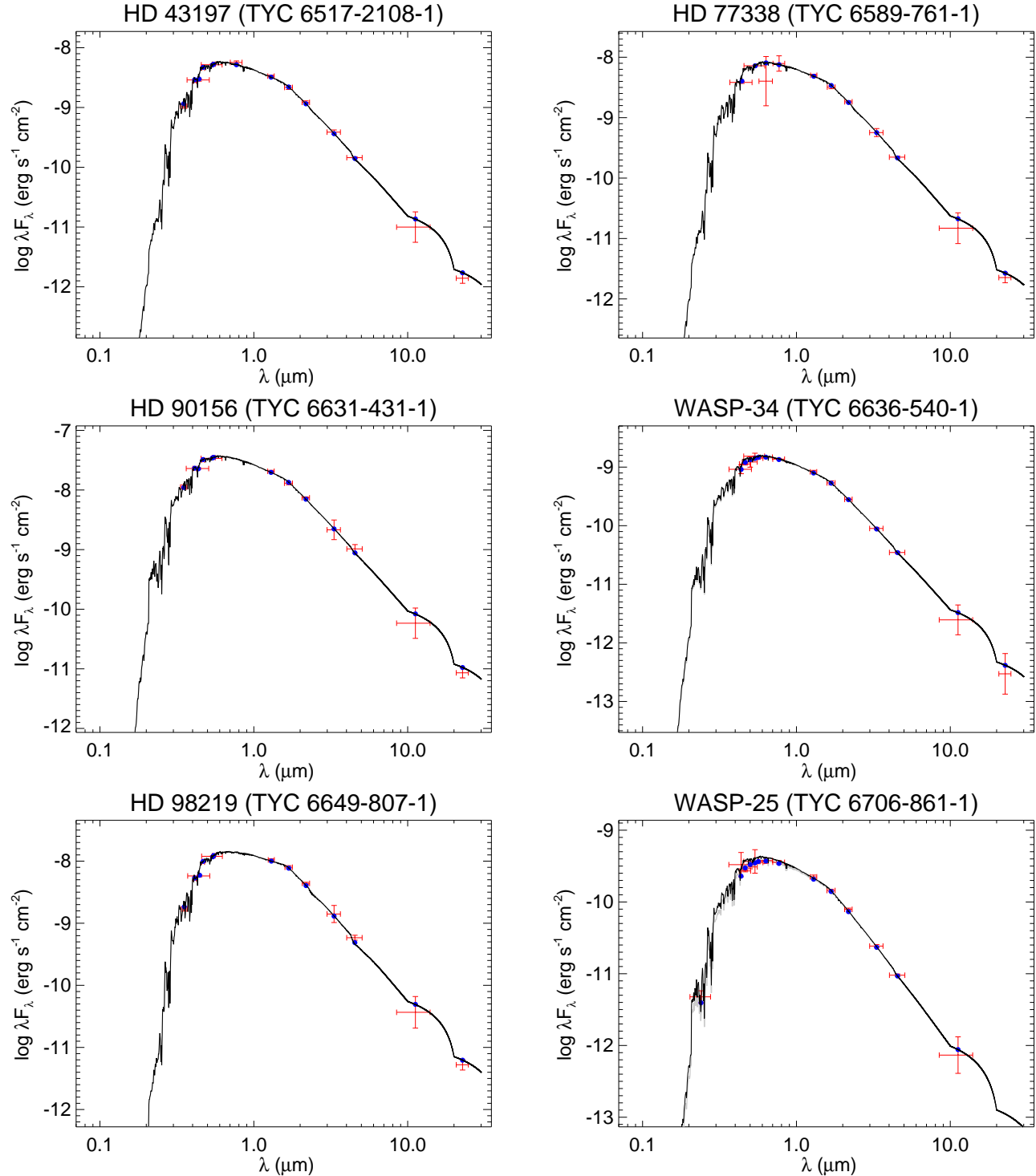


Figure 75. All labels, lines, symbols, and colors as in Figure 14.

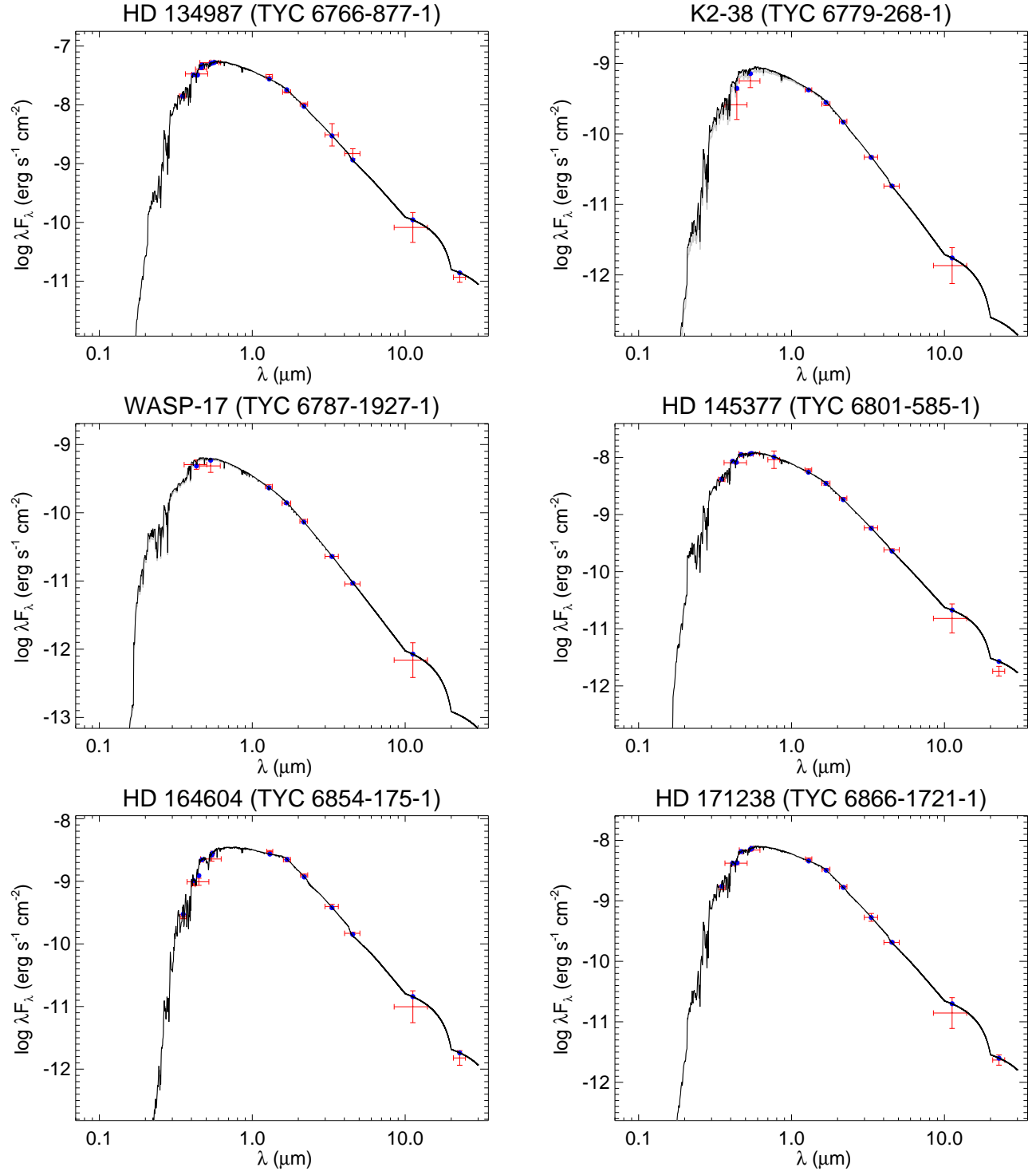


Figure 76. All labels, lines, symbols, and colors as in Figure 14.

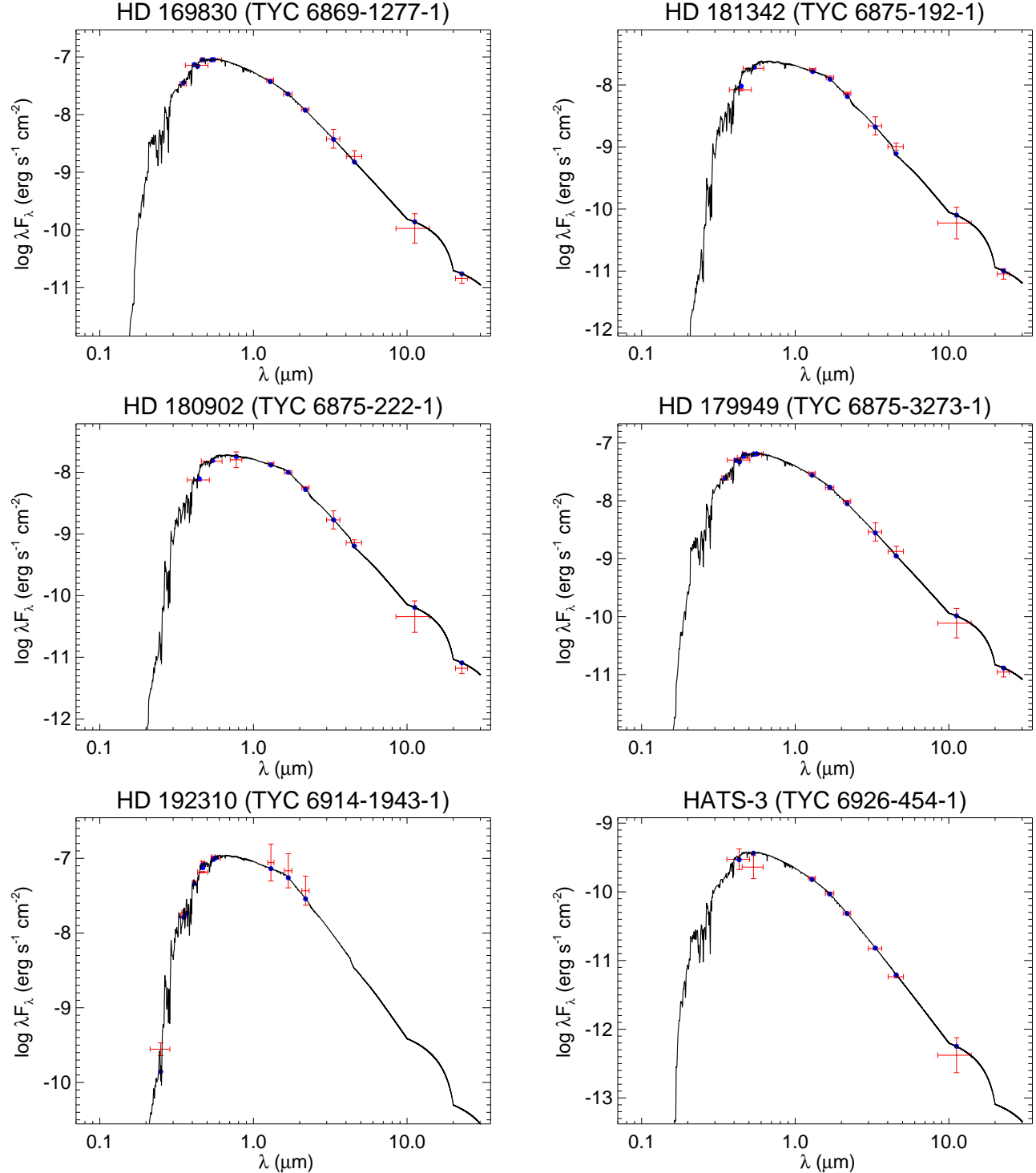


Figure 77. All labels, lines, symbols, and colors as in Figure 14.

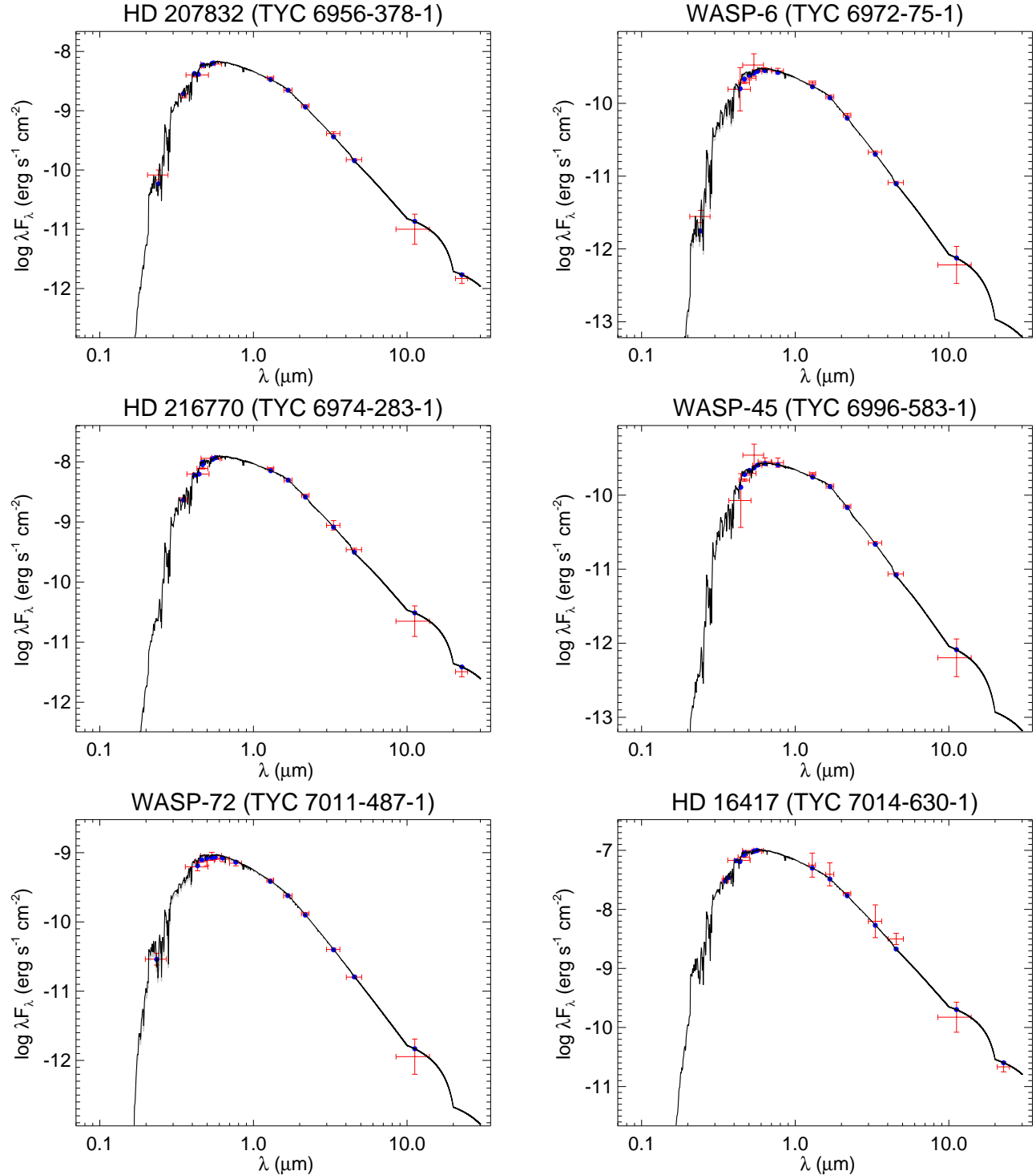


Figure 78. All labels, lines, symbols, and colors as in Figure 14.

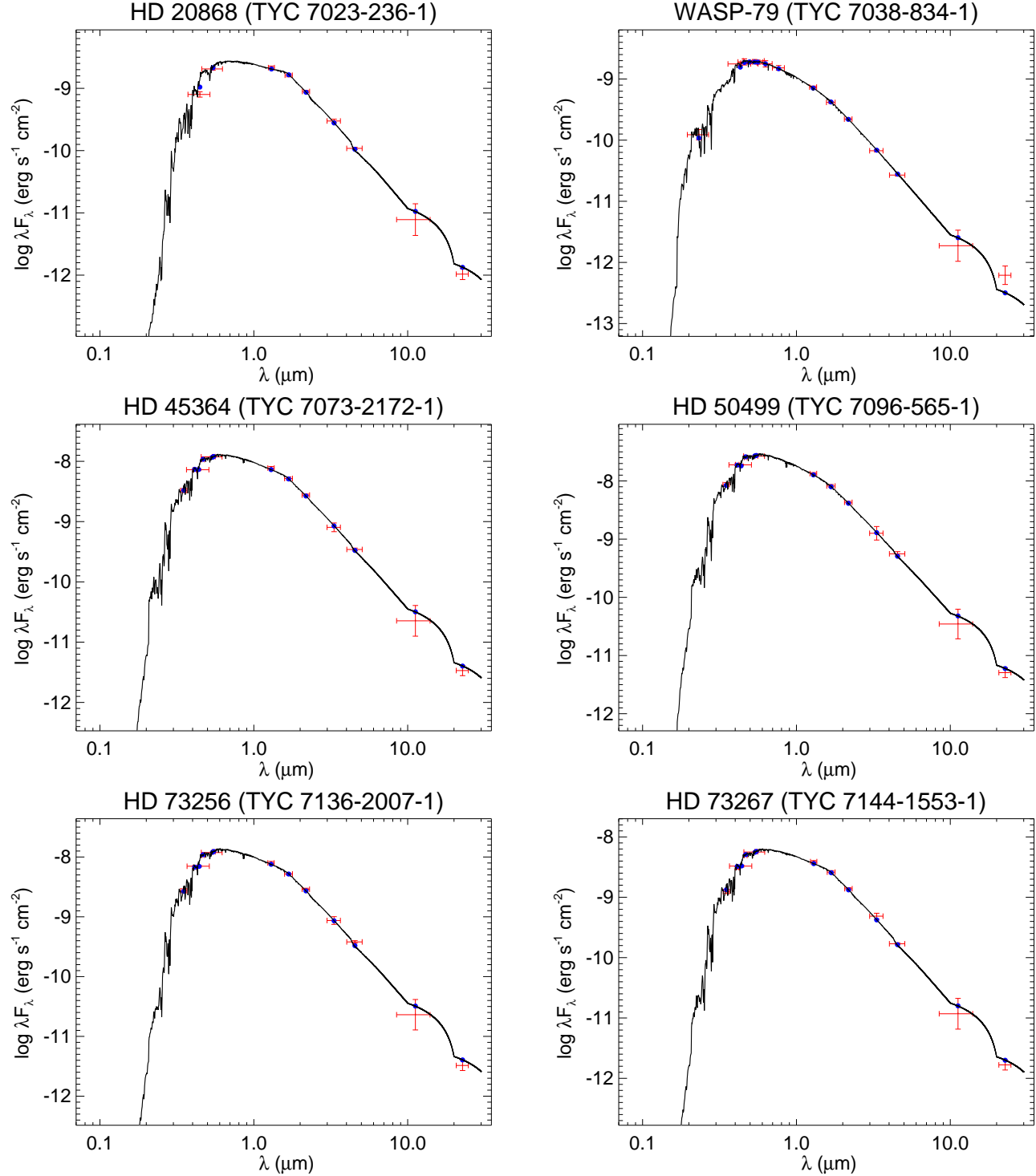


Figure 79. All labels, lines, symbols, and colors as in Figure 14.

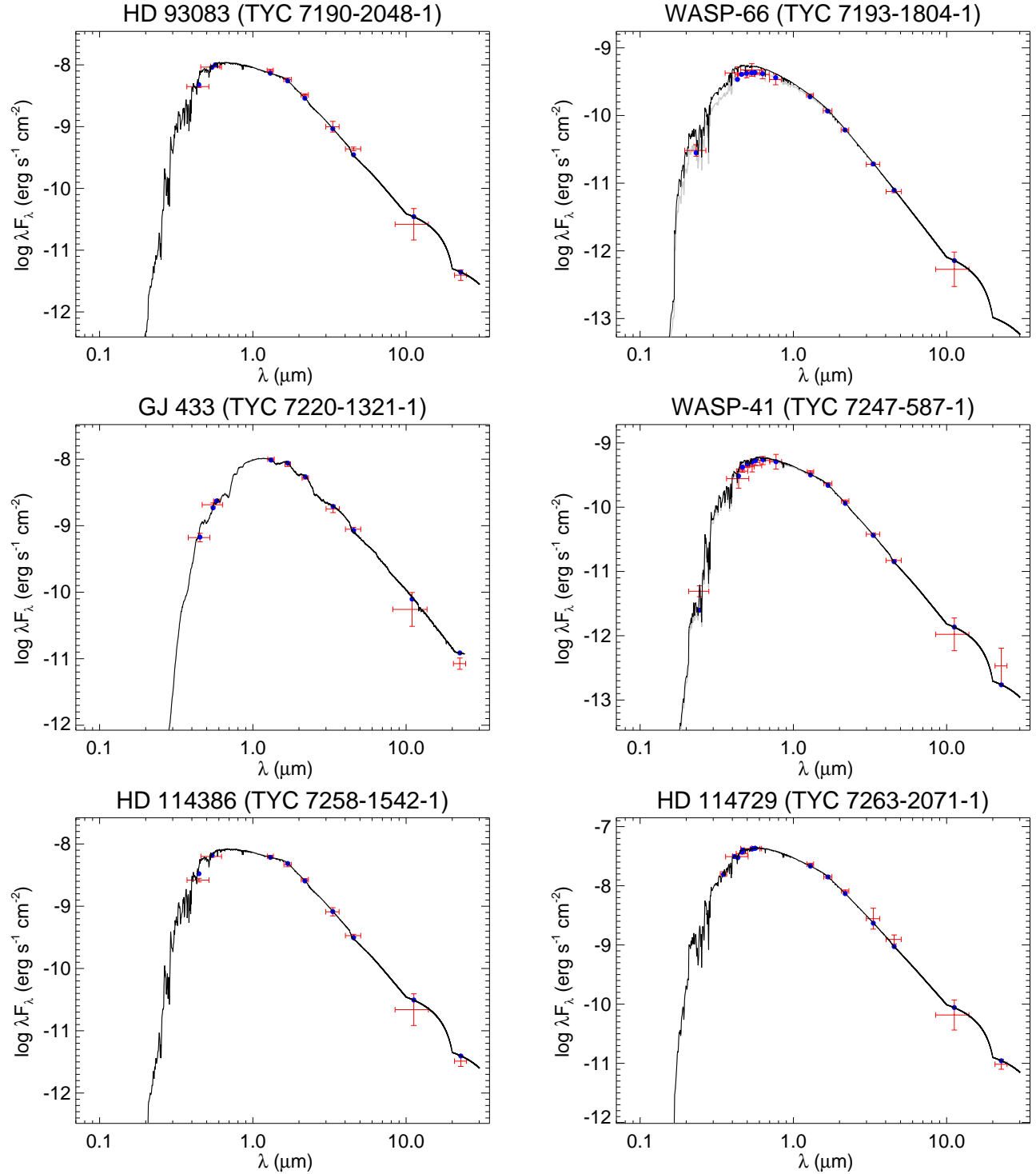


Figure 80. All labels, lines, symbols, and colors as in Figure 14.

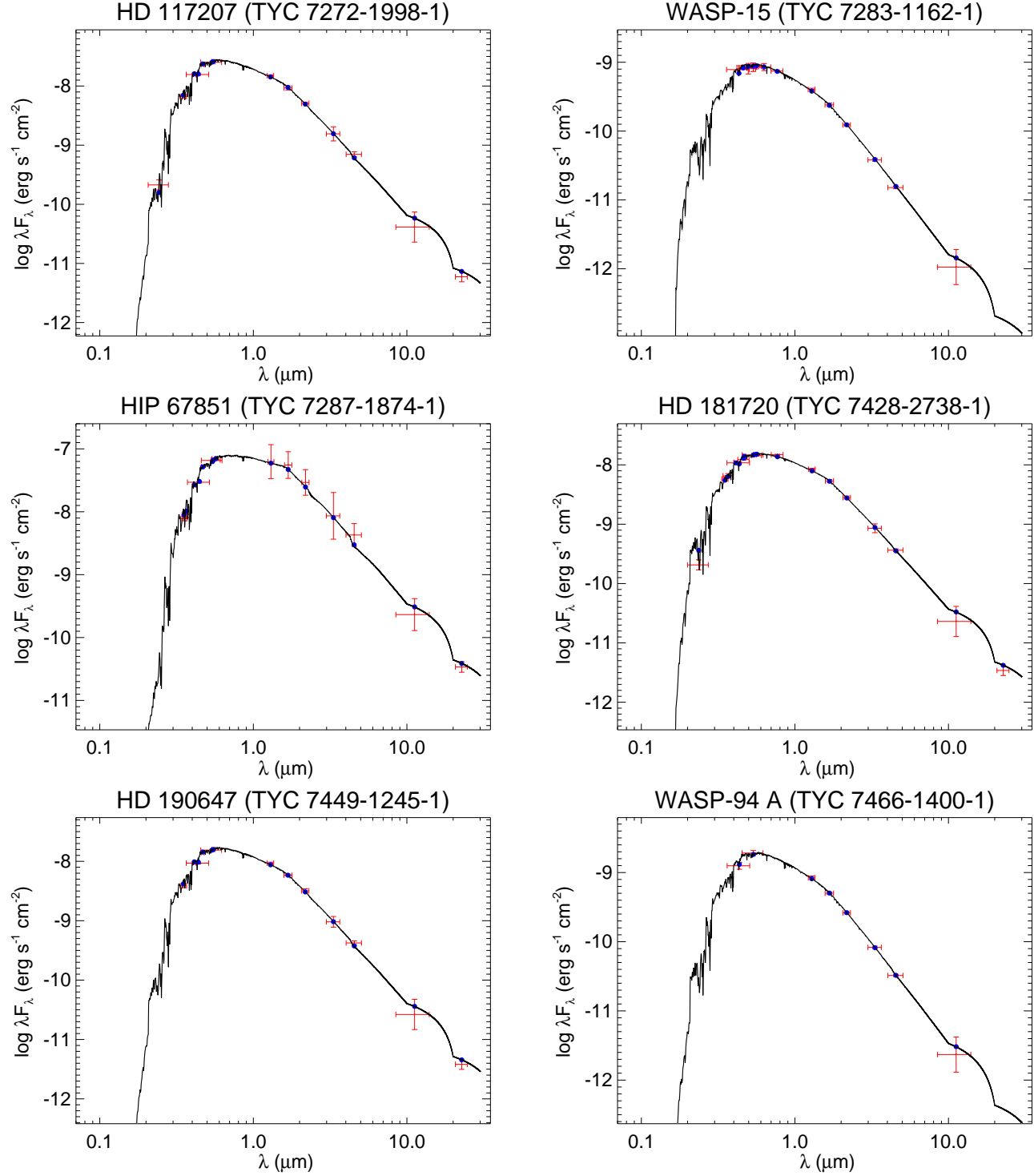


Figure 81. All labels, lines, symbols, and colors as in Figure 14.

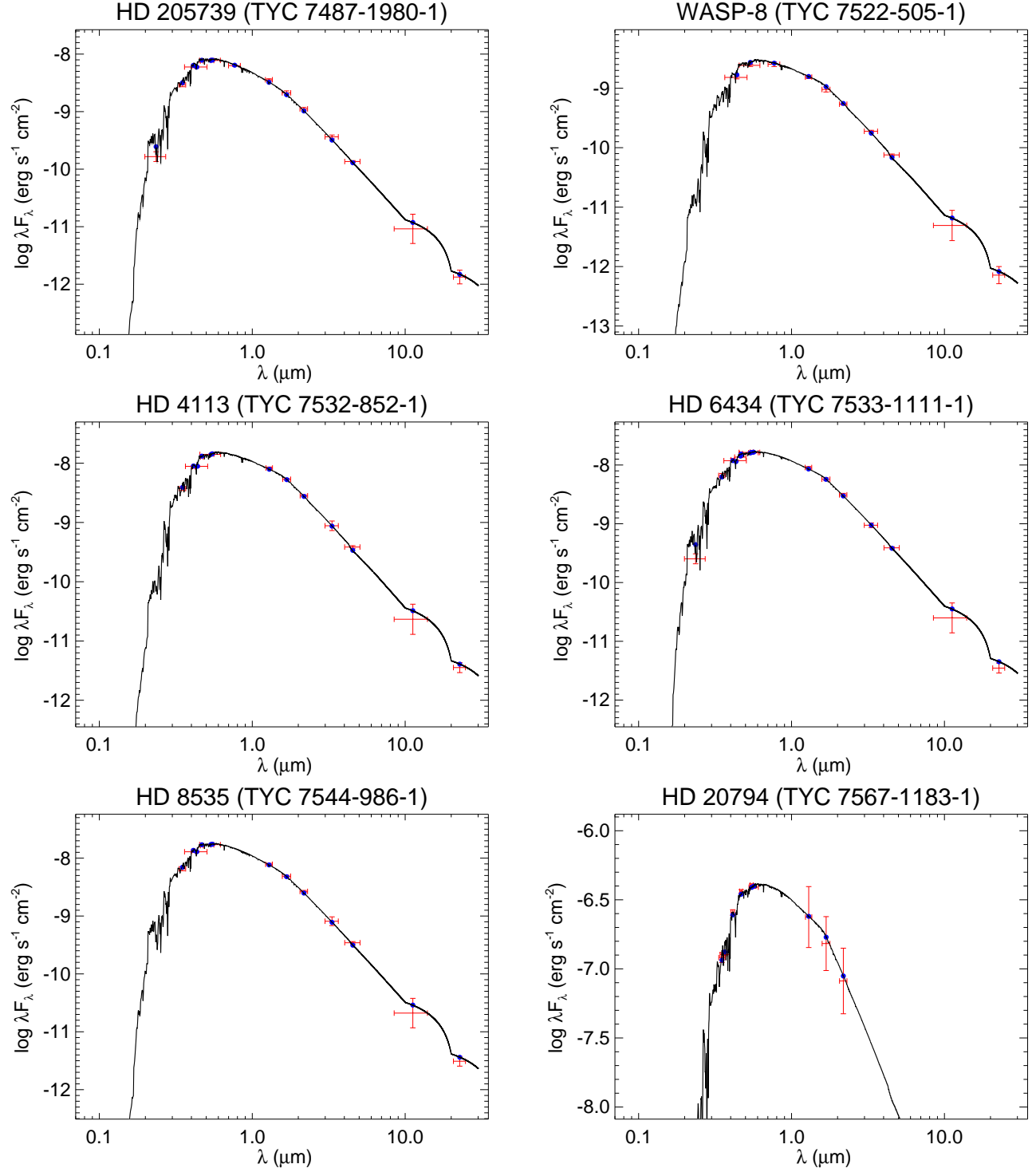


Figure 82. All labels, lines, symbols, and colors as in Figure 14.

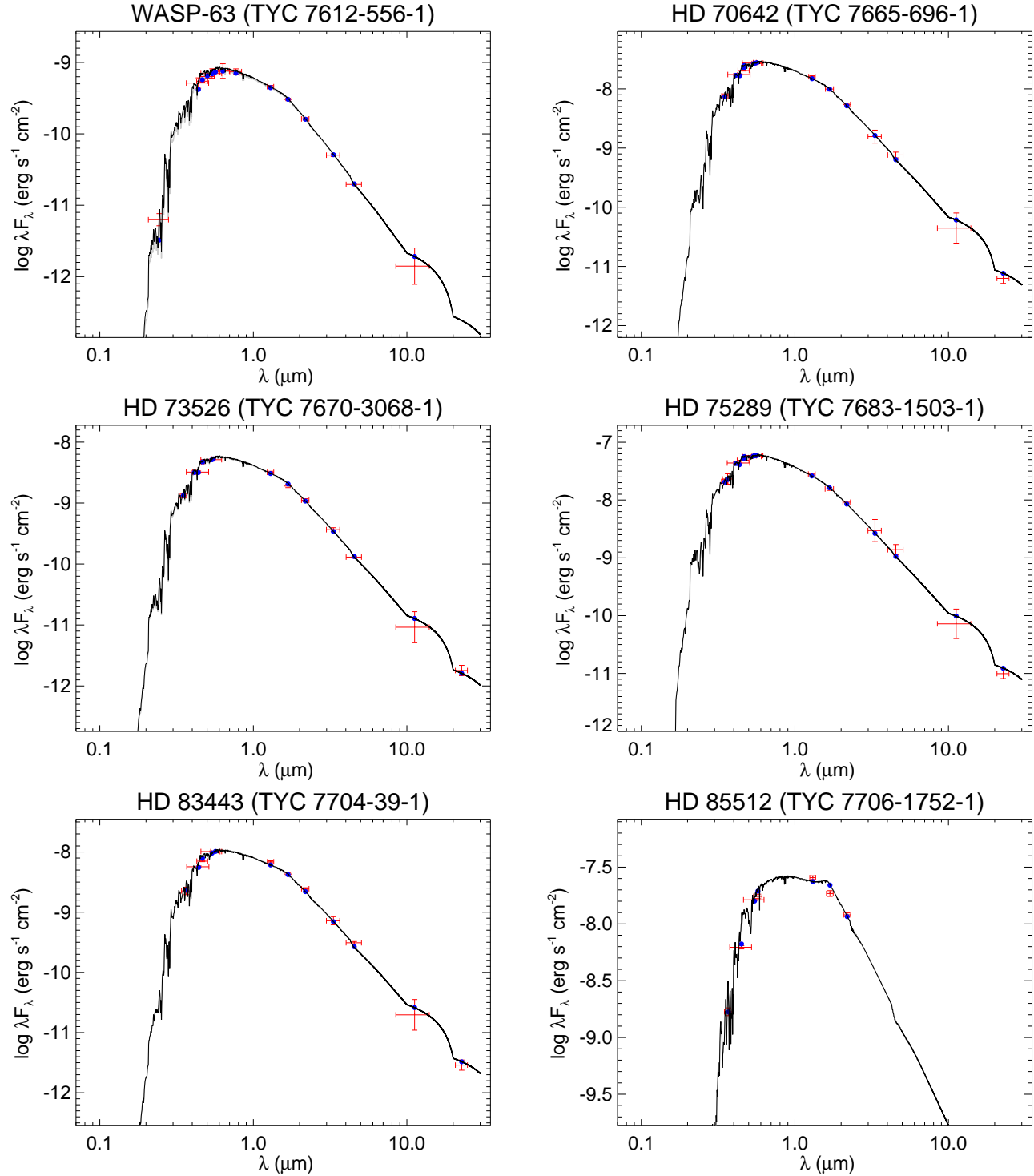


Figure 83. All labels, lines, symbols, and colors as in Figure 14.

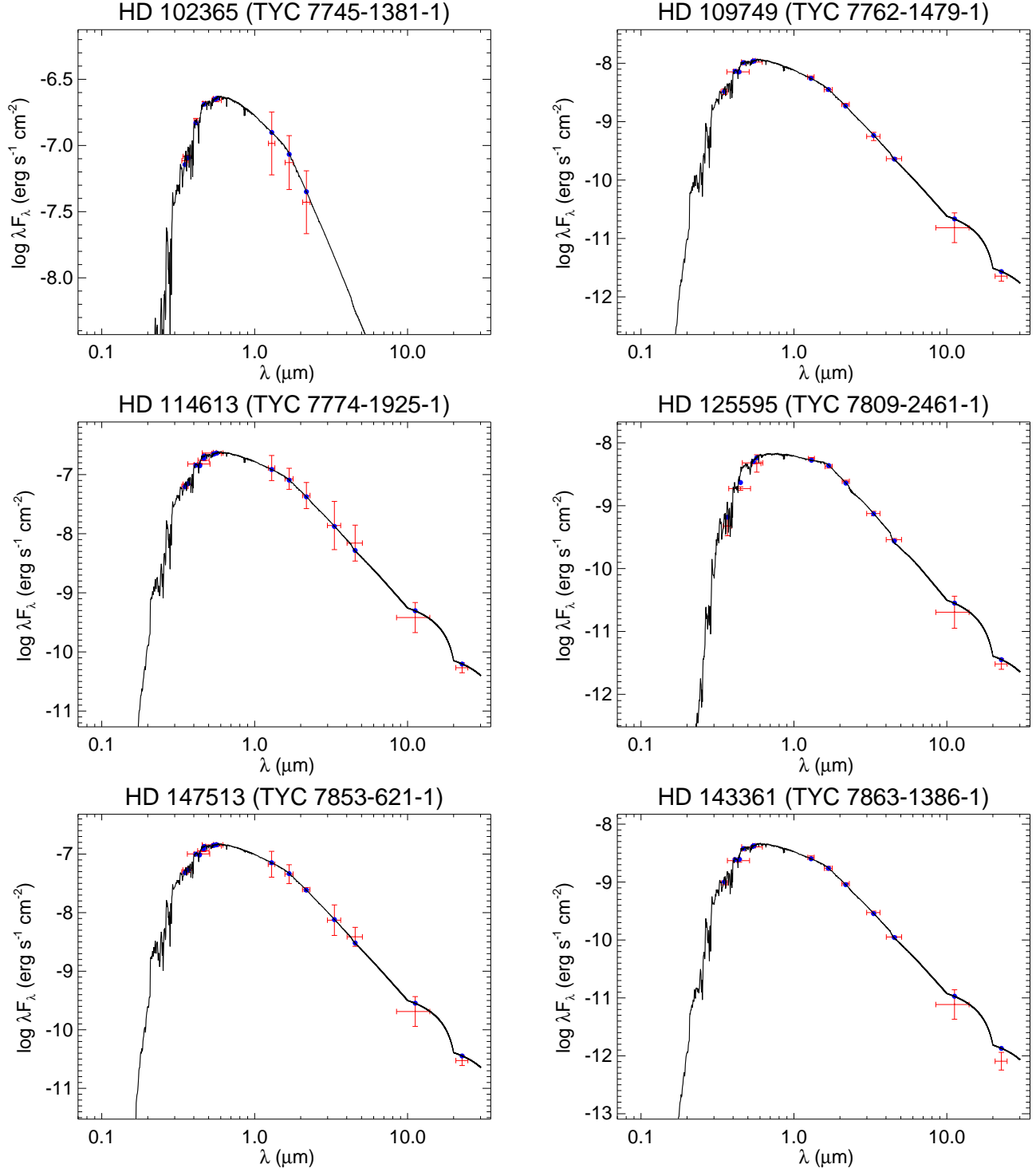


Figure 84. All labels, lines, symbols, and colors as in Figure 14.

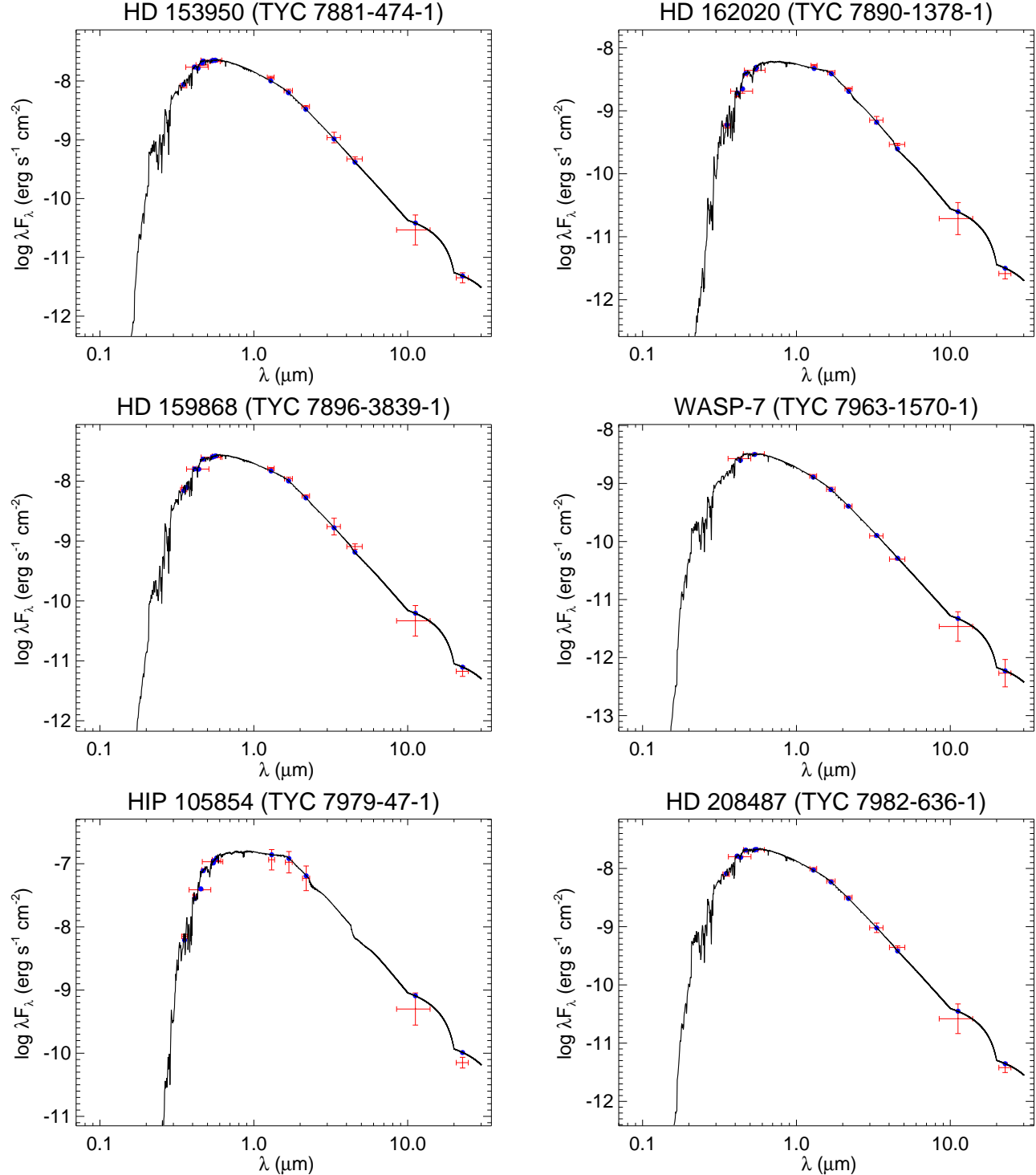


Figure 85. All labels, lines, symbols, and colors as in Figure 14.

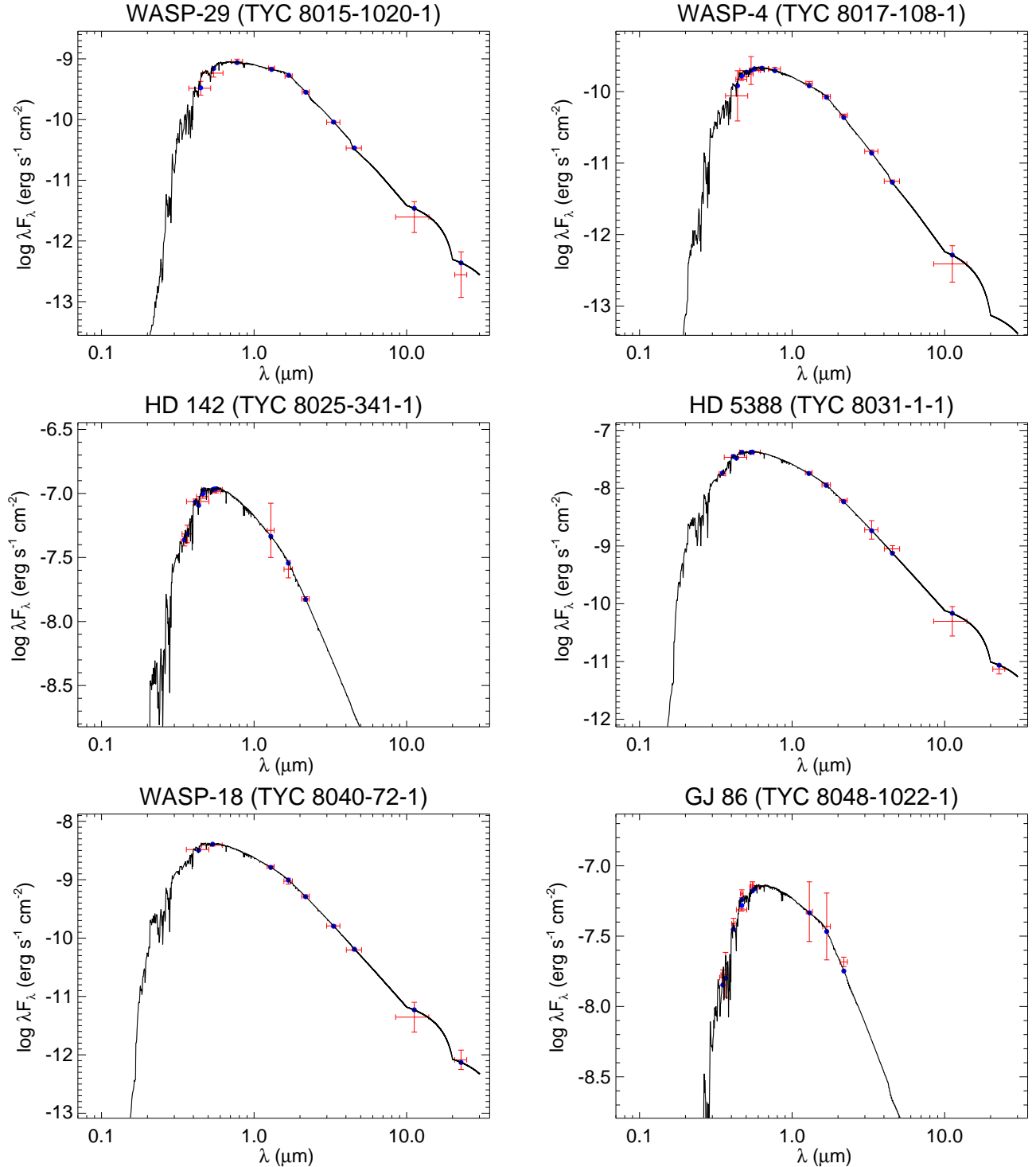


Figure 86. All labels, lines, symbols, and colors as in Figure 14.

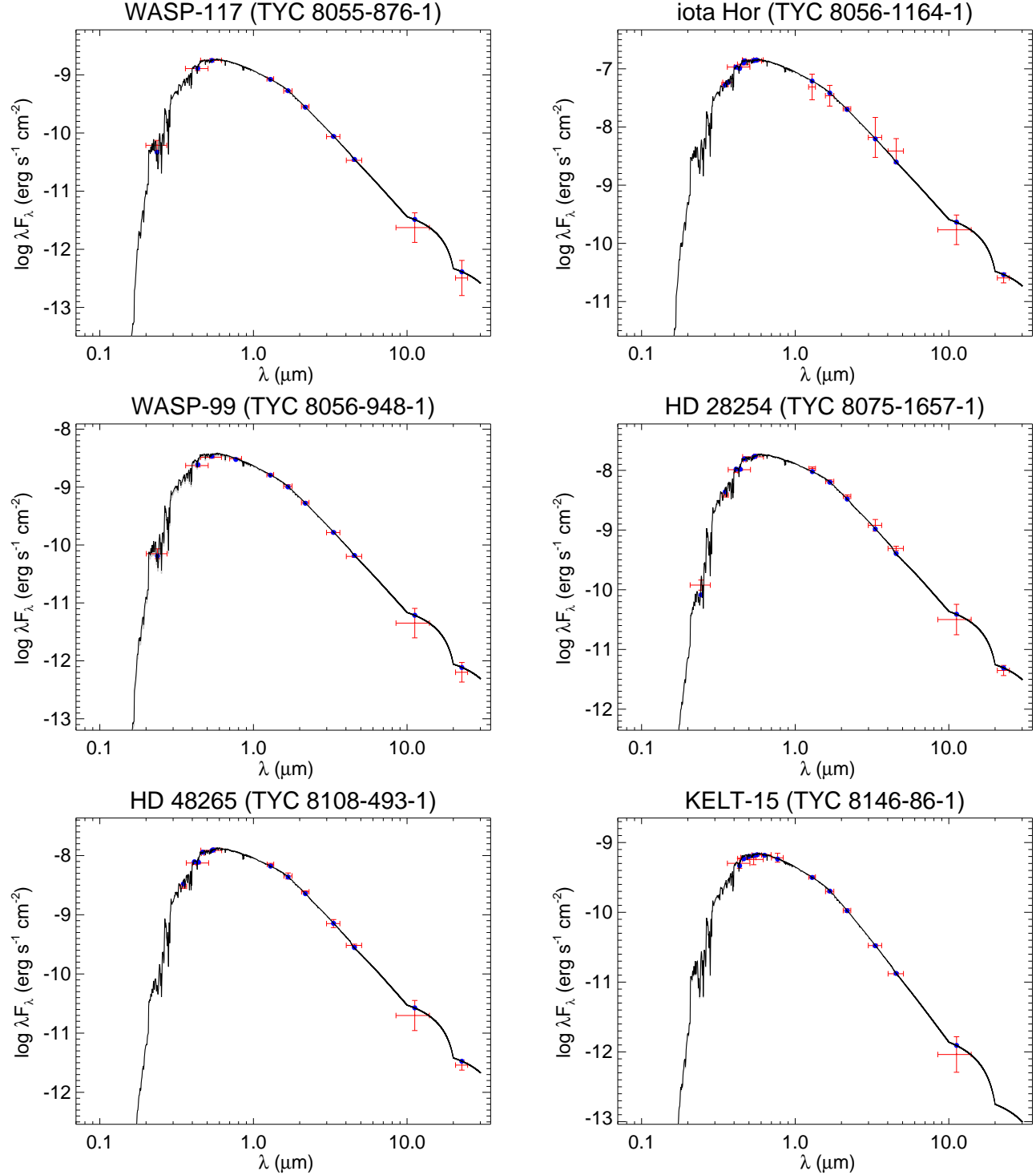


Figure 87. All labels, lines, symbols, and colors as in Figure 14.

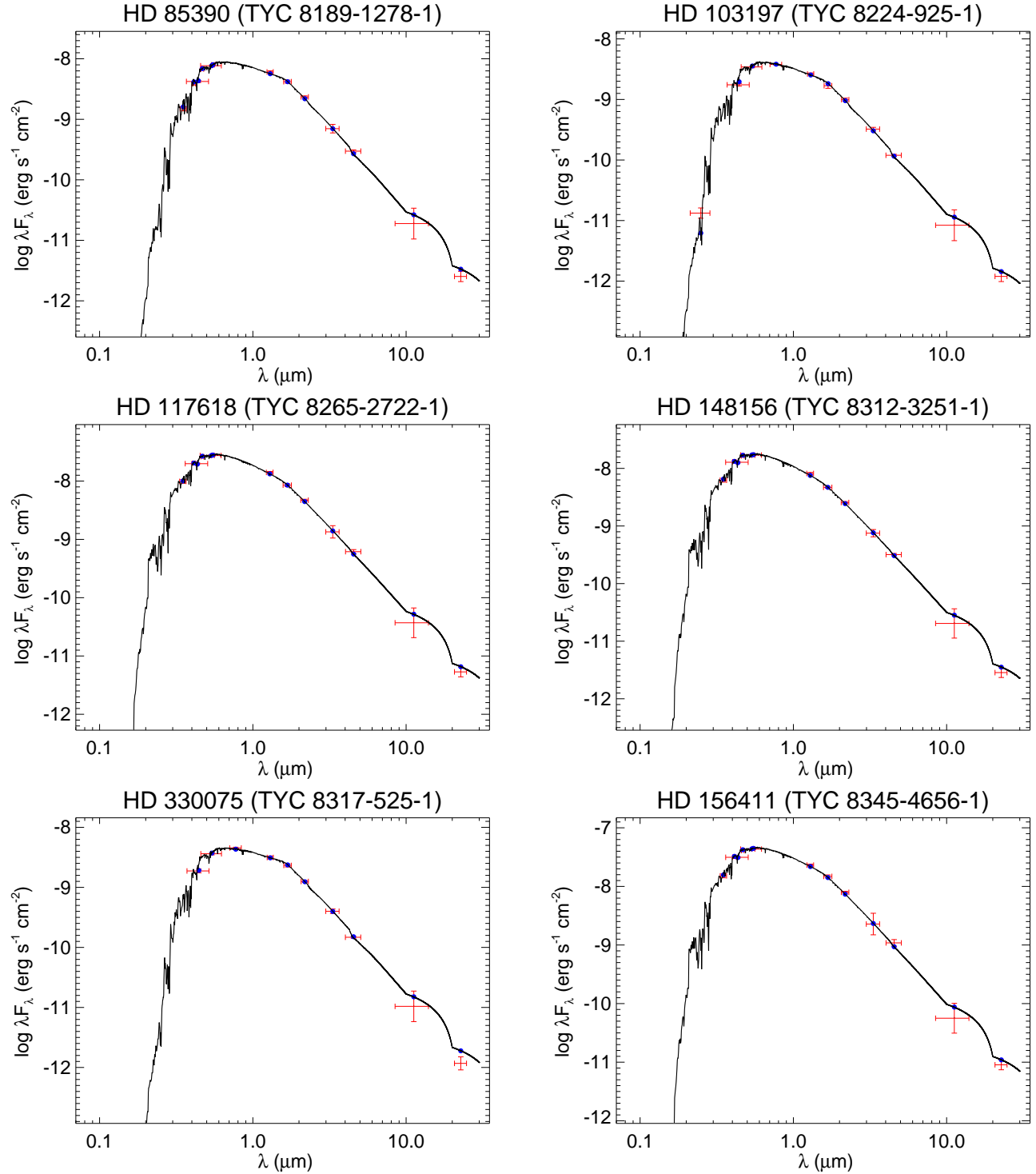


Figure 88. All labels, lines, symbols, and colors as in Figure 14.

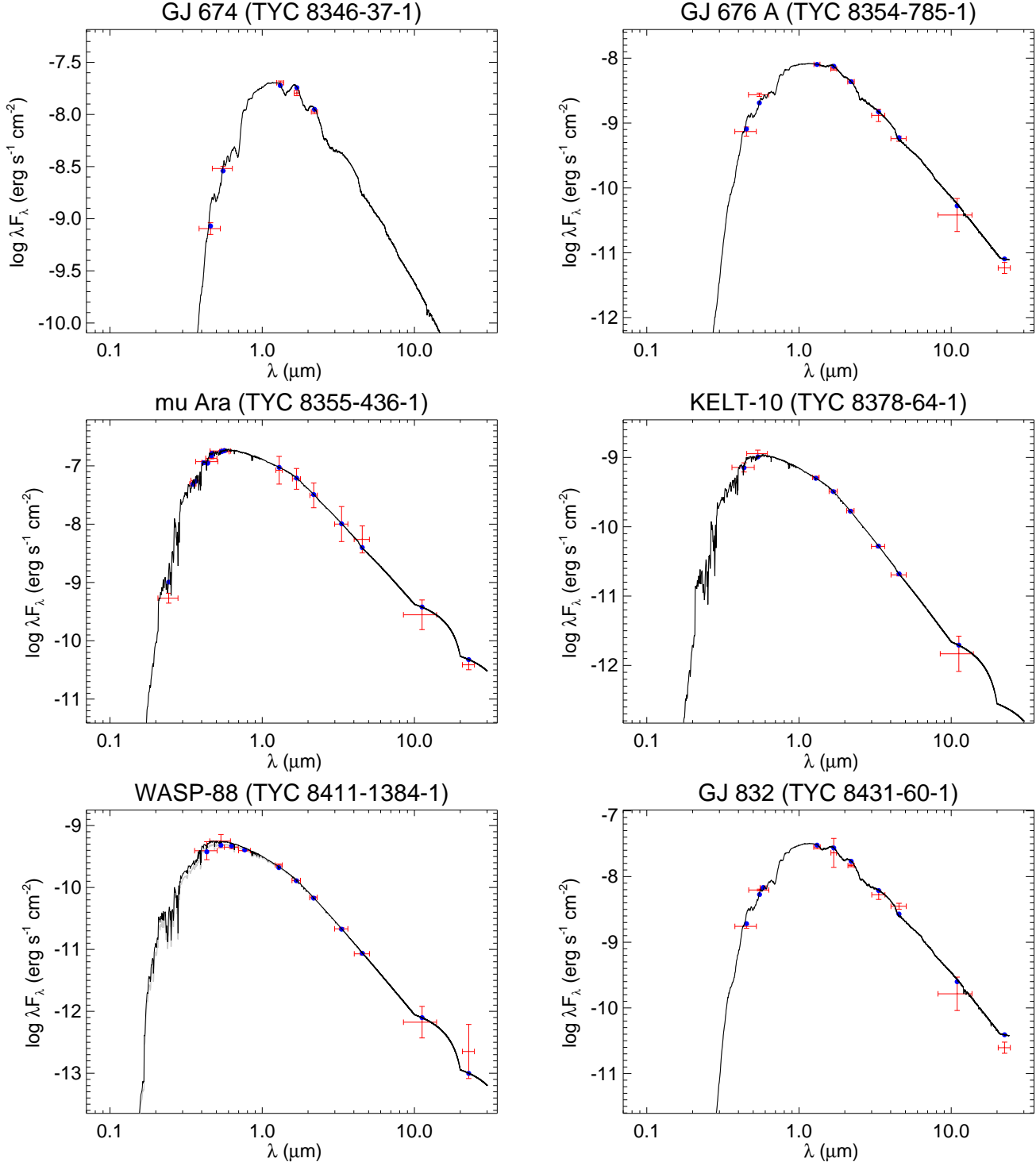


Figure 89. All labels, lines, symbols, and colors as in Figure 14.

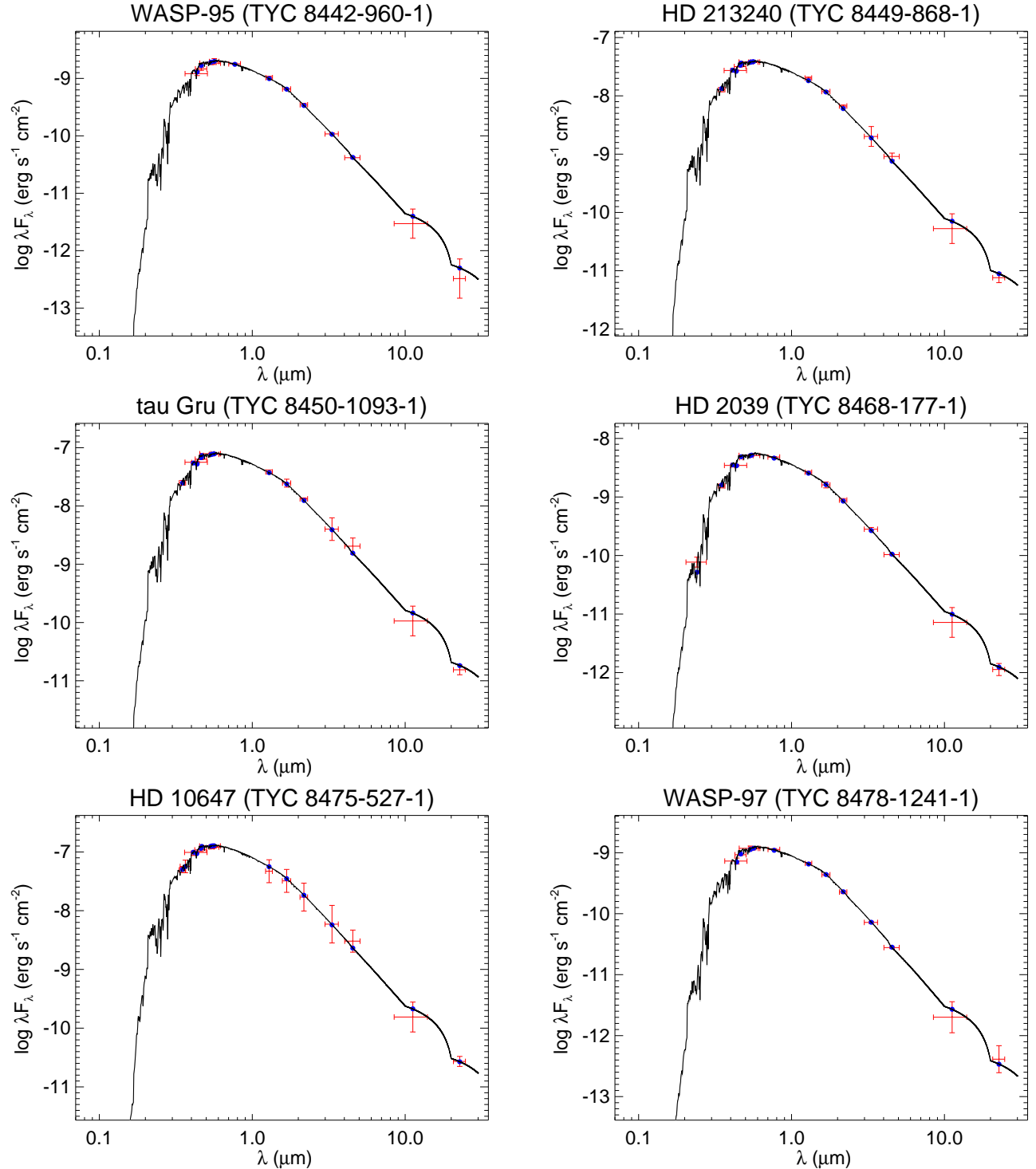


Figure 90. All labels, lines, symbols, and colors as in Figure 14.

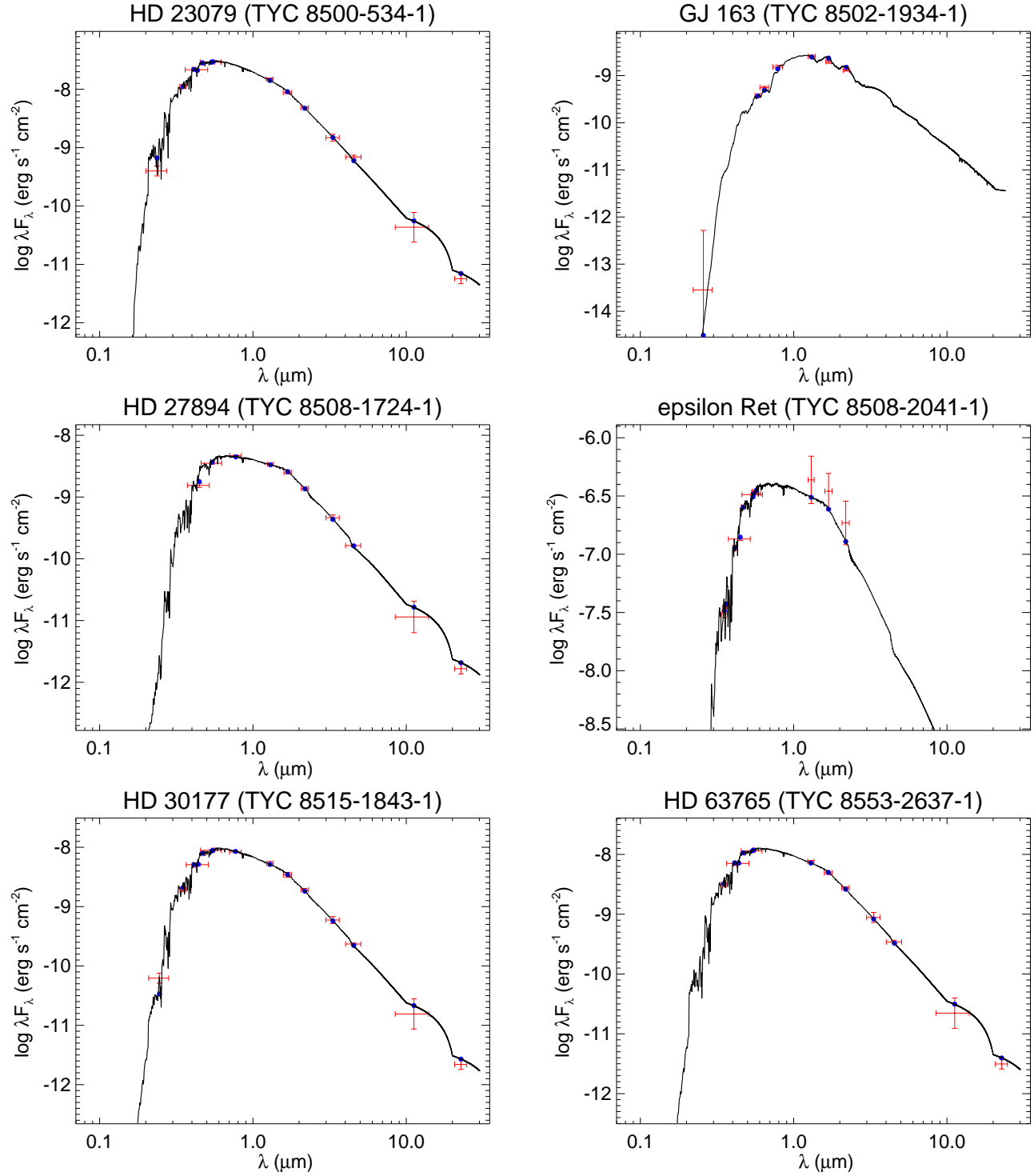


Figure 91. All labels, lines, symbols, and colors as in Figure 14.

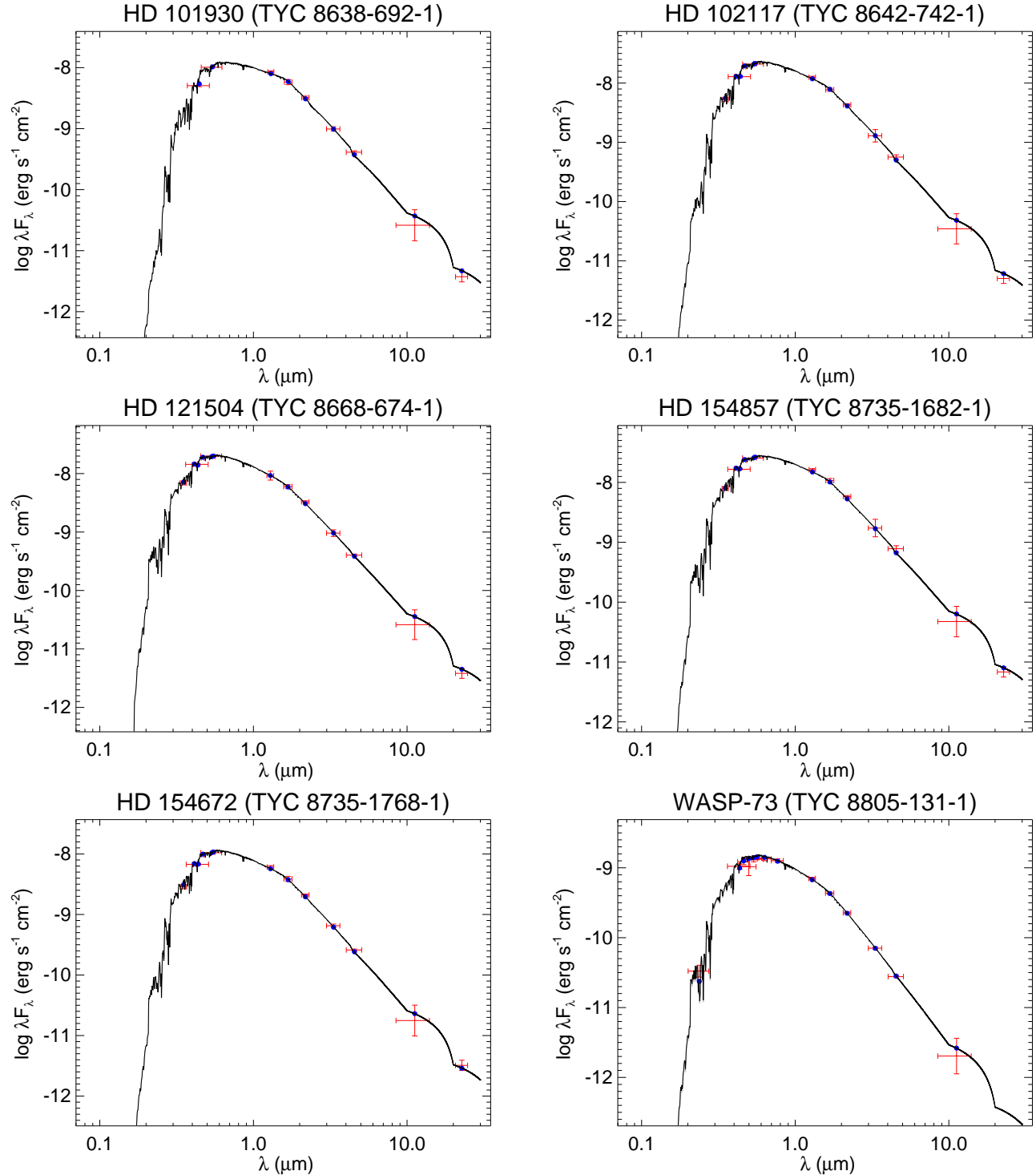


Figure 92. All labels, lines, symbols, and colors as in Figure 14.

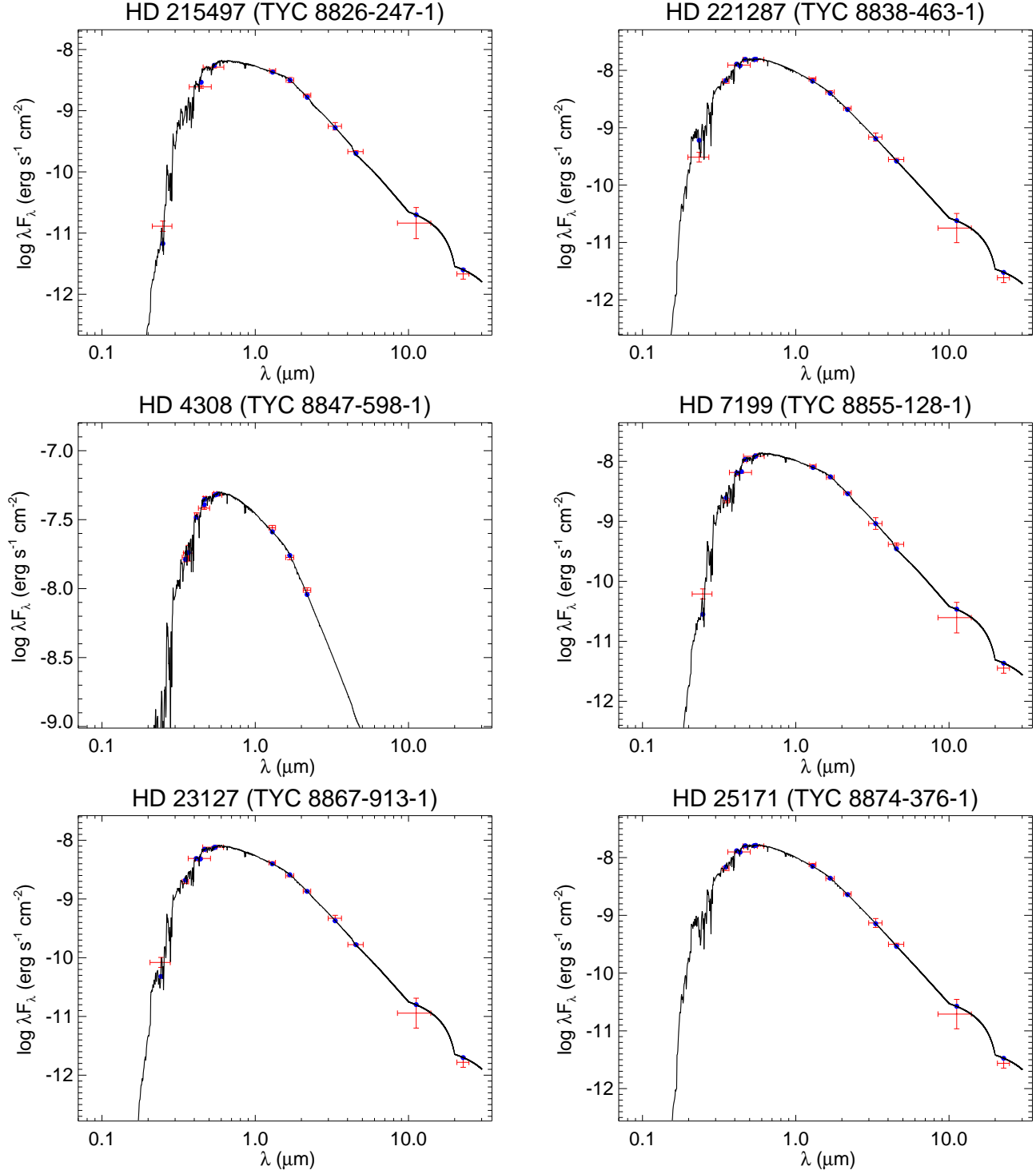


Figure 93. All labels, lines, symbols, and colors as in Figure 14.

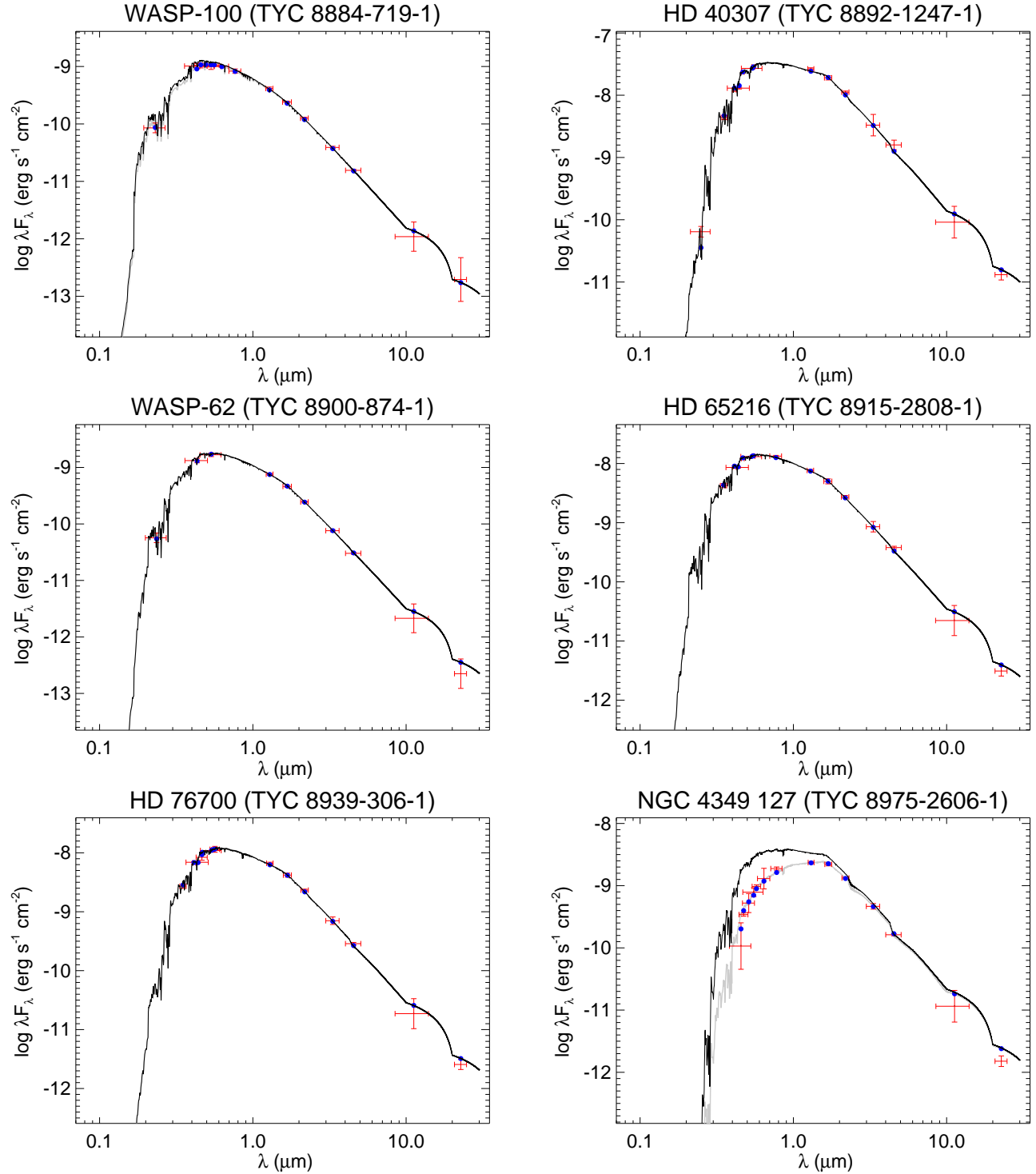


Figure 94. All labels, lines, symbols, and colors as in Figure 14.

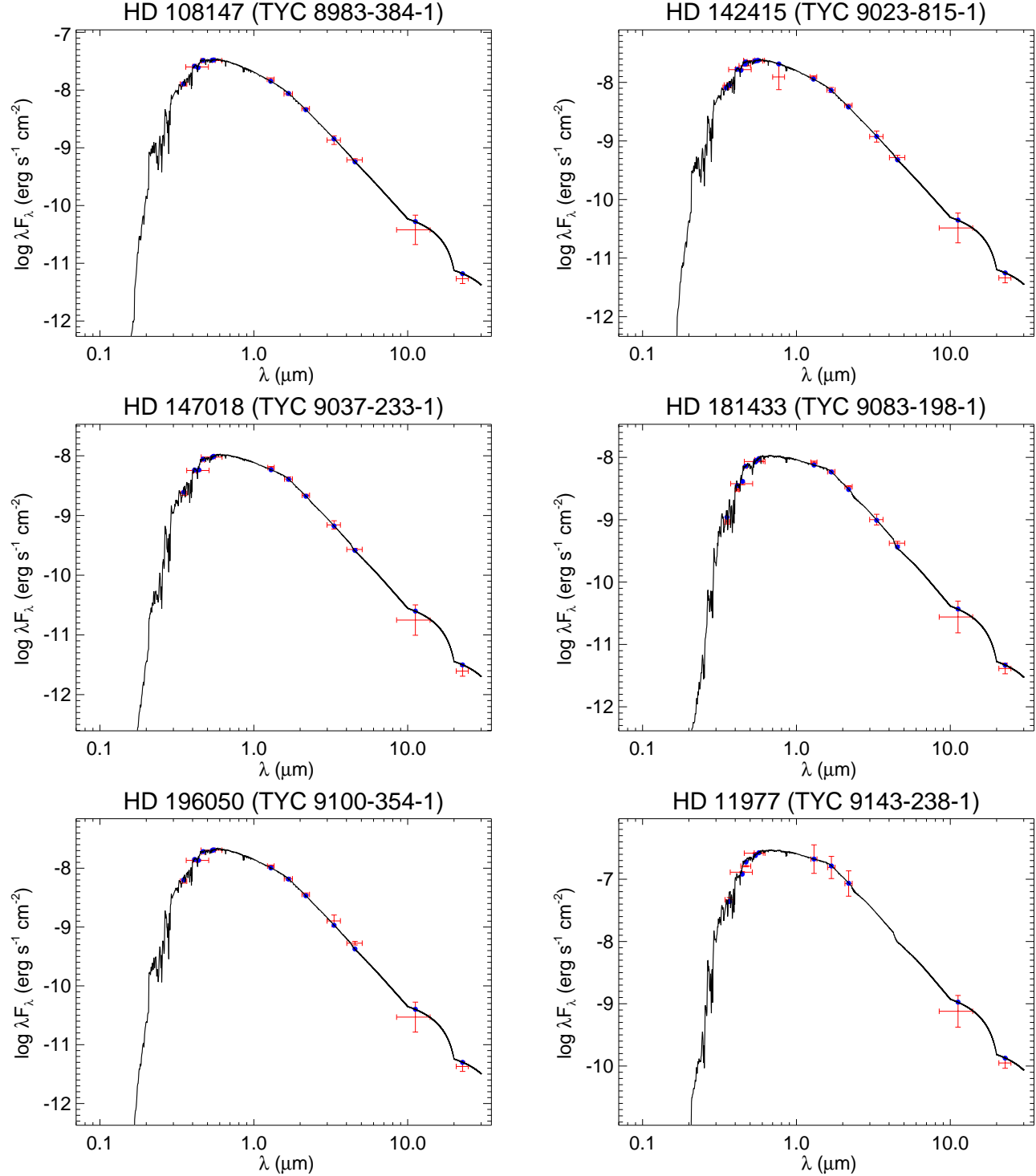


Figure 95. All labels, lines, symbols, and colors as in Figure 14.

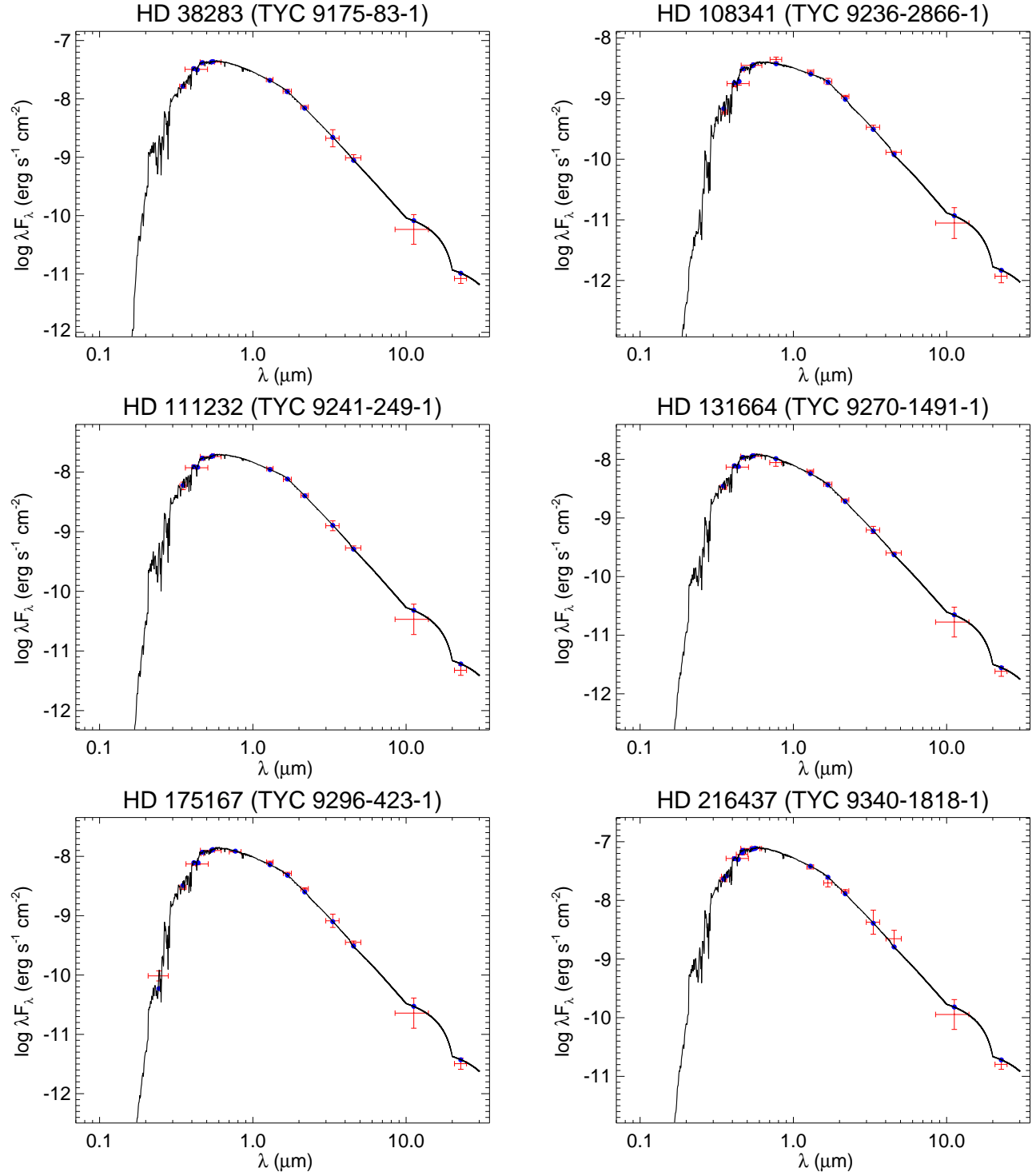


Figure 96. All labels, lines, symbols, and colors as in Figure 14.

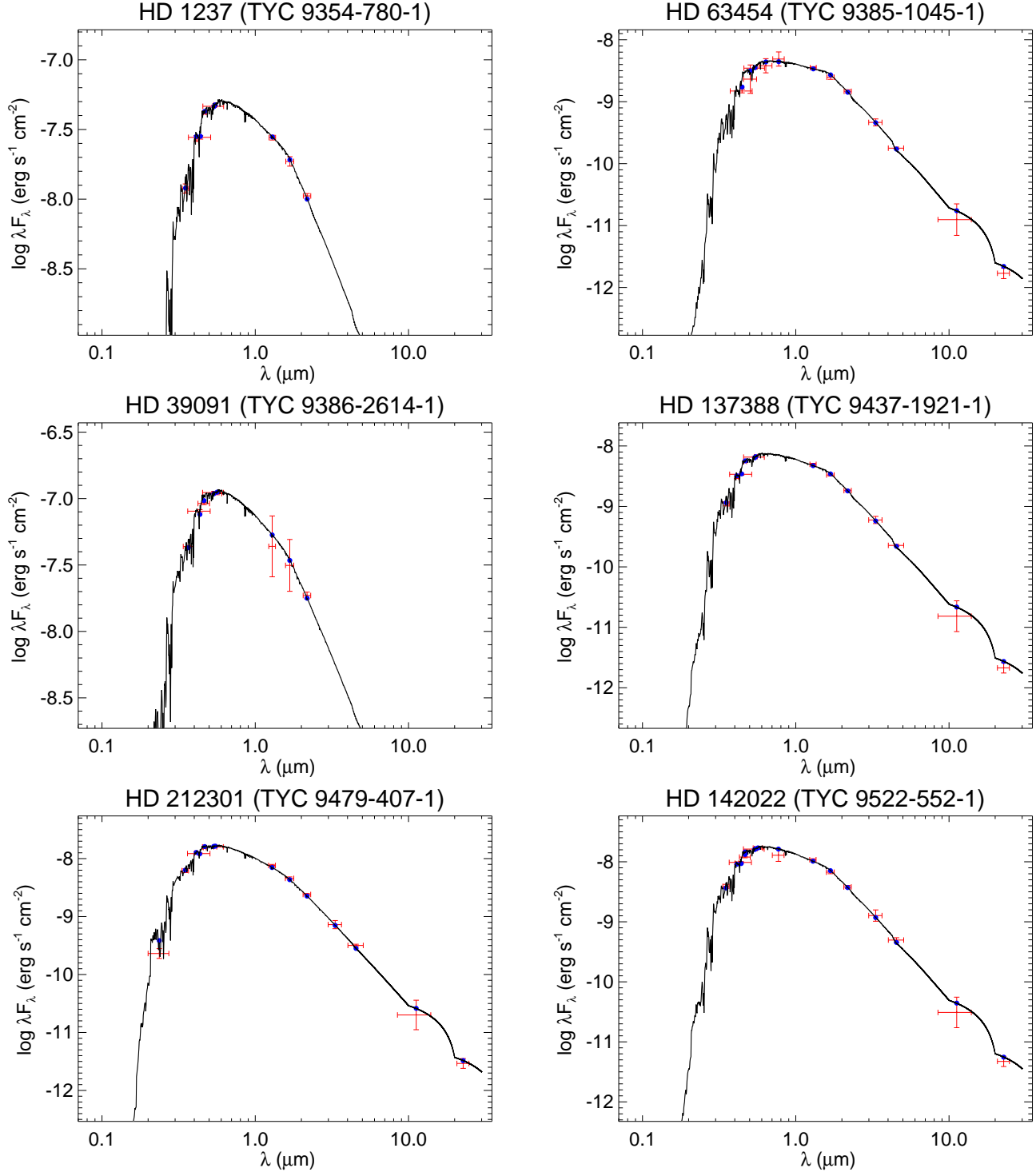


Figure 97. All labels, lines, symbols, and colors as in Figure 14.